TECHNISCHE UNIVERSITÄT WIEN
Vienna | Austria

PhD Thesis

Dissertation

New Monomers for Tough Photopolymers

ausgeführt zum Zwecke der Erlangung des akademischen Grades
eines Doktors der technischen Wissenschaften

unter der Leitung von

Univ.Prof. DI Dr.techn. Robert Liska

und

DI Dr.techn. Christian Gorsche

E163 – Institut für Angewandte Synthesechemie

eingereicht an der Technischen Universität Wien
Fakultät für Technische Chemie

von

DI Johannes Steindl

e0926235

Withalmstraße 9/1B/16, 2120 Wolkersdorf

Wolkersdorf, am 26. Februar 2021

Die approbierte gedruckte Originalversion dieser Dissertation ist an der TU Wien Bibliothek verfügbar.
The approved original version of this doctoral thesis is available in print at TU Wien Bibliothek.
TU Bibliothek Your knowledge hub WIEN

Die approbierte gedruckte Originalversion dieser Dissertation ist an der TU Wien Bibliothek verfügbar.
The approved original version of this doctoral thesis is available in print at TU Wien Bibliothek.

“Unkraut vergeht nicht!”

Danksagung

Während der Erstellung der vorliegenden Arbeit haben mich viele Personen begleitet und unterstützt. An dieser Stelle möchte ich mich herzlich bedanken:

Herrn Prof. Robert Liska und Prof. Jürgen Stampfl möchte ich für die interessante Themenstellung der Dissertation, die Möglichkeit, diese in ihren Arbeitsgruppen durchführen zu können, und für die Freiheit, die mir beim Erstellen dieser Arbeit gewährt wurde, danken. Weiters gilt mein Dank Dr. Christian Gorsche für die ausgezeichnete Betreuung.
Beim gesamten Arbeitsbereich für Makromolekulare Chemie – unter der Leitung von Prof. Simone Knaus – möchte ich mich für das angenehme Arbeitsklima, die hervorragende Zusammenarbeit und viele gemütliche Stunden mit dem ein oder anderen Bier bedanken. Nirgendwo hätte ich die Jahre lieber verbracht als in dieser Arbeitsgruppe! Nico, Paul, Lukas, Sandra, Kathi, Ricki, Roli, Chris, Sebi, Pazi, Lisl, Lunzer, Gitti, Moritz, Philip, Ralle, Sascha, Babsi, AD, Hofi, György, David, Anna, Lisa, Larissa, Bettina, Kury, Olga, Helfert, Sarah, Daniel, Erika, Davide, Stefan, Knäcksi, Mia und Konzi, Ihr habt die Zeit unvergesslich gemacht, danke! Besonders hervorzuheben ist jedoch das H31, das beste Labor aller Zeiten: Pauli, Daniel, Raffi, Schnölli und Gernot. Ohne Euch hätte das Ganze kaum Spaß gemacht.
Weiters gilt mein Dank auch meinen Praktikanten, die zum Gelingen dieser Arbeit tatkräftig beigetragen haben: Florian, Isabella und Michael.
Allen Institutsangestellten – im besonderen Walter Dazinger, die gute Seele des Arbeitsbereichs –, ohne die ein Laborbetrieb in dieser Form nicht möglich wäre, möchte ich aufrichtig meinen Dank aussprechen.

Bei Lisa muss ich mich für die Motivation und Kraft bedanken, diese Arbeit noch abschließen zu können. Deine ewige Geduld mit mir gibt mir den nötigen Rückhalt. Du gibst mir Hoffnung, Vertrauen und Unterstützung, wenn ich sie am dringendsten brauche. Danke – Ich liebe dich!
Ein besonders großes Dankeschön gilt meinen Eltern, Geschwistern und Großeltern: danke, dass ihr mir dieses Studium ermöglicht und mich dabei auch immer unterstützt habt; danke, dass ihr mir Flügel verliehen und Wurzeln gegeben habt; danke für die Vermittlung von Selbstständigkeit, Vertrauen und Respekt; danke für den Halt, die Werte und die Orientierung.

Macromolecular Chemistry

Wolkersdorf, im Februar 2021

Johannes Steindl

Die approbierte gedruckte Originalversion dieser Dissertation ist an der TU Wien Bibliothek verfügbar.
The approved original version of this doctoral thesis is available in print at TU Wien Bibliothek.
TU Bibliothek Your knowledge hub WIEN

Abstract

Photopolymers are a widely spread class of materials. They are utilised in thin layer applications such as inks and protective and decorative coatings to more sophisticated uses like medical applications or additive manufacturing technologies. Nevertheless, lack of toughness still limits utilisation of bulk materials in industry. For this purpose, several promising concepts were already published in literature to overcome these drawbacks (*e.g.* toughening additives or modification of the polymer network). However, they exhibit other disadvantages such as high viscosity, decrease of other (thermo)mechanical properties in exchange for toughness or are quite simply too expensive for many areas.

Therefore, the aim of this thesis was to investigate new approaches to tackle brittleness in photopolymers. Thus, two different independent plans were pursued and studied in detail ranging from resin characterisation to determination of (thermo)mechanical properties of the final materials.

On the one hand, new cross-linking monomers were synthesised containing blocked isocyanates, which could be cleaved thermally. So, a change in network architecture from highly cross-linked to linear thermoplastic polymers was achieved.

On the other hand, a concept was developed, which was modelled on ABS as a very prominent and tough engineering plastic. Unfortunately, ABS cannot be photopolymerised. Thus, new terpolymers based on maleimide, styrene and polybutadiene were explored to mimic structure and properties of ABS. Furthermore, additional derivatives were synthesised to optimise monomer and material characteristics and to acquire a deeper understanding of these novel transparent ABS-like photopolymers. Finally, three different potential applications were shown (reactive diluent for commercial highly viscous resins, frontal polymerisation and 3D printing), which could pave the way for this new promising photopolymer class in research and industry.

Die approbierte gedruckte Originalversion dieser Dissertation ist an der TU Wien Bibliothek verfügbar.
The approved original version of this doctoral thesis is available in print at TU Wien Bibliothek.
TU Bibliothek Your knowledge hub WIEN

Kurzfassung

Photopolymere stellen eine weitverbreitete Materialklasse dar und werden für eine Vielzahl an Anwendungen von Tinten und Beschichtungen, aber auch für medizinische Materialien und Additive Manufacturing (3D Druck) eingesetzt. Der Mangel an Zähigkeit verhindert jedoch nach wie vor eine breitere Verwendung in der Industrie. Um diese Nachteile zu überwinden, wurden in der Literatur bereits einige vielversprechende Konzepte veröffentlicht (z.B. Additive oder Modifizierung der Polymerstruktur). Diese Ansätze bringen aber andere Nachteile einher, wie hohe Viskosität, Verschlechterung verschiedener anderer (thermo)mechanischer Eigenschaften im Austausch für eine hohe Zähigkeit oder sind einfach zu teuer für viele Anwendungen.

Daher war das Ziel dieser Arbeit, neue Ansätze zur Verringerung der Sprödigkeit in Photopolymeren zu finden. Dazu wurden zwei unterschiedliche Konzepte verfolgt und im Detail – beginnend bei Formulierungseigenschaften bis hin zu (thermo)mechanischen Eigenschaften des fertigen Materials – untersucht.

Einerseits wurden neue vernetzende Monomere mit geblockten Isocyanaten hergestellt, die thermisch gespalten werden können. Dadurch gelang es, die Netzwerkarchitektur von einem stark vernetzten hin zu einem linearen thermoplastischen Polymer zu verändern.

Andererseits wurde ein Konzept entwickelt, welches ABS als bekannten und zähen Kunststoff zum Vorbild nahm. Da ABS nicht photopolymerisiert werden kann, wurden neue Terpolymere basierend auf Maleimid, Styrol und Polybutadien entwickelt, um die Struktur und Eigenschaften von ABS nachzuahmen. Darüber hinaus wurden weitere Monomere synthetisiert, um verschiedene Monomer- und Materialeigenschaften zu optimieren und ein besseres Verständnis für diese neuartigen transparenten ABS-ähnlichen Photopolymere zu entwickeln. Schlussendlich konnten drei mögliche Anwendungen (Reaktivverdünner für kommerzielle hochviskose Harze, Frontalpolymerisation und 3D Druck) aufgezeigt werden, welche den Weg für diese neue vielversprechende Photopolymerklasse ebnen können.

Die approbierte gedruckte Originalversion dieser Dissertation ist an der TU Wien Bibliothek verfügbar.
The approved original version of this doctoral thesis is available in print at TU Wien Bibliothek.
TU WIEN Bibliothek Your knowledge hub

Table of Contents

Introduction	1	
Objective	13	
General Part / Experimental Part	14 / 166	
	Gen.	Exp.
1. UV-Curable (Meth)Acrylates containing Blocked Isocyanates	14	166
1.1. State of the art	16	
1.2. Model compounds	21	166
1.2.1. Model isocyanurates	21	166
1.2.1.1. Determination of structure and functionality	22	
1.2.1.2. Determination of deblocking temperature	27	166
1.2.2. Model C-H acidic blocking agent	32	
1.3. Syntheses of methacrylates containing BICs	33	167
1.3.1. Synthesis of C3D1	36	167
1.3.2. Synthesis of BICMA1	38	168
1.3.3. Synthesis of BICMA2	38	
1.4. Melt viscosity	41	
1.5. Deblocking reactions in solution	43	169
1.5.1. Deblocking reaction of BICMA1	43	
1.5.2. Deblocking reaction of VIC2	45	
1.6. (Thermo)mechanical properties	46	169
1.6.1. DMTA	48	
1.6.2. Tensile tests	52	
1.6.3. Impact resistance	54	
1.7. Influence of the matrix on deblocking reactions	54	171
1.7.1. Matrix polarity	55	
1.7.2. Soft matrix	55	171
1.7.2.1. DMTA	56	
1.7.2.2. Tensile tests	57	

Die approbierte gedruckte Originalversion dieser Dissertation ist an der TU Wien Bibliothek verfügbar.
The approved original version of this doctoral thesis is available in print at TU Wien Bibliothek.
TU WIEN Bibliothek Your knowledge hub

2. ABS-like Photopolymers 60 172
2.1. State of the art 60
2.2. Preliminary experiments 62 172
2.2.1. Syntheses of itaconimides and citraconimides 63 172
2.2.1.1. Synthesis of PrII and PrCI 63 172
2.2.1.2. Synthesis of BnII and BnCI 66 173
2.2.2. Volatility 66
2.2.3. Comparison of itaconimide, citraconimide and maleimide 68
2.2.4. Comparison of fumaric and maleic acid esters and maleimide 72
2.2.5. Maleimide-styrene-methacrylate terpolymerisation 75
2.3. Model maleimide-styrene-system (MISt1) 81 175
2.3.1. Volatility 82
2.3.2. Storage stability 83
2.3.3. Viscosity 84
2.3.4. Potential self-initiation 84
2.3.5. Photo-DSC 86
2.3.6. RT-NIR-photorheology 89
2.3.7. Swellability 94 175
2.3.8. (Thermo)mechanical properties 96 175
2.3.8.1. DMTA 96
2.3.8.2. Tensile tests 98
2.3.8.3. Impact resistance 99
2.3.9. AFM 100
2.3.10. Thermal stability 102
2.4. Further mechanistic studies on MI-St-copolymerisation 104 176
2.4.1. Influence of polybutadienes on MISt1 104
2.4.2. Cross-linking behaviour in MI-St-copolymers 111 176
2.4.2.1. Synthesis of FESt 112 176
2.4.2.2. Volatility of FESt 113
2.4.2.3. Swellability 114 177

Die approbierte gedruckte Originalversion dieser Dissertation ist an der TU Wien Bibliothek verfügbar.
The approved original version of this doctoral thesis is available in print at TU Wien Bibliothek.
TU Bibliothek Your knowledge hub WIEN

2.5. Variation of MI substituent 116 178
2.5.1. Monomer syntheses 118 178
2.5.1.1. Synthesis of MMI 118 178
2.5.1.2. Synthesis of EHMI 120 179
2.5.2. Volatility 121
2.5.3. Storage stability 122
2.5.4. UV-Vis absorbance 123
2.5.5. Melt viscosity 125
2.5.6. Photo-DSC 129
2.5.7. RT-NIR-photorheology 134
2.5.8. Swellability 139 180
2.5.9. (Thermo)mechanical properties 141 180
2.5.9.1. DMTA 142
2.5.9.2. Tensile tests 144
2.5.9.3. Impact resistance 146
2.5.10. AFM 148
2.5.11. Thermal stability 150
2.5.12. Conclusion 152
2.6. Potential applications 153 181
2.6.1. Reactive diluent (RD) 153 181
2.6.1.1. Melt viscosity 154
2.6.1.2. DMTA 155
2.6.1.3. Tensile tests 156
2.6.1.4. Impact resistance 158
2.6.2. Frontal polymerisation (FP) 159 181
2.6.3. 3D printing 162 181

Materials, Devices and Analyses 182
Summary 192
Abbreviations 200
Bibliography 201
Appendix 217
Curriculum Vitae 221

Die approbierte gedruckte Originalversion dieser Dissertation ist an der TU Wien Bibliothek verfügbar.
The approved original version of this doctoral thesis is available in print at TU Wien Bibliothek.
TU WIEN Bibliothek Your knowledge hub

Introduction

Photopolymerisation is the process to solidify liquid resins by electromagnetic irradiation and plays an essential role in research as well as in industry [1]. Radical photopolymerisation gives a lot of advantages such as high curing speed, bulk polymerisation without the need of solvents, high energy efficiency and low production costs. Furthermore, materials with good (thermo)mechanical properties are obtained (*e.g.* heat deflection temperature, hardness, stiffness).

The most important fields of applications of radically cured photopolymers are

- Inks
- Paints [2]
- Coatings [3-4]
- Adhesives
- Medical applications: Bone replacement [5-6], dental fillings [7], hydrogels [8-9],...
- Frontal polymerisation (FP) [10-11]
- Additive manufacturing technologies (AMT) [5, 12-14]

Formulations for photopolymerisation typically contain several components – optimised for each application:

- Photoinitiator (PI)
- Monomers
- Additives

Die approbierte gedruckte Originalversion dieser Dissertation ist an der TU Wien Bibliothek verfügbar.
The approved original version of this doctoral thesis is available in print at TU Wien Bibliothek.
TU Bibliothek Your knowledge hub WIEN

Introduction

The most crucial resin component is the PI, which enables the photopolymerisation process. It absorbs the applied UV/Vis light and generates the reactive species (*i.e.* radicals), which consequently initiate the radical polymerisation reaction.

The first step is the absorption of one photon by the PI, which excites the molecule from the ground state (S_0) to the excited singlet state (S_1). A transition to a excited triplet state (T_1) can be achieved by intersystem crossing (Figure 1). Since triplet states exhibit longer lifetimes compared to singlet states (by a factor of ~ 1000), energy transfers or (side) reactions (*e.g.* quenching by O_2) are much more likely. Fluorescence, phosphorescence and radiation free relaxation are competing processes.

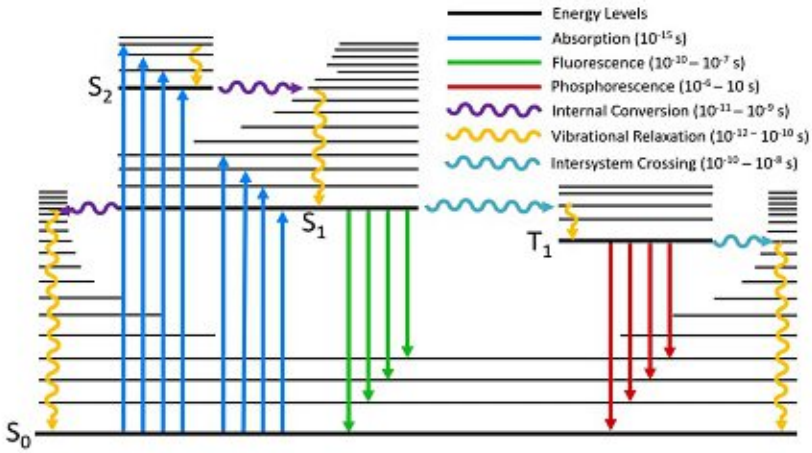

Figure 1: Jablonski scheme [15]

The absorption of a photon occurs either directly by the PI or by an indirect photosensitising process. Due to their different mechanisms for generating radicals, two different kinds of PIs are known [16-18]:

- Type I (Figure 2): Homolytic bond cleavage (monomolecular reaction), see Figure 3
- Type II (Figure 4): H-abstraction or electron-proton-transfer (bimolecular reaction), see Figure 5

Die approbierte gedruckte Originalversion dieser Dissertation ist an der TU Wien Bibliothek verfügbar.
The approved original version of this doctoral thesis is available in print at TU Wien Bibliothek.
TU Bibliothek Your knowledge hub WIEN

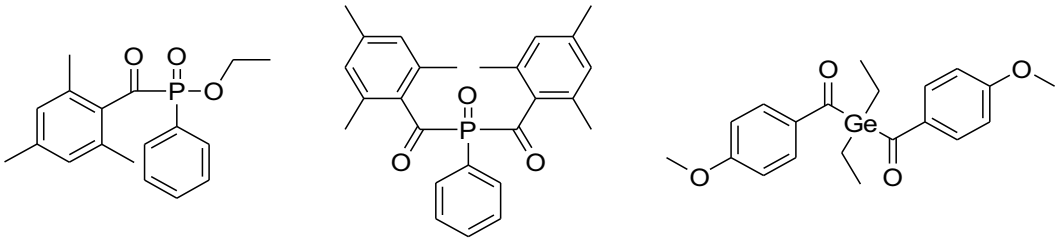

Figure 2: Prominent examples of type I photoinitiators

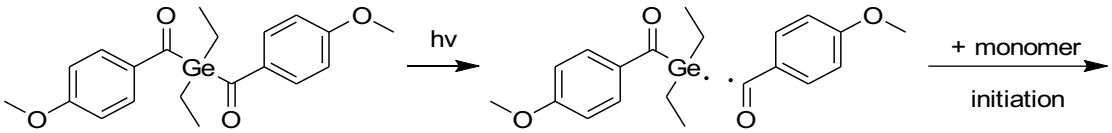

Figure 3: Decomposition of Ivocerin via α-cleavage

Figure 3 shows Ivocerin as a prominent type I PI and the homolytic scission of the bond in α-position to a carbonyl group, which generates radicals to initiate the polymerisation reaction.

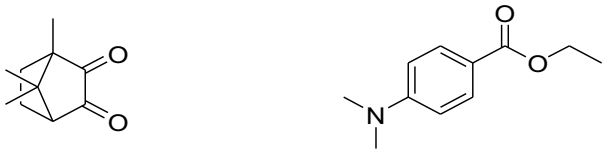

camphorquinone (CQ)

ethyl-4-(dimethylamino)benzoate (EDB)

Figure 4: Prominent example of a type II photoinitiator system

Die approbierte gedruckte Originalversion dieser Dissertation ist an der TU Wien Bibliothek verfügbar.
The approved original version of this doctoral thesis is available in print at TU Wien Bibliothek.

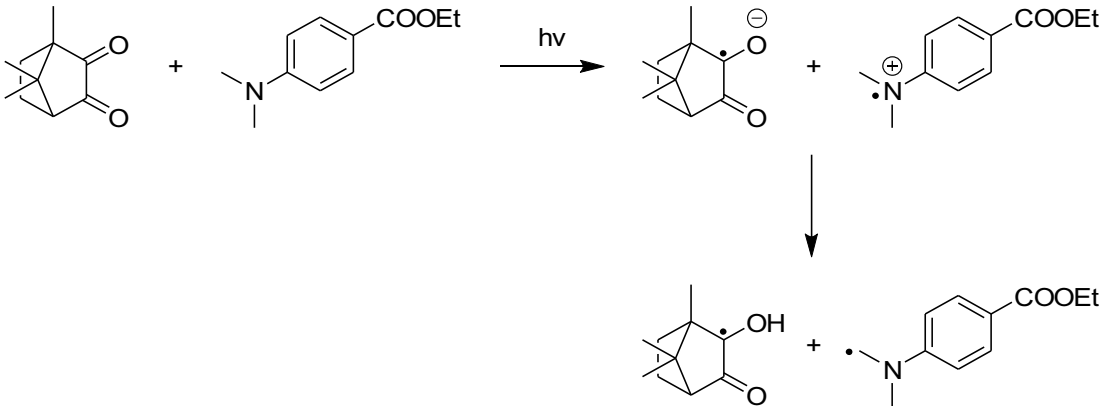

Figure 5: Initiation mechanism of the CQ/EDB-photoinitiator systems via an electron-proton-transfer

As can be seen in Figure 5 a coinitiator (*e.g.* tertiary amine) transfers a electron to the chromophore, which was excited by the absorption of a photon. Afterwards, the reactive coinitiator radical is formed in a second reaction by proton transfer.

Additionally, radically polymerisable monomers are needed, which form networks upon polymerisation and thus significantly determine the final material properties. A general base monomer structure as well as examples for monofunctional and multifunctional monomers are given in Figure 6.

Die approbierte gedruckte Originalversion dieser Dissertation ist an der TU Wien Bibliothek verfügbar.
The approved original version of this doctoral thesis is available in print at TU Wien Bibliothek.

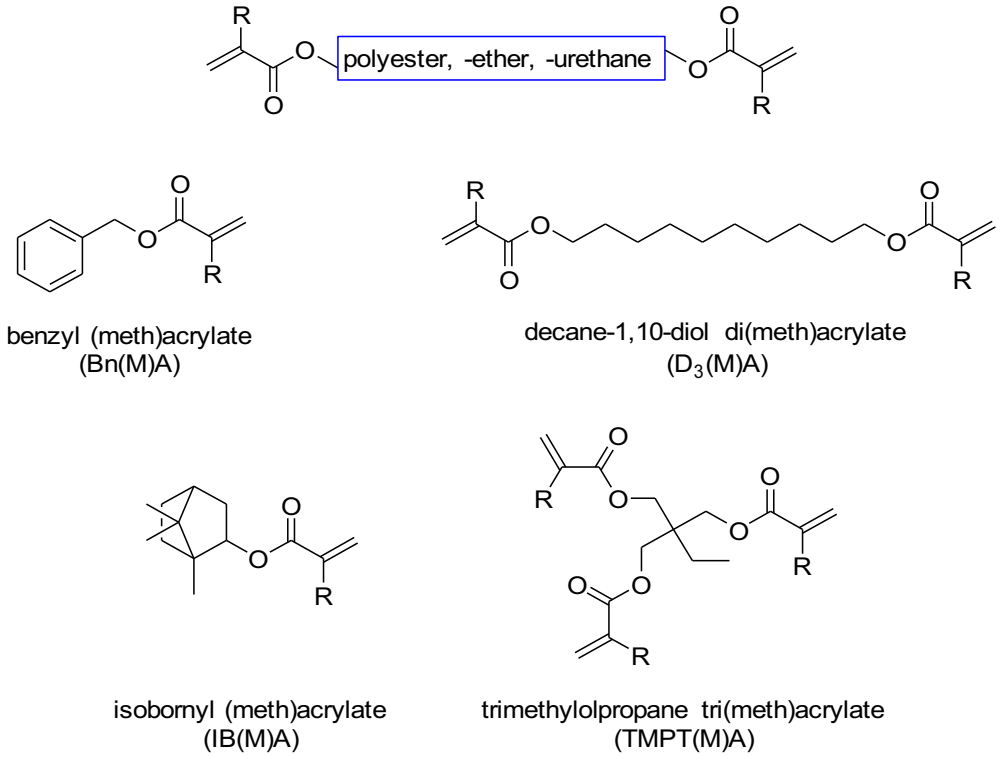

Figure 6: Structure of common monomers and examples for reactive diluents: acrylates (R = H) and methacrylates (R = Me)

Chemical parameters like toxicity [19], curing speed, O_2 inhibition [20-21] and conversion are significantly determined by the monomer. Furthermore, thermo(mechanical) properties such as glass transition temperature (T_g), scratch resistance, moduli and toughness [22] can be tuned by the proper choice of monomers as well.

The chemical structure of the monomers determines many monomer and polymer properties, since the reactive functional groups are usually linked by polyester, polyether or polyurethane moieties (compare Figure 6). Hence, these spacers have a huge influence on material characteristics (*e.g.* soft polyether or rigid polyurea groups). Additionally, the number of functionalities also changes network architecture from linear chains (monofunctional monomers) to networks with different amounts of cross-linking density (functionality ≥ 2) (see Figure 7).

Die approbierte gedruckte Originalversion dieser Dissertation ist an der TU Wien Bibliothek verfügbar.
The approved original version of this doctoral thesis is available in print at TU Wien Bibliothek.
TU Bibliothek Your knowledge hub WIEN

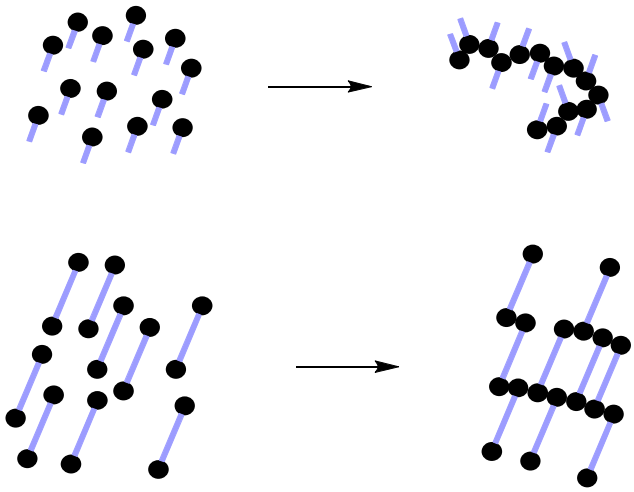

Figure 7: Linear polymer vs. polymer network

Unfortunately, many of these base monomers exhibit high viscosities due to the high molecular weight of the polyester, polyether or polyurethane spacers and thus can only be processed after addition of reactive diluents (RDs). The low viscous RDs decrease the resin viscosity to an acceptable level. Furthermore, they copolymerise with the monomers and therefore are covalently bonded in the polymer matrix. Thus, toxicological issues are reduced, because lower amounts of uncured substances are able to migrate to the surface and hence cannot interact with the environment. One of the industrially most prominent RD isobornyl (meth)acrylate (IB(M)A) is already mentioned in Figure 6 above.

Finally, photopolymer resins also contain a variety of different additives depending on the targeted application area such as RDs, cross-linking agents, stabilisers, inhibitors, fillers, dyes, flame retardants or surface active substances.

One of the main issues of photopolymerisation is the typically high brittleness of the obtained polymers, which dramatically lowers material performance and thus hinders wide industrial utilisation. This low impact resistance can be neglected in thin films (*e.g.* coatings), but is especially crucial for bulk applications like dental fillings or 3D printing [22].

Die approbierte gedruckte Originalversion dieser Dissertation ist an der TU Wien Bibliothek verfügbar.
The approved original version of this doctoral thesis is available in print at TU Wien Bibliothek.
TU WIEN Bibliothek Your knowledge hub

There are several different approaches known in literature to tackle the poor toughness:

- Additives
- Reduction of internal stress via network modification
- Polymer architecture
- Matrix morphology

Additives are already used in polymer science to change and further improve material properties since the beginning of the 20th century. The polymers are compounded with various fibres, inorganic particles or rubber to yield polymer composites. Moreover, application of inorganic nanoparticles, core-shell-particles, liquid rubbers or block copolymers further increases toughening efficiency due to their smaller size resulting in an increased surface to volume ratio compared to macroscopic and microscopic fillers. Hence, interaction of the polymer matrix with the additive – and therefore the impact on material properties – is much more enhanced, which enables usage in significant lower loadings [23-27].

A high contribution to brittleness of radically cured photopolymers originates from the internal stress in the material. The stress is formed, because of an uncontrolled free radical chain growth mechanism, which yields a highly cross-linked and inhomogeneous polymer network structure. This leads to high shrinkage stress during the polymerisation reaction (Figure 8) and consequently to high internal stress as well [28-29].

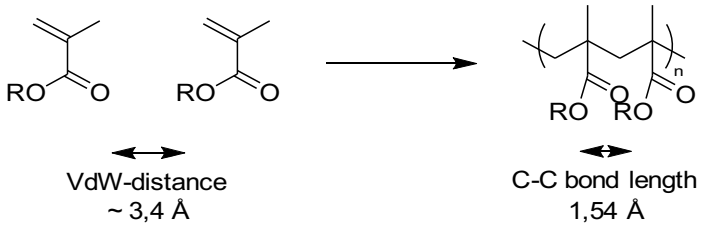

Figure 8: Origin of shrinkage during a polymerisation reaction

Die approbierte gedruckte Originalversion dieser Dissertation ist an der TU Wien Bibliothek verfügbar.
The approved original version of this doctoral thesis is available in print at TU Wien Bibliothek.
TU Bibliothek Your knowledge hub WIEN

A popular approach to tackle this problem is to regulate the free radical polymerisation reaction with chain transfer agents (CTAs) [30]. In literature several different CTAs are known like thiols (thiol-ene chemistry [31-33]) or silanes (silane-ene chemistry [34-36]) (Figure 9). Furthermore, addition fragmentation chain transfer (AFCT) reagents (Figure 9) are established CTAs as well [37-41].

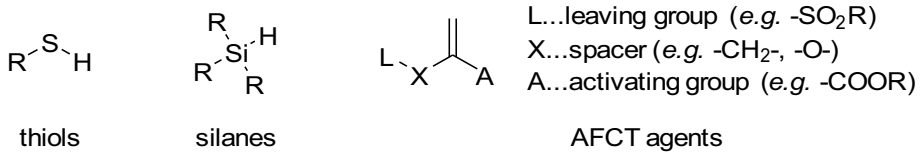

Figure 9: Structures of different CTAs

The mentioned CTAs all apply – with different chemical mechanisms – a regulated radical (step growth like) polymerisation reaction and thereby shift the gelation of the resin to higher conversions. Thus, the system has more time to flow and so stress relaxation is still possible (compare Figure 10) [42].

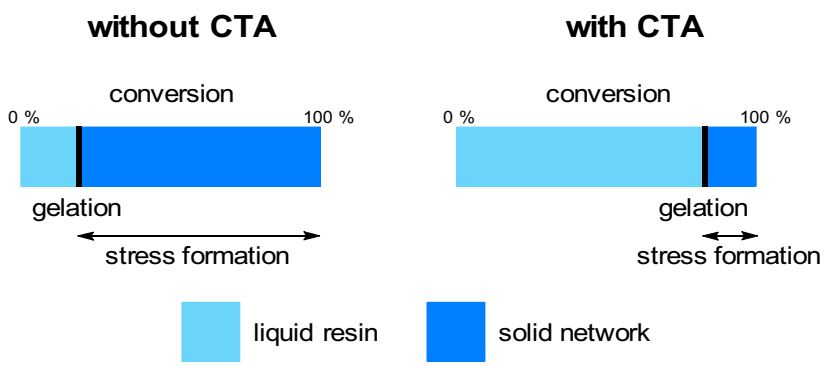

Figure 10: Correlation of gelation and shrinkage stress

The second effect of a regulated polymerisation reaction is that in the end a better distribution of the cross-linking points and thus a more homogeneous network structure is obtained (Figure 11) [43-44]. Therefore, network modification improves very efficiently toughness and thermomechanical properties of the material [45].

Die approbierte gedruckte Originalversion dieser Dissertation ist an der TU Wien Bibliothek verfügbar.
The approved original version of this doctoral thesis is available in print at TU Wien Bibliothek.
TU Bibliothek Your knowledge hub WIEN

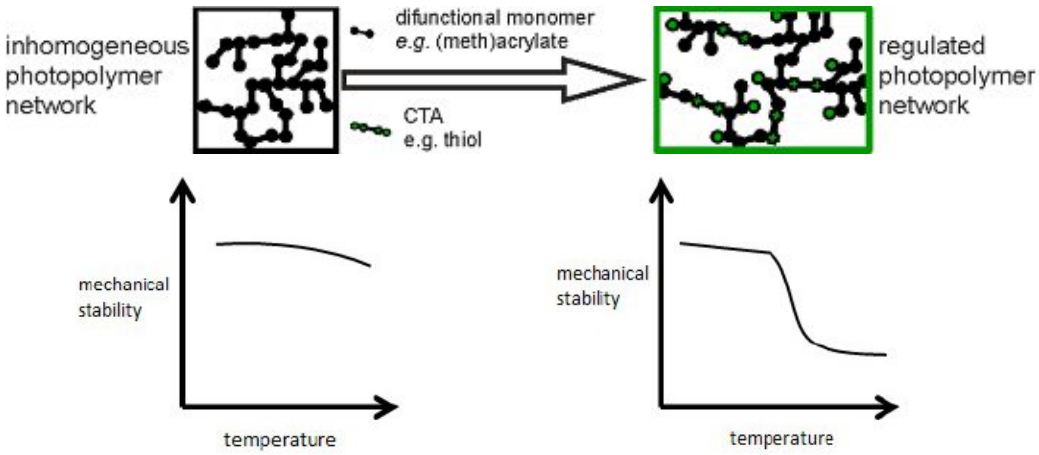

Figure 11: Inhomogeneous vs. homogeneous network structures and their thermal behaviour [46]

Another point, which is very crucial for material properties, is the polymer architecture. Three groups of polymers are (more or less precisely) classified according to their molecular structure and amount of covalent cross-links, which is determined by the monomer functionality: thermosets, elastomers and thermoplastics (see Figure 12) [47].

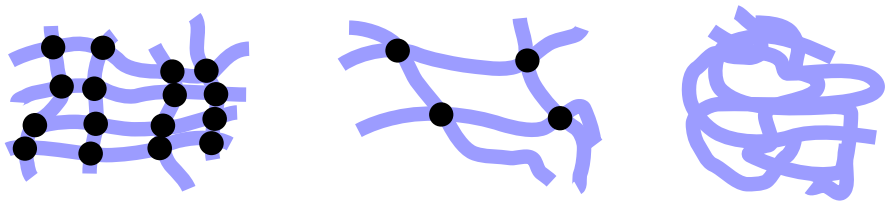

Figure 12: Structure of thermosets (left), elastomers (middle) and thermoplastics (right)

The architecture apparently determines a lot of macroscopic material properties. Tensile properties are shown exemplarily in Figure 13.

Die approbierte gedruckte Originalversion dieser Dissertation ist an der TU Wien Bibliothek verfügbar.
The approved original version of this doctoral thesis is available in print at TU Wien Bibliothek.
TU Bibliothek Your knowledge hub WIEN

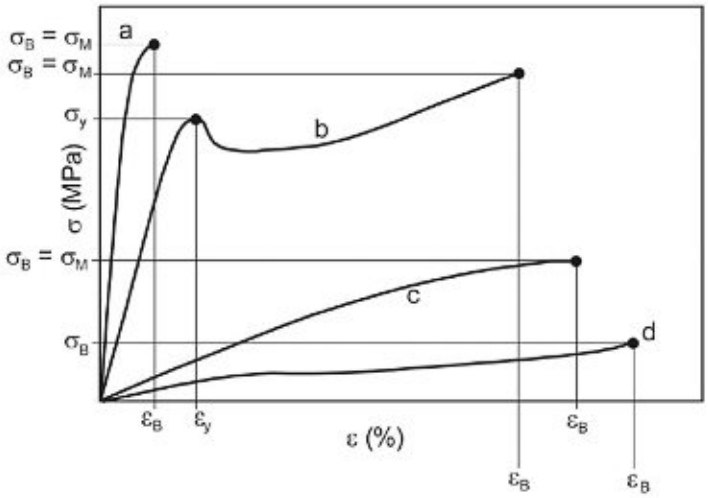

Figure 13: Exemplarily stress-strain curves of a brittle (a), tough (b+c) and an elastomeric material [22]

As Figure 13 shows, highly cross-linked thermosets give high strength but also are very brittle. In contrast, linear thermoplastics exhibit no covalent cross-links and only reversible intermolecular interactions and thus are also meltable. Finally, also the flexibility and elasticity of elastomers can be explained because of their high molecular weight and low degree of cross-linking, which yields very loose polymer networks. Therefore, the amount of cross-linking and network density in the polymer architecture significantly defines (thermo)mechanical material properties. Furthermore, thereby their behaviour under stress and possible energy dissipation in the polymer is determined as well [47-48].

One possible approach to enhance thermomechanical properties in photopolymers is to add additional inter- or intramolecular forces to the polymer network [22]. For that purpose, different non-covalent bonds are suitable, because these can be reversibly cleaved and reformed (supramolecular structures):

- Van der Waals interactions
- Hydrogen bonds
- Ionic bonds (ionomers) [49]

Die approbierte gedruckte Originalversion dieser Dissertation ist an der TU Wien Bibliothek verfügbar.
The approved original version of this doctoral thesis is available in print at TU Wien Bibliothek.
TU Bibliothek Your knowledge hub WIEN

Especially polymers, which are capable of forming intermolecular H-bonds, exhibit good material properties, *e.g.* polyurethanes (PUs), polyamides (PAs), etc., because they give additional reversible cross-links between different polymer chains (see Figure 14).

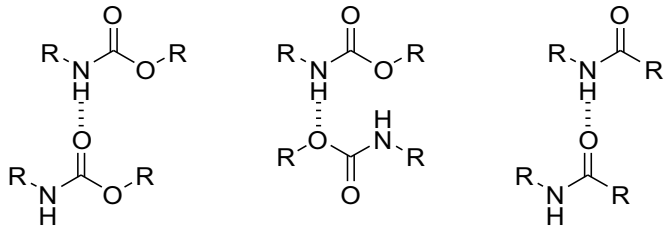

Figure 14: H-bonds in polyurethanes (left, middle) and polyamides (right)

However, the H-bonds also interact in the liquid monomer, which results in highly viscous monomers, which are more difficult to process [50]. Therefore, a need is given for (reactive) diluents, which decrease the viscosity of the final resin. But these diluents – usually small molecules – exhibit also some problematic properties like volatility or if final conversion is not sufficiently high, residual monomers are capable of migrating out of the polymer [51].

The morphology of the polymer matrix exhibits an important contribution to (thermo)mechanical material properties as well. Firstly, occurrence and ratio of hard and rigid crystalline domains and soft and ductile amorphous phases obviously determine a lot of thermomechanical characteristics of the polymer (compare *e.g.* polyurethane chemistry). In addition, phase separation of not miscible phases is a second effect, which can be very beneficial especially for high toughness [48]. A heterogeneous morphology dramatically raises the needed force for material failure due to an increased breaking route (compare Figure 15) [52].

Die approbierte gedruckte Originalversion dieser Dissertation ist an der TU Wien Bibliothek verfügbar.
The approved original version of this doctoral thesis is available in print at TU Wien Bibliothek.
TU Bibliothek Your knowledge hub WIEN

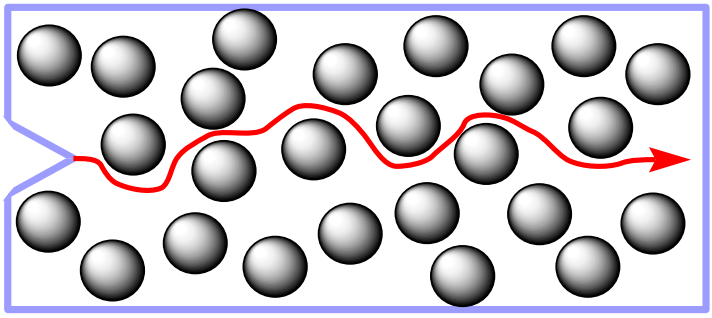

Figure 15: Increased crack path in heterogeneous materials

Moreover, crack propagation can be hindered by an efficient energy dissipation like induction of micro cracks, crack bridging, crazing or void formation with straining (see Figure 16). Hence, also tougher materials are obtained, when crack formation and/or crack growth are restrained [53].

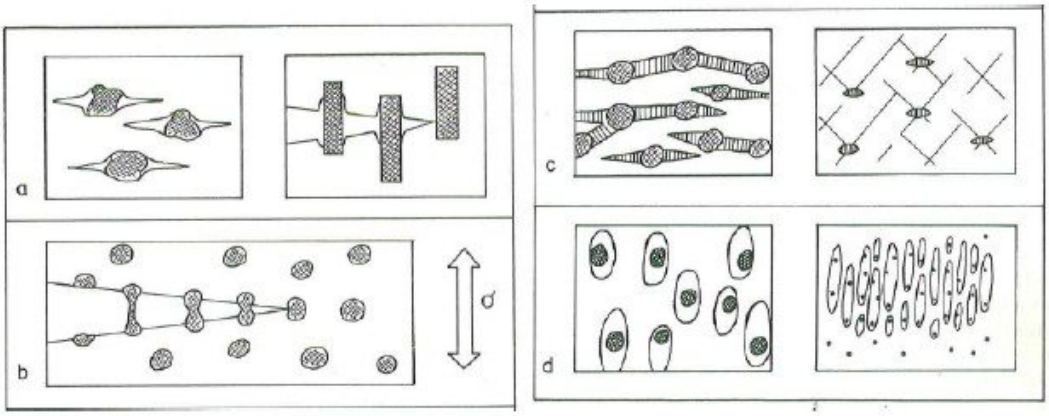

Figure 16: Toughening mechanisms in heterogeneous polymers [54]

Most prominent for this kind of toughening mechanism is the thermoplastic acrylonitrile butadiene styrene terpolymer (ABS), which is also a benchmark for tough engineering plastics. In ABS the inhomogeneous morphology consisting of soft polybutadiene domains in a hard and rigid poly(styrene-*co*-acrylonitrile) matrix yields a very tough material while maintaining other important properties like stiffness or heat resistance. Unfortunately, at the same time the phase separation also leads to one of the main drawbacks of ABS: it is opaque and thus not suitable for many applications [47].

Die approbierte gedruckte Originalversion dieser Dissertation ist an der TU Wien Bibliothek verfügbar.
The approved original version of this doctoral thesis is available in print at TU Wien Bibliothek.
TU Bibliothek Your knowledge hub WIEN

Objective

Photopolymers are an important class of materials, due to their advantageous characteristics like fast curing, no need of solvents, spatial control over the curing reaction and low production costs compared to conventional polymerisation techniques. Unfortunately, lack of toughness limits many applications in industry.

The aim of this thesis is to investigate two different concepts for toughening of photopolymers and evaluate their potential for industrial utilisation.

The first approach is to change polymer architecture from a highly cross-linked thermoset to a linear thermoplastic material via degradation of thermally labile motives (blocked isocyanates) and thus combining benefits from both polymer classes. Therefore, model compounds have to be tested regarding their potential for cleavage under suitable conditions. The selected moieties should be incorporated into new photopolymerisable monomers. Finally, the polymers have to be characterised before and after degradation of the polymer network according to their (thermo)mechanical properties with DMTA, tensile tests and impact resistance.

In addition, a second approach will be studied to mimic ABS, which is a very popular engineering plastic, because it exhibits favourable material properties due to a heterogeneous morphology. Since ABS cannot be photopolymerised, a concept will be developed to circumvent this issue (copolymerisation of maleimide and styrene derivatives). The most promising monomers should be studied in detail. Hence, photopolymerisable formulations (volatility, storage stability, melt viscosity), curing reactions (conversion, molecular weight, photo-DSC, RT-NIR-photorheology) as well as final material properties (DMTA, tensile and Dynstat impact tests) will be characterised. Finally, different potential applications should be evaluated for this new promising photopolymer class.

Die approbierte gedruckte Originalversion dieser Dissertation ist an der TU Wien Bibliothek verfügbar.
The approved original version of this doctoral thesis is available in print at TU Wien Bibliothek.
TU Bibliothek Your knowledge hub WIEN

General Part

1. UV-Curable (Meth)Acrylates containing Blocked Isocyanates

Monomers with H-bond forming moieties like urethanes and urea derivatives possess on the one hand beneficial features in the final material such as a large range of feasible mechanical properties but on the other hand some drawbacks (*e.g.* high viscosity). Hence, the idea is to generate the H-bond forming structures in a second reaction step in bulk after photopolymerisation of the resin.

A promising approach for reaching this goal are blocked isocyanates (BICs, Figure 17). The blocking agent (BIH) could easily be cleaved off thermally in a second annealing step at moderate temperatures before degradation of the polymer would occur. So the liberated isocyanates (ICs) are able to react with nucleophiles (chain extenders; *e.g.* alcohols or amines) to form a thermally stable urethane/urea moiety [55-58].

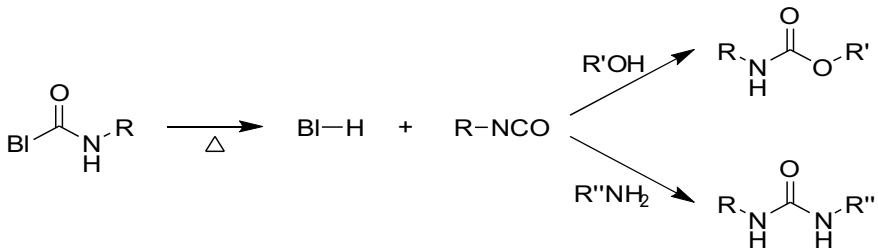

Figure 17: Deblocking of BICs and reaction with chain extenders

In addition, presence of chain extenders decreases viscosity of the photopolymerisable resin and thus further enhances processability.

Die approbierte gedruckte Originalversion dieser Dissertation ist an der TU Wien Bibliothek verfügbar.
The approved original version of this doctoral thesis is available in print at TU Wien Bibliothek.
TU Bibliothek Your knowledge hub WIEN

Furthermore, Figure 18 nicely depicts the second feature of this introduced approach: the polymer architecture will be changed due to deblocking of the BICs. Firstly, a highly cross-linked poly(meth)acrylate is synthesised by photopolymerisation, which is very beneficial for fast curing and mechanical stability of the green part. Afterwards, thermal treatment degrades the cross-linking and yields a polyurethane or polyurea. This second linear polymer further enhances material properties due to its thermoplastic character (in addition to the already mentioned formation of H-bonds).

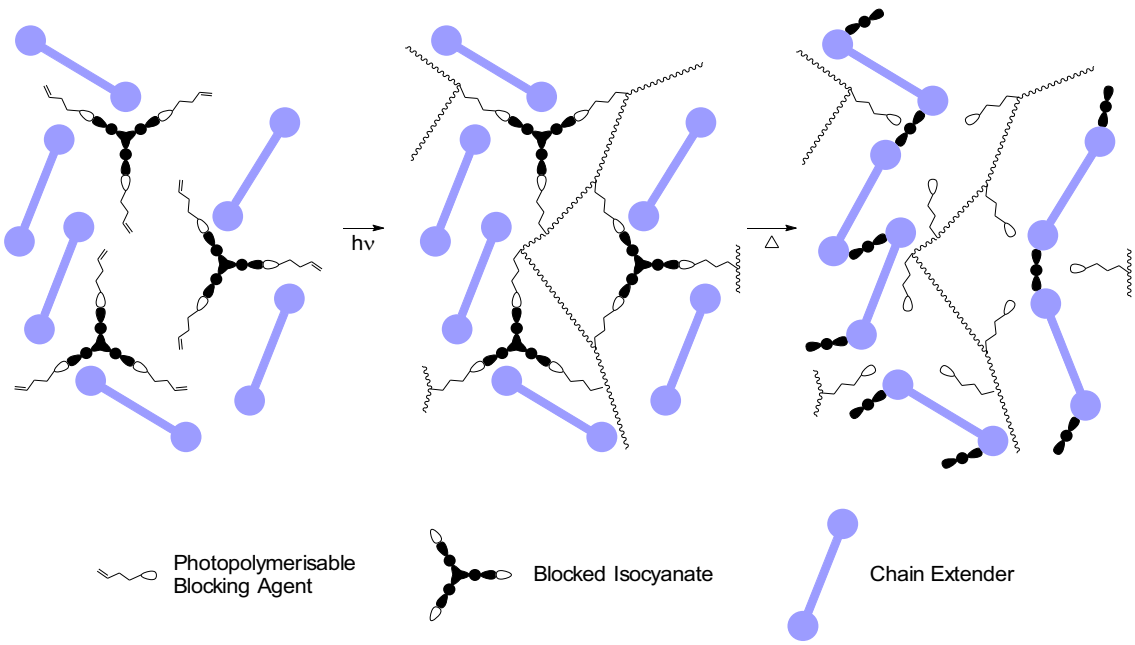

Figure 18: Concept of thermally cleavable BICs in photopolymer network formation

Thus, materials with good thermomechanical properties could be photopolymerised in the presented way, while circumventing the rather high viscosity of such resins. Hence, this approach offers a huge variety of new potential application fields, which could not be considered before for photopolymers.

Die approbierte gedruckte Originalversion dieser Dissertation ist an der TU Wien Bibliothek verfügbar.
The approved original version of this doctoral thesis is available in print at TU Wien Bibliothek.
TU WIEN Bibliothek Your knowledge hub

1.1. State of the art

Polyurethanes (PUs) can be tuned very easily to a broad range of applications by varying molecular compositions, cross-linking and intermolecular forces. So they seized a huge field of applications in a lot of different industries due to their versatility (thermosets, thermoplastics or elastomers) [59-63].

Unfortunately, classical PUs cannot be prepared directly by photopolymerisation. Thus, low molecular weight (P)Us are capped with (meth)acrylates, which enable radical photopolymerisation. Methacrylates are less reactive than acrylates, but also less toxic, which is crucial for all kinds of medical applications. These urethane (meth)acrylates (U(M)As) offer a lot of different properties, which can be tuned for optimised properties for each utilisation [64-71]. A prominent example of an industrially applied low molecular weight UMA is UDMA (Figure 19), which is used in dental applications [7].

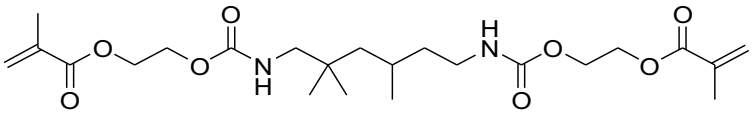

Figure 19: Structure of UDMA

PU properties can be altered easily within a broad range with changes of the phase separation and morphology in the polymer. This variability is caused by hard and soft blocks, which can be tuned in their molecular structure, molecular weight, length and linkages [72]. The soft segments usually consist of polyether or polyester based macrodiols (see Figure 20) [73]. The soft block provides flexibility, low T_g, low moduli and strength and high elongation to the material [74-75].

Die approbierte gedruckte Originalversion dieser Dissertation ist an der TU Wien Bibliothek verfügbar.
The approved original version of this doctoral thesis is available in print at TU Wien Bibliothek.
TU Bibliothek Your knowledge hub WIEN

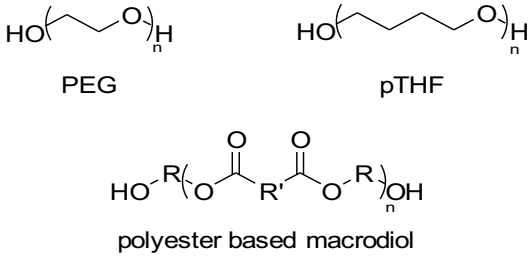

Figure 20: Structure of different macrodiols

In contrast, the hard domains are formed by rigid urethane moieties, which are obtained from the reaction of the alcohol with an isocyanate. The hard segments are crucial for high rigidity, T_g and tensile strength. In addition, they give efficient phase separation via partial crystallisation caused by their H-bonds (compare Figure 15), which is necessary to yield good (thermo)mechanical properties [76-78]. Some commercially popular difunctional ICs are depicted in Figure 21.

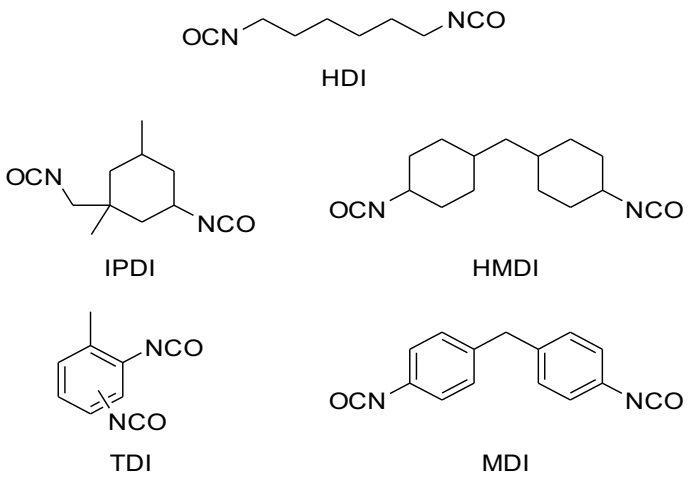

Figure 21: Structure of different difunctional ICs

The urethane structures can introduce crystallinity into the polymer with their H-bonds. So microphase phase separation is achieved (see Figure 22). This microphase morphology contributes a significant factor for the high toughness of PUs [79-81].

Die approbierte gedruckte Originalversion dieser Dissertation ist an der TU Wien Bibliothek verfügbar.
The approved original version of this doctoral thesis is available in print at TU Wien Bibliothek.
TU Bibliothek Your knowledge hub WIEN

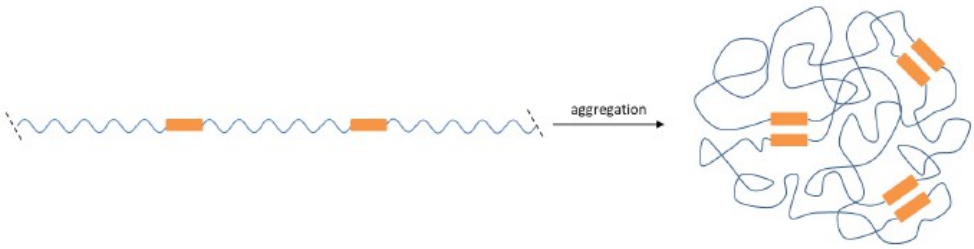

Figure 22: Phase separation of soft (--) and hard segments (--) in PUs [82]

PUs are usually prepared by either a one-shot-approach (mixing all starting products, followed by immediate curing) or via prepolymers. Therefore, macrodiols are capped with an excess of difunctional IC and are cured afterwards with the addition of low molecular weight multifunctional alcohols or amines. Additionally, water can be added for foaming [62].

Thus, two-component (2K) formulations are always needed for PUs to prevent reaction of IC and alcohol/amine prior to application. Therefore, 1K (one-component) PU formulations – and waterborne resins as well [83] – were developed to overcome this drawback [84-85]. The important improvement was achieved by using blocking agents, which block the IC motive and thus prevent a curing reaction (Figure 23) [55, 86].

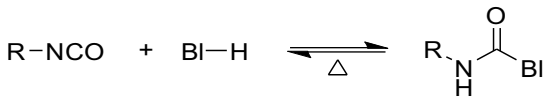

Figure 23: Blocking and deblocking of BICs

Some commercially applied BIHs are shown in Figure 24.

Die approbierte gedruckte Originalversion dieser Dissertation ist an der TU Wien Bibliothek verfügbar.
The approved original version of this doctoral thesis is available in print at TU Wien Bibliothek.
TU Bibliothek Your knowledge hub WIEN

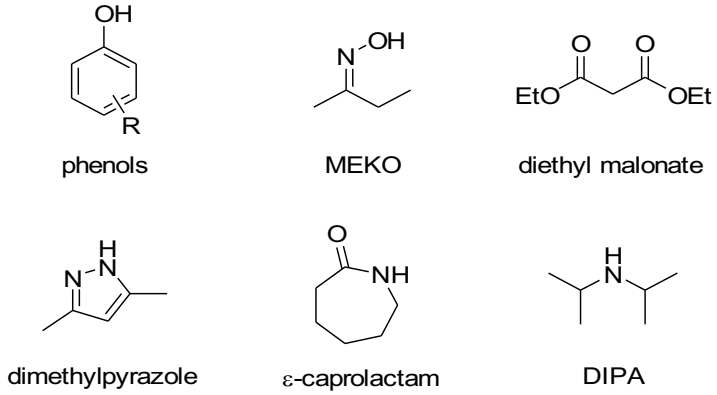

Figure 24: Different BIHs

The curing reaction is initiated by heating, which cleaves the BICs. Thus, the IC is liberated and reacts with the alcohol/amine forming a polymer. The needed temperature for the deblocking reaction (T_{db}) is influenced by several factors [87-90]:

- IC: Aliphatic ICs are more stable than aromatic ICs
- BIH: Aliphatic BIHs are more stable than aromatic BIHs
- Solvent polarity: The more polar the lower T_{db}
- Presence of a catalyst
- Presence of a nucleophile (*e.g.* alcohol or amine)

In addition, it is known in literature, that steric hindrance on the BIH also lowers T_{db} (compare *e.g.* amine DIPA in Figure 24) [91-94].

So when teaming U(M)As with BICs the best of two worlds can be combined to benefit from each strengths like photopolymerisation and low viscosity. This approach was applied by Velankar *et al.* [95-96] and later Carbon3D [97-100] as well. They blocked various (macro)diisocyanates based on polyethers or polyesters with sterically hindered amines (*i.e.* *t*-butyl amine groups) and further functionalised the ends with methacrylates. After photopolymerisation a second annealing step was performed at elevated temperatures (> 100 °C), the BIC was

Die approbierte gedruckte Originalversion dieser Dissertation ist an der TU Wien Bibliothek verfügbar.
The approved original version of this doctoral thesis is available in print at TU Wien Bibliothek.
TU Bibliothek Your knowledge hub WIEN

cleaved and the regenerated IC reacted with an incorporated chain extender. Different low as well as high molecular weight difunctional alcohols or amines were used as nucleophiles (see Figure 25).

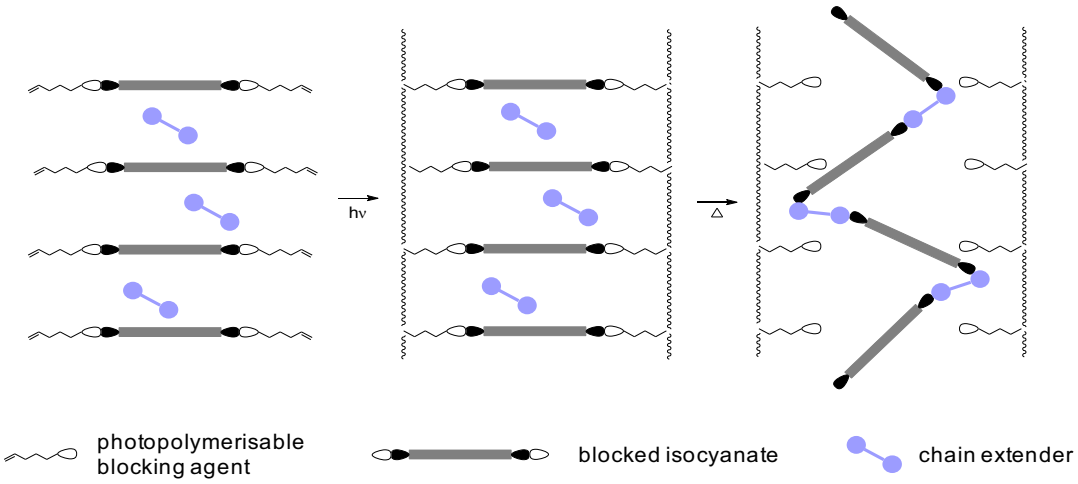

Figure 25: Concept of thermally cleavable BICs in photopolymer network formation

They both succeeded in synthesising a PU/polyurea within a linear as well as a cross-linked photopolymer network, but struggled with low conversion in the second annealing reaction and obtained only very soft elastomer like materials with low modulus. Nevertheless, the prepared polymers exhibited increased T_gs and Young's moduli compared to traditional linear or cross-linked PUs/polyureas with similar structure, which were synthesised as reference compounds. However, tensile properties of classical 2K PUs could not be achieved in almost all tested samples. This drawback can be attributed to less efficient phase separation of the PU/polyurea, which is hindered in the presence of the photopolymer.

Die approbierte gedruckte Originalversion dieser Dissertation ist an der TU Wien Bibliothek verfügbar.
The approved original version of this doctoral thesis is available in print at TU Wien Bibliothek.
TU Bibliothek Your knowledge hub WIEN

1.2. Model compounds

In the beginning some model BICs have to be examined for a proof-of-concept. Therefore, dimers and trimers of an IC were chosen, because they offer higher IC concentrations in the final formulations compared to conventional BICs (see chapter 1.1). This approach gives the opportunity to increase the chain extender content, which makes resin development easier and a lot more flexible regarding final material properties, since a huge variety of (multifunctional) alcohols and amines is commercially available.

In addition, also an IC blocked with a C-H acidic blocking agent should be tested for comparison, because they are popular blocking agents in industry [85] and were already applied in our working group for other applications [101].

1.2.1. Model isocyanurates

Although isocyanate dimers (uretdiones, Figure 26) show promising deblocking temperatures in bulk of 150 – 200 °C, this IC regeneration is dramatically lowered in solution in the presence of residual catalysts or nucleophiles to 10 – 80 °C. Hence, uretdiones already react slowly at room temperature with nucleophiles (*e.g.* alcohols or amines) [56]. Therefore, their application is limited to powder coatings [102]. In contrast, isocyanate trimers (isocyanurates, Figure 26) exhibit less reactivity due to decreased ring stress compared to uretdiones (6-membered ring vs. 4-membered ring).

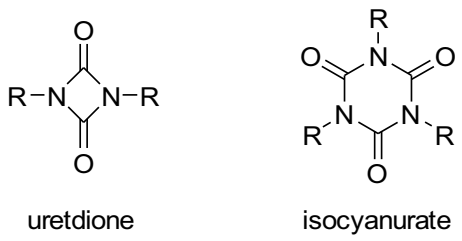

Figure 26: Structures of uretdiones and isocyanurates

Die approbierte gedruckte Originalversion dieser Dissertation ist an der TU Wien Bibliothek verfügbar.
The approved original version of this doctoral thesis is available in print at TU Wien Bibliothek.

No detailed deblocking temperatures are available in literature for isocyanurates in solution, but they are generally known to be more thermally stable than uretdiones. Hence, isocyanurates were investigated to ensure storage stability of final resins over long time periods.

Thus, commercial BIC samples were chosen, which are explicitly claimed as isocyanate trimer or isocyanurates and also do not contain additives or solvents. In addition, aliphatic BICs were selected as aromatic ICs can give undesired discolouration (see Figure 27).

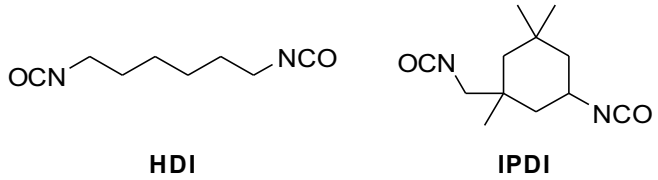

Figure 27: Common commercially available ICs

So isocyanurates based on **HDI** (easier analysis because of simple structure, Desmodur N3300) and **IPDI** (good (thermo)mechanical properties like a high T_g due to a rigid ring structure, Vestanat T1890/100) were used for preliminary studies. All chosen samples were commercial resins (in technical grade) without an exact molecular structure given. Furthermore, Vestanat T1890/100 exhibits a broad melting range of 95-115 °C. Hence, obtained samples probably do not only contain trimerised ICs of **HDI** or **IPDI**. Thus, some further characterisation is necessary.

1.2.1.1. Determination of structure and functionality

The “real structures” (degree of oligomerisation, Figure 28) – or at least the ratio of free to blocked isocyanates – has to be known for modification (*e.g.* syntheses) of the 2 received commercial isocyanurates, Desmodur N3300 and Vestanat T1890/100.

Die approbierte gedruckte Originalversion dieser Dissertation ist an der TU Wien Bibliothek verfügbar.
The approved original version of this doctoral thesis is available in print at TU Wien Bibliothek.
TU Bibliothek Your knowledge hub WIEN

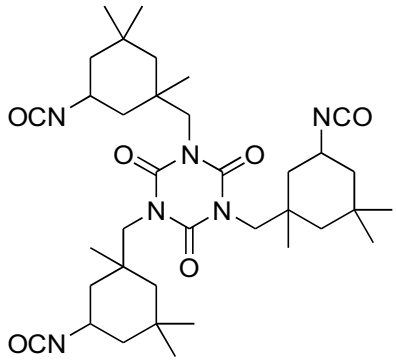

Figure 28: Idealized structure of the isocyanurate based on **IPDI**

a) ATR-IR spectroscopy

First of all, ATR-IR spectra were recorded to prove the isocyanurate structure, because the carbonyl groups show a very characteristic signal at 1690 cm^{-1} [103]. In contrast, uretdiones, which can also be formed during trimerisation of ICs, exhibit the corresponding carbonyl peak at 1760 cm^{-1} [103].

ATR-IR spectra of **HDI** and **IPDI** and their corresponding isocyanurates are shown in Figure 29 and 30.

Die approbierte gedruckte Originalversion dieser Dissertation ist an der TU Wien Bibliothek verfügbar.
The approved original version of this doctoral thesis is available in print at TU Wien Bibliothek.
TU Bibliothek Your knowledge hub WIEN

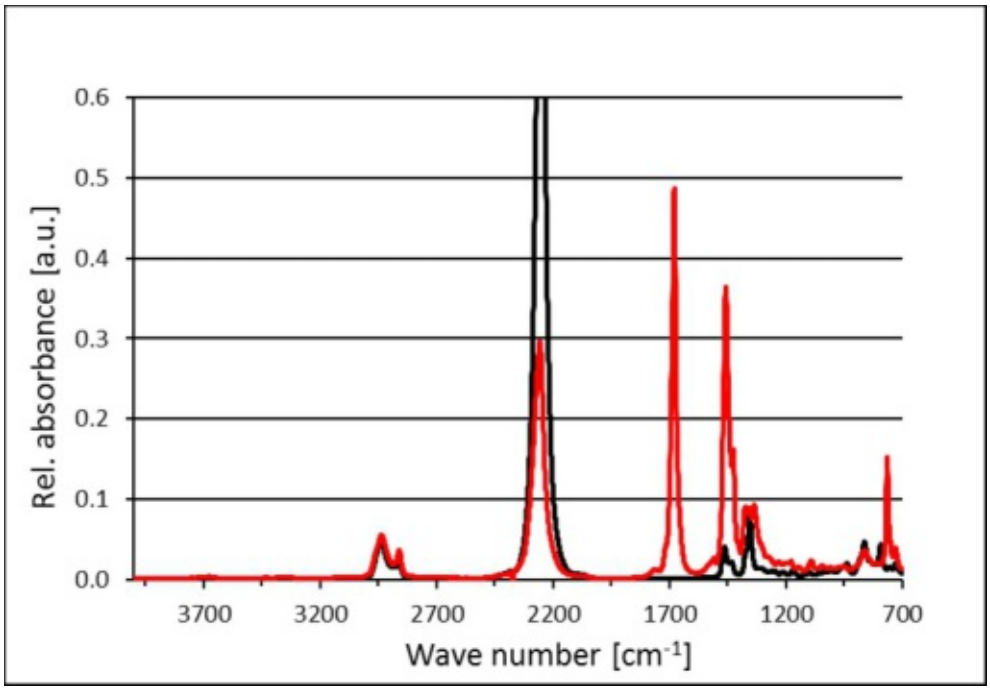

Figure 29: ATR-IR spectra of **HDI** (—) and Desmodur N3300 (—)

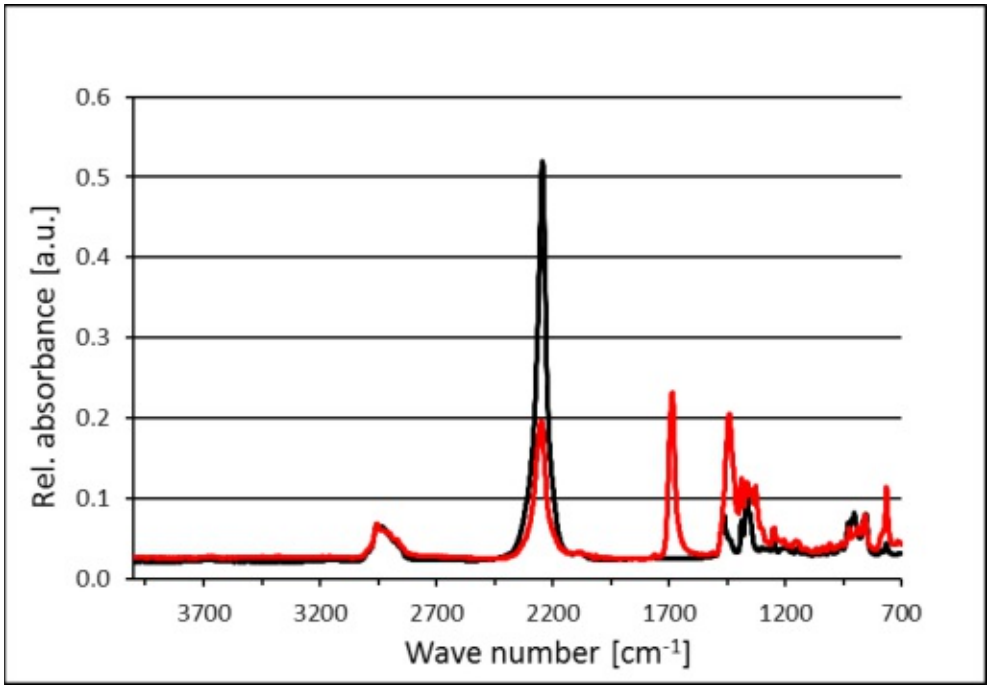

Figure 30: ATR-IR spectra of **IPDI** (—) and Vestanat T1890/100 (—)

Die approbierte gedruckte Originalversion dieser Dissertation ist an der TU Wien Bibliothek verfügbar.
The approved original version of this doctoral thesis is available in print at TU Wien Bibliothek.
TU Bibliothek Your knowledge hub WIEN

As can be seen in the figures above, both commercial isocyanurates contain almost no uretdiones (~ 1760 cm^{-1}). Additionally, the characteristic peaks of a free IC group (~ 2250 cm^{-1}) and the carbonyl moiety of an isocyanurate structure (~ 1690 cm^{-1}) can be identified.

b) NMR spectroscopy

Since IR spectroscopy gives no information regarding the degree of oligomerisation, NMR spectra of the samples were measured as well.
Desmodur N3300 was chosen for the tests, since analysis is a lot easier, because of the simple structure of the corresponding IC **HDI**. NMR spectroscopy analysis of **IPDI**-based Vestanat T1890/100 is not possible, due to a lot of overlapping peaks in the ^{1}H as well as in the ^{13}C-NMR spectra. This can be attributed to a lot of potential isomers: already 8 different stereoisomers can be found, if only the primary IC group would react and also if only the trimer and no higher oligomers would be formed.

So the isocyanurate Desmodur N3300 was mixed with an excess of Bu_2NH (compare DIN EN ISO 11909 and ASTM D 2572), dissolved in C_6D_6 and ^{1}H- and APT NMR spectra were recorded. The APT spectrum shows:

- Isocyanurate peak (~ 150 ppm) still present
- Complete disappearance of IC peak (~ 120 ppm)
- New peak at ~ 160 ppm (characteristic shift for urea derivatives) from the reaction product of isocyanate with Bu_2NH

Thus, a quantitative reaction of free isocyanate with amine can be assumed.
But as there is still the possibility of amine reacting with the isocyanurate motive, the ^{1}H-NMR spectrum was investigated more closely. So the CH_2 signals next to the free IC group, the isocyanurate moiety and the formed urea derivative are monitored at ~ 3.00 – 3.80 ppm: the ratio of isocyanurate to urea, which is generated by the reaction of free IC with Bu_2NH, remains unchanged compared to the ratio of isocyanurate to free IC in a reference spectrum without added

Die approbierte gedruckte Originalversion dieser Dissertation ist an der TU Wien Bibliothek verfügbar.
The approved original version of this doctoral thesis is available in print at TU Wien Bibliothek.
TU Bibliothek Your knowledge hub WIEN

amine. Thus, no ring opening of the isocyanurate with the used amine occurs. Furthermore, a ratio of 0.88 of free to blocked IC groups can be calculated. Therefore, a degree of oligomerisation of ~ 11.4 is determined, which is higher than the idealised 3 units of the IC trimer (compare also isocyanurate motive in Figure 28).

These estimated results from the NMR spectra are in good accordance to the data given in the product data sheets of the used commercial isocyanurates Desmodur N3300 and Vestanat T1890/100, where the IC content (in w%) is estimated by titration (DIN EN ISO 11909 or ASTM D 2572). The amount of free IC can be converted from the claimed IC concentration in w% with equation 1.

$$IC = \frac{\Delta V * c}{m} * 4.2 \qquad (1)$$

ΔV... Difference in consumption of diluted HCl between blank sample and sample [mL]
c... Real concentration of diluted HCl [mol/l]
m... Weighted sample [g]

So the following ratios of free IC groups per IC monomer of the 2 commercial isocyanurates could be calculated from the corresponding data sheets of the manufacturer: Table 1.

Table 1: Structure of used commercial isocyanurates

Isocyanurate	IC content [w%]	Free IC/monomer [-]	Average degree of oligomerisation [-]
Desmodur N3300	21.8	0.873	11.5
Vestanat T1890/100	17.3	0.916	10.9

Hence, both commercial isocyanurate samples contain higher oligomers than trimers.

Die approbierte gedruckte Originalversion dieser Dissertation ist an der TU Wien Bibliothek verfügbar.
The approved original version of this doctoral thesis is available in print at TU Wien Bibliothek.
TU Bibliothek Your knowledge hub WIEN

1.2.1.2. Determination of deblocking temperature

The second necessary preliminary study was performed to measure deblocking temperature (T_{db}) of the used BIC moieties (isocyanurates). Although the deblocking reaction depends on several factors like matrix polarity and presence of (residues of) catalysts or nucleophiles some basic tests were performed to get an idea of the temperature range of deblocking reactions.

a) STA

Since deblocking reactions of isocyanurates should come along with a change in heat flow, DSC measurements were performed. The tests were conducted on an STA to additionally get information on thermal stability. Furthermore, BIC mixtures with an excess of a high boiling amine were investigated as well to study the influence of a nucleophile on the deblocking reaction.

The BIC monomers were dissolved in 10 eq. of amine 1-laurylamine. IR spectra proved complete conversion of free IC with amine. Afterwards, STA measurements were executed under N_2 atmosphere from 25 to 300 °C with a heating rate of 10 K/min.

The obtained results for the **HDI** and **IPDI**-based BICs are shown in Figures 31 and 32.

Die approbierte gedruckte Originalversion dieser Dissertation ist an der TU Wien Bibliothek verfügbar.
The approved original version of this doctoral thesis is available in print at TU Wien Bibliothek.
TU Bibliothek Your knowledge hub WIEN

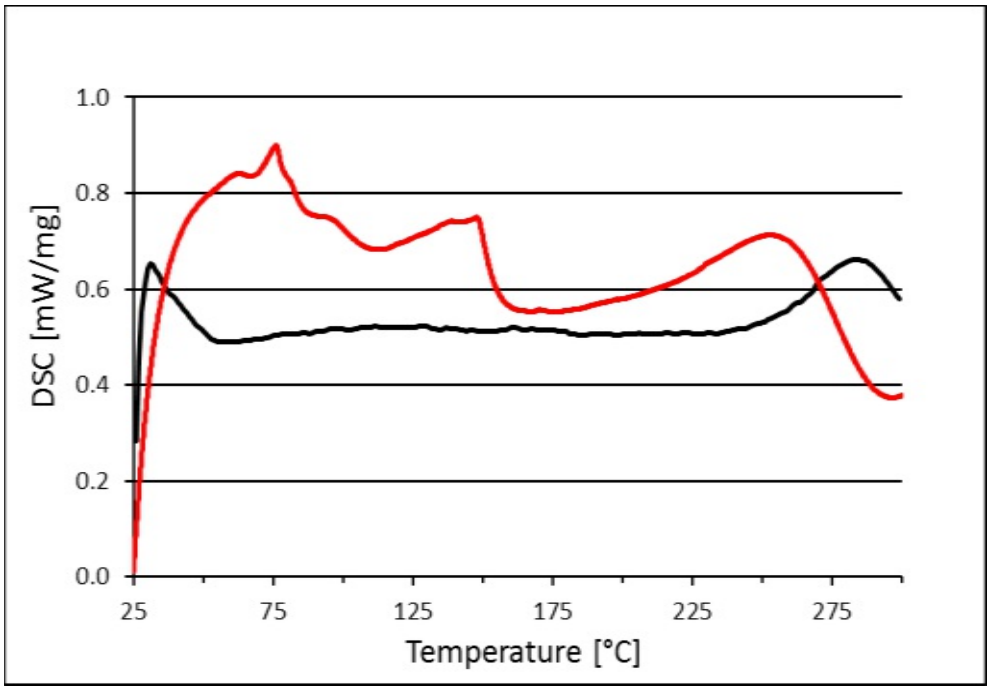

Figure 31: DSC curve of Desmodur N3300 without (—) and with amine (—)

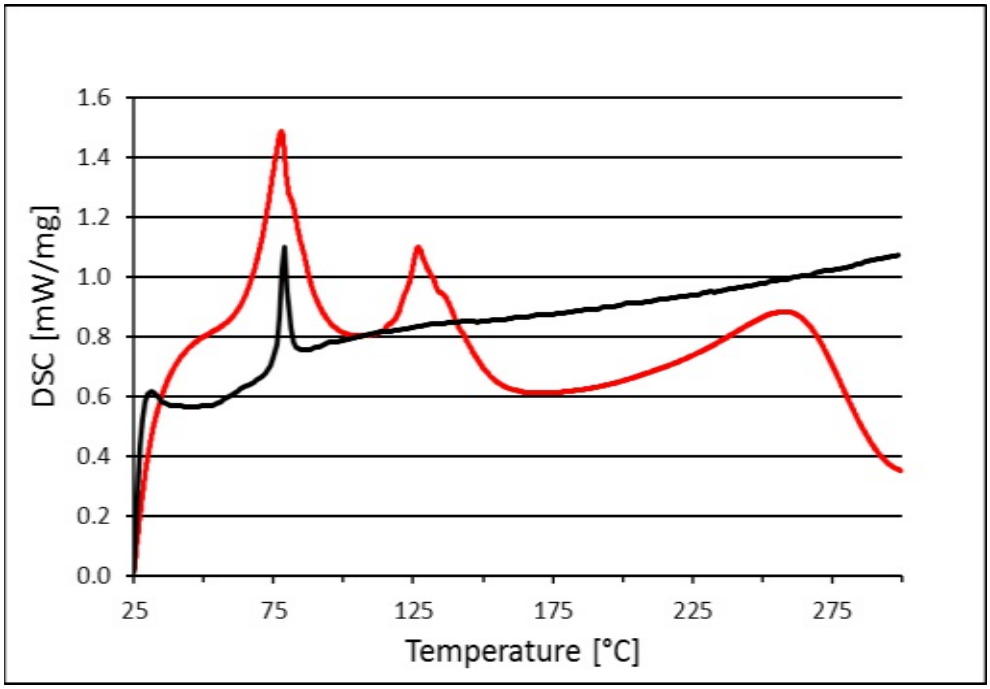

Figure 32: DSC curve of Vestanat T1890/100 without (—) and with amine (—)

Die approbierte gedruckte Originalversion dieser Dissertation ist an der TU Wien Bibliothek verfügbar.
The approved original version of this doctoral thesis is available in print at TU Wien Bibliothek.
TU Bibliothek Your knowledge hub WIEN

As can be seen in Figures 31 and 32, without addition of amine **HDI**-based isocyanurate Desmodur N3300 shows decomposition starting from ~ 250 °C and **IPDI**-based Vestanat T1890/100 exhibits only the endothermic signal originating from melting. Thus, DSC signals do not indicate any thermally induced reactions in the blank isocyanurate samples.

In contrast, an excess of amine provokes a endothermic reaction at ~ 150 °C for the **HDI**-based isocyanurate. The same peak is observed for the **IPDI**-based BIC at ~ 130 °C. Unfortunately, it is not possible to assign the observed endothermic signals to a particular reaction. Furthermore, melting of the reaction product of amine and **HDI** isocyanurate can be seen at ~ 75 °C.

Finally, the broad endothermic peaks in both figures at ~ 250 °C originate from evaporation of 1-laurylamine.

b) ATR-IR spectroscopy

As STA measurements yielded strong hints but did not prove the occurrence of deblocking reactions and T_{db}, ATR-IR spectra were recorded of thermally treated samples. Again mixtures of BICs and an amine were examined as well to investigate its influence on the deblocking reaction.

The experiments were performed under Ar atmosphere to prevent reactions with moisture. Samples of the 2 different commercial isocyanurates Desmodur N3300 and Vestanat T1890/100 were heated in an Al-block at 160 °C for 1 h without and with an excess (10 eq.) of 1-laurylamine. After cooling to room temperature ATR-IR spectra were recorded and compared to an untreated reference spectrum of the corresponding BIC or BIC amine mixture.

However, no change in IR spectra could be observed in samples without added amine. Thus, the experiments were repeated at 200 °C for 5 h. Again no reaction can be identified (see exemplarily Figure 33 for the **HDI**-based Desmodur

Die approbierte gedruckte Originalversion dieser Dissertation ist an der TU Wien Bibliothek verfügbar.
The approved original version of this doctoral thesis is available in print at TU Wien Bibliothek.
TU WIEN Bibliothek Your knowledge hub

N3300). So either no deblocking reaction occurs up to 200 °C in pure monomer, or the “reblocking” reaction is already completed in some minutes when cooling a sample to room temperature.

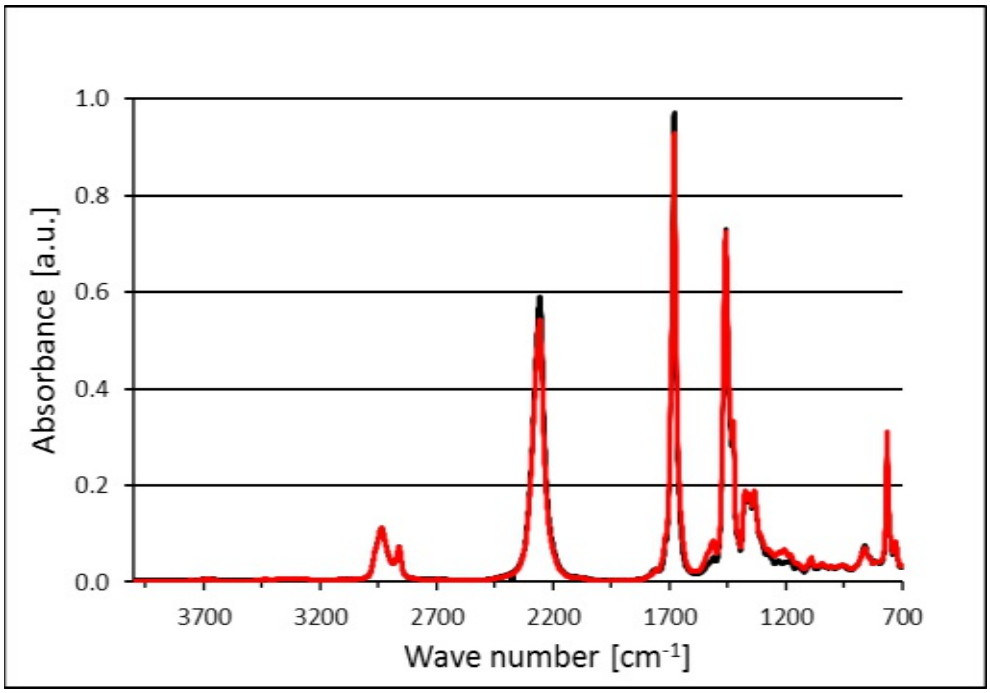

Figure 33: ATR-IR spectra of Desmodur N3300 before (—) and after (—) heating to 200 °C

A deblocking reaction of the 2 commercial isocyanurates based on **HDI** and **IPDI** was achieved at 160 °C with the addition of amine laurylamine. IR spectra presented in Figures 34 and 35 verify the successful deblocking of both tested BICs during thermal treatment due to an increase of the urea N-H signals, which are formed by the reaction of liberated IC with amine.

Die approbierte gedruckte Originalversion dieser Dissertation ist an der TU Wien Bibliothek verfügbar.
The approved original version of this doctoral thesis is available in print at TU Wien Bibliothek.
TU Bibliothek Your knowledge hub WIEN

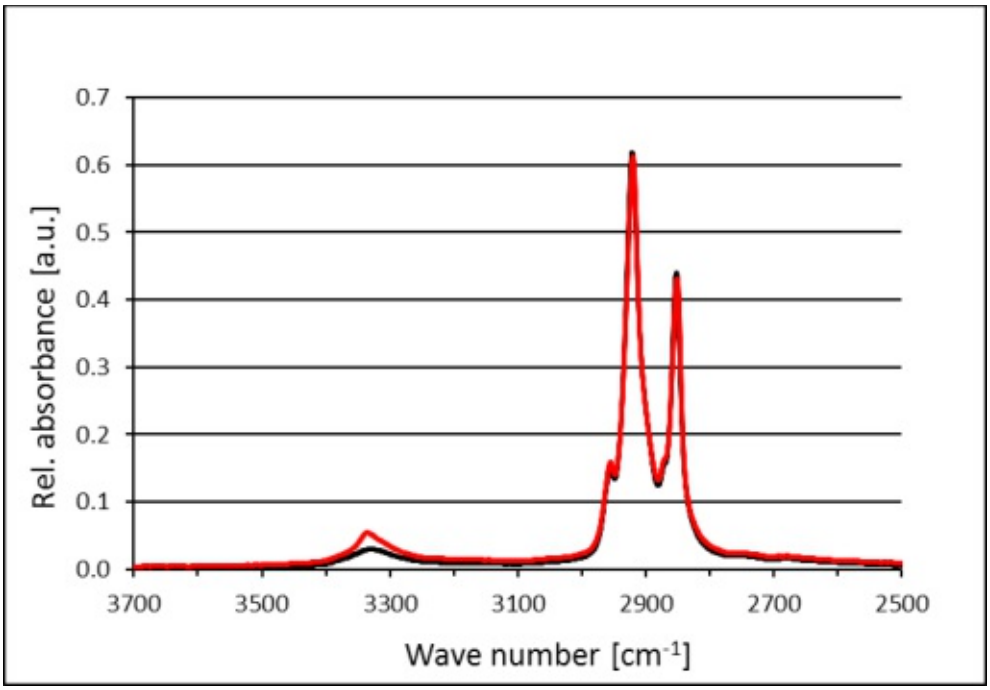

Figure 34: IR spectra of Desmodur N3300 with amine before (—) and after (—) heating

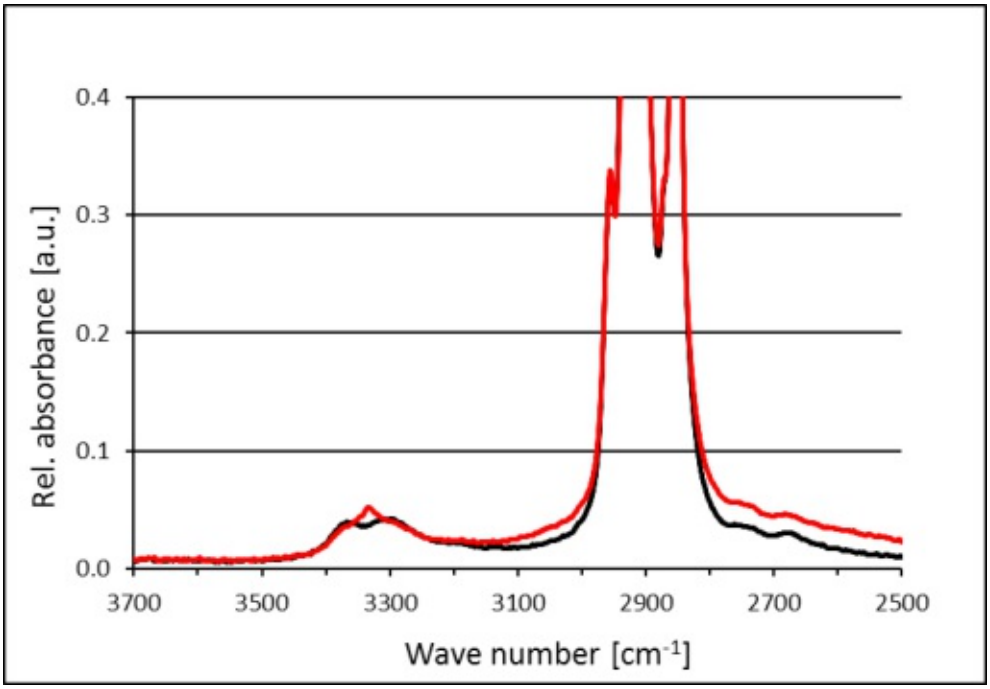

Figure 35: IR spectra of Vestanat T1890/100 with amine before (—) and after (—) heating

Die approbierte gedruckte Originalversion dieser Dissertation ist an der TU Wien Bibliothek verfügbar.
The approved original version of this doctoral thesis is available in print at TU Wien Bibliothek.
TU Bibliothek Your knowledge hub WIEN

With these promising preliminary experiments on the deblocking reactions of isocyanurates, they will be used to synthesise UV-curable multifunctional methacrylates, which contain BIC structures as spacer, for the preparation of photopolymers.

1.2.2. Model C-H acidic blocking agent

VIC2 (Figure 36, kindly provided by Ivoclar Vivadent) was used as representative for an IC blocked by a C-H acidic blocking agent.

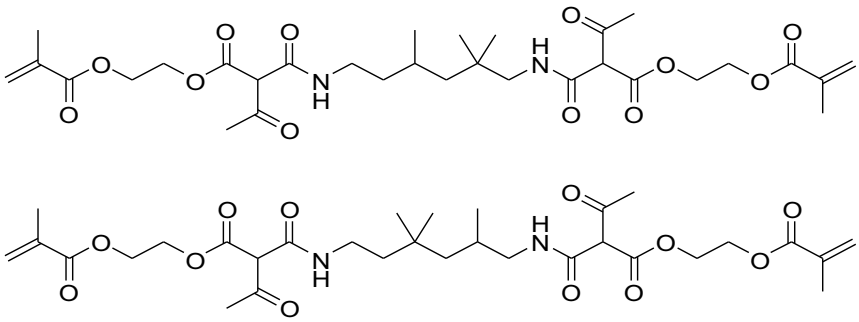

Figure 36: Isomeric structure of **VIC2**

Since this monomer was already established in a PhD thesis of our group [46, 101], no further preliminary studies are necessary on **VIC2**. In the thesis it was used as photopolymerisable cross-linker containing thermally labile BIC groups for debonding-on-demand in dental adhesives. A T_{db} of 154 °C of 4 mol% **VIC2** in a poly-*N*-acryloylmorpholine (**pNAM**, Figure 37) matrix could be determined.

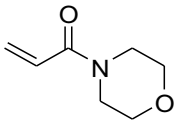

Figure 37: Structure of **NAM**

Die approbierte gedruckte Originalversion dieser Dissertation ist an der TU Wien Bibliothek verfügbar.
The approved original version of this doctoral thesis is available in print at TU Wien Bibliothek.
TU Bibliothek Your knowledge hub WIEN

1.3. Syntheses of methacrylates containing BICs

After first results in preliminary studies on model structures a UV-curable difunctional methacrylate containing a isocyanurate as spacer should be synthesised to prove the usability of this BIC concept. Furthermore, it should be compared to a difunctional methacrylate with an incorporated C-H acidic BIC and also to a similar monomer from Carbon3D [97-99].

At the beginning one model compound patented from Carbon3D [98], which shows good mechanical properties in a photopolymer network, was selected for comparison: **C3D1** (Figure 38).

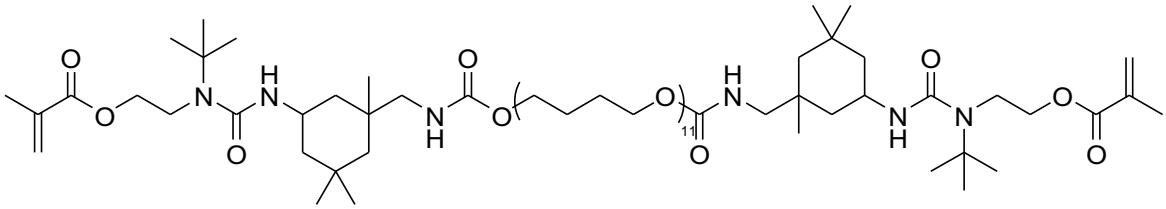

Figure 38: Structure of **C3D1**

The molecular structure of the monomer **C3D1** was transferred to our concept with isocyanurates as BICs to get a comparable polymer structure. Therefore, also isophorone diisocyanate (**IPDI**) as IC component and 2-(*t*-butyl amino)ethyl methacrylate (**tBAEMA**) as double bond functionality for photopolymerisation were chosen: **BICMA1** (Figure 39). However, the pTHF structure in the centre of **C3D1**, which gives the system flexibility, is applied in our concept as the chain extender, where bis(3-aminopropyl) terminated pTHF of same molecular weight (**DA**, Figure 39) is used.

Die approbierte gedruckte Originalversion dieser Dissertation ist an der TU Wien Bibliothek verfügbar.
The approved original version of this doctoral thesis is available in print at TU Wien Bibliothek.
TU Bibliothek Your knowledge hub WIEN

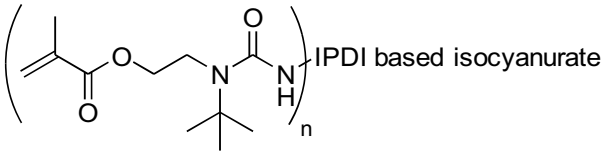

BICMA1

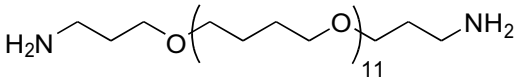

DA

Figure 39: Structures of **BICMA1** and **DA**

A huge benefit of the isocyanurate concept is, that due to the isocyanurate moiety 2 times more ICs can be released (compare Figure 40) and thus more low viscous chain extender can be added to reduce the viscosity of the final formulation.

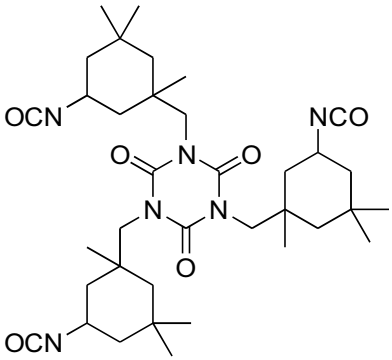

Figure 40: Idealized structure of the isocyanurate based on **IPDI**

In addition higher double bond functionality of the monomer leads to faster gelation of the resin and thus less time is needed for polymerisation of a green part. Furthermore, higher green part shape stability can be reached due to a higher degree of cross-linking.

Die approbierte gedruckte Originalversion dieser Dissertation ist an der TU Wien Bibliothek verfügbar.
The approved original version of this doctoral thesis is available in print at TU Wien Bibliothek.
TU Bibliothek Your knowledge hub WIEN

Additionally, a molecule should be synthesised with a structure according to monomer **C3D1** and isocyanurate based **BICMA1** with the C-H acidic blocking agent of **VIC2** (**BICMA2**, Figure 41). Hence, better comparability of the different systems will be achieved.

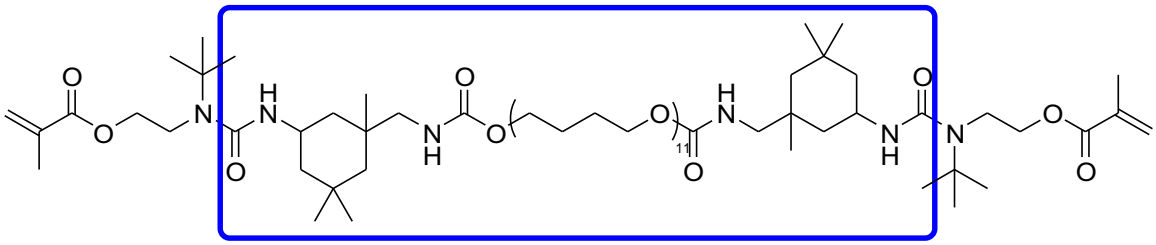

C3D1

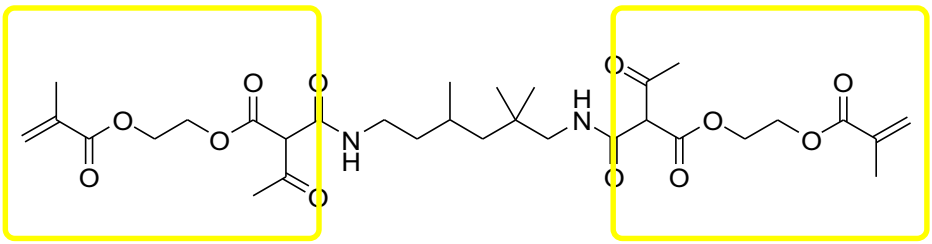

VIC2

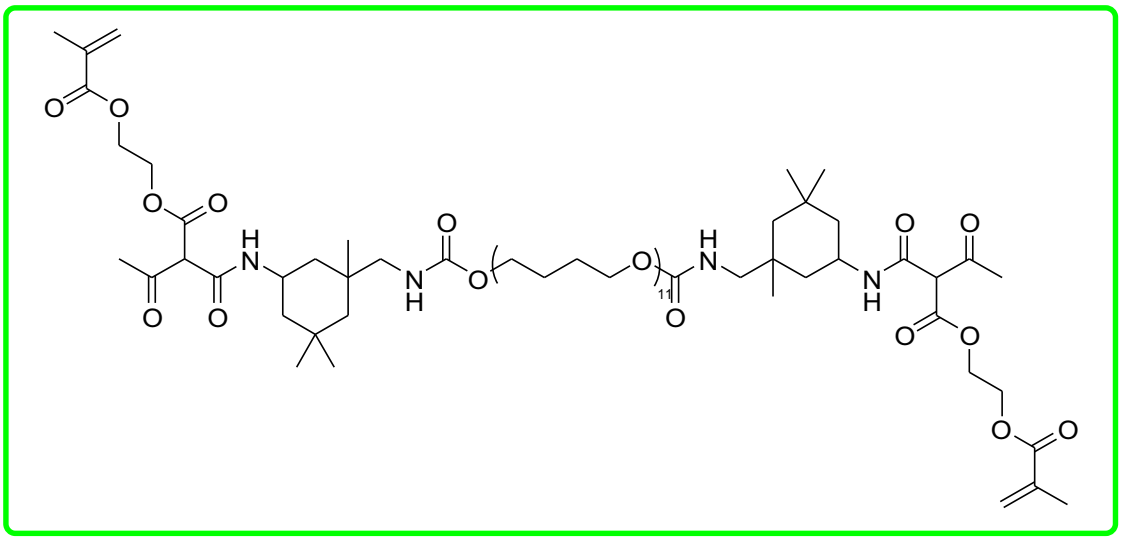

BICMA2

Figure 41: Structures of **C3D1**, **VIC2** and **BICMA2**

Die approbierte gedruckte Originalversion dieser Dissertation ist an der TU Wien Bibliothek verfügbar.
The approved original version of this doctoral thesis is available in print at TU Wien Bibliothek.

*1.3.1. Synthesis of **C3D1***

Synthesis of reference compound **C3D1** was performed according to literature [98]. Since the monomer is used as a reference, the synthesis was conducted strictly according to cited literature: difunctional alcohol and diisocyanate were mixed with the Sn-catalyst and stirred at 70 °C for few hours. Afterwards, a radical inhibitor and the methacrylate were added at lower temperature to prevent polymerisation (40 °C). The mixture was stirred for almost one day to complete the reaction (see Figure 42 and also chapter 1.3.1 of the experimental part).

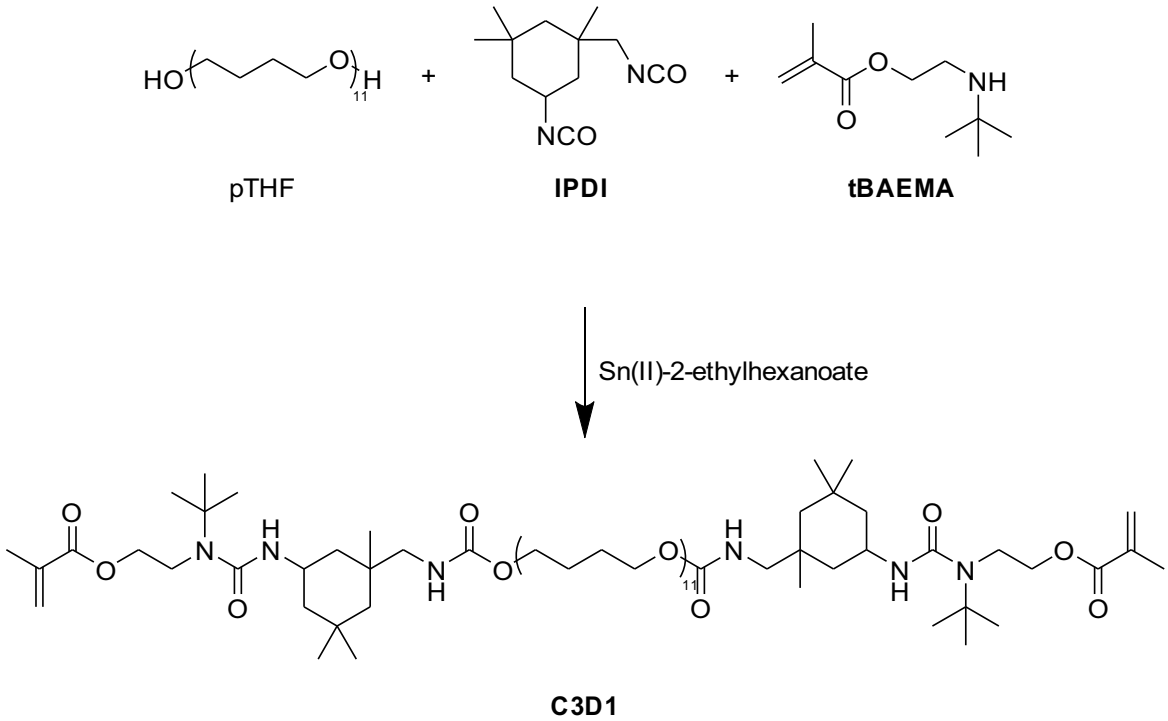

Figure 42: Synthesis of **C3D1**

It has to be mentioned, that – due to the experimental procedure – the shown structure of **C3D1** in Figure 42 is only the idealized one. With addition of the Sn-catalyst the primary as well as the secondary IC moiety of **IPDI** can react with the primary hydroxy groups of pTHF. Thus, this workflow yields also higher addition

Die approbierte gedruckte Originalversion dieser Dissertation ist an der TU Wien Bibliothek verfügbar.
The approved original version of this doctoral thesis is available in print at TU Wien Bibliothek.
TU Bibliothek Your knowledge hub WIEN

products and afterwards due to residual **IPDI** to structures like **tBAEMA-IPDI-tBAEMA**. The existence of monomers with different molecular weights was proved by GPC (Figure 43).

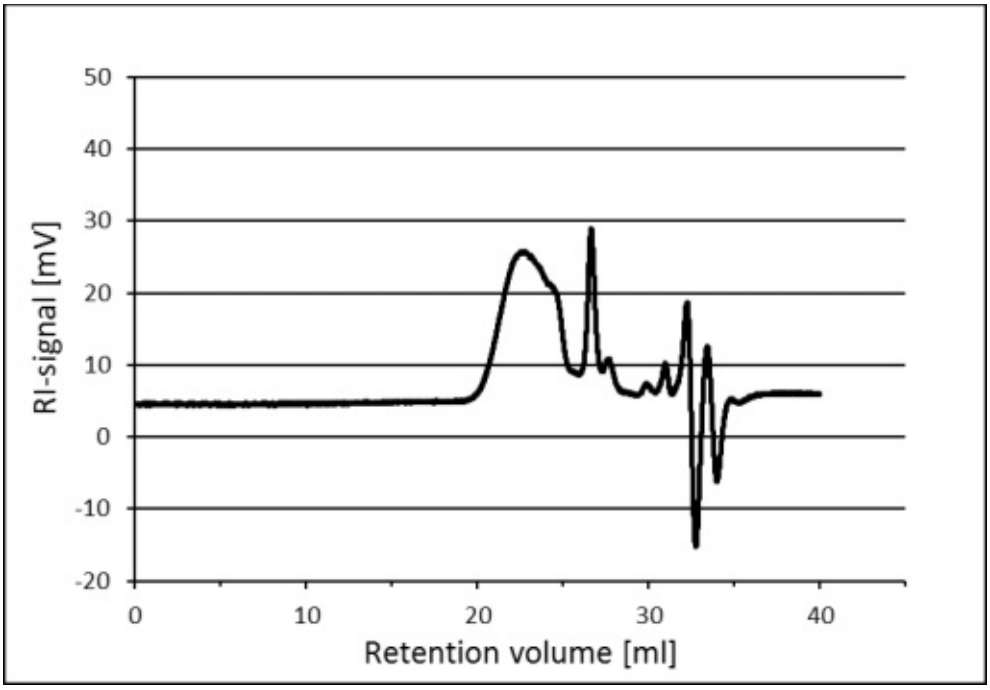

Figure 43: GPC of **C3D1**

The chromatogram in Figure 43 evidences the presence of several different reaction products:

- The main peak at M_n ~ 3.2 kDa corresponds to higher addition products.
- The visible shoulder at M_n ~ 1.6 kDa fits well to the idealised **C3D1** structure with a molecular weight of 1626.33 g/mol.
- All other peaks are beyond the calibrated range, but indicate structures like **tBAEMA-IPDI-tBAEMA**.

However, the crude product was used without any purification for further studies according to literature [98].

Die approbierte gedruckte Originalversion dieser Dissertation ist an der TU Wien Bibliothek verfügbar.
The approved original version of this doctoral thesis is available in print at TU Wien Bibliothek.
TU Bibliothek Your knowledge hub WIEN

*1.3.2. Synthesis of **BICMA1***

Synthesis of isocyanurate based **BICMA1** was performed according to Cooper *et al.* [96]. After **IPDI**-based isocyanurate was dissolved in THF, the methacrylic blocking agent and a Sn-catalyst were added. A reaction time of 48 h at room temperature was necessary to receive complete conversion. Finally, the solvent was removed under reduced pressure and **BICMA1** was obtained as a white powder (see Figure 44 and also chapter 1.3.2 of the experimental part).

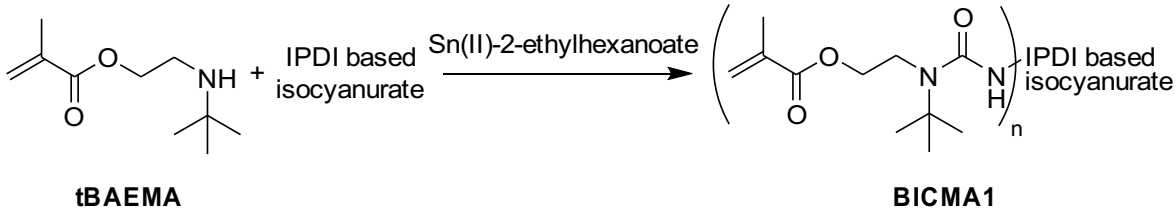

Figure 44: Synthesis of **BICMA1**

It has to be mentioned, that commercially available **IPDI**-based isocyanurate (Vestanat T1890/100) is not only a trimer (as shown in Figure 40), it also contains higher oligomers, which is indicated by the broad melting range of ~ 20 °C. Therefore, the used equivalents of all starting materials have been adjusted according to the previously determined free IC content (compare chapter 1.2.1.1 and see chapter 1.3.2 of the experimental part).
Furthermore, ^{1}H-NMR and ATR-IR spectra proved quantitative conversion and also the preservation of the isocyanurate moiety in **BICMA1**, while no formation of uretdione, due to the presence of a Sn-catalyst, can be observed [104]. Hence, monomer **BICMA1** is also used without further purification.

*1.3.3. Synthesis of **BICMA2***

The synthesis of **BICMA2**, which contains a C-H acidic BIC, was performed in accordance to different procedures established in our working group [46, 105]. The reaction scheme is shown in Figure 45.

Die approbierte gedruckte Originalversion dieser Dissertation ist an der TU Wien Bibliothek verfügbar.
The approved original version of this doctoral thesis is available in print at TU Wien Bibliothek.
TU Bibliothek Your knowledge hub WIEN

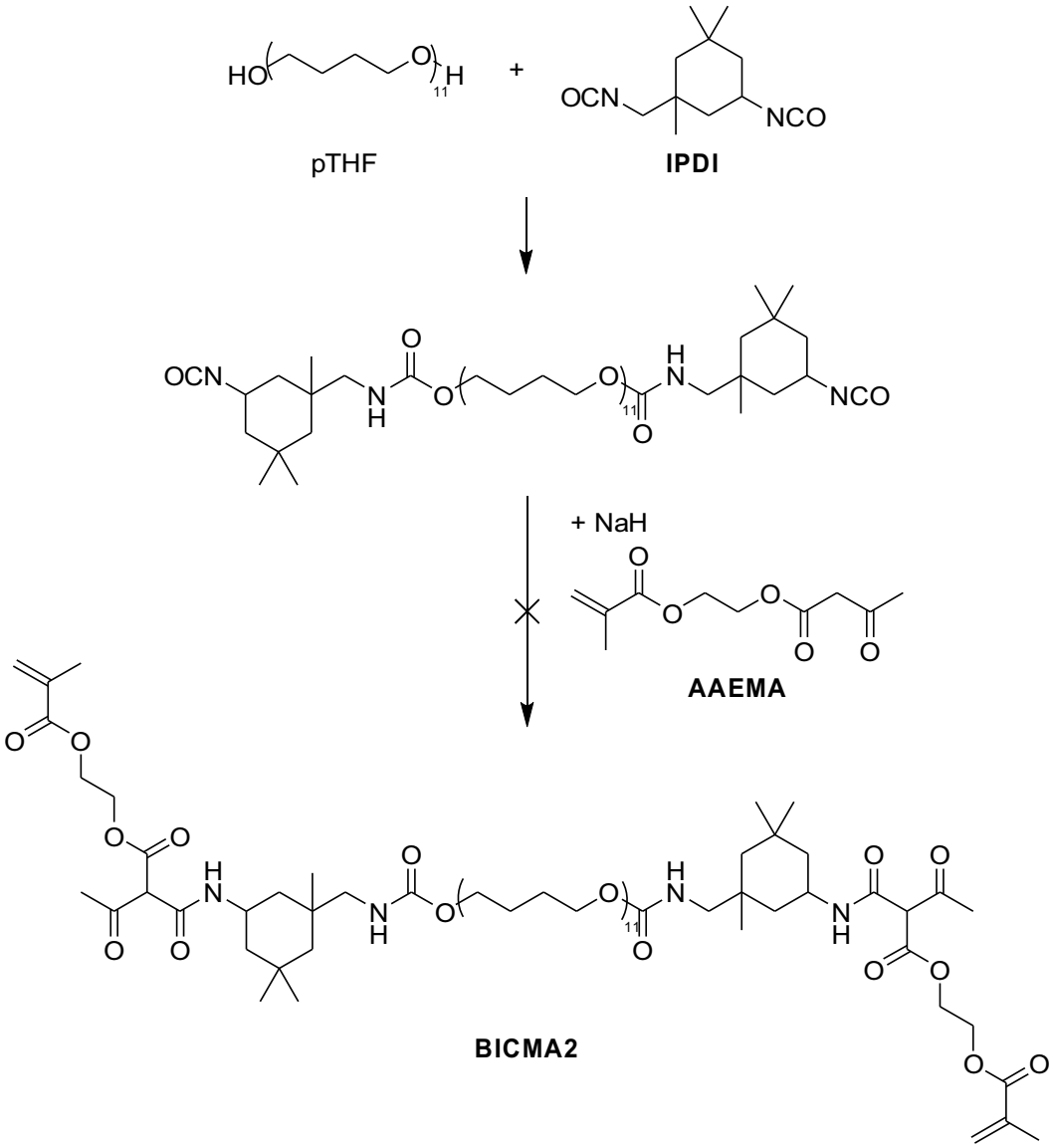

Figure 45: Synthesis of **BICMA2**

Therefore, first **IPDI** and dry pTHF were mixed in the presence of a catalyst (Sn(II)-2-ethylhexanoate) under Ar atmosphere as already done for the syntheses of **C3D1** and **BICMA1** (see chapter 1.3.1 and 1.3.2). In the meantime a second flask was charged also under Ar atmosphere with NaH and dry Et_2O and **AAEMA** was added slowly while cooling the solution with an ice bath. The reaction was heated under reflux for 12 h to ensure full deprotonation. After completion of both reactions, which were monitored with IR (IC peak at ~ 2250 cm^{-1}) and ^{1}H-NMR spectroscopy (protons in α-position to the reactive

Die approbierte gedruckte Originalversion dieser Dissertation ist an der TU Wien Bibliothek verfügbar.
The approved original version of this doctoral thesis is available in print at TU Wien Bibliothek.
TU Bibliothek Your knowledge hub WIEN

hydroxy and IC moieties at ~ 3.00 – 3.80 ppm), the solutions were mixed and refluxed overnight. Finally, the crude product was washed with 1 N HCl and with deionised H_2O (2 times each). Unfortunately, the desired product could not be verified by NMR and IR spectra.

Hence, reaction conditions like equivalents of NaH, amount of solvent, temperatures, reaction time and extraction procedure were varied. Finally, – after some tries – it was possible to receive a crude product, which could be the desired **BICMA2**. On the other hand, no further purification is possible as the pTHF block makes already aqueous extraction extremely difficult and time consuming and also column chromatography or recrystallisation is not possible due to the high molecular weight of **BICMA2**.

However, also all previously in our group synthesised BICs with an acidic C-H moiety as blocking agent had to be purified by recrystallisation or column chromatography. This drawback is caused by the highly reactive carbanion, which is formed as intermediate after deprotonation and hence can undergo several side reactions, which dramatically decreases the obtained purity and yield.

Furthermore, the other synthesis sequence, which starts with first blocking IC **IPDI** with **AAEMA** followed by the reaction with pTHF, is not possible, because no regioselectivity is given in the reaction of the carbanion with the two different IC groups of **IPDI**. Hence, both IC structures of **IPDI** would be blocked by **AAEMA**.

Consequently, the synthesis of **BICMA2** could not be achieved in sufficient purity.

So **VIC2** (see chapter 1.2.2), which is also based on a C-H acidic BIC, has to be used as representative for this class of blocking agents for further studies.

Die approbierte gedruckte Originalversion dieser Dissertation ist an der TU Wien Bibliothek verfügbar.
The approved original version of this doctoral thesis is available in print at TU Wien Bibliothek.
TU Bibliothek Your knowledge hub WIEN

1.4. Melt viscosity

Melt viscosities of **C3D1**, **BICMA1** and **VIC2** are crucial for evaluation of potential applications to ensure processability. Hence, viscosities were measured at different temperatures on a rheometer.

For a better comparability of the different monomer systems, they were studied with their corresponding chain extenders (Figure 46):

- **C3D1** with **HMDA**
- **BICMA1** with **DA** as corresponding soft block to **C3D1** for comparability of the monomers
- **VIC2** with **HMDA**

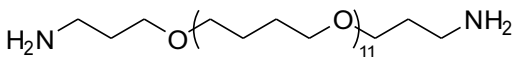

DA

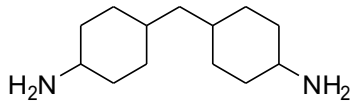

HMDA

Figure 46: Structures of the chain extenders **DA** and **HMDA**

Chain extender concentration was calculated that in the resin an equimolar ratio of BIC moieties to NH_2-groups is provided. Therefore, the concentrations shown in Table 2 were applied in the rheology experiments.

Table 2: Resin composition

Formulation	Monomer [w%]	Amine [w%]
C3D1 and **HMDA**	88.5	11.5
BICMA1 and **DA**	29.8	70.2
VIC2 and **HMDA**	75.2	24.8

Die approbierte gedruckte Originalversion dieser Dissertation ist an der TU Wien Bibliothek verfügbar.
The approved original version of this doctoral thesis is available in print at TU Wien Bibliothek.
TU Bibliothek Your knowledge hub WIEN

So the results shown in Figure 47 and exemplarily given for 80 °C in Table 3 were obtained.

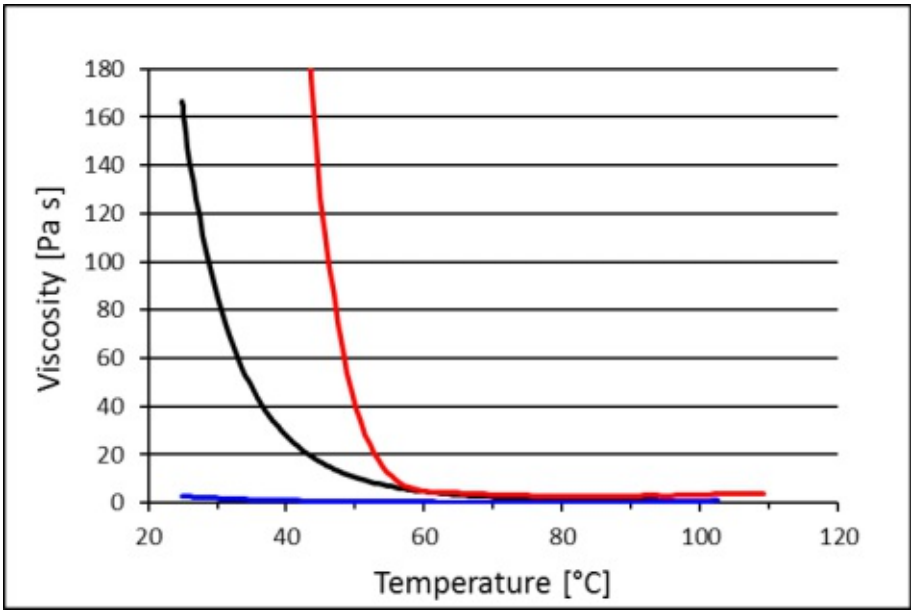

Figure 47: Melt viscosities of **C3D1** (—), **BICMA1** (—) and **VIC2** (—) with corresponding chain extenders

Table 3: Viscosities of tested formulations

Mixture	Viscosity at 80 °C [Pa s]
C3D1 with **HMDA**	1.54
BICMA1 with **DA**	0.22
VIC2 with **HMDA**	2.79

As can be seen in Figure 47, viscosity of **BICMA1** resin is obviously lower than the comparable mixture with **C3D1**, which was one important aim of the isocyanurate approach (see chapter 1.2.1). Additionally, usage of toxic **HMDA** as chain extender can be avoided. Furthermore, viscosity of **VIC2** resin is very high due to the absence of a soft and liquid pTHF structure in the monomer.

Moreover, all 3 tested formulations exhibit a viscosity rise at elevated temperatures (~ 95 – 110 °C). Since the resins were stabilized with high amounts of an inhibitor (0.5 mg phenothiazine in ~ 85 µL sample) and methacrylates are

Die approbierte gedruckte Originalversion dieser Dissertation ist an der TU Wien Bibliothek verfügbar.
The approved original version of this doctoral thesis is available in print at TU Wien Bibliothek.
TU Bibliothek Your knowledge hub WIEN

usually thermally stable up to ~ 140 °C, it seems likely, that deblocking of the isocyanate and consequently reaction with the diamine triggers the viscosity increase. This observation is in good accordance with results obtained from STA experiments in chapter 1.2.1.2, which showed an onset of deblocking reaction of isocyanurate in the presence of an amine at ~ 115 °C. Furthermore, patent literature claims thermal treatment for deblocking of the BIC moiety in a **C3D1**-based photopolymer at > 105 °C [98].

However, above 65 °C the viscosities of all tested formulations are already < 5 Pa s and comparable to the reference BIC-amine-system with **C3D1** [98]. Thus, a variety of potential applications is enabled with this low viscosity.

1.5. Deblocking reactions in solution

Since threshold temperatures needed for deblocking the different classes of BICs (T_{db}) could be determined in chapter 1.2.1.2 for pure BICs, new experiments with the synthesised multifunctional methacrylates containing BICs as spacer should be performed as well. The monomers were studied in solution with an excess of nucleophile (alcohol or amine) as solvent, because matrix polarity also influences T_{db} [56].

The model compound **C3D1** was not tested in these studies, because successful deblocking of the BIC moiety is already demonstrated in the patent [98]. It is shown, that thermal treatment (2 – 4 h at 125 °C) of photopolymers containing BIC **C3D1** and amines as chain extenders reduces cross-linking density and thus a change in network architecture towards a thermoplastic-like behaviour is achieved.

*1.5.1. Deblocking reaction of **BICMA1***

For a proof-of-concept **BICMA1** was dissolved in an excess of a high boiling alcohol or amine. Therefore, 1-lauryl alcohol and 1-laurylamine were selected.

Die approbierte gedruckte Originalversion dieser Dissertation ist an der TU Wien Bibliothek verfügbar.
The approved original version of this doctoral thesis is available in print at TU Wien Bibliothek.
TU WIEN Bibliothek Your knowledge hub

The monomer was dissolved in 10 eq. of alcohol or amine and was stirred 5 h under Ar atmosphere at 125 °C. IR spectra were recorded before and after thermal treatment (see Figure 48).

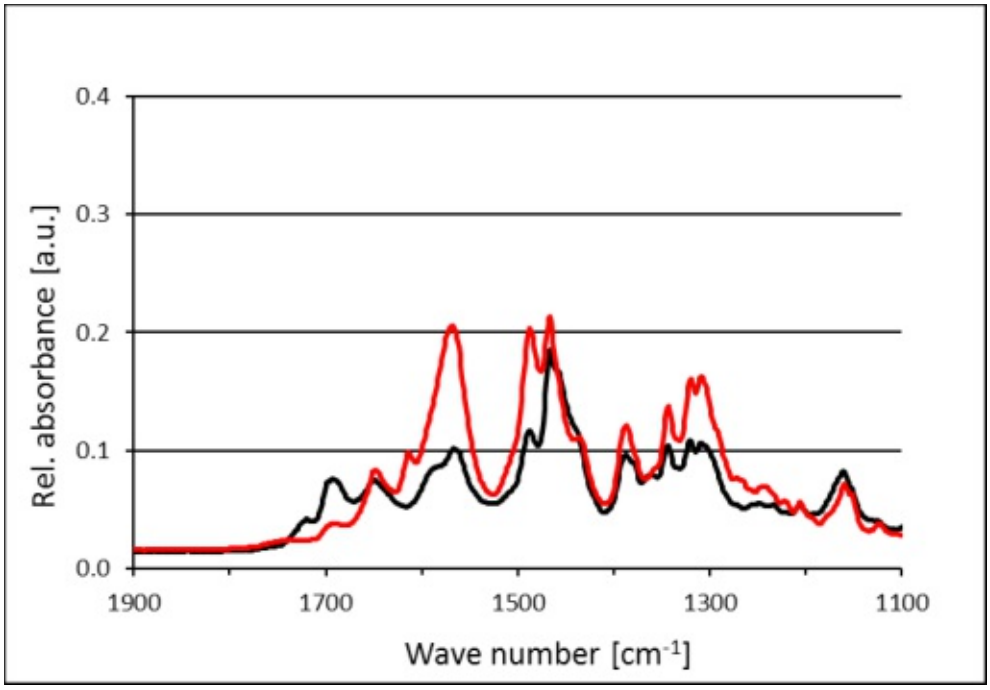

Figure 48: ATR-IR spectra of **BICMA1** before (—) and after (—) thermal treatment in the presence of amine

In alcoholic solution IR spectra showed no reduction in isocyanurate carbonyl signal intensity (~ 1690 cm^{-1}). However, **tBAEMA** blocked IC probably was released partially, because the signal at ~ 1640 cm^{-1} originating from urea carbonyl lost intensity.

In contrast, almost complete deblocking of isocyanurate moiety was observed with the amine (see Figure 48). This can be attributed to higher nucleophilicity of amines compared to alcohols. No information can be gained for **tBAEMA** deblocking, due to product being also an urea derivative and so carbonyl signals are not distinguishable. Furthermore, the urea N-H bond (~ 3300 cm^{-1}) is overlaid with the intense amine N-H signals (~ 3200 – 3350 cm^{-1}), so these peaks cannot be used for reaction monitoring.

Die approbierte gedruckte Originalversion dieser Dissertation ist an der TU Wien Bibliothek verfügbar.
The approved original version of this doctoral thesis is available in print at TU Wien Bibliothek.
TU Bibliothek Your knowledge hub WIEN

*1.5.2. Deblocking reaction of **VIC2***

Experiments were conducted in the same way as for **BICMA1** before (chapter 1.5.1), to investigate the deblocking reaction of **VIC2**. The monomer was dissolved as well in an excess of 1-lauryl alcohol or 1-laurylamine. In contrast, reaction analysis was performed with NMR spectroscopy, because no significant carbonyl signals can be observed in IR spectra, due to the structure of the C-H acidic blocking agent. Additionally, since **VIC2** always polymerised under the used reaction conditions, a shorter reaction time had to be applied, which was compensated by a slightly increased temperature.

The monomer and phenothiazine were dissolved in 10 eq. of alcohol or amine and were stirred 15 min under Ar atmosphere at 150 °C. Pure **VIC2** was used as reference system. Samples were taken before and after thermal treatment and ^{1}H and ^{13}C-NMR spectra were recorded.

Whereas pure **VIC2** only polymerised, the solutions containing alcohol or amine showed bubble formation, which can indicate a reaction of released ICs with residues of water and hence CO_2 formation. But NMR spectra evidence for the experiment with alcohol only (thermal) degradation/decarboxylation. In contrast, when using amine deblocking reaction of the BIC occurs and several new peaks (*e.g.* amide, ester, urea) were identified in the ^{13}C-NMR spectrum (see Figure 49). Furthermore, biuret formation could not be observed, since corresponding peaks (~ 155-160 ppm [106-108]) are absent. This lack of side reactions is expected, because applied IC/amine ratio is low.

Die approbierte gedruckte Originalversion dieser Dissertation ist an der TU Wien Bibliothek verfügbar.
The approved original version of this doctoral thesis is available in print at TU Wien Bibliothek.
TU Bibliothek Your knowledge hub WIEN

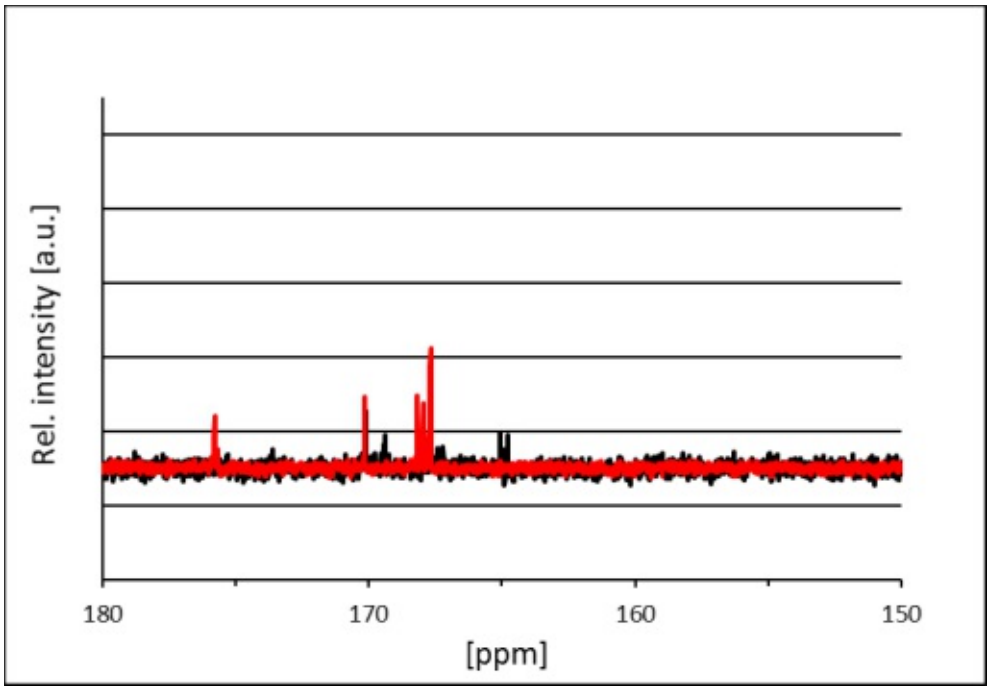

Figure 49: APT NMR spectra of **VIC2** before (—) and after (—) thermal treatment in the presence of amine

Thus, also for C-H acidic BIC **VIC2** deblocking could be achieved in the presence of an amine.

1.6. (Thermo)mechanical properties

For a characterisation of the (thermo)mechanical properties of the synthesised methacrylates containing BICs several studies were performed. In addition, influence of thermal treatment after UV curing on material properties should be investigated.

Resins were formulated according to double bond percent (DB%) of the patent [98] for better comparability (see Table 4, Figure 50).

Die approbierte gedruckte Originalversion dieser Dissertation ist an der TU Wien Bibliothek verfügbar.
The approved original version of this doctoral thesis is available in print at TU Wien Bibliothek.
TU Bibliothek Your knowledge hub WIEN

Table 4: Patented resin composition **REF** [98]

Component	w‰ [‰]	mol% [%]	eq. [-]	DB% [%]
C3D1	700	22.5	1.00	43.4
E3MA	206	57.2	2.54	55.2
PEGDMA (M_w = 750 Da)	10	0.7	0.03	1.4
HMDA	74	18.4	0.82	-
Irgacure 819	10	1.2	0.06	-

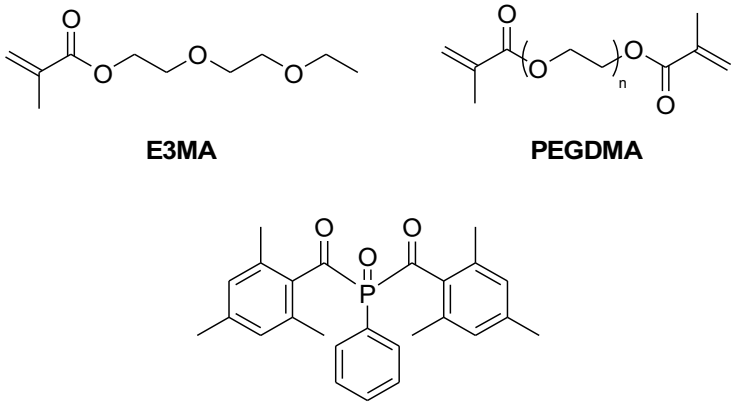

Figure 50: Structures of reactive diluent **E3MA**, cross-linking agent **PEGDMA** and PI Irgacure 819

As can be seen in Table 4 an insufficient amount of diamine **HMDA** is used, probably to ensure that no toxic residues diffuse out of the cured material. Nevertheless, formulations containing **BICMA1** (**RES1**) and **VIC2** (**RES2**) were mixed according to DB% used in **C3D1** resin (**REF**). Only amine **DA** was used in an “equimolar” ratio, which means that one amino functionality is taken into account for each BIC moiety: Table 5.

Die approbierte gedruckte Originalversion dieser Dissertation ist an der TU Wien Bibliothek verfügbar.
The approved original version of this doctoral thesis is available in print at TU Wien Bibliothek.

Table 5: Resin compositions **RES1** and **RES2**

Component	DB% [%]	**RES1** [w%]	**RES2** [w%]
BICMA1	43.4	25.0	-
DA	-	58.4	-
VIC2	43.4	-	45.5
HMDA	-	-	15.0
E3MA	55.2	14.9	36.7
PEGDMA (M_w = 750 Da)	1.4	0.7	1.8
Irgacure 819	-	1.0	1.0

All specimens were cured in transparent silicon moulds for 10 min on each side in the Lumamat oven (see the general procedure in chapter 1.6 of the experimental part). Afterwards, half of the samples were stored 14 h at 125 °C, where all polymers became darker, less sticky and seemed to be harder and tougher.

Additionally, ATR-IR spectra were recorded before and after annealing, but no difference could be observed. Furthermore, no NMR spectroscopy is possible, because cured samples are not soluble (as well as parts without cross-linking agent **PEGDMA**).

Finally, annealing temperature for small test samples was raised to 150 and 200 °C, whereby also no difference in ATR-IR spectra can be observed and polymers are still insoluble.

Nevertheless, DMTA, tensile and Dynstat impact tests were performed to compare (thermo)mechanical properties of the cured photopolymers without and with thermal treatment.

1.6.1. DMTA

DMTA studies were performed to estimate thermomechanical material properties as well as thermal phase transitions (*e.g.* T_g).

Die approbierte gedruckte Originalversion dieser Dissertation ist an der TU Wien Bibliothek verfügbar.
The approved original version of this doctoral thesis is available in print at TU Wien Bibliothek.
TU Bibliothek Your knowledge hub WIEN

All DMTA experiments were executed in torsion mode with a heating rate of 2 °C/min and constant normal force.

So data shown in Figures 51-53 was obtained.

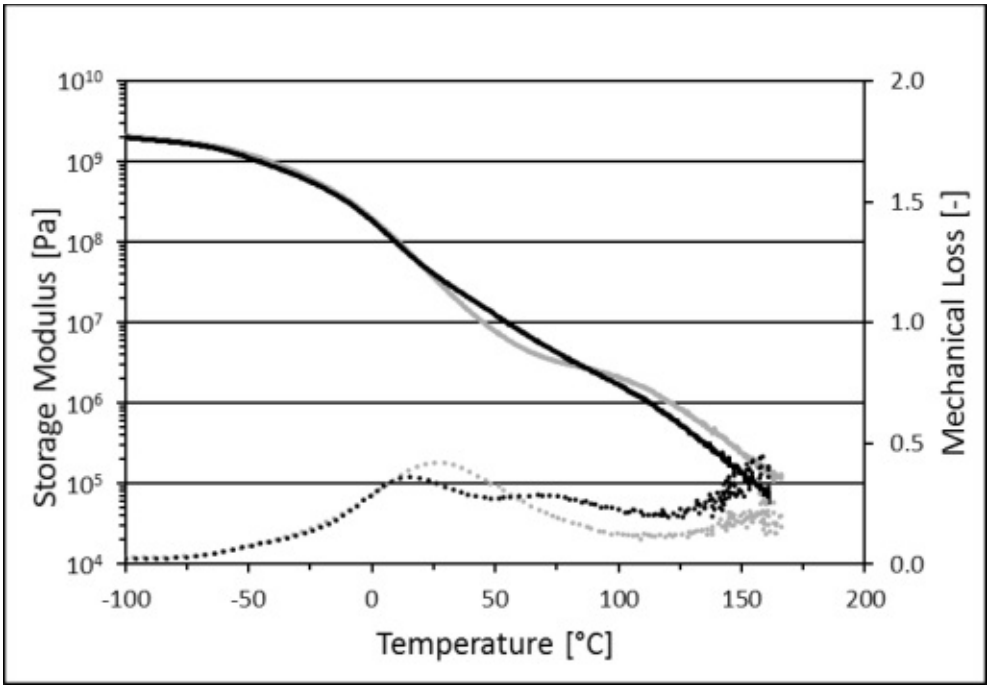

Figure 51: Storage modulus (—) and mechanical loss (···) of **pREF** before (—) and after annealing 14 h at 125 °C (—)

As can be seen in Figure 51 nearly no significant difference in thermomechanical properties before and after thermal treatment of **pREF** can be observed. Only mechanical loss of annealed **pREF** indicates a second peak (T_g) at ~ 75 °C, that probably can be attributed to partial deblocking of the BIC and formation of the desired polyurea phase.

Die approbierte gedruckte Originalversion dieser Dissertation ist an der TU Wien Bibliothek verfügbar.
The approved original version of this doctoral thesis is available in print at TU Wien Bibliothek.
TU Bibliothek Your knowledge hub WIEN

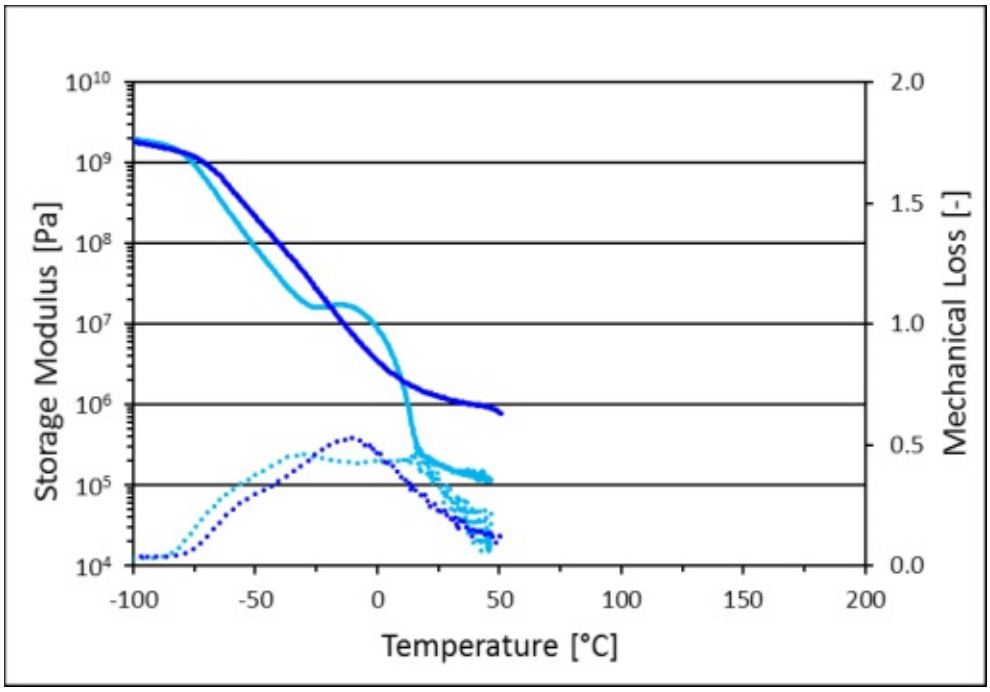

Figure 52: Storage modulus (—) and mechanical loss (···) of **pRES1** before (—) and after annealing 14 h at 125 °C (—)

Figure 52 shows that storage modulus in the rubbery-elastic area is higher after annealing for **pRES1**, which indicates that cross-linking density raises after thermal treatment. This effect could be caused by thermal postcuring or reaction of difunctional amine **DA** with the ester moiety of **E3MA** (ester aminolysis), which yields also in an increased cross-linking density.

Die approbierte gedruckte Originalversion dieser Dissertation ist an der TU Wien Bibliothek verfügbar.
The approved original version of this doctoral thesis is available in print at TU Wien Bibliothek.
TU Bibliothek Your knowledge hub WIEN

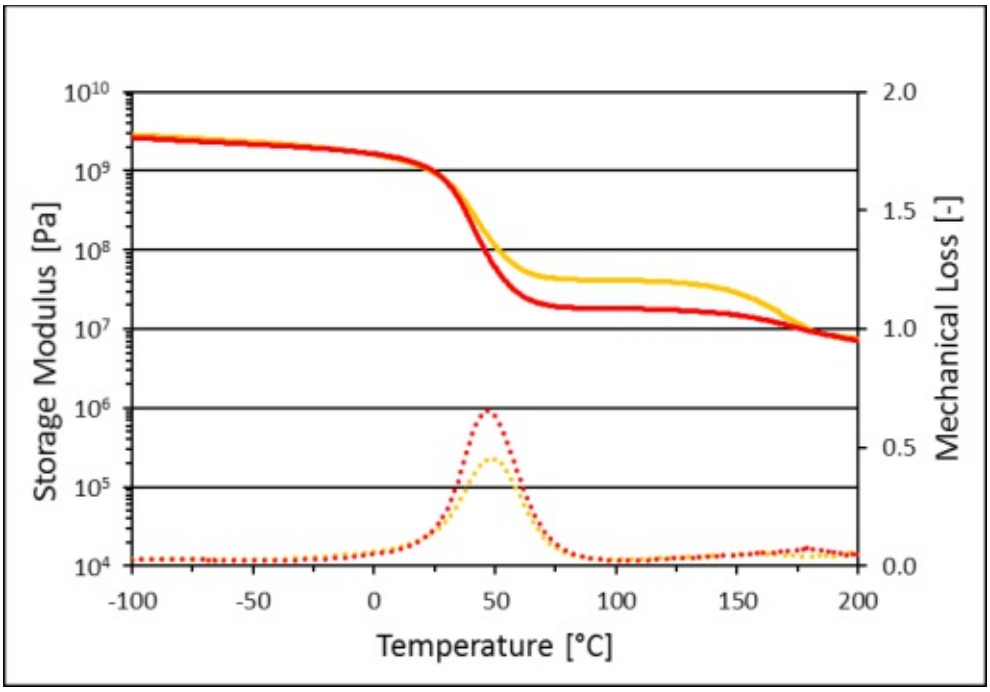

Figure 53: Storage modulus (—) and mechanical loss (···) of **pRES2** before (—) and after annealing 14 h at 125 °C (—)

As Figure 53 shows, DMTA curves of **pRES2** give very promising results. The T_g is not changed after thermal curing and the G' in the rubbery-elastic area is lower, which indicates lower cross-linking density. So deblocking reactions may occur and would partially break up cross-linking points.

Finally, Figure 54 displays a comparison of the annealed **pREF**, **pRES1** and **pRES2**.

Die approbierte gedruckte Originalversion dieser Dissertation ist an der TU Wien Bibliothek verfügbar.
The approved original version of this doctoral thesis is available in print at TU Wien Bibliothek.
TU Bibliothek Your knowledge hub WIEN

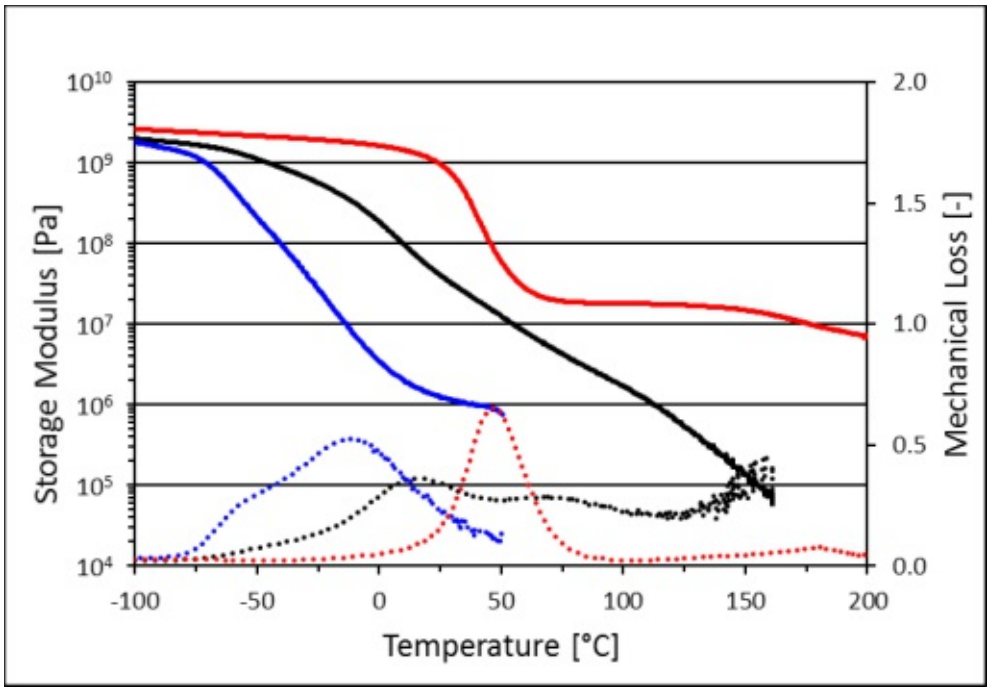

Figure 54: Storage modulus (—) and mechanical loss (···) of annealed **pREF** (—), **pRES1** (—) and **pRES2** (—)

Figure 54 illustrates the difference between **pREF**, **pRES1** and **pRES2** polymers in annealed state. It can be seen, that T_g is lowered with an increased amount of soft pTHF and that G' remains quite high for the **pRES1** and especially for the **pRES2** system in rubbery-elastic area. Additionally, it shows that **pRES2** exhibits significant higher storage modulus at room temperature and T_g, since no soft pTHF structure is present in the polymer.

1.6.2. Tensile tests

Furthermore, tensile tests were performed to compare stress-strain curves of the different BIC systems based on **pREF**, **pRES1** and **pRES2**.

All tensile tests were executed according to ISO 527 with specimen shape 5B and a traverse speed of 5 mm/min.
So the results shown in Figure 55 and summarized in Table 6 were obtained.

Die approbierte gedruckte Originalversion dieser Dissertation ist an der TU Wien Bibliothek verfügbar.
The approved original version of this doctoral thesis is available in print at TU Wien Bibliothek.
TU Bibliothek Your knowledge hub WIEN

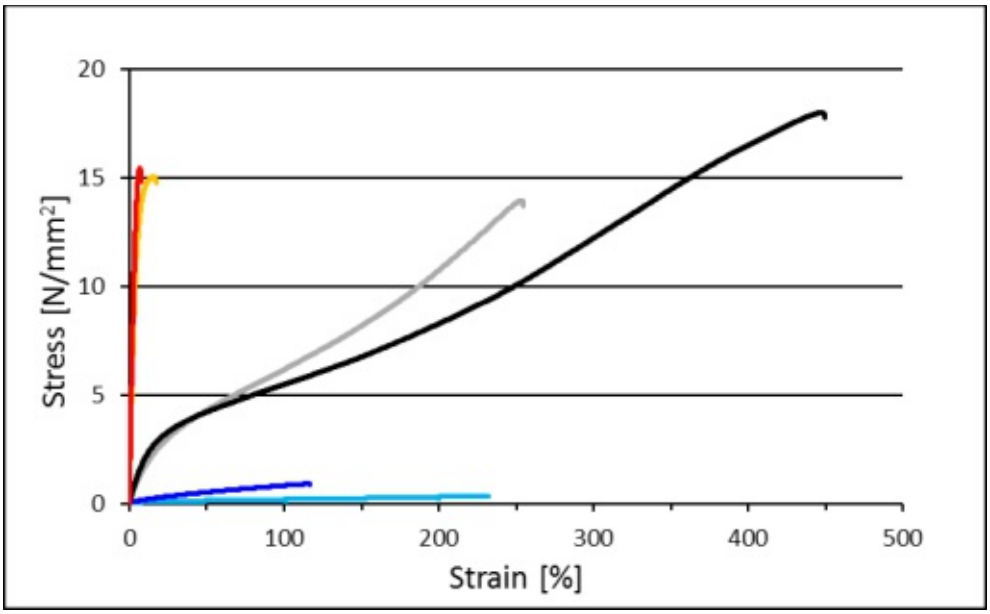

Figure 55: Exemplary stress-strain curves of **pREF** (—), **pREF AN** (—), **pRES1** (—), **pRES1 AN** (—), **pRES2** (—) and **pRES2 AN** (—)

Table 6: Estimated stress and strain at break of **pREF**, **pRES1** and **pRES2**

Sample	$Stress_{max}$ [MPa]		$Strain_{Break}$ [%]	
	Average	s	Average	s
pREF	13.8	0.7	244.1	14.2
pREF AN	18.5	2.5	450.1	29.7
pRES1	0.34	0.09	233.0	26.9
pRES1 AN	0.88	0.06	117.2	6.1
pRES2	14.9	0.9	16.7	2.3
pRES2 AN	15.2	0.4	7.5	2.7

Figure 55 and Table 6 show that polymer **pREF** containing reference monomer **C3D1** dramatically outperforms the **BICMA1** (**RES1**) as well as **VIC2** (**RES2**) approach regarding tensile properties. One reason is probably the stability of the isocyanurate ring in **BICMA1**, whereby cross-links in the polymer network do not break – and actually even increase with thermal treatment – (see also chapter

Die approbierte gedruckte Originalversion dieser Dissertation ist an der TU Wien Bibliothek verfügbar.
The approved original version of this doctoral thesis is available in print at TU Wien Bibliothek.
TU Bibliothek Your knowledge hub WIEN

1.6.1), which causes less elastic behaviour. In addition, higher storage modulus of **pRES2** compared to **pREF** at the annealing temperature (125 °C, see DMTA curves in chapter 1.6.1) may hinder efficient deblocking reactions.

1.6.3. Impact resistance

Furthermore, impact strengths according to the Dynstat approach of treated and untreated photopolymerised **pREF**, **pRES1** and **pRES2** were measured.

All impact tests were performed according to DIN 51230 with a 20 kpcm hammer. In addition, measured data was normalised to the cross section of the corresponding test specimen.

However, untreated **pRES1** is too soft and flexible to break, annealed **pRES1** and both **pREF** photopolymers are too tough: they are always kicked out of the sample mount instead of breaking.
In contrast, for cured **pRES2** polymers following values could be calculated:

- **pRES2**: 2.3 ± 1.0 kJ/m^2
- **pRES2 AN**: 1.3 ± 0.6 kJ/m^2

Again reference **pREF** dramatically outperforms isocyanurate based **pRES1** and C-H acidic BIC based **pRES2**.

1.7. Influence of the matrix on deblocking reactions

One possible explanation for poor results in thermomechanical tests is, that maybe no or only an insufficient amount of deblocking reactions occur, and thus no polyurea is formed. Therefore, the influence of the polymer matrix should be investigated in detail.

Die approbierte gedruckte Originalversion dieser Dissertation ist an der TU Wien Bibliothek verfügbar.
The approved original version of this doctoral thesis is available in print at TU Wien Bibliothek.
TU Bibliothek Your knowledge hub WIEN

1.7.1. Matrix polarity

Since deblocking of isocyanurate failed in a matrix from literature, which was chosen for better comparability, a more polar matrix monomer was used, because a higher polarity of the chemical environment facilitates deblocking reactions of BICs [56].

Hence, **HEMA** (Figure 56) was chosen, because matrix polarity is thereby increased drastically by the presence of hydroxy groups.

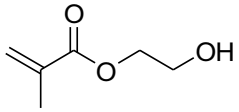

Figure 56: Structure of **HEMA**

So small samples of a formulation containing 49.5 w% “equimolar” **BICMA1** and **DA** (like it was used already before in chapter 1.6), 49.5 w% **HEMA** and 1 w% Ivocerin were cured in the Lumamat oven.

Finally, also in this very polar matrix no deblocking of the isocyanurate functionality could be observed after 14 h at 150 °C via ATR-IR spectroscopy, although polymer feels much more stiffer and tougher. In addition, NMR spectroscopy is not possible since the samples are insoluble (compare also chapter 1.6).

1.7.2. Soft matrix

As **VIC2** did not give the expected results in the patented formulation (chapter 1.6), a second softer matrix was tested for deblocking **VIC2**, because lower G' should facilitate diffusion. Thus, desired polyurea formation in the solid polymer matrix should be enabled.

Die approbierte gedruckte Originalversion dieser Dissertation ist an der TU Wien Bibliothek verfügbar.
The approved original version of this doctoral thesis is available in print at TU Wien Bibliothek.
TU Bibliothek Your knowledge hub WIEN

The used composition of resin **RES3** is shown in Table 7. Amine **HMDA** is again applied in equimolar ratio to BIC **VIC2**.

Table 7: Composition of formulation **RES3**

Component	DB% [%]	w% [%]
VIC2	10	14.1
HMDA	-	4.6
E3MA	90	80.3
Irgacure 819	-	1.0

Photopolymerisation, thermal curing and specimen preparation for DMTA and tensile tests were executed under the same conditions as before in chapter 1.6 (see also chapter 1.6 of the experimental part) to get comparable data.

1.7.2.1. DMTA

DMTA measurements were performed again to investigate the influence of matrix polarity on thermal deblocking reaction and on material properties like T_g.

The DMTA experiments were conducted in torsion mode with a heating rate of 2 °C/min and constant normal force.
So the data given in Figure 57 was obtained for **pRES3**.

Die approbierte gedruckte Originalversion dieser Dissertation ist an der TU Wien Bibliothek verfügbar.
The approved original version of this doctoral thesis is available in print at TU Wien Bibliothek.
TU Bibliothek Your knowledge hub WIEN

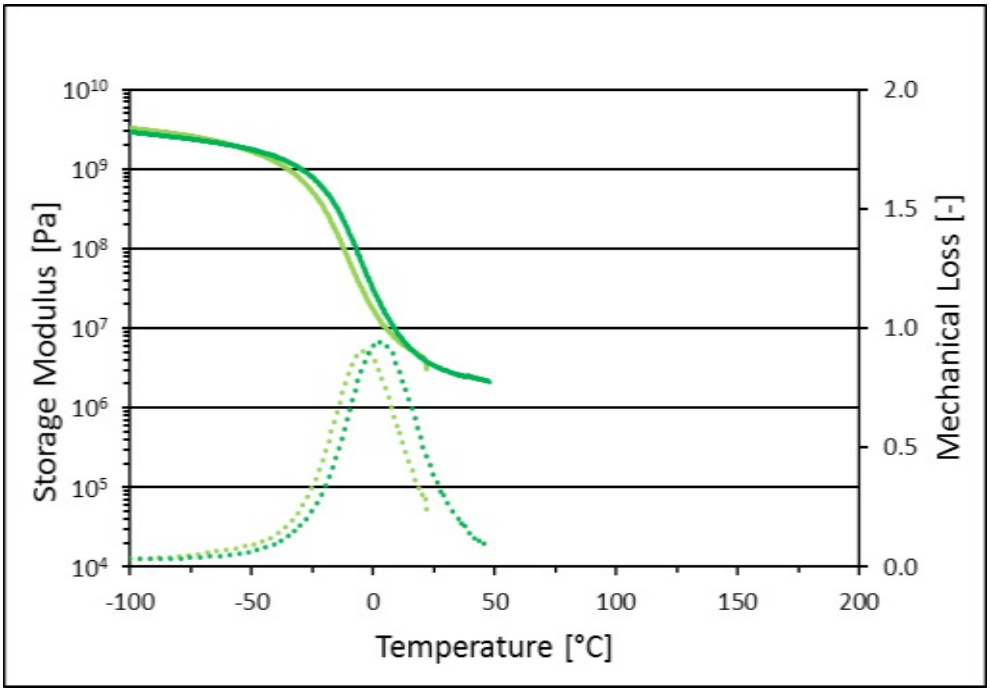

Figure 57: Storage modulus (—) and mechanical loss (···) of **pRES3** before (—) and after annealing (—)

As can be seen in Figure 57 almost no change in storage modulus curve and T_g can be observed due to thermal treatment. Similar results were already obtained for **pRES2** (see chapter 1.6.1), where T_g also remains constant but G' drops in rubbery-elastic area, due to thermal treatment.

So again DMTA curves give no indication of deblocking reaction and urea formation.

1.7.2.2. Tensile tests

Finally, tensile tests of the soft **pRES3** material were performed to check tensile properties before and after annealing.

Tensile tests were conducted according to ISO 527 with specimen shape 5B and a traverse speed of 5 mm/min.

Thus, stress-strain curves, which are given exemplarily in Figure 58, were measured. All results are summarised in Table 8.

Die approbierte gedruckte Originalversion dieser Dissertation ist an der TU Wien Bibliothek verfügbar.
The approved original version of this doctoral thesis is available in print at TU Wien Bibliothek.
TU Bibliothek Your knowledge hub WIEN

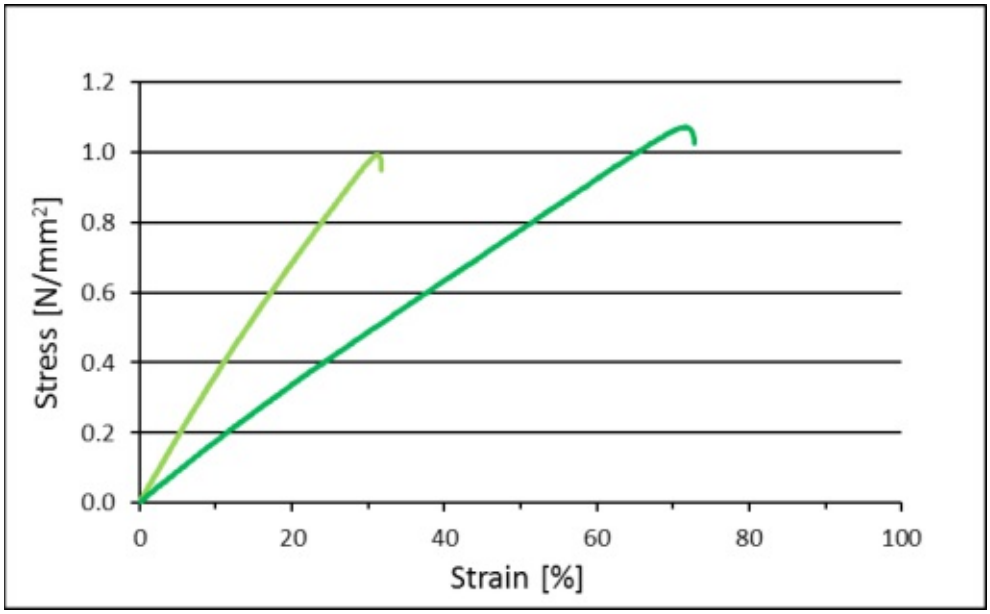

Figure 58: Exemplary stress-strain curves of **pRES3** before (—) and after annealing (—)

Table 8: Estimated stress and strain at break of **pRES3**

Sample	$Stress_{max}$ [MPa]		$Strain_{Break}$ [%]	
	Average	s	Average	s
pRES3	1.0	0.0	32.8	1.8
pRES3 AN	1.1	0.2	69.1	6.4

As can be seen in Figure 58 and Table 8 annealing increases maximum strain by a factor of 2, while maximum stress remains constant. This behaviour indicates, that deblocking reactions and furthermore polyurea formation occur in the soft matrix and hence the polymer architecture is changed from a network towards linear chains.

However, in the meantime Covestro [109-110] and Canon [111] patented some (meth)acrylates containing BICs for lithography based AMT (L-AMT). The inventions are explicitly described with special blocking agents, which will not be released into environment after deblocking reaction and thus a lower

Die approbierte gedruckte Originalversion dieser Dissertation ist an der TU Wien Bibliothek verfügbar.
The approved original version of this doctoral thesis is available in print at TU Wien Bibliothek.
TU Bibliothek Your knowledge hub WIEN

concentration of volatile organic compounds (VOCs) can be achieved. The claimed blocking agents are cyclic ketones with an ester or nitrile motive in α-position, glycerine carbonate, lactams and finally isocyanates themselves (uretdiones or isocyanurates) (see Figure 59).

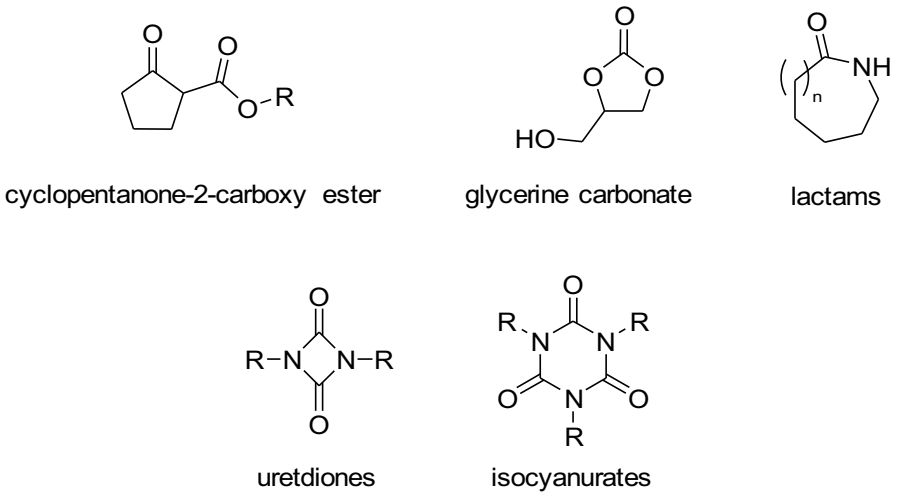

Figure 59: Structures of blocking agents patented by Covestro

In contrast, all given examples in the patents use **HDI**-based uretdiones as BICs and multifunctional amines as chain extenders, although uretdiones are known to react slowly with amines at room temperature.

For example formulations containing a monomer based on PPG, **HDI**-based uretdione, **HEMA** and multifunctional amines as chain chain extender are photopolymerised. Afterwards the green bodies are thermally cured at 120 °C for 1 h. For that purpose, a ratio of NH_2-groups to uretdiones of 1 to 5 is used, which may explain the increased storage stability of the claimed resins. Finally, polymers with increased maximum stress (11-17 MPa) and strain at break (65-85%) are obtained, although only ~ 44% of present uretdione groups are cleaved.

As a consequence another approach to enhance toughness in photopolymers should be evaluated.

Die approbierte gedruckte Originalversion dieser Dissertation ist an der TU Wien Bibliothek verfügbar.
The approved original version of this doctoral thesis is available in print at TU Wien Bibliothek.

2. ABS-like Photopolymers

When talking about toughness of polymers one cannot pass ABS as benchmark for tough high-performance engineering plastics. So the second tested approach for toughening of photopolymers is to mimic ABS.

2.1. State of the art

The favourable thermomechanical properties within a broad application range from -20 – 80 °C, good processability (injection moulding, extrusion) and versatile post-processing (*e.g.* bonding, welding, electroplating, printing) enabled a lot of application fields for ABS. Only some of the most important uses are household and consumer goods, pipes, toys (Lego), automotive and electrical industry, all kinds of cases, music instruments and filament for 3D printing (fused deposition modelling, FDM) [47, 112].

The beneficial characteristics of ABS originate on the one hand from the used monomers (Figure 60), but also on the morphology of the final material.

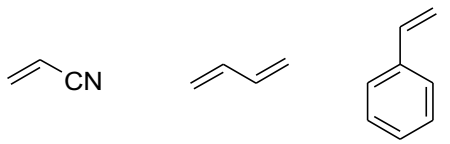

Figure 60: Monomers of ABS

In the terpolymer acrylonitrile (15 – 35%) forms strong polar interactions, which enhance thermomechanical properties, and is also responsible for hardness, increased heat distortion temperature, weatherability and good chemical resistance of ABS. In contrast, elastomeric butadiene (5 – 30%) is the soft component, which yields high elongation and high toughness even at low temperatures. Lastly, styrene (40 – 60%) gives gloss and stiffness in the final polymer (and a low price as well) [47].

Die approbierte gedruckte Originalversion dieser Dissertation ist an der TU Wien Bibliothek verfügbar.
The approved original version of this doctoral thesis is available in print at TU Wien Bibliothek.
TU Bibliothek Your knowledge hub WIEN

As already mentioned before, ABS is an amorphous heterogeneous thermoplastic material and thus exhibits opaque and not transparent optical properties. In addition, morphology has a great influence on the material properties as well [48]. The heterogeneity of ABS arises from the incompatibility of polybutadiene and poly(styrene-*co*-acrylonitrile) (SAN), which is grafted from the primarily synthesised polybutadiene particles. So phase separation of the soft elastomeric polybutadiene and the rigid and brittle SAN matrix occurs (see Figure 61).

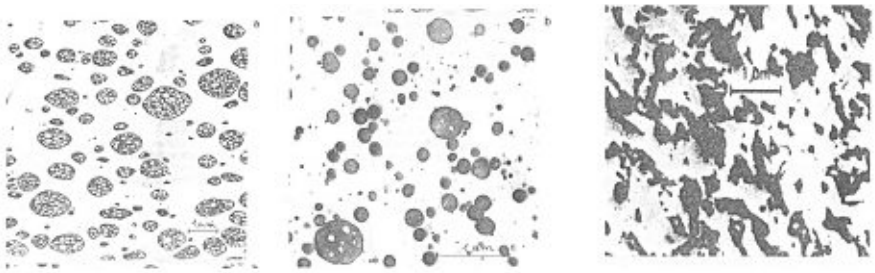

Figure 61: SEM pictures of ABS (bulk/suspension polymerisation (a), emulsion polymerisation (b) or blend type (c)) stained with OsO_4 [113]

As a consequence of the heterogeneous structure crazes form at the interface layer of the 2 phases already at comparable low strains, when the polymer is stressed. But the high elasticity of the polybutadiene very efficiently prevents crack growth. This mechanism can be seen also in macroscopic scale as stress whitening [52-53, 114].

However, ABS cannot be photopolymerised at room temperature. Although there are also special applications for photopolymerisation, where increased temperatures are applied, it is usually utilised at room temperature, since no need for heating is one of the main advantage of photopolymerisation compared to conventional polymerisation techniques. So monomer volatility must be dramatically reduced for polymerisation at elevated temperatures, because preventing monomer evaporation with increased pressure (*e.g.* autoclave) is not

Die approbierte gedruckte Originalversion dieser Dissertation ist an der TU Wien Bibliothek verfügbar.
The approved original version of this doctoral thesis is available in print at TU Wien Bibliothek.
TU Bibliothek Your knowledge hub WIEN

a practicable method for photopolymerisation. In contrast, a second approach is to circumvent the thermodynamic control by an alternating copolymerisation with a second monomer and thus enabling polymerisation at room temperature.

Hence, different possible electron rich and electron poor monomers should be tested to find a suitable highly reactive monomer system for alternating copolymerisation. Furthermore, toughening agent butadiene should be used already as polybutadiene and thus have to be soluble in the photopolymerisable formulation.

2.2. Preliminary experiments

Some preliminary studies were performed for a proof-of-concept and to get more insights into key monomer properties like volatility, stability and reactivity. So potential applications for the new monomer systems should be evaluated.

Therefore, a set of different promising imide structures (electron poor double bonds) was chosen for first tests, because good (thermo)mechanical properties of the final polymers like a high T_g can be expected due to their rigid ring motive (Figure 62) [115]:

- Maleimide (MI)
- Itaconimide (II)
- Citraconimide (CI)

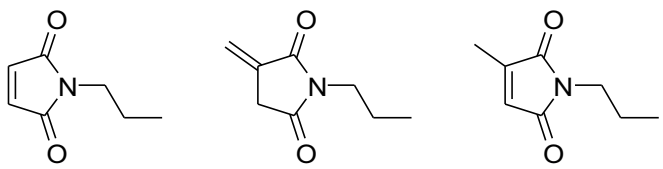

PrMI **PrII** **PrCI**

Figure 62: Structures of studied MI **PrMI**, II **PrII** and CI **PrCI**

Die approbierte gedruckte Originalversion dieser Dissertation ist an der TU Wien Bibliothek verfügbar.
The approved original version of this doctoral thesis is available in print at TU Wien Bibliothek.
TU Bibliothek Your knowledge hub WIEN

In addition, 3 different electron rich double bond moieties were investigated regarding their copolymerisation behaviour with imides (Figure 63):

- Vinyl ether
- Allyl ether
- Styrene derivative (styrene itself is very volatile)

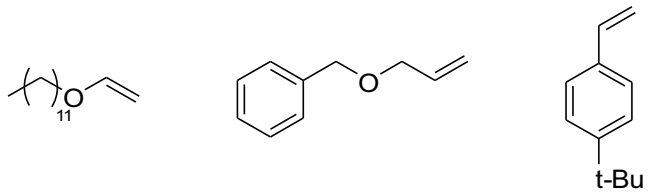

LVE **ABE** **tBuSt**

Figure 63: Structures of vinyl ether **LVE**, allyl ether **ABE** and styrene derivative **tBuSt**

Maleimide **PrMI** and all comonomers are commercially available, so only itaconimide **PrII** and citraconimide **PrCI** had to be synthesised.

2.2.1. Syntheses of itaconimides and citraconimides

In addition to commercially available MI **PrMI**, also II **PrII** and CI **PrCI** should be tested to study the influence of double bond position on the copolymerisation behaviour. IIs and CIs are especially interesting and more favourable than MIs, because they can be obtained from biological resources [116]. Furthermore, IIs exhibit slightly higher reactivity in radical homopolymerisation than CIs or MIs [117].

*2.2.1.1. Synthesis of **PrII** and **PrCI***

Synthesis of II **PrII** and CI **PrCI** was performed according to patent WO 2005118537 [118] (Figure 64, see also chapter 2.2.1.1 of the experimental part) with a Dean-Stark-apparatus and toluene as entrainer. With this synthetic route

Die approbierte gedruckte Originalversion dieser Dissertation ist an der TU Wien Bibliothek verfügbar.
The approved original version of this doctoral thesis is available in print at TU Wien Bibliothek.
TU Bibliothek Your knowledge hub WIEN

both monomers can be synthesised in one pot, because bases (*i.e.* starting material 1-propylamine) catalyse double bond isomerisation. The obtained ratio of II and CI depends on the basicity of used nucleophile and reaction conditions.

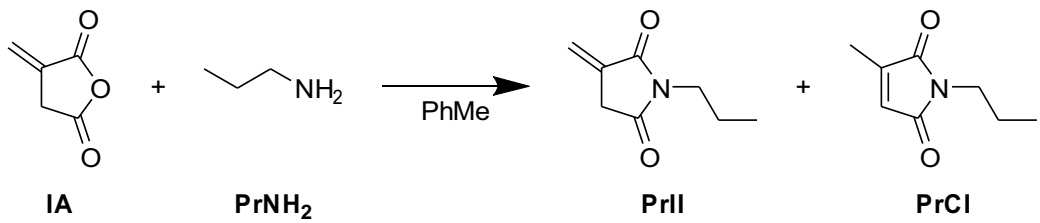

Figure 64: Synthesis of **PrII** and **PrCI**

However, due to high basicity of propylamine ($pK_a \sim 10.71$) double bond isomerisation is a serious problem. The ratio of isolated II : CI is only 1 : 3.7. Furthermore, yields are very low (~ 5% of theory), because Michael addition of the amine to the activated double bonds also occurs very efficiently (Figure 65).

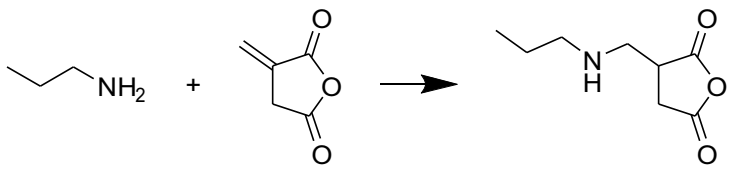

Figure 65: Side reaction Michael addition

There are several other promising synthesis routes known in literature for IIs like **PrII**. Some potential ways are depicted in Figure 66.

Die approbierte gedruckte Originalversion dieser Dissertation ist an der TU Wien Bibliothek verfügbar.
The approved original version of this doctoral thesis is available in print at TU Wien Bibliothek.
TU Bibliothek Your knowledge hub WIEN

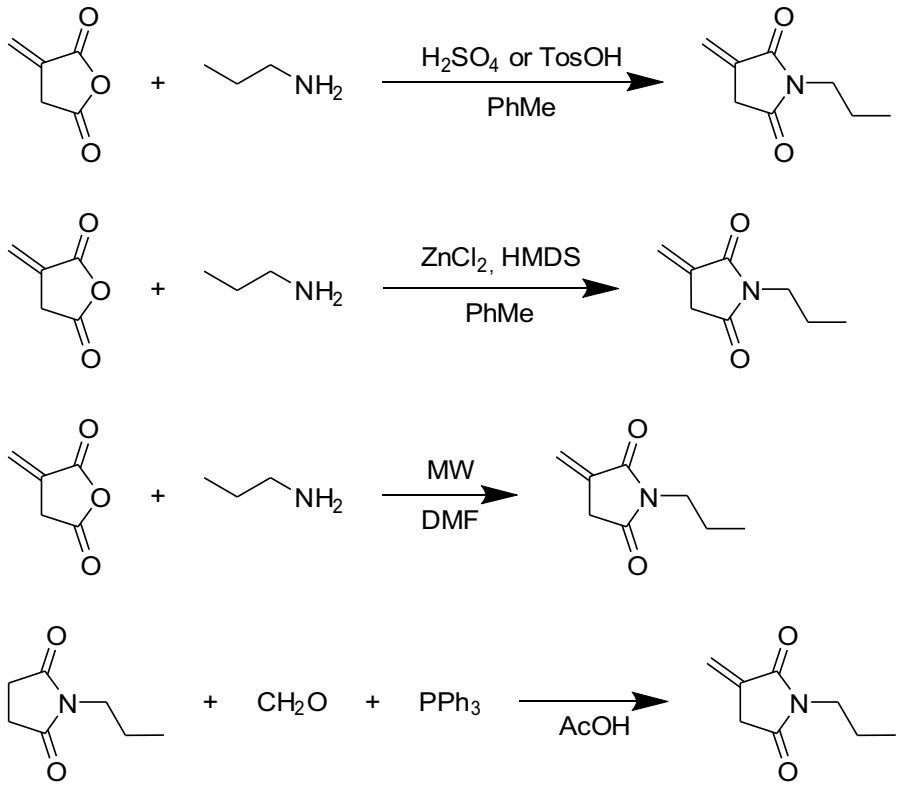

Figure 66: Further possible synthetic routes for **PrII** with acid catalysis [119-120], lewis acid catalyst [121], microwave irradiation [122] or with succinimide as starting material [123]

Synthetic pathways shown in Figure 66 are either known to give low yield or require sensitive/expensive reactants (*e.g.* HMDS) and thus are not suitable for syntheses of big batches.

Additionally, it is possible to protect the anhydride double bond before the reaction with an amine and afterwards regenerate the methylene group. But this approach would extend the needed syntheses by two steps.

However, since there is no need to attach exactly a propyl group on the N atom, it is easier to change the substituent. So benzylamine is used as alternative, due to its lower basicity (pK_a ~ 9.34) compared to propylamine (pK_a ~ 10.71). Hence, double bond isomerisation should be reduced significantly.

Die approbierte gedruckte Originalversion dieser Dissertation ist an der TU Wien Bibliothek verfügbar.
The approved original version of this doctoral thesis is available in print at TU Wien Bibliothek.
TU Bibliothek Your knowledge hub WIEN

2.2.1.2. Synthesis of ***BnII*** and ***BnCI***

Synthesis of II **BnII** and CI **BnCI** was conducted again according to patent WO 2005118537 [118] (see Figure 67 and also chapter 2.2.1.2 of the experimental part). At the same time always corresponding CI will form, because the more basic the amine is, the more effective is double bond isomerisation [120]. This also implies, that for syntheses of IIs always isomerisation occurs, if bases as reagents or catalysts are used.

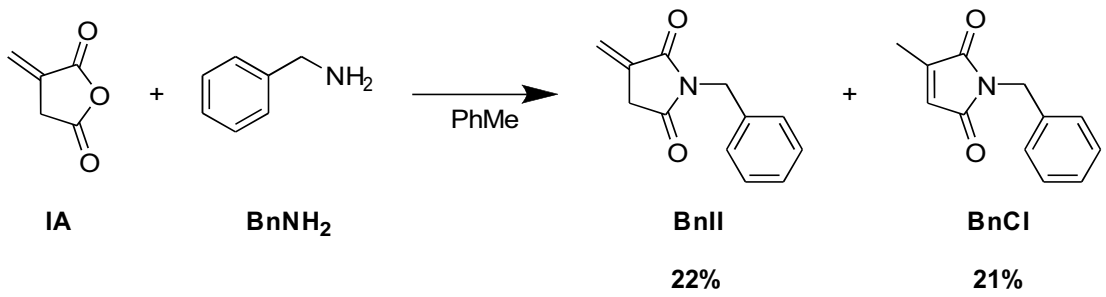

Figure 67: Synthesis of **BnII** and **BnCI**

However, it was possible to reduce the amount of isomerisation to approximately equimolar ratio of II and CI. Furthermore, obtained yields are higher due to less Michael addition. Separation of isomers is easily possible with column chromatography.

So finally it was possible to get a set of 3 different comparable imides for further characterisation, since corresponding MI **BnMI** is commercially available.

2.2.2. Volatility

For some potential applications like Hot-Lithography [124-125] monomers have to be stable and not volatile over some hours also at elevated temperatures. Therefore, volatility of used (co)monomers at different temperatures was measured with STA.

Die approbierte gedruckte Originalversion dieser Dissertation ist an der TU Wien Bibliothek verfügbar.
The approved original version of this doctoral thesis is available in print at TU Wien Bibliothek.
TU Bibliothek Your knowledge hub WIEN

Methacrylate **IBMA** was used as a reference, because it is a well-known reactive diluent in radical photopolymerisation, which is too volatile to be used at elevated temperatures.

So mass loss of (co)monomers, which are summarised in Figure 68, was measured for 3 h under N_2 atmosphere at 50 or 90 °C with STA. Thus, data given in Table 9 was obtained.

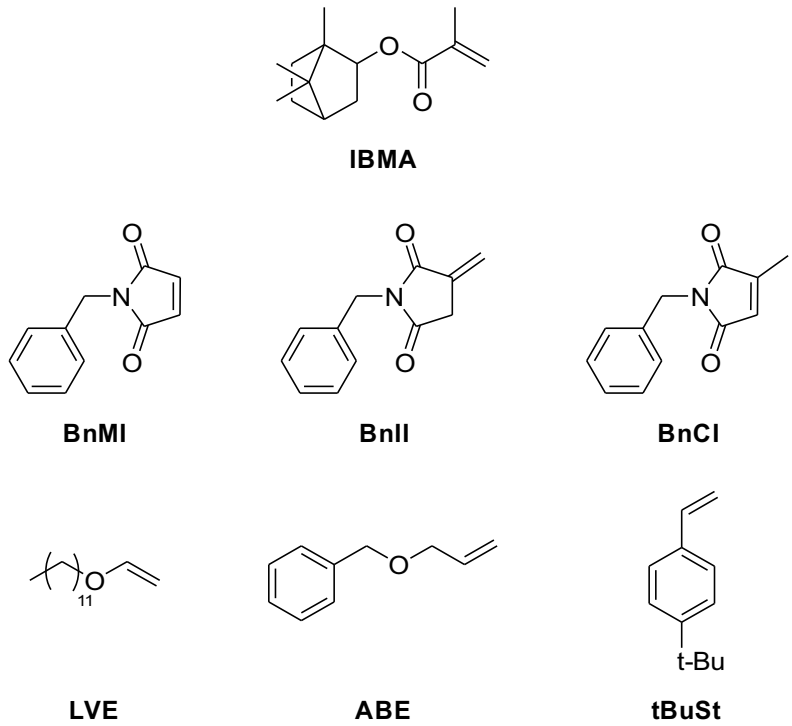

Figure 68: (Co)monomer structures

Die approbierte gedruckte Originalversion dieser Dissertation ist an der TU Wien Bibliothek verfügbar.
The approved original version of this doctoral thesis is available in print at TU Wien Bibliothek.

Table 9: Volatility of used monomers after 3 h

Monomer	Mass loss at 50 °C [%]	Mass loss at 90 °C [%]
IBMA	7	10
BnMI	n.d.*	1
BnII	n.d.*	< 1
BnCI	n.d.*	1
LVE	10	58
ABE	4	7
tBuSt	5	16**

* not determined

** polymerised

The experiments show that the investigated benzyl imides are not volatile – even at 90 °C. In contrast, already at 50 °C a significant amount of MA **IBMA** and of all 3 tested comonomers evaporates after 3 h. Therefore, formulations containing one of these comonomers can only be used at room temperature.

2.2.3. Comparison of itaconimide, citraconimide and maleimide

Finally, photo-DSC studies were performed to investigate the influence of double bond position on the reactivity in (co)polymerisation of obtained imides MI, II and CI. For a better comparability, all imides were substituted with a benzyl group on the N atom (MI **BnMI**, II **BnII** and CI **BnCI**, Figure 69). Furthermore, used comonomers (vinyl ether **LVE**, allyl ether **ABE** and styrene derivative **tBuSt**) are also shown in Figure 69.

Die approbierte gedruckte Originalversion dieser Dissertation ist an der TU Wien Bibliothek verfügbar.
The approved original version of this doctoral thesis is available in print at TU Wien Bibliothek.
TU Bibliothek Your knowledge hub WIEN

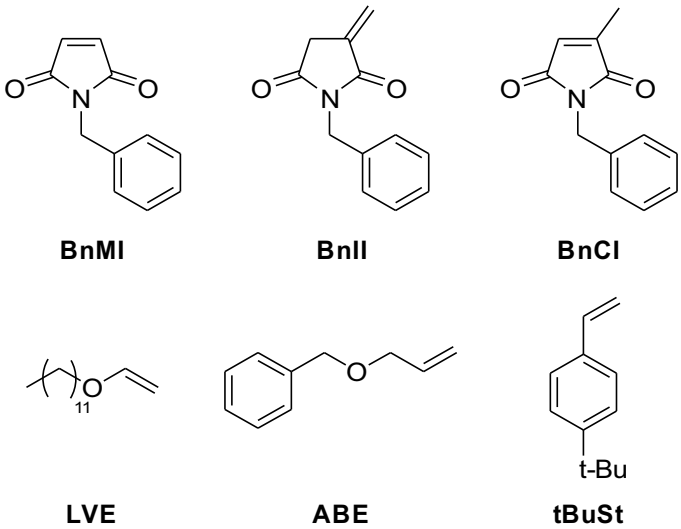

Figure 69: Structure of imides and used comonomers

Since MI **BnMI** is solid at room temperature (T_m = 69 °C) and not soluble in used comonomers, an additional second photo-DSC study was performed at 90 °C. But used comonomers are too volatile for elevated temperatures, thus only a comparison of the homopolymerisation of different imides **BnMI**, **BnII** and **BnCI** is possible.

Both photo-DSC studies were performed under following conditions:

- Equimolar concentration of imide and comonomer
- Temperature: 25 °C or 90 °C
- PI: 1 w% Ivocerin
- Irradiation: 400 – 500 nm
- ^{1}H-NMR spectroscopy and GPC of each sample

So photo-DSC curves shown in Figure 70 and summarised in Table 10 were measured at 25 °C.

Die approbierte gedruckte Originalversion dieser Dissertation ist an der TU Wien Bibliothek verfügbar.
The approved original version of this doctoral thesis is available in print at TU Wien Bibliothek.
TU Bibliothek Your knowledge hub WIEN

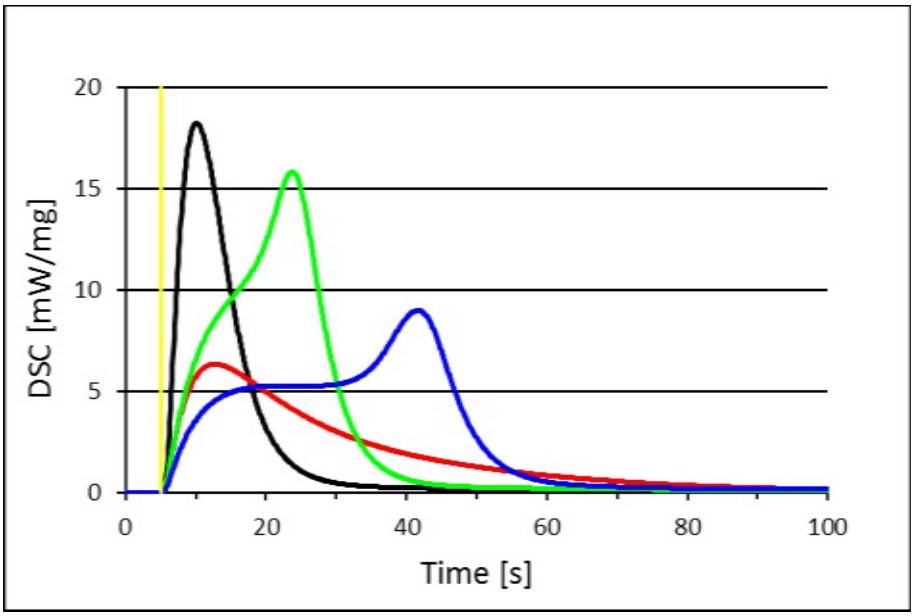

Figure 70: Photo-DSC curves at 25 °C of **BnII** without (—) and with **ABE** (—) or **tBuSt** (—) and **BnCI** with **tBuSt** (—); start of irradiation (—)

Table 10: Results of photo-DSC measurements at 25 °C, NMR spectroscopy and GPC measurements

Imide	Co-monomer	Photo-DSC			NMR spectroscopy		GPC	
		Peak max [s]	$t_{95\%}$ [s]	Area [J/g]	DBC imide [%]	DBC co-monomer [%]	M_n [kDa]	Đ [-]
BnII	-	5.5	35.2	177.7	85	-	24.7	3.4
	LVE	not miscible						
	ABE	7.6	77.7	183.0	96	83	6.7	2.1
	tBuSt	19.0	46.1	267.0	75	87	25.5	4.8
BnCI	-	10.9	186.8	34.4	0	-	-	-
	LVE	10.8	166.4	56.7	0	0	-	-
	ABE	10.1	157.4	28.0	0	0	-	-
	tBuSt	36.8	53.8	259.9	65	76	19.3	6.0
BnMI	-	solid						
	LVE	not soluble						
	ABE	not soluble						
	tBuSt	not soluble						

Die approbierte gedruckte Originalversion dieser Dissertation ist an der TU Wien Bibliothek verfügbar.
The approved original version of this doctoral thesis is available in print at TU Wien Bibliothek.
TU Bibliothek Your knowledge hub WIEN

As can be seen in Figure 70 and Table 10 above – and as expected from literature [119, 126-127] –, II **BnII** is much more reactive than CI **BnCI** due to the less sterically hindered 1,1-disubstituted double bond. Nevertheless, CI **BnCI** shows interestingly only a slightly reduced reactivity with St **tBuSt**. This behaviour makes the copolymerisation with styrene derivatives a lot more interesting and promising, because CIs are always formed during the syntheses of IIs. So it would make separation of the two simultaneously formed imide isomers unnecessary.

Additionally, homopolymerisation at 90 °C gave the DSC curves shown in Figure 71 and summarised in Table 11.

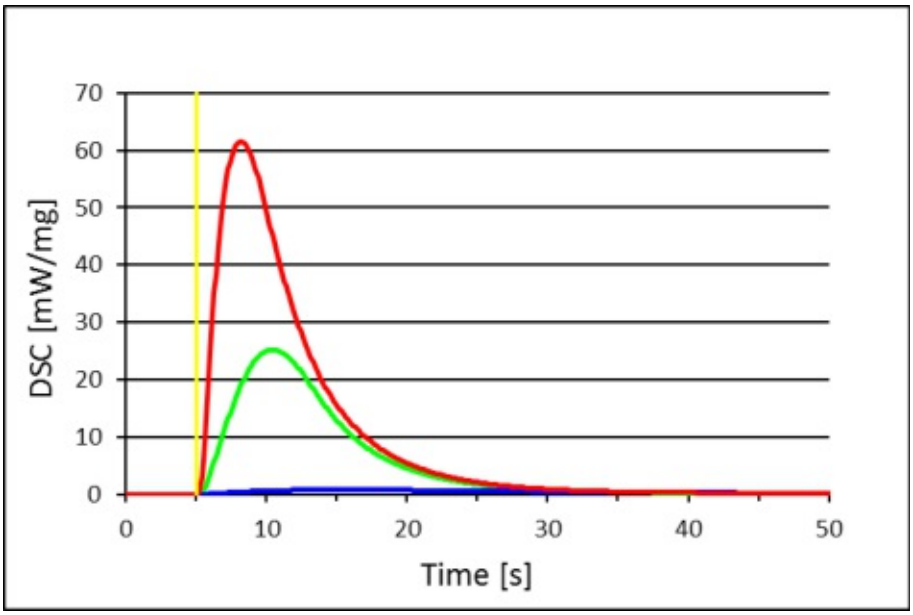

Figure 71: Photo-DSC curves at 90 °C of **BnII** (—), **BnCI** (—) and **BnMI** (—); start of irradiation (—)

Die approbierte gedruckte Originalversion dieser Dissertation ist an der TU Wien Bibliothek verfügbar.
The approved original version of this doctoral thesis is available in print at TU Wien Bibliothek.
TU Bibliothek Your knowledge hub WIEN

Table 11: Results of photo-DSC experiments at 90 °C, NMR spectroscopy and GPC measurements

Monomer	Photo-DSC			NMR spectroscopy	GPC	
	Peak max [s]	$t_{95\%}$ [s]	Area [J/g]	DBC [%]	M_n [kDa]	Đ [-]
BnII	5.5	22.2	239.1	98	36.1	1.9
BnCI	10.2	57.2	21.2	0	-	-
BnMI	3.2	18.3	455.1	not soluble		

Figure 71 and Table 11 underline again, that CI **BnCI** is less reactive than II **BnII**. Furthermore, the tested II **BnII** offers a high DBC and only a slightly slower reaction than the MI **BnMI**. Additionally, it can be seen, that (at least) homopolymerisation of maleimide **BnMI** is even faster than of the corresponding II. Since polymerised **BnMI** is not soluble any more, only the leachable part was measured with NMR spectroscopy and GPC to get an idea of minimum DBC and molecular weight. They showed a DBC of > 97% and a M_n of 42.1 kDa (3.0 PDI) of the soluble fraction, which is quite good for first preliminary tests.

2.2.4. Comparison of fumaric and maleic acid esters and maleimide

An additional photo-DSC study was performed to check if the ring structure of tested imides is needed to obtain high reactivity, because a lot of different monomers without this moiety (*e.g.* unsaturated ester) are commercially available and are also easier to synthesise.

Hence, two different unsaturated esters, which also possess activated double bonds with comparable structures but without ring strain, were chosen: fumaric and maleic acid esters (**DEF** and **DEM**, Figure 72). So information on the influence of double bond configuration can be gained at the same time. MI **PrMI** (Figure 72) is used for better comparability with studied esters.

Die approbierte gedruckte Originalversion dieser Dissertation ist an der TU Wien Bibliothek verfügbar.
The approved original version of this doctoral thesis is available in print at TU Wien Bibliothek.
TU Bibliothek Your knowledge hub WIEN

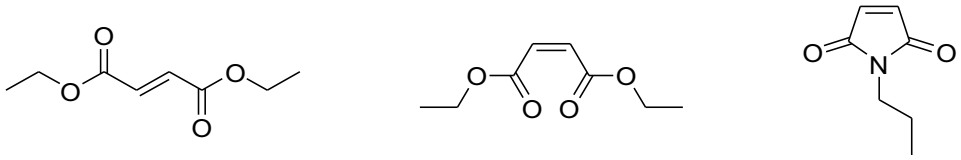

DEF **DEM** **PrMI**

Figure 72: Structures of **DEF**, **DEM** and **PrMI**

Furthermore, copolymerisation with vinyl ether **LVE**, allyl ether **ABE** and styrene derivative **tBuSt** is investigated as well (compare chapter 2.2.3).

Photo-DSC measurements were performed under following conditions:

- Equimolar concentration of ester/imide and comonomer
- Temperature: 25 °C
- PI: 1 w% Ivocerin
- Irradiation: 400 – 500 nm
- ^{1}H-NMR spectroscopy and GPC of each sample

The tests showed that only MI **PrMI** photopolymerises under these conditions with all comonomers. Thus, only the **PrMI** series is presented in Figure 73. In contrast, all gained data is summarised in Table 12.

Die approbierte gedruckte Originalversion dieser Dissertation ist an der TU Wien Bibliothek verfügbar.
The approved original version of this doctoral thesis is available in print at TU Wien Bibliothek.
TU Bibliothek Your knowledge hub WIEN

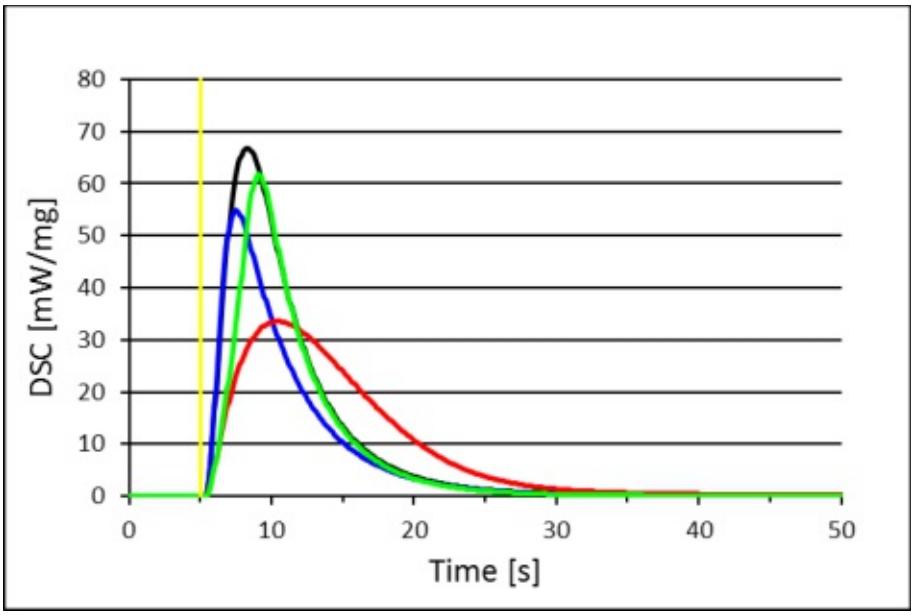

Figure 73: Photo-DSC curves of **PrMI** without (—) and with **LVE** (—), **ABE** (—) and **tBuSt** (—); start of irradiation (—)

Table 12: Results of photo-DSC, NMR spectroscopy and GPC measurements

Monomer	Co-monomer	Photo-DSC			NMR spectroscopy		GPC	
		Peak max [s]	$t_{95\%}$ [s]	Area [J/g]	DBC MI [%]	DBC co-monomer [%]	M_n [kDa]	Đ [-]
DEF	-	11.1	110.0	56.5	30	-	2.7	2.3
	LVE	not miscible						
	ABE	9.7	63.9	61.8	*	*	1.6	1.6
	tBuSt	11.8	100.3	152.9	70	92	15.2	5.6
DEM	-	10.2	66.9	27.7	11	-	0.9	1.5
	LVE	9.1	67.8	240.6	97	91	12.6	2.2
	ABE	8.5	59.0	36.4	*	*	1.2	1.3
	tBuSt	8.8	69.5	27.1	12	22	2.4	3.5
PrMI	-	3.2	20.9	427.6	not soluble			
	LVE	2.5	16.2	332.3	not soluble			
	ABE	5.6	22.7	394.9	not soluble			
	tBuSt	4.1	15.3	363.4	not soluble			

* poor solubility, thus no suitable spectra possible

Die approbierte gedruckte Originalversion dieser Dissertation ist an der TU Wien Bibliothek verfügbar.
The approved original version of this doctoral thesis is available in print at TU Wien Bibliothek.
TU Bibliothek Your knowledge hub WIEN

As can be seen in Table 12 above, fumaric and maleic esters **DEF** and **DEM** exhibit low reactivity. They yield only high conversions with St **tBuSt** or vinyl ether **LVE**, respectively. All other monomer combinations give some low molecular weight oligomers. This completely different reaction behaviour likely originates from their different *E/Z*-isomerisation and therefore sterical hindrance at the reaction centres. However, recorded NMR spectra of **DEF** and **DEM** samples are not that reliable due to a lot of overlapping peaks. So photo-DSC gives a lot more accurate comparison of monomer reactivities, although exact heats of polymerisation are not known for the different monomer combinations.
In contrast, maleimide **PrMI** exhibits a high reactivity with all tested comonomers. Unfortunately, polymers are not completely soluble, so no NMR spectra or GPC can be measured. Nevertheless, ^{1}H-NMR spectra of the soluble parts show no remaining MI double bonds, but still a high content of vinyl or allyl ether. On the other hand, the formulation containing St **tBuSt** has a significantly more similar consumption of the two monomers, which indicates better copolymerisation.

So it is demonstrated, that ring strain in the monomers with activated double bonds is necessary to reach high reactivity in (co)polymerisation. Hence, MIs in combination with Sts are investigated further, because commercial availability and also synthetic accessibility of these monomer classes are a lot better than for vinyl ether and allyl ether. So MI **PrMI** will be used due to its good miscibility and St derivative **tBuSt** is utilised as comonomer for further investigations.

2.2.5. Maleimide-styrene-methacrylate terpolymerisation

Fast and highly exothermic copolymerisation of MI and St monomers was already successfully shown in previous chapters. However, common photopolymer formulations usually consist of MAs, thus terpolymerisation of a MI-St-system with an MA is of interest as well. So experiments were performed

Die approbierte gedruckte Originalversion dieser Dissertation ist an der TU Wien Bibliothek verfügbar.
The approved original version of this doctoral thesis is available in print at TU Wien Bibliothek.
TU Bibliothek Your knowledge hub WIEN

to investigate the possibility of terpolymerisation of a MI-St-system with MAs, because this approach would make an incorporation into common methacrylic photopolymer resins easily possible.
Hence, RT-NIR-photorheology experiments were performed to study reactivity of MI-St-MA-terpolymerisation. Additionally, online information on the photopolymerisation reaction is obtained.

For this purpose MI **PrMI** and St **tBuSt** were used in equimolar ratio. In addition, MI-St-mixtures containing different MA **BnMA** concentrations (Figure 74; 10, 33 and 90 mol%) as well as pure **BnMA** were tested to check, if there is a threshold concentration for added monomers, which hinders copolymerisation/charge-transfer complexes of MI **PrMI** and St **tBuSt**.

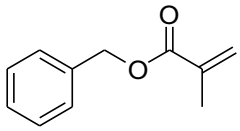

Figure 74: Structure of **BnMA**

PI TPO-L (Figure 75) is applied in a concentration of 0.2 w%, because this amount was estimated as maximum PI concentration for moulding thicker specimens without bubble formation. So more realistic results regarding potential applications can be achieved.

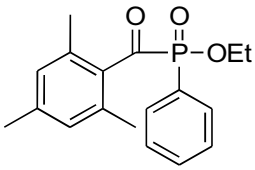

Figure 75: Structure of TPO-L

As it is not possible to distinguish between different C=C double bond signals in the MIR (~ 1630 cm^{-1}) and to meet absorption limits when tracking significant =C-H-absorption bands of MIs (~ 695 cm^{-1}), only NIR region can be used to

Die approbierte gedruckte Originalversion dieser Dissertation ist an der TU Wien Bibliothek verfügbar.
The approved original version of this doctoral thesis is available in print at TU Wien Bibliothek.
TU Bibliothek Your knowledge hub WIEN

monitor the photopolymerisation reaction. But unfortunately NIR peaks originating from double bond overtones are not fully separated (see Figure 76). Nevertheless, rheological information and also overall DBCs can be measured.

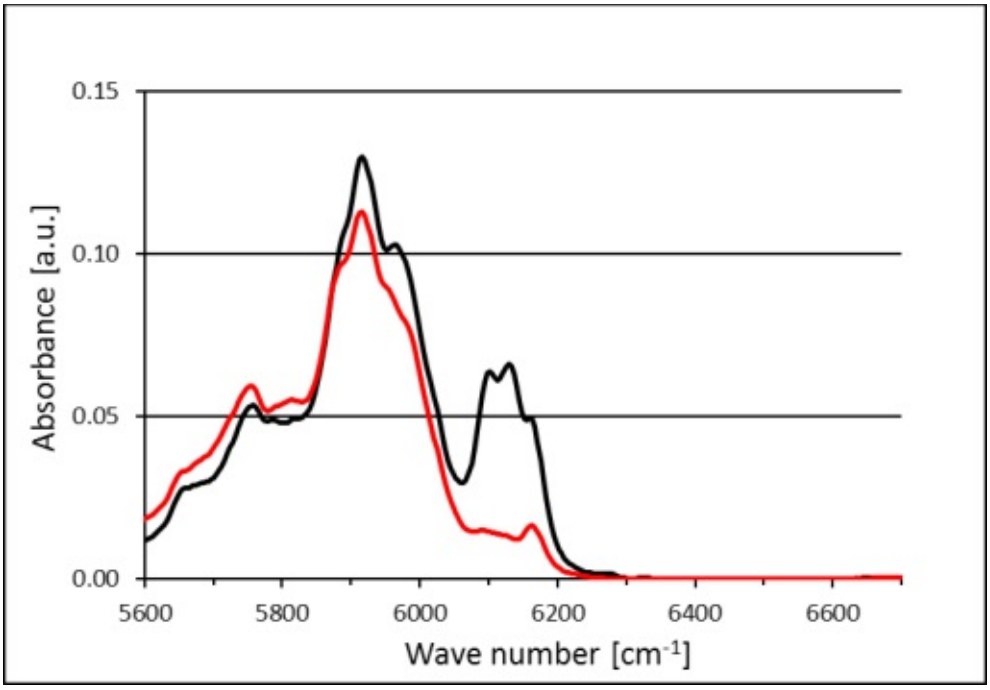

Figure 76: NIR spectra of an equimolar mixture of **PrMI**, **tBuSt** and **BnMA** before (—) and after irradiation (—)

The experiments were conducted with following measurements parameters:

- Equimolar concentrations of MI **PrMI** and St **tBuSt** containing 10, 33 or 90 mol% MA **BnMA**
- Temperature: 25 °C
- PI: 0.2 w% TPO-L
- Irradiation: 320 – 500 nm

So data shown in Figures 77-79 and summarised in Table 13 was obtained.

Die approbierte gedruckte Originalversion dieser Dissertation ist an der TU Wien Bibliothek verfügbar.
The approved original version of this doctoral thesis is available in print at TU Wien Bibliothek.
TU Bibliothek Your knowledge hub WIEN

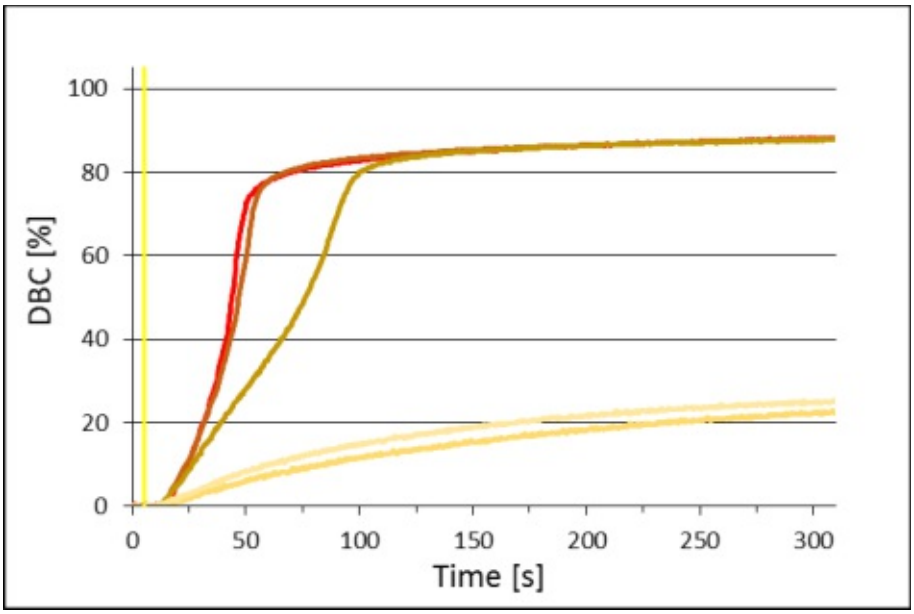

Figure 77: DBC of an equimolar mixture of **PrMI** and **tBuSt** without (—) and with 10 (—), 33 (—) or 90 mol% (—) **BnMA** and pure **BnMA** (—); start of irradiation (—)

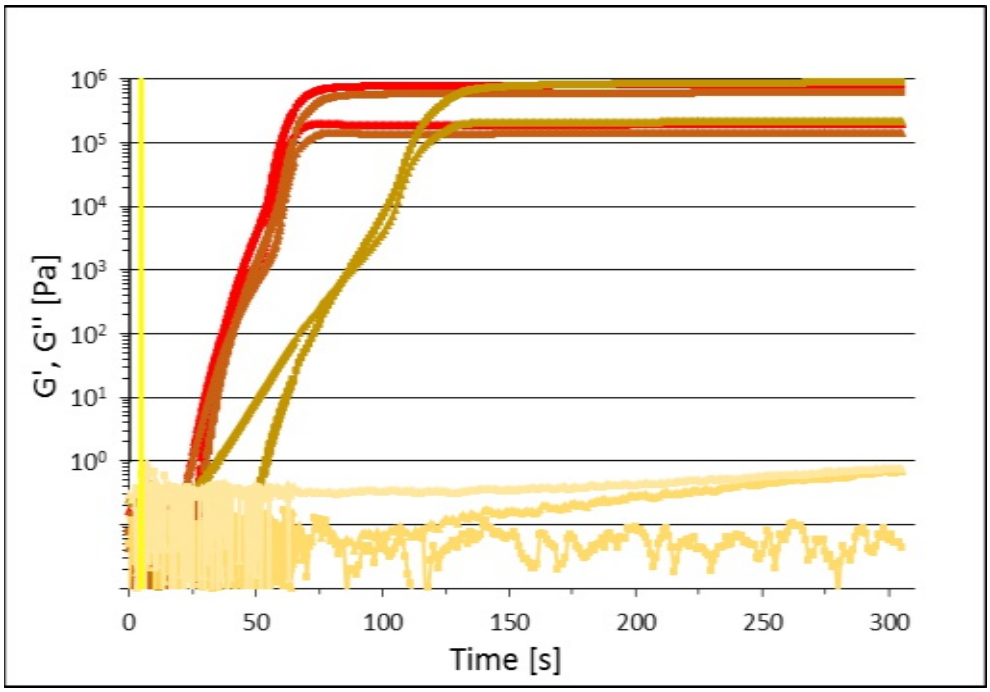

Figure 78: Storage modulus (—■—) and loss modulus (—▲—) of an equimolar mixture of **PrMI** and **tBuSt** without (—) and with 10 (—), 33 (—) or 90 mol% (—) **BnMA** and pure **BnMA** (—); start of irradiation (—)

Die approbierte gedruckte Originalversion dieser Dissertation ist an der TU Wien Bibliothek verfügbar.
The approved original version of this doctoral thesis is available in print at TU Wien Bibliothek.
TU Bibliothek Your knowledge hub WIEN

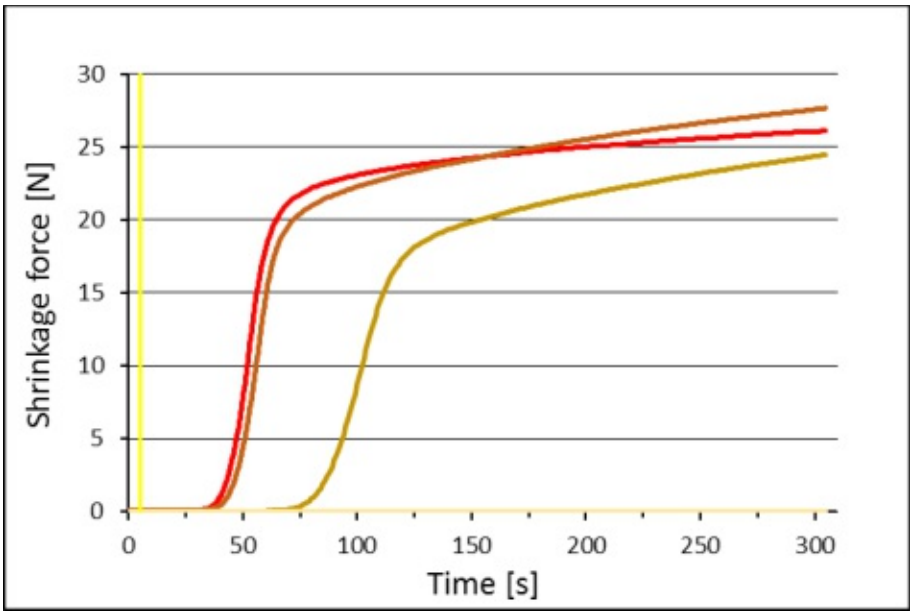

Figure 79: Evolution of shrinkage force of an equimolar mixture of **PrMI** and **tBuSt** without (—) and with 10 (—), 33 (—) or 90 mol% (—) **BnMA** and pure **BnMA** (—); start of irradiation (—)

Table 13: Results of photorheology measurements

Formulation [mol%]			R_p [%/s]	t_{gp} [s]	DBC_{gp} [%]	$t_{95\%}$ [s]	DBC_{end} [%]	Shrinkage force [N]
PrMI	**tBuSt**	**BnMA**						
50	50	0	1.2	34.1	37	112.0	89	28.6
45	45	10	1.1	39.4	41	102.4	89	27.0
33	33	33	0.8	82.7	64	118.9	87	23.7
5	5	90	0.2	-	-	271.7	23	0.0
0	0	100	0.2	-	-	257.0	26	0.0

As results above show, an increasing MA concentration leads to lower polymerisation rates and retardation of gelation, but also higher DBC at gel point can be achieved. However, the equimolar mixture of **PrMI** and **tBuSt** containing 90 mol% **BnMA** and pure MA do not solidify any more and also $t_{95\%}$ and final DBC decrease dramatically. Furthermore, $t_{95\%}$ and final DBC remain almost constant, if **BnMA** content does not get too high.

Die approbierte gedruckte Originalversion dieser Dissertation ist an der TU Wien Bibliothek verfügbar.
The approved original version of this doctoral thesis is available in print at TU Wien Bibliothek.
TU Bibliothek Your knowledge hub WIEN

Addition of a further reactive monomer induces – as expected – a retardation of the copolymerisation of MI and St due to probably disturbance of the charge-transfer complexes and furthermore of course also lower concentrations. On the other hand, storage stability is increased of resins with high MA concentration (> 3 months), while the pure equimolar mixture of **PrMI** and **tBuSt** polymerises already after few days.

Finally, Figure 76 already indicates, that DBCs of MI and St are higher than MA DBC. Thus, peak deconvolution was performed and the DBCs, which are listed in Table 14, were calculated.

Table 14: Peak deconvolution results

Formulation [mol%]			$DBC_{photorheology}$ [%]	DBC_{MI} [%]	DBC_{St} [%]	DBC_{MA} [%]
PrMI	**tBuSt**	**BnMA**				
50	50	0	89	94	88	-
45	45	10	89	93	87	82
33	33	33	87	96	91	67
5	5	90	23	25	22	26
0	0	100	26	-	-	26

As can be seen in Table 14 DBCs determined with peak deconvolution show the same trends and are approximately in accordance with the overall DBCs estimated with the IR spectrometer of the NIR-photorheology device. The obtained results demonstrate once more, that higher additive contents interfere with the MI-St-copolymerisation, because MI and St DBCs decrease. Furthermore, **BnMA** conversion is reduced as well at lower **PrMI/tBuSt** concentrations. So MA homopolymerisation seems to be less efficient than copolymerisation with the MI/St monomers under the applied conditions.

Die approbierte gedruckte Originalversion dieser Dissertation ist an der TU Wien Bibliothek verfügbar.
The approved original version of this doctoral thesis is available in print at TU Wien Bibliothek.
TU Bibliothek Your knowledge hub WIEN

Since preliminary experiments gave very promising results like high reactivity and high double bond conversions, a closer look should be taken into resin characteristics, photopolymerisation reaction and also material properties of a MI-St-system based on MI **PrMI** and St **tBuSt** (→ model MI-St-system MISt1).

2.3. Model maleimide-styrene-system (**MISt1**)

Preliminary studies showed the high potential of MI-St-copolymerisation (see chapter 2.2). So further investigations will be conducted to test more chemical but also (thermo)mechanical properties of this new class of materials.

Therefore, one formulation was selected for an expanded chemical and (thermo)mechanical study to gain further insights into a model system. Thus, St derivative **tBuSt** is used as comonomer with MI **PrMI**. Both monomers were always used in equimolar ratio to promote strict alternating copolymerisation (→ MI-St-system 1, **MISt1**).

Furthermore, a monofunctional methacrylate (**IBMA**) will be tested for comparison with **MISt1**, because methacrylates are typical monomers for photopolymerisation for various applications.

Additionally, BUNA CB24 (a > 96% *cis*-1,4-polybutadiene from Arlanxeo, **CB24**) was added as a filler and to increase toughness (compare ABS). **CB24** has a molecular weight (M_n) of 180 kDa and a polydispersity of 2.1.

TPO-L was used again as photoinitiator in a concentration of 0.2 w%, because higher contents or more reactive photoinitiators (like *e.g.* Ivocerin) lead to bubble formation during curing of thicker specimens for mechanical tests.

First of all, the maximum soluble amount of BR **CB24** in MI-St-system **MISt1** was estimated. At higher concentrations (> ~ 20 w%) **CB24** was swollen with **MISt1** monomers instead of rubber being dissolved in the resin. Additionally,

Die approbierte gedruckte Originalversion dieser Dissertation ist an der TU Wien Bibliothek verfügbar.
The approved original version of this doctoral thesis is available in print at TU Wien Bibliothek.
TU Bibliothek Your knowledge hub WIEN

formulations with a BR content above 50 w% are not processable any more. Hence, for all experiments **MISt1** containing 0, 10, 20, 30 and 50 w% **CB24** is used. Similar mixtures with methacrylate **IBMA** were tested for comparison.
Following nomenclature for formulations will be used to facilitate reading: resin "**M_x**" represents monomer "M" (either MI-St-system **MISt1** or reference MA **IBMA**), which contains a BR **CB24** concentration of x w%.

2.3.1. Volatility

As already mentioned in chapter 2.2.2 before, volatility of monomers is a crucial property for many applications.
Since used St derivative **tBuSt** in **MISt1** and MA **IBMA** were already tested regarding their volatility in chapter 2.2.2, only MI **PrMI** had to be measured.

So mass loss of MI **PrMI** was measured for 3 h under N_2 atmosphere at 50 or 90 °C with STA.
Thus, data listed in Table 15 was obtained. Furthermore, MA **IBMA** and comonomer St **tBuSt** are also shown.

Table 15: Volatility of used monomers

Monomer	Mass loss at 50 °C [%]	Mass loss at 90 °C [%]
IBMA	7	10
PrMI	9	53
tBuSt	5	16*

* polymerised

As can be seen clearly above, MI **PrMI**, St **tBuSt** and MA **IBMA** show significant mass loss already at 50 °C over 3 h. Therefore, formulations based on **MISt1** or **IBMA** can be used only at room temperature.

Die approbierte gedruckte Originalversion dieser Dissertation ist an der TU Wien Bibliothek verfügbar.
The approved original version of this doctoral thesis is available in print at TU Wien Bibliothek.
TU Bibliothek Your knowledge hub WIEN

2.3.2. Storage stability

Storage stability of (photo)polymerisable formulations is not only important for daily use in research but even more crucial for industrial applications. Hence, some stability tests of **MISt1** were performed.

Therefore, **MISt1_0** resin (**MISt1** without rubber **CB24**) was stored without additional inhibitors under air and under light protection at room temperature. Stability of the formulation was assessed by periodically recording ^{1}H-NMR spectra. Reference monomer MA **IBMA_0** was not tested, because MAs are known to be storage stable at room temperature over years.

The spectra do not change over 3 days, but on the 4th day already some solids can be seen optically (Figure 80), which are not fully soluble in $CDCl_3$ any more. This result is in accordance with previous photo-DSC experiments (compare chapters 2.2.3 and 2.2.4), where samples containing MIs are also not soluble after polymerisation.

Figure 80: MISt1_0 formulation after 4 days

So sufficient storage stability of resins based on **MISt1** is given for further experiments. If this instability is too high for a certain application, there is still the possibility to add stabilizers.

Die approbierte gedruckte Originalversion dieser Dissertation ist an der TU Wien Bibliothek verfügbar.
The approved original version of this doctoral thesis is available in print at TU Wien Bibliothek.
TU Bibliothek Your knowledge hub WIEN

2.3.3. Viscosity

Another important property of resins is their viscosity, because if it is too high processing becomes challenging.

Since monomers used in **MISt1** and **IBMA** are highly volatile, viscosities were only measured at room temperature with a rheometer. Furthermore, it has to be mentioned, that only resins with a BR **CB24** content below 20 w% can be tested, because higher concentrations give a rubber swollen with monomers instead of a liquid formulation. Hence, no rheological measurements are possible.

So viscosities given in Table 16 were measured at 25 °C.

Table 16: Viscosities of tested resins

Formulation	Viscosity [mPa s]
MISt1_0	1
MISt1_10	5240
MISt1_20	28700
IBMA_0	7
IBMA_10	10790
IBMA_20	33200

As can be seen in Table 16 addition of high molecular weight **CB24** induces a strong increase in viscosity. Nevertheless, viscosity of resins based on **MISt1** is always lower than comparable **IBMA**-based ones.

2.3.4. Potential self-initiation

First of all, **PrMI** and **MISt1** formulations were tested on a Photo-DSC to exclude self-initiation under the used irradiation conditions, which is known for exposure of MIs, MIs combined with photosensitizers and tertiary amines or MI-St-

Die approbierte gedruckte Originalversion dieser Dissertation ist an der TU Wien Bibliothek verfügbar.
The approved original version of this doctoral thesis is available in print at TU Wien Bibliothek.
TU Bibliothek Your knowledge hub WIEN

complexes to UV-light of a broadband Hg-bulb [128-132]. Therefore, resins without PI and with a type II PIS **BP** (without and with **MDEA**, Figure 81) were studied.

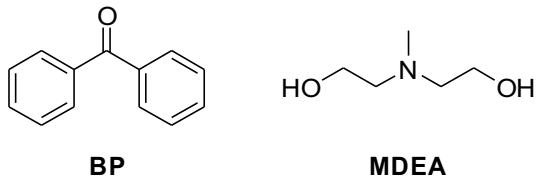

Figure 81: Structures of **BP** and **MDEA**

Photo-DSC experiments were conducted under the following conditions:

- Temperature: 25 °C
- PI (and coinitiator) concentration: 1 w%
- Irradiation: 320 – 500 nm
- ^{1}H-NMR spectroscopy and GPC of each sample

So results listed in Table 17 were obtained.

Table 17: Results of photo-DSC, NMR spectroscopy and GPC measurements

Monomer	PI	Photo-DSC			NMR spectroscopy		GPC	
		Peak max [s]	$t_{95\%}$ [s]	Area [J/g]	DBC MI [%]	DBC St [%]	M_n [kDa]	Đ [-]
PrMI	-	-	-	-	0	-	-	-
PrMI	**BP**	-	-	-	0	-	-	-
PrMI	**BP + MDEA**	-	-	-	0	-	-	-
MISt1_0	-	-	-	-	0	0	-	-

The data presented in Table 17 shows, that no photopolymerisation occurs in **PrMI** as well as **MISt1_0** without PI, with sensitizer **BP** or with a type II PIS (**BP** and **MDEA**) at the used irradiation conditions. Interestingly, 20 years ago most prominent Hoyle and Jönsson [128-131] but also others [132-134] always described MI and MI-comonomer acceptor-donor charge-transfer complexes as self-initiating monomers or already as PI *e.g.* for photopolymerisation of

Die approbierte gedruckte Originalversion dieser Dissertation ist an der TU Wien Bibliothek verfügbar.
The approved original version of this doctoral thesis is available in print at TU Wien Bibliothek.
TU Bibliothek Your knowledge hub WIEN

acrylates. In contrast, these results now support data in a new publication from Friesen *et al.* [135], where perfluorated MIs are utilised as self-initiating monomers also with an Omnicure UV-lamp system. But they had to use unfiltered UV-light of the Hg-bulb to initiate photopolymerisation. If a filter was applied, no polymerisation occurred without addition of a radical PI (Darocur 1173).

2.3.5. Photo-DSC

Photo-DSC studies were performed to investigate the reactivity of **MISt1** containing different amounts of BR **CB24** and to check, if there is a change in copolymerisation kinetics due to the presence of the rubber. In addition, MA **IBMA** was again used as reference methacrylic monomer.
Furthermore, MI **PrMI** without comonomer was measured as second reference and for comparison with preliminary studies, where another PI(-concentration) and irradiation conditions were applied (compare chapter 2.2.4).

Photo-DSC experiments were executed under the following conditions:

- Temperature: 25 °C
- PI: 0.2 w% TPO-L
- Irradiation: 320 – 500 nm
- ^{1}H-NMR spectroscopy and GPC of each sample

So results depicted in Figures 82-83 and summarised in Table 18 were measured.

Die approbierte gedruckte Originalversion dieser Dissertation ist an der TU Wien Bibliothek verfügbar.
The approved original version of this doctoral thesis is available in print at TU Wien Bibliothek.
TU Bibliothek Your knowledge hub WIEN

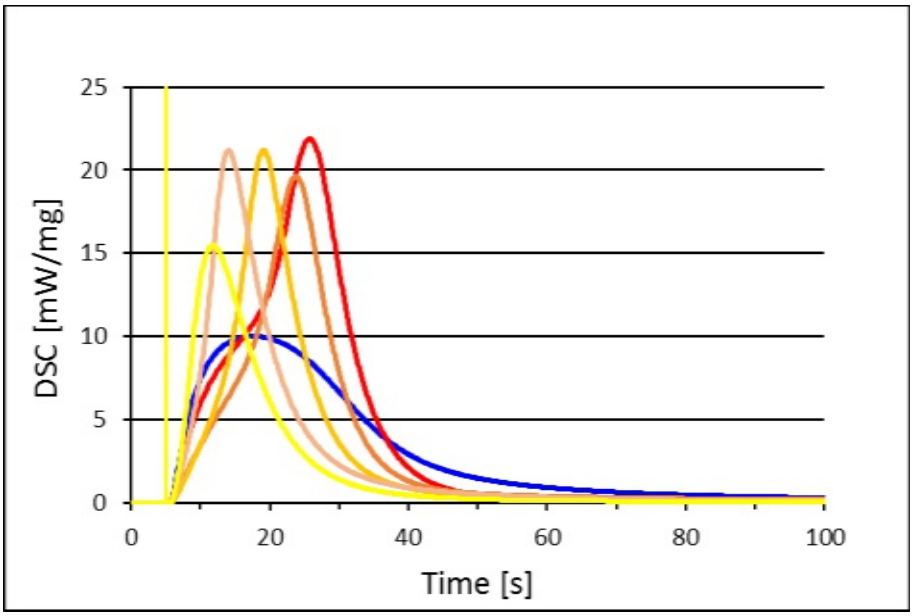

Figure 82: Photo-DSC curves of **PrMI** (—) and **MISt1** without (—) and with 10 (—), 20 (—), 30 (—) or 50 w% (—) **CB24**; start of irradiation (—)

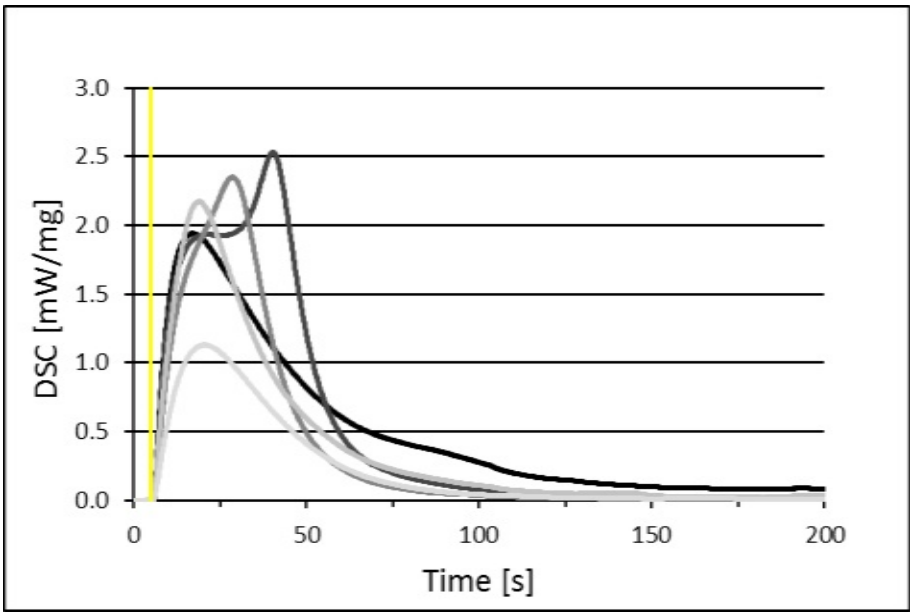

Figure 83: Photo-DSC curves of **IBMA** without (—) and with 10 (—), 20 (—), 30 (—) or 50 w% (—) **CB24**; start of irradiation (—)

Die approbierte gedruckte Originalversion dieser Dissertation ist an der TU Wien Bibliothek verfügbar.
The approved original version of this doctoral thesis is available in print at TU Wien Bibliothek.
TU Bibliothek Your knowledge hub WIEN

Table 18: Results of photo-DSC, NMR spectroscopy and GPC measurements of **PrMI**, **MISt1** and **IBMA** formulations

Formulation	Photo-DSC			NMR spectroscopy		GPC	
	Peak max [s]	$t_{95\%}$ [s]	Area [J/g]	DBC MI/MA [%]	DBC co-monomer [%]	M_n [kDa]	Đ [-]
PrMI	12.7	82.3	313.3	not soluble		not soluble	
MISt1_0	21.1	41.0	372.2	not soluble		not soluble	
MISt1_10	18.7	63.1	306.8	not soluble		not soluble	
MISt1_20	14.3	57.9	288.0	not soluble		not soluble	
MISt1_30	9.1	53.6	262.5	not soluble		not soluble	
MISt1_50	7.2	30.6	183.7	not soluble		not soluble	
IBMA_0	11.9	176.9	94.6	47	-	37.4	6.6
IBMA_10	35.4	91.9	101.2	52	-	38.1	8.7
IBMA_20	22.0	92.6	87.8	53	-	43.4	8.1
IBMA_30	14.0	120.5	74.1	55	-	48.7	11.1
IBMA_50	16.0	84.6	42.1	31	-	69.6	8.5

As can be seen in Table 18, **MISt1** formulations interestingly show a reduction in time to reach peak maximum with an increasing polybutadiene content, whereas $t_{95\%}$ is higher with added **CB24**, but decreases with increasing BR content. These effects can be attributed to the increased viscosities, which originate from higher rubber amounts, and also because cross-linking reactions may occur with **CB24** double bonds.

In contrast, no tendency can be seen in photo-DSC data of **IBMA** resins. Only DBC stays constant, except for the highest **CB24** concentration, where it drops probably due to the high viscosity of the resin. Interestingly, only the formulations containing 10 w% (and also very weak 20 w%) BR exhibit a Trommsdorff effect and therefore peak maximum is delayed. On the other hand, molecular weight increases with higher polybutadiene **CB24** content.

Die approbierte gedruckte Originalversion dieser Dissertation ist an der TU Wien Bibliothek verfügbar.
The approved original version of this doctoral thesis is available in print at TU Wien Bibliothek.
TU Bibliothek WIEN Your knowledge hub

However, insolubility of **pMISt1** samples need additional experiments, since as they should build polymer chains, they should be soluble in suitable solvents. Nevertheless, studies on the photopolymerisation reaction will be completed, before polymer insolubility of the model MI-St-system is investigated further.

2.3.6. RT-NIR-photorheology

RT-NIR-photorheology measurements were performed to further characterise **MISt1** resins and to get some more insights into photopolymerisation of MI-St-BR-based mixtures.

Additionally, **IBMA** was again used for comparison with a monofunctional MA, since this monomer class is the most prominent in industry for radically curable formulations. Furthermore, MI **PrMI** without comonomer was measured for comparison with preliminary studies, where another PI(-concentration) and irradiation conditions were applied (compare chapter 2.2.4).

Finally, it should be mentioned again, that only resins with a BR **CB24** content below 20 w% could be tested, because higher concentrations give a rubber swollen with monomers instead of a liquid formulation. Hence, no rheological measurements are possible (compare also chapter 2.3.3).

The experiments were conducted under standard measurements parameters:

- Temperature: 25 °C
- PI: 0.2 w% TPO-L
- Irradiation: 320 – 500 nm

Furthermore, it has to be mentioned once more, that it is not possible to distinguish between different double bond signals in the MIR as well as to meet absorption limits when tracking significant =C-H-absorption bands of MIs (~ 695 cm^{-1}). So only NIR region can be used to monitor the photopolymerisation reaction. But IR peaks in the NIR region originating from first DB overtones from MI (~ 6100 cm^{-1}) and St (~ 6130 cm^{-1}) are not fully separated, due to strong

Die approbierte gedruckte Originalversion dieser Dissertation ist an der TU Wien Bibliothek verfügbar.
The approved original version of this doctoral thesis is available in print at TU Wien Bibliothek.
TU Bibliothek Your knowledge hub WIEN

overlapping (in contrast signal of polybutadiene **CB24** does not intersect): Figure 84. Nevertheless, rheological information and overall conversion of both reactive monomers can be measured.

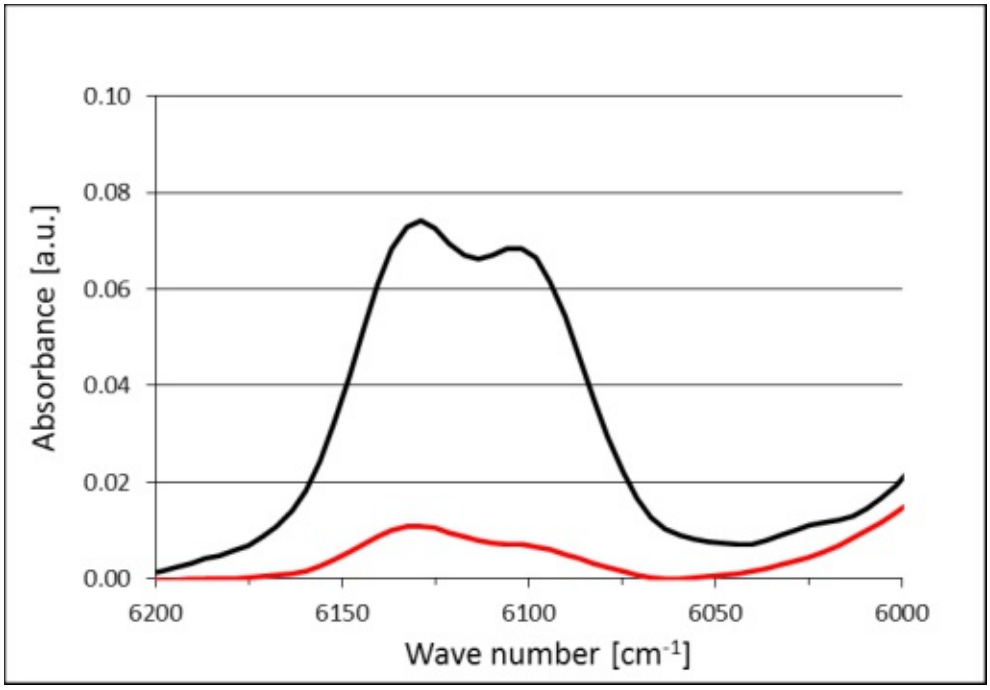

Figure 84: Overlapping of double bond signals of **PrMI** and **tBuSt** before (—) and after irradiation (—)

So the data presented in Figures 85-87 and summarised in Table 19 was obtained.

Die approbierte gedruckte Originalversion dieser Dissertation ist an der TU Wien Bibliothek verfügbar.
The approved original version of this doctoral thesis is available in print at TU Wien Bibliothek.
TU Bibliothek Your knowledge hub WIEN

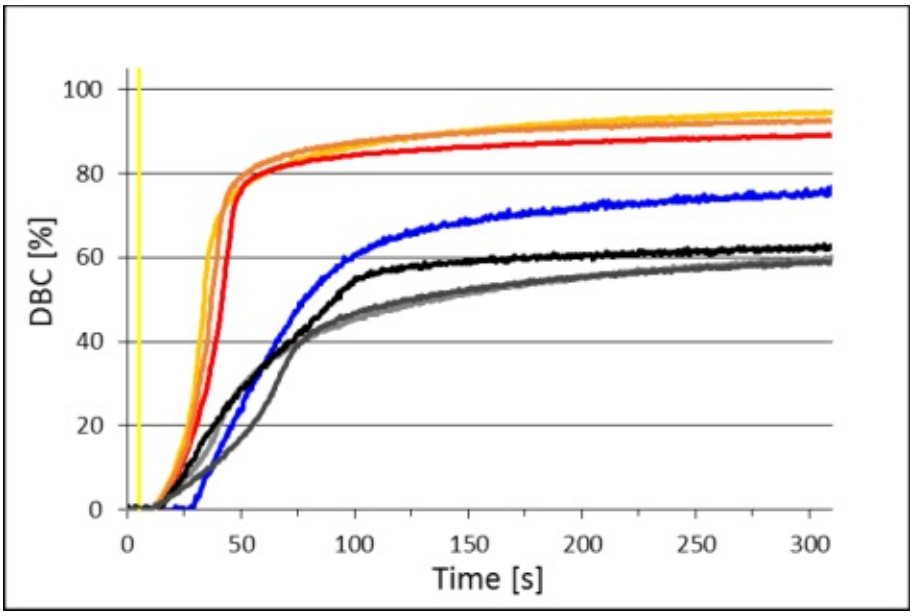

Figure 85: DBC of **PrMI** (—), **MISt1** without (—) and with 10 (—) or 20 w% (—) **CB24** and **IBMA** without (—) and with 10 (—) or 20 w% (—) **CB24**; start of irradiation (—)

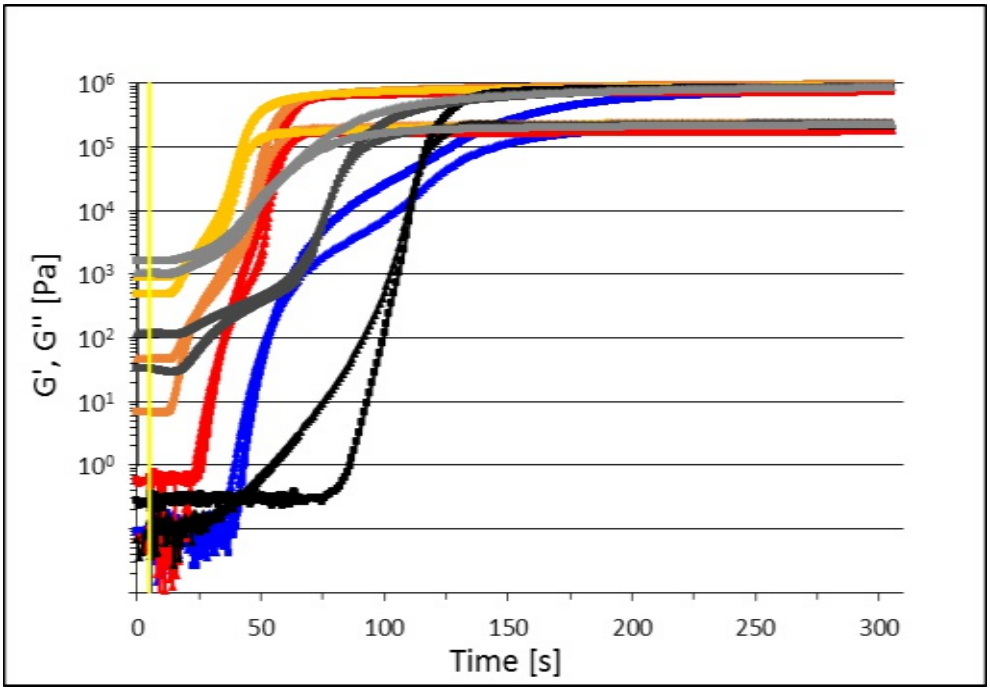

Figure 86: Storage modulus (—■—) and loss modulus (—▲—) of **PrMI** (—), **MISt1** without (—) and with 10 (—) or 20 w% (—) **CB24** and **IBMA** without (—) and with 10 (—) or 20 w% (—) **CB24**; start of irradiation (—)

Die approbierte gedruckte Originalversion dieser Dissertation ist an der TU Wien Bibliothek verfügbar.
The approved original version of this doctoral thesis is available in print at TU Wien Bibliothek.
TU Bibliothek Your knowledge hub WIEN

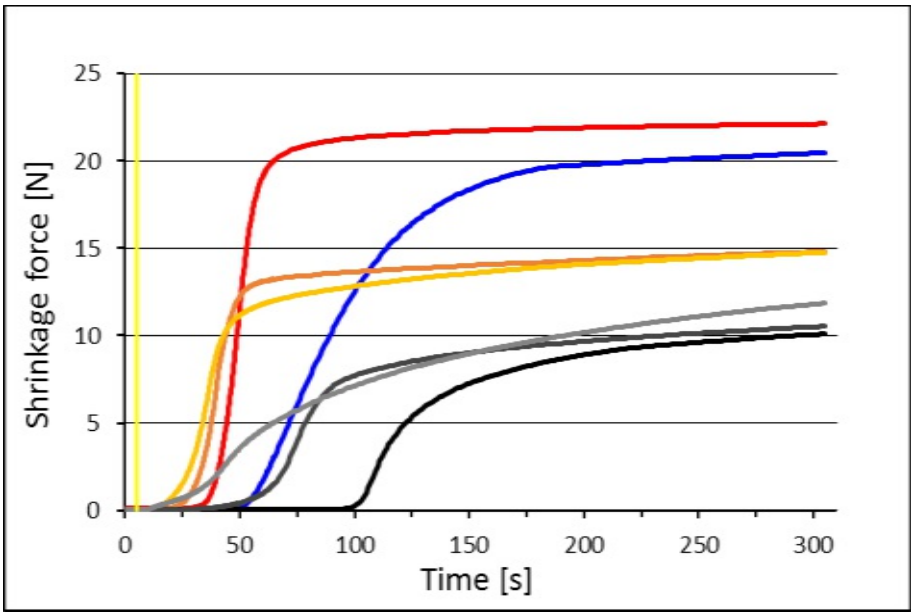

Figure 87: Evolution of shrinkage force of **PrMI** (—), **MISt1** without (—) and with 10 (—) or 20 w% (—) **CB24** and **IBMA** without (—) and with 10 (—) or 20 w% (—) **CB24**; start of irradiation (—)

Table 19: Results of photorheology measurements

Formulation	R_p [%/s]	t_{gp} [s]	DBC_{gp} [%]	$t_{95\%}$ [s]	DBC_{end} [%]	Shrinkage force [N]
PrMI	1.1	52.4	32	193.3	75	20.2
MISt1_0	1.1	31.2	36	100.9	88	22.9
MISt1_10	1.1	21.2	17	108.5	92	14.6
MISt1_20	1.2	19.3	15	141.0	95	15.5
IBMA_0	0.8	120.5	55	166.6	60	9.1
IBMA_10	0.4	78.5	43	211.2	59	10.5
IBMA_20	0.5	46.5	30	225.0	60	11.8

The conversion curves in Figure 85 support again our approach to use MI-St-copolymerisation instead of pure maleimide homopolymerisation, because the copolymerisation is faster (R_p, t_{gp} as well as $t_{95\%}$), due to less retardation and reaches higher DBCs in the end. On the other hand, produced shrinkage stress is slightly higher, but it is with ~ 23 N not very high.

Die approbierte gedruckte Originalversion dieser Dissertation ist an der TU Wien Bibliothek verfügbar.
The approved original version of this doctoral thesis is available in print at TU Wien Bibliothek.
TU Bibliothek Your knowledge hub WIEN

As expected addition of polybutadiene **CB24** yields in both systems to faster gelation at lower DBCs, while the DBC_{end} remains nearly unchanged (and $t_{95\%}$ little bit increased). Beyond that, it significantly reduces formed shrinkage stress in **MISt1**.

A comparison with results of **IBMA** is not really fair, because the used photoinitiator concentration is optimised for **MISt1** and too low for **IBMA**, but as already explained in the beginning higher PI contents give bubbles when curing thicker samples of **MISt1_0**. However, a Trommsdorff effect can be observed again for both formulations containing 10 w% BR and **IBMA_20**, as it was already seen in the photo-DSC studies in chapter 2.3.5.

Finally, shrinkage force is measured as well, but the absolute values are quite low (< 23 N), due to the monofunctionality of the tested monomers and therefore late gelation at high DBCs.

In addition, peak deconvolution was performed to check literature known very efficient alternating copolymerisation of MI and St [116, 136-138]. Therefore, DBCs, which are listed in Table 20, were calculated for each monomer.

Table 20: Results of photorheology measurements and peak deconvolution

Formulation	$DBC_{photorheology}$ [%]	MI DBC [%]	St DBC [%]
MISt1_0	88	90	87
MISt1_10	92	93	89
MISt1_20	95	97	93

As can be seen in Table 20, DBCs calculated with peak deconvolution show the same trend and are in accordance with the overall DBCs estimated with IR spectroscopy from NIR-photorheology. Furthermore, effective alternating copolymerisation of MIs and Sts could be confirmed, since very similar DBCs are found for both monomers.

Die approbierte gedruckte Originalversion dieser Dissertation ist an der TU Wien Bibliothek verfügbar.
The approved original version of this doctoral thesis is available in print at TU Wien Bibliothek.
TU Bibliothek Your knowledge hub WIEN

Finally, all polymerised **pMISt1** samples cannot be dissolved fully although they actually should be soluble in suitable solvents. Thus, swellability studies were performed to clarify this surprising finding.

2.3.7. Swellability

Since all **pMISt1**-based polymers are only swelling very strongly, but do not fully dissolve, it seems that cross-linking may occur in the MI-St-system. Polymerised samples are also not soluble in the monomers **PrMI** or **tBuSt**. Furthermore, the influence of *cis*-1,4-polybutadiene **CB24** double bonds on swellability behaviour should also be examined. In contrast, all **pIBMA** samples without and with BR **CB24** are still soluble. So swellability tests were performed to finally clarify, if cross-linking reactions in the MI-St-BR-system happen.

Therefore, harsh solvents for swellability tests (an apolar and a polar one) were used to definitely prove insolubility, rather than checking degree of swelling: $CHCl_3$ and EtOH. Formulations based on **IBMA** could not be investigated for comparison, because they are completely soluble in both tested solvents.

So polymerised samples were submerged for 7 d in $CHCl_3$ or EtOH. Sample mass was recorded before and after swelling and after drying (see chapter 2.3.7 of the experimental part).
Thus, swellability and gel fraction in $CHCl_3$ (Table 21) and EtOH (Table 22) were calculated.

Die approbierte gedruckte Originalversion dieser Dissertation ist an der TU Wien Bibliothek verfügbar.
The approved original version of this doctoral thesis is available in print at TU Wien Bibliothek.
TU Bibliothek Your knowledge hub WIEN

Table 21: Swellability and gel fraction in $CHCl_3$

Sample	Swellability [%]	Gel fraction [%]
pMISt1_0	1648	87.5
pMISt1_10	1213	88.6
pMISt1_20	1107	92.5
pMISt1_30	944	95.1
pMISt1_50	962	96.0

Table 22: Swellability and gel fraction in EtOH

Sample	Swellability [%]	Gel fraction [%]
pMISt1_0	129.8	93.7
pMISt1_10	125.0	92.6
pMISt1_20	121.8	96.3
pMISt1_30	115.0	98.2
pMISt1_50	109.9	98.9

As can be seen in Tables 21 and 22, swellability tests show, that pure **pMISt1_0** swells extremely, but does not dissolve. So interestingly cross-linking in **MISt1**-based systems occurs, which can be supposedly caused by hydrogen abstraction reactions either next to the N atom of the MI **PrMI** or maybe from the MI backbone (Figure 88).

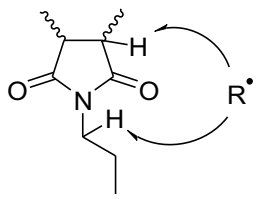

Figure 88: Possible cross-linking mechanisms

Die approbierte gedruckte Originalversion dieser Dissertation ist an der TU Wien Bibliothek verfügbar.
The approved original version of this doctoral thesis is available in print at TU Wien Bibliothek.
TU Bibliothek Your knowledge hub WIEN

In addition, data shows, that higher BR concentrations give lower degrees of swelling and higher gel fractions. So network density increases with higher rubber content. Furthermore, leachable fractions are smaller than BR content. Hence, these results prove that polybutadiene **CB24** is definitely covalently linked with the **pMISt1** matrix.

Finally, higher swellability values in $CHCl_3$ than EtOH are due to a lower polarity of the solvent and therefore more efficient swelling of the rather apolar MI-St-matrix.

2.3.8. (Thermo)mechanical properties

For further characterisation of material properties of MI-St-BR-terpolymers several studies were performed to also determine (thermo)mechanical properties of **pMISt1** polymers, which contain different amounts of polybutadiene **CB24**.

Formulations based on **IBMA** could not be tested, since they do not fully solidify under used PI concentration. A higher initiator content is not possible, because then **MISt1** formulations would become too hot and give bubbles during curing.

The specimens for all (thermo)mechanical tests were prepared by moulding the resins according to the general procedure described in chapter 2.3.8 of the experimental part.

2.3.8.1. DMTA

DMTA studies were performed to estimate thermomechanical properties as well as thermal phase transitions like glass transition temperature (T_g).

All DMTA experiments were executed in torsion mode with a heating rate of 2 °C/min and constant normal force.

So the data shown in Figure 89 was obtained.

Die approbierte gedruckte Originalversion dieser Dissertation ist an der TU Wien Bibliothek verfügbar.
The approved original version of this doctoral thesis is available in print at TU Wien Bibliothek.
TU Bibliothek Your knowledge hub WIEN

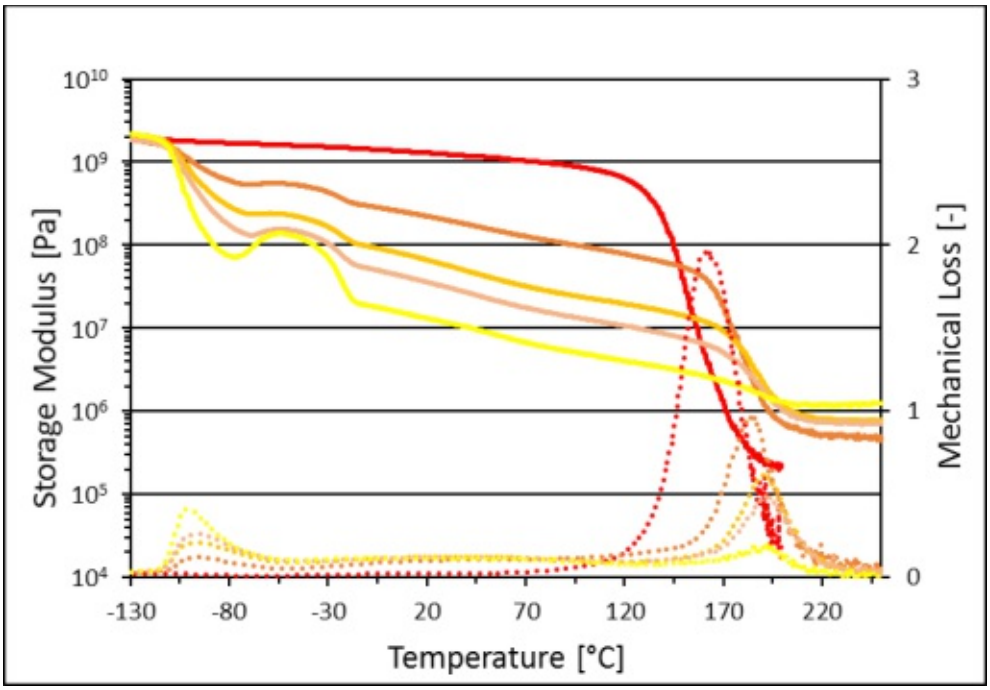

Figure 89: Storage modulus (—) and mechanical loss (···) of **pMISt1** without (—) and with 10 (—), 20 (—), 30 (—) or 50 w% (—) **CB24**

As can be seen in Figure 89 **pMISt1** and **CB24** are not fully miscible, because there are still both peaks of the glass transitions present (peak at ~ -96 °C corresponds to the BR and ~ 175 °C originates from **pMISt1**). In addition, T_gs of the hard phase (**pMISt1**) are shifted to higher temperatures (161 °C → 192 °C) with increasing polybutadiene content, which indicates partial compatibility of the **pMISt1**-**CB24**-system. These results are even more surprising since all tested sample specimens are clear transparent polymers.

The observed peaks at ~ -50 °C in G', which increase with higher **CB24** contents, could originate from crystallisation processes of the BR, but DSC measurements showed no exothermic signals in this temperature range. On the other hand, also different thermal expansions and thus formation of compression stress of the MI-St phase and the BR phase could explain the increase of G' and G".

Die approbierte gedruckte Originalversion dieser Dissertation ist an der TU Wien Bibliothek verfügbar.
The approved original version of this doctoral thesis is available in print at TU Wien Bibliothek.
TU Bibliothek Your knowledge hub WIEN

2.3.8.2. Tensile tests

In addition to DMTA studies also tensile tests were performed to further characterise mechanical properties of the model MI-St-BR-system **pMISt1**.

Tensile tests were conducted according to ISO 527 with specimen shape 5B and a traverse speed of 5 mm/min.

So stress-strain curves shown exemplary in Figure 90 and summarised in Table 23 were obtained.

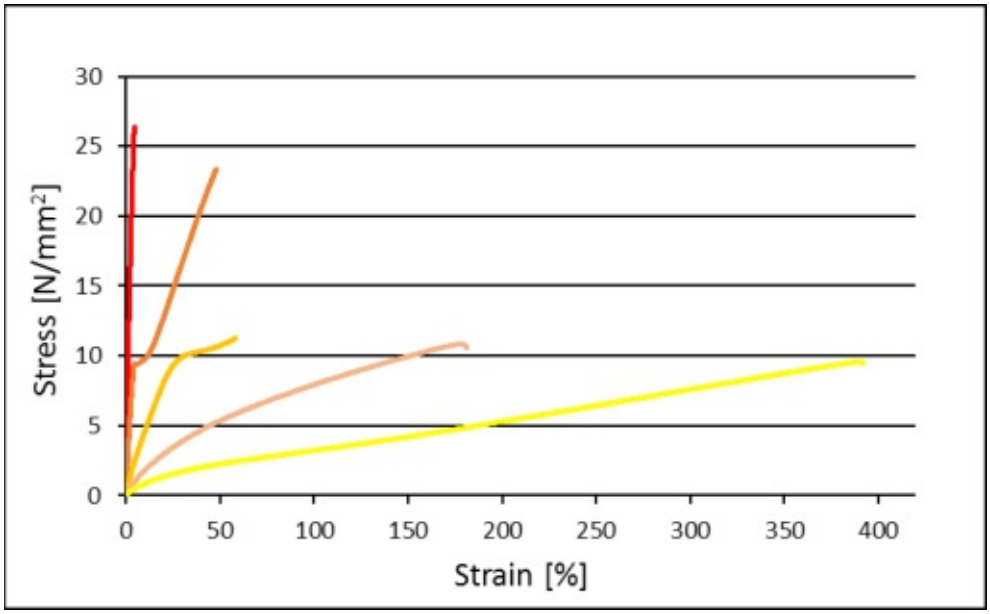

Figure 90: Exemplary stress-strain curves of **pMISt1** without (—) and with 10 (—), 20 (—), 30 (—) or 50 w% (—) **CB24**

Table 23: Results of tensile tests of **pMISt1**

Sample	$Stress_{max}$ [MPa]		$Strain_{Break}$ [%]	
	Average	s	Average	s
pMISt1_0	27.5	3.0	4.3	0.7
pMISt1_10	22.0	2.5	45.6	7.0
pMISt1_20	12.4	0.6	54.6	3.9
pMISt1_30	13.1	1.9	182.9	35.0
pMISt1_50	8.4	1.3	389.7	84.4

Die approbierte gedruckte Originalversion dieser Dissertation ist an der TU Wien Bibliothek verfügbar.
The approved original version of this doctoral thesis is available in print at TU Wien Bibliothek.
TU Bibliothek Your knowledge hub WIEN

Figure 90 shows the brittle behaviour of **pMISt1_0**, which becomes more and more ductile with increasing BR content. Additionally, stress-strain curves of **pMISt1_10** and **pMISt1_20** exhibit a yield point, whereas higher amounts of polybutadiene **CB24** lead to more elastomer like properties.

2.3.8.3. Impact resistance

Finally, also impact resistance was measured to conclude characterisation of the model MI-St-BR-system **pMISt1**. Therefore, Dynstat impact tests were performed, since they need only very small sample specimens compared to other impact resistance experiments like Charpy or Izod.

Impact resistance was measured with the Dynstat approach according to DIN 51230.

The experiments show, that **pMISt1_0** specimens are quite brittle (1.8 ± 0.5 kJ/m^2). All specimen containing polybutadiene **CB24** do not break even with the heaviest hammer (40 kpcm). They only get some graces instead of breaking (Figure 91).

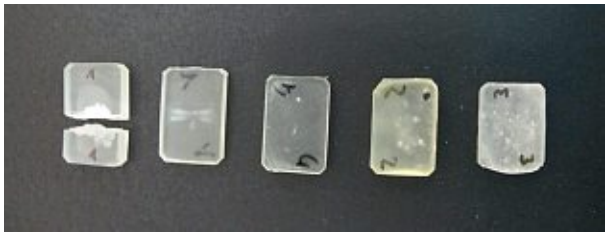

Figure 91: Samples after impact test: **pMISt1** without (1.) and with 10 (2.), 20 (3.), 30 (4.) or 50 w% (5.) **CB24**

Furthermore, SEM pictures of Dynstat impact test specimen were taken to get more information on the morphology of the (not) broken samples.

Die approbierte gedruckte Originalversion dieser Dissertation ist an der TU Wien Bibliothek verfügbar.
The approved original version of this doctoral thesis is available in print at TU Wien Bibliothek.
TU Bibliothek Your knowledge hub WIEN

So the images shown in Figure 92 were obtained for the fracture surface of a broken **pMISt1_0** impact test specimen.

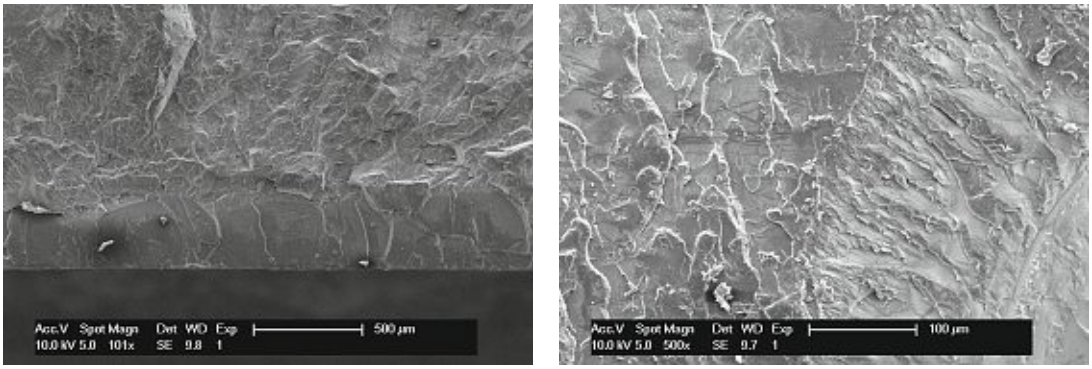

Figure 92: Broken Dynstat impact test specimen of **pMISt1_0**

As can be seen in Figure 92 **pMISt1_0** gives a rather smooth fracture surface, which explains the low impact resistance.

Furthermore, no phase separation of hard MI-St phase and soft rubber phase, which can explain the very high impact resistance and that was also seen in the corresponding DMTA curves (see chapter 2.3.8.1), can be observed in SEM images in **pMISt1** samples containing BR **CB24**.
Since differentiation of different organic phases in SEM is quite difficult and staining with Os or Ru-based staining agents is not possible in this case, AFM measurements were used to visualise phase separation.

2.3.9. AFM

AFM pictures were taken to show the phase separation of the MI-St matrix **pMISt1** and rubber **CB24**. Therefore, Young's modulus was measured with AFM on the surface of **pMISt1** samples containing rubber, due to the very significant difference in the moduli of hard and soft domains.

Die approbierte gedruckte Originalversion dieser Dissertation ist an der TU Wien Bibliothek verfügbar.
The approved original version of this doctoral thesis is available in print at TU Wien Bibliothek.
TU Bibliothek Your knowledge hub WIEN

All AFM experiments were performed in an area of 5*5 µm^2 and with a resolution of 256*256 pixels.

So the images shown in Figure 93 were obtained.

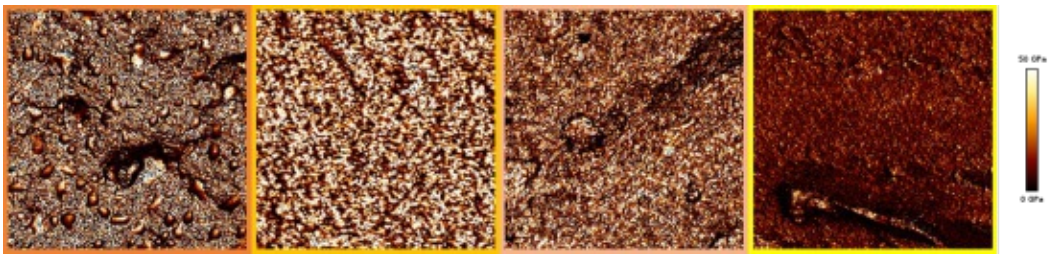

Figure 93: Young's moduli of **pMISt1** samples with 10 (—), 20 (—), 30 (—) or 50 w% (—) **CB24**

Although sample preparation of materials with phase separation is tricky and it is in this study also probably not ideal, the pictures in Figure 93 nevertheless nicely illustrate the separation of the hard MI-St and the soft BR phase in **pMISt1**-based photopolymers, which was already indicated in the DMTA measurements (compare chapter 2.3.8.1). They show very small areas of the two different phases (< 50 nm). Therefore, the transparency of the terpolymers can be explained (see Figure 91), because domain size is significantly lower than the wavelength of visible light. In contrast, the dimension of the phases is one of the reasons for the opaque appearance of ABS.

Furthermore, the obtained Young's moduli are in the same order as the moduli indicated by the tensile tests (chapter 2.3.8.2). However, tensile tests do not yield Young's moduli due to the applied experimental parameters.

Finally, the pictures become darker (lower moduli) and resolution becomes less with higher rubber content due to the very small size of the two different phases. Thus, measurement volume (~ 40 nm depth) is in the same size range than the domain size and therefore an AFM experiment always measures more than one domain in a single experiment. So a levelling effect is observed and the determined moduli seem to be lower with increasing BR concentrations.

Die approbierte gedruckte Originalversion dieser Dissertation ist an der TU Wien Bibliothek verfügbar.
The approved original version of this doctoral thesis is available in print at TU Wien Bibliothek.
TU WIEN Bibliothek Your knowledge hub

2.3.10. Thermal stability

Finally, thermal stability of model MI-St-BR-terpolymers was tested to conclude characterisation of this new class of photopolymers. Therefore, STA measurements were performed.

The experiments were conducted under N_2 atmosphere according to DIN EN ISO 11358 on an STA.
So obtained TGA curves are shown in Figure 94 and the estimated temperatures of beginning mass loss (T_A) and the temperatures of the inflexion point (T_C) are summarised in Table 24.

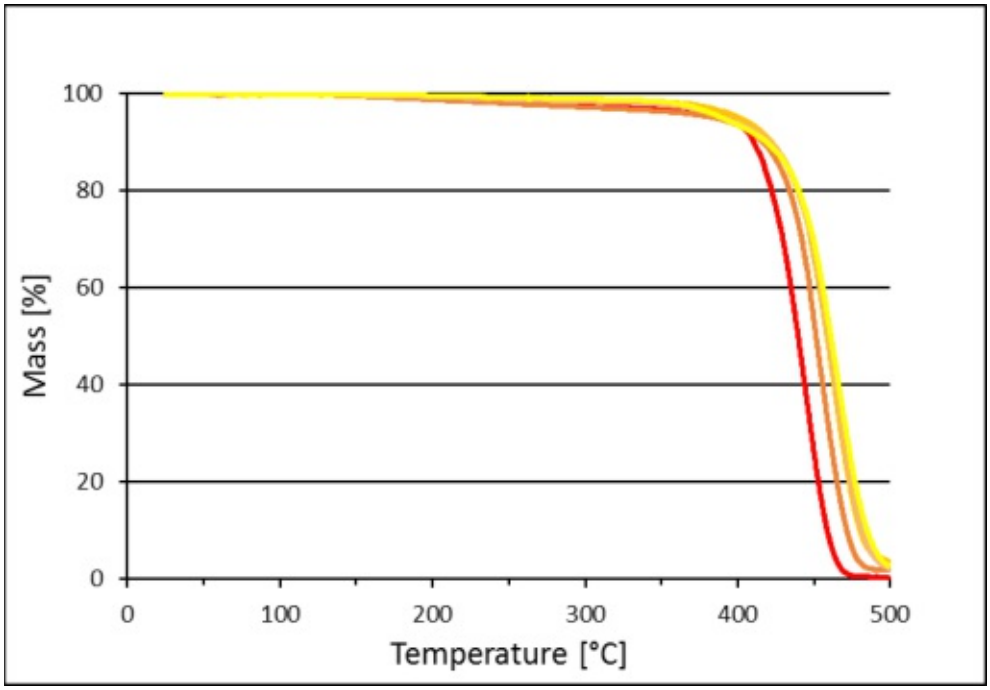

Figure 94: TGA of **pMISt1** without (—) and with 10 (—), 20 (—), 30 (—) or 50 w% (—) **CB24**

Die approbierte gedruckte Originalversion dieser Dissertation ist an der TU Wien Bibliothek verfügbar.
The approved original version of this doctoral thesis is available in print at TU Wien Bibliothek.
TU Bibliothek Your knowledge hub WIEN

Table 24: Thermal stability of **pMISt1**

Sample	T_A [°C]	T_C [°C]
pMISt1_0	418	446
pMISt1_10	431	448
pMISt1_20	434	464
pMISt1_30	435	464
pMISt1_50	436	464

Figure 94 and Table 24 show, that **pMISt1** possesses quite high thermal stability, which increases also slightly with the addition of BR **CB24**. Compared to ABS the thermal degradation is ~ 45 °C higher for the MI-St-BR-terpolymer [139].

Hence, already first tested model MI-St-system **MISt1** exhibits high reactivity and good (thermo)mechanical properties such as high T_g, high strain at break and very high impact resistance. Nevertheless, there are still some drawbacks, which strongly limit their potential applications (*e.g.* volatility or storage stability).
Nevertheless, first some more basic studies have to be performed to get a better understanding of MI-St-BR-terpolymers, before optimisation of MI and St monomers regarding enhanced material properties can be done.

Die approbierte gedruckte Originalversion dieser Dissertation ist an der TU Wien Bibliothek verfügbar.
The approved original version of this doctoral thesis is available in print at TU Wien Bibliothek.
TU WIEN Bibliothek Your knowledge hub

2.4. Further mechanistic studies on MI-St-copolymerisation

Before optimisation of material properties of MI-St-based photopolymers can be done, further basic investigations should be performed to clarify some observed effects in model MI-St-BR-system **MISt1**:

- Influence of BR
- Insolubility due to cross-linking reactions

*2.4.1. Influence of polybutadienes on **MISt1***

Polybutadiene **CB24** was already applied successfully to enhance toughness in brittle model MI-St-system **pMISt1**. Besides the used **CB24**, additional polybutadienes (Table 25, kindly provided by Cray Valley) with lower molecular weight – but completely different microstructures – were tested to get an idea of the influence of the rubber component in the MI-St-matrix **pMISt1**.

Table 25: Used polybutadienes

Trade name	M_n [kDa]	Molecular structure	Remarks
Krasol LBH-P 3000	3.2	65% Vinyl	Both ends terminated with primary hydroxy groups
Krasol HLBH-P 3000	3.1	65% Ethyl	Hydrogenated BR (HBR); Both ends terminated with primary hydroxy groups
Ricon 134	8.0	28% Vinyl	
Krasol LBH 5000 M	5.0	65% Vinyl	1 end terminated with a primary hydroxy group
Ricon 154	5.2	90% Vinyl	

Incorporation of all these low molecular weight polybutadienes in the **pMISt1** matrix will lead to quite brittle polymers (similar to **pMISt1** without added rubber), but the aim of this approach is to understand the effects of different BR structures on the photopolymer **pMISt1** and not to increase toughness.

Die approbierte gedruckte Originalversion dieser Dissertation ist an der TU Wien Bibliothek verfügbar.
The approved original version of this doctoral thesis is available in print at TU Wien Bibliothek.
TU Bibliothek Your knowledge hub WIEN

DMTA studies were performed to investigate if remaining double bonds of the polybutadiene have an influence on the material. Therefore, 10 w% Krasol LBH-P 3000 (BR) or Krasol HLBH-P 3000 (= hydrogenated version of Krasol LBH-P 3000, HBR) were incorporated into **pMISt1**.

All specimens for DMTA tests were prepared by moulding the resins according to the general procedure described in chapter 2.3.8 of the experimental part. The DMTA experiments were executed in torsion mode with a heating rate of 2 °C/min and constant normal force.
So following DMTA curves were measured (Figure 95). In addition, **pMISt1_0** and **pMISt1_10** are shown as well for comparison with high molecular weight BR **CB24**.

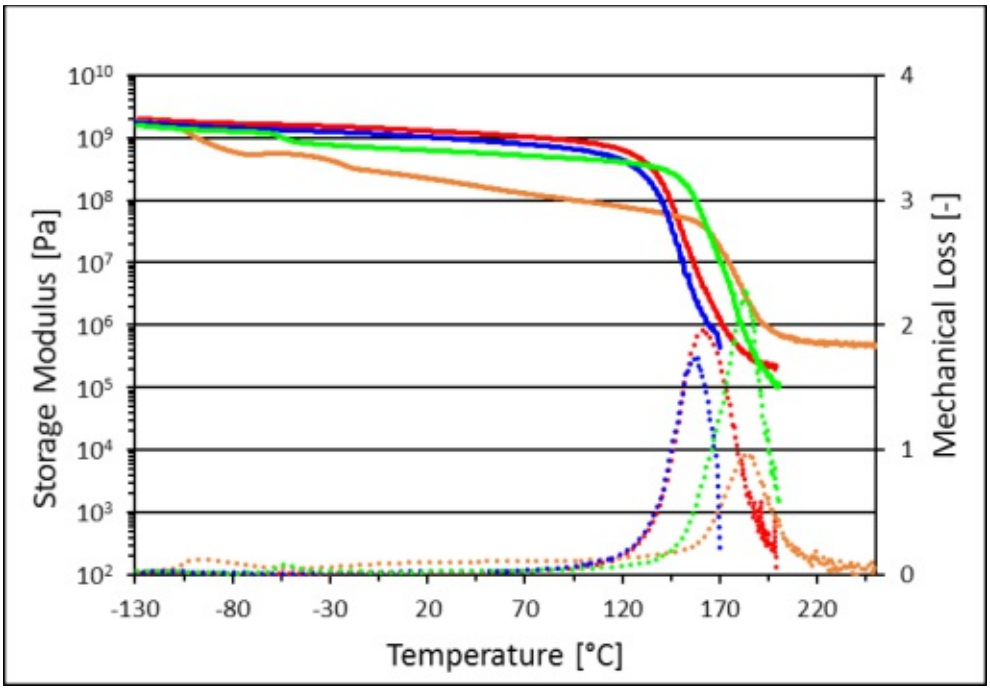

Figure 95: Storage modulus (—) and mechanical loss (▪▪▪) of **pMISt1** without (—) and with 10 w% **CB24** (—), HBR (—) or BR (—)

Die approbierte gedruckte Originalversion dieser Dissertation ist an der TU Wien Bibliothek verfügbar.
The approved original version of this doctoral thesis is available in print at TU Wien Bibliothek.
TU Bibliothek Your knowledge hub WIEN

As can be seen in Figure 95 the low molecular weight polybutadiene with vinyl groups (blue curves) interestingly does not drastically change modulus or glass transition temperature. Furthermore, no phase separation could be observed – neither in DMTA data nor optically (see also Figure 96).

Figure 96: DMTA specimen of **pMISt1** with 10 w% BR (left) or corresponding HBR (right)

In contrast, – as Figure 95 above also shows – addition of the hydrogenated BR (green curves) leads to 2 glass transitions and a small increase in glass transition temperature of the MI-St phase similar to high molecular weight BR **CB24**, which is covalently bonded with the MI-St matrix. The rise in the polymer containing HBR is caused probably by incomplete miscibility of the different phases, because no cross-linking reactions between remaining BR double bonds and MI/St monomer radicals can occur, which is also underlined by a lower storage modulus in the rubbery-elastic area. Finally, this approach is further supported by the observation, that the polymer containing the hydrogenated rubber is not transparent (see Figure 96 again).

Hence, SEM pictures of the specimens were taken to further prove this theory: Figures 97 and 98.

Die approbierte gedruckte Originalversion dieser Dissertation ist an der TU Wien Bibliothek verfügbar.
The approved original version of this doctoral thesis is available in print at TU Wien Bibliothek.
TU Bibliothek Your knowledge hub WIEN

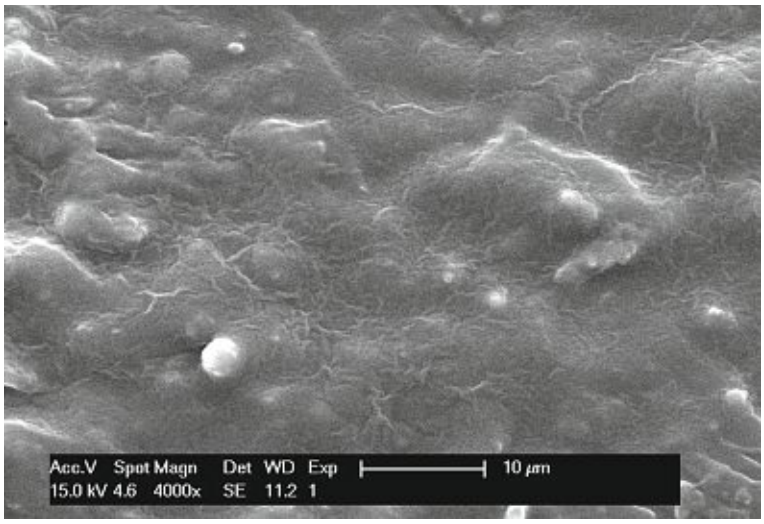

Figure 97: Broken DMTA specimen of **pMISt1** with 10 w% BR

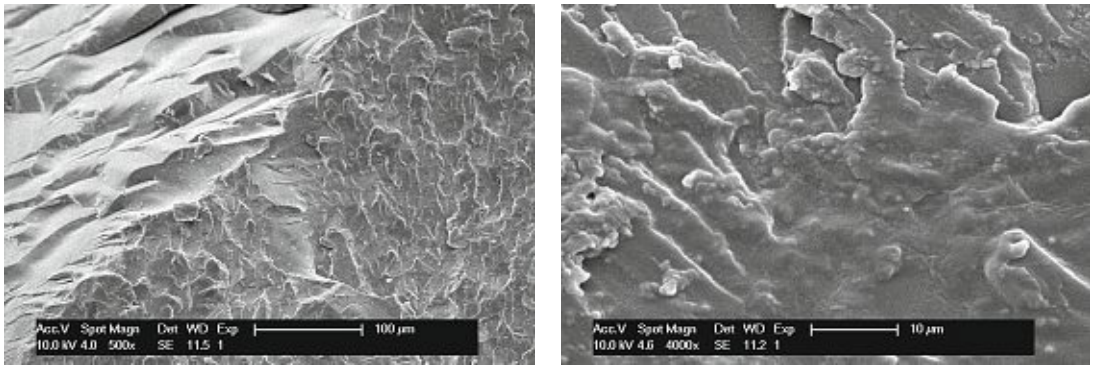

Figure 98: pMISt1 with 10 w% BR

SEM images also indicate, that there is only one homogeneous phase present in the photopolymer containing the polybutadiene with double bonds.

In contrast, a distinct phase separation is present in samples with the corresponding HBR (Figures 99 and 100).

Die approbierte gedruckte Originalversion dieser Dissertation ist an der TU Wien Bibliothek verfügbar.
The approved original version of this doctoral thesis is available in print at TU Wien Bibliothek.
TU WIEN Bibliothek Your knowledge hub

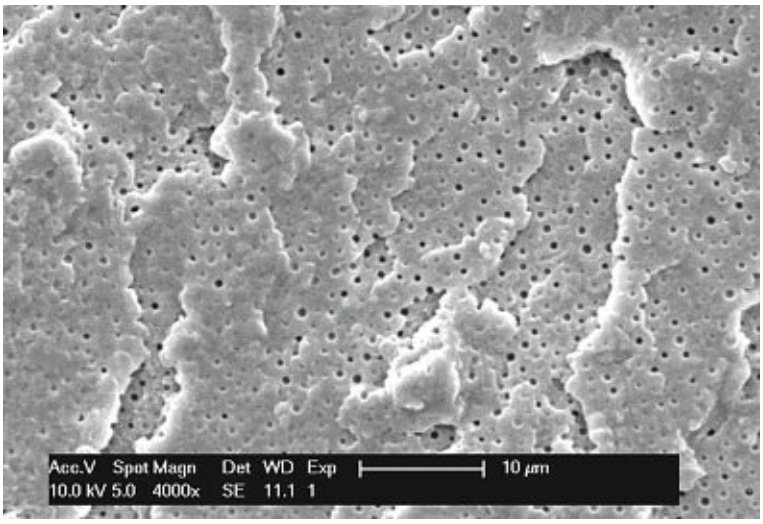

Figure 99: Broken DMTA specimen of **pMISt1** with 10 w% HBR

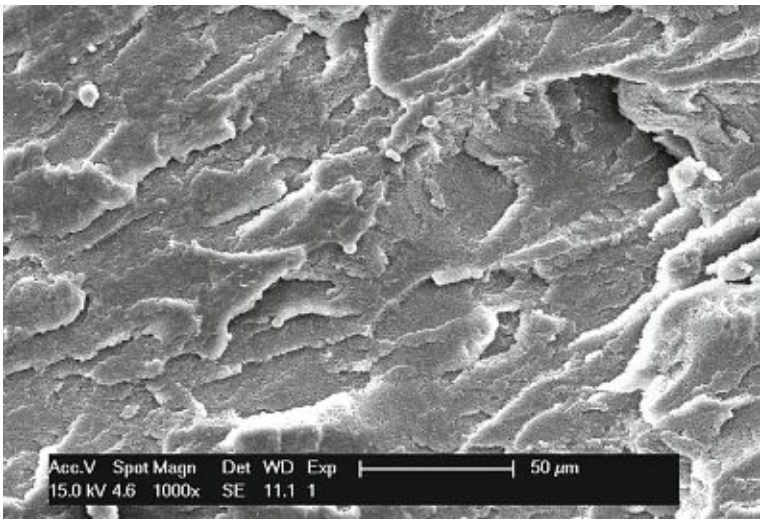

Figure 100: pMISt1 with 10 w% HBR

The size of the second minor domains (polybutadiene) is approximately 400 – 700 nm, which is exactly the wavelength of visible light, thus explaining the opacity of the polymer.

Additionally, SEM pictures prove that addition of HBR Krasol HLBH-P 3000 to **MISt1** leads to polymerisation induced phase separation, since the liquid formulation is homogeneous and transparent.

Die approbierte gedruckte Originalversion dieser Dissertation ist an der TU Wien Bibliothek verfügbar.
The approved original version of this doctoral thesis is available in print at TU Wien Bibliothek.
TU Bibliothek Your knowledge hub WIEN

In addition, rubbers with slightly higher molecular weights (compare Table 25) and with different structures were studied as well according to their effect on model MI-St-system **pMISt1**:

- **pMISt1** with 10 w% Ricon 134 (28% vinyl, M_n = 8.0 kDa): White polymer
- **pMISt1** with 10 w% Krasol LBH 5000 M (65% vinyl, M_n = 5.0 kDa): Almost transparent material
- **pMISt1** with 10 w% Ricon 154 (90% vinyl, M_n = 5.2 kDa): Transparent material

The optical phase separation (shown in Figure 101) of **pMISt1** containing Ricon 134 could either be explained due to the higher molecular weight compared to the other ones or also because of a low vinyl group content (28%).

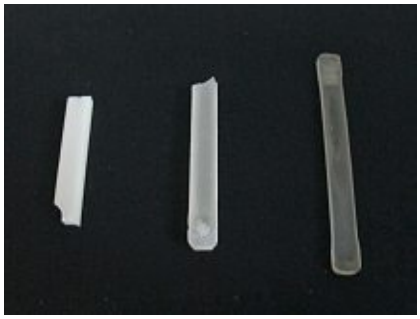

Figure 101: Samples of **pMISt1** with 10 w% Ricon 134 (left), Krasol LBH 5000 M (middle) or Ricon 154 (right)

Furthermore, DMTA was measured again to prove first optical impressions as well as to investigate the influence of polybutadienes on thermomechanical properties.

The DMTA experiments were conducted with the same experimental parameters as before, to obtain comparable results (see chapter 2.4.1).
So DMTA results given in Figure 102 were obtained.

Die approbierte gedruckte Originalversion dieser Dissertation ist an der TU Wien Bibliothek verfügbar.
The approved original version of this doctoral thesis is available in print at TU Wien Bibliothek.
TU Bibliothek Your knowledge hub WIEN

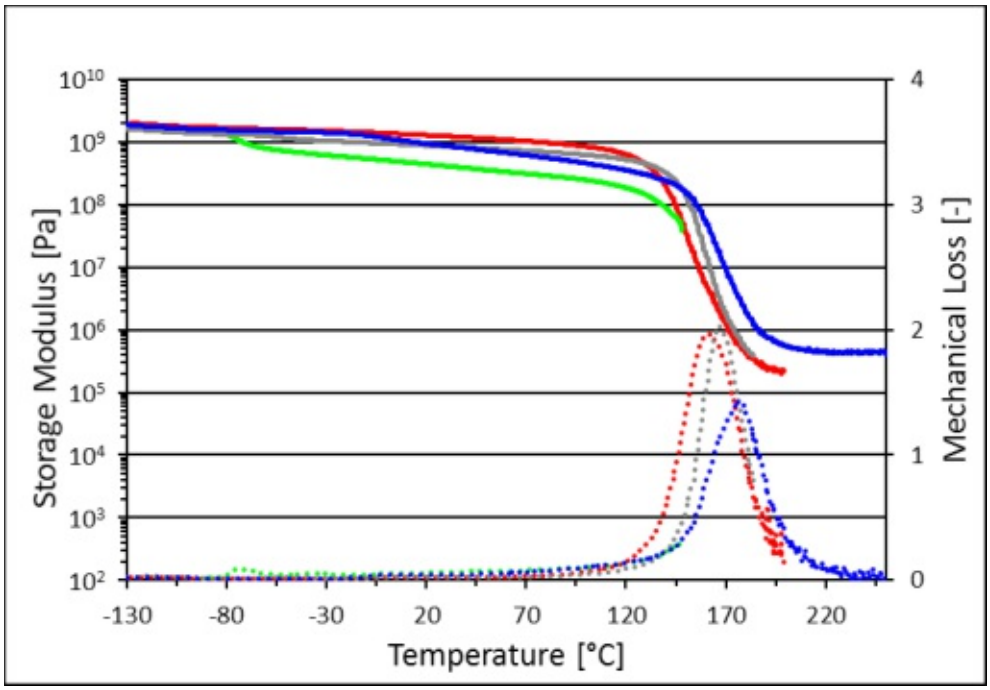

Figure 102: Storage modulus (—) and mechanical loss (···) of **pMISt1** without (—) and with 10 w% Ricon 134 (—), Krasol LBH 5000M (—) or Ricon 154 (—)

DMTA demonstrates, that the low molecular weight polybutadienes increase the T_g slightly with an increasing vinyl content, due to the steric demand of the vinyl groups and a little bit higher degrees of cross-linking. Furthermore, only the "high" molecular weight (8 kDa) Ricon 134, which has the lowest vinyl concentration and also shows optically phase separation, exhibits 2 glass transitions.

So it seems, that either "high" (> 6 kDa) molecular weight or low content of vinyl groups trigger phase separation. On the other hand, **CB24** with an M_n of 180 kDa and almost no vinyl groups (> 96% *cis*-1,4-polybutadiene) yields transparent polymers when incorporated into **MISt1**, but still possesses 2 glass transitions (originating from soft BR phase and hard MI-St phase).

Die approbierte gedruckte Originalversion dieser Dissertation ist an der TU Wien Bibliothek verfügbar.
The approved original version of this doctoral thesis is available in print at TU Wien Bibliothek.
TU Bibliothek Your knowledge hub WIEN

2.4.2. Cross-linking behaviour in MI-St-copolymers

Since insolubility of MI-St-copolymers of pure **pMISt1_0** but also **pMISt1** containing various different rubbers was observed already several times (compare *e.g.* chapters 2.3.7 or 2.4.1), a closer look is necessary to analyse this unexpected property.

The idea is that either H-abstraction occurs on the MI ring, then all MI-St-based photopolymers should be insoluble, or a H atom on the substituent next to the N atom is abstracted, then solubility can be controlled by the choice of the substituent (see also Figure 88).

Thus, swellability tests with a MI without an α-H atom next to the N atom were planned in order to investigate the cross-linking reaction. So aromatic substituted *N*-phenylmaleimide **PhMI** was used, because it exhibits – compared to other MIs – a very low melting point (T_m = 88 – 91 °C). Since **PhMI** is solid and also cannot be dissolved in St **tBuSt**, the need is given for a new St comonomer. A key feature of the new monomer has to be a very high boiling point and additionally low volatility as well, to make dissolving of MI **PhMI** at elevated temperatures possible.
Therefore, a new St derivative (**FESt**) was introduced, which can be applied in combination with MI **PhMI** for MI-St-sytem 2 (**MISt2**, Figure 103) also at high temperatures.
Again 0.2 w% TPO-L were always used as PI in all formulations of **MISt2**.

Die approbierte gedruckte Originalversion dieser Dissertation ist an der TU Wien Bibliothek verfügbar.
The approved original version of this doctoral thesis is available in print at TU Wien Bibliothek.
TU WIEN Bibliothek Your knowledge hub

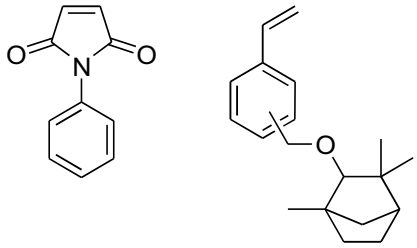

Figure 103: Monomers used for **MISt2**

MI **PhMI** was kindly provided by HOS-Technik (Homide 105), thus only St derivative **FESt** had to be synthesised.

*2.4.2.1. Synthesis of **FESt***

Synthesis of St derivative **FESt** was performed according to Kobayashi *et al.* [140] (Figure 104). It has to be mentioned, that the starting material vinylbenzyl chloride (**VBnCl**) is a mixture of m- and p-substituted styrene in an approximately equimolar ratio (51 : 49 according to GC-MS chromatogram).

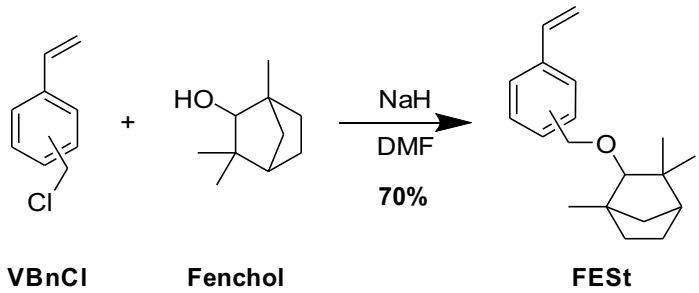

Figure 104: Synthesis of **FESt**

The synthesis was also conducted in THF instead of DMF, because this solvent would be easier to remove, but then conversion dropped to ~ 10% (according to ^{1}H-NMR spectrum) after 24 h compared to 78% isolated product in DMF with a reaction time of ~ 16 h. The low conversion may be optimised with even longer

Die approbierte gedruckte Originalversion dieser Dissertation ist an der TU Wien Bibliothek verfügbar.
The approved original version of this doctoral thesis is available in print at TU Wien Bibliothek.
TU Bibliothek Your knowledge hub WIEN

reaction times or elevated temperatures. However, St monomer **FESt** could be successfully synthesised with the known procedure in big batch sizes (> 35 g), which is a sufficient amount for all planned studies.

*2.4.2.2. Volatility of **FESt***

First of all, volatility of St **FESt** was checked, as it is a main drawback of the previous applied St derivative **tBuSt**, which was used in **MISt1** resins. Furthermore, this property is crucial for the utilisation in combination with MI **PhMI** in MI-St-system **MISt2**.
In addition, the results were compared to MA **IBMA** (as industrial relevant monofunctional monomer) and to the former used St **tBuSt** as well (compare also chapter 2.3.1).

Therefore, mass loss was measured again with STA at 90 °C for 3 h under N_2 atmosphere.
So the data summarised in Table 26 was obtained:

Table 26: Volatility at 90 °C after 3 h

Monomer	Mass loss [%]
IBMA	10
tBuSt	16*
FESt	< 1

* polymerised

Table 26 shows, that the new St moiety **FESt** exhibits only an mass loss of < 1% after 3 h at 90 °C. Additionally, no homopolymerisation or solidification can be observed.
This result makes St **FESt** perfectly suitable for dissolving MI **PhMI** at elevated temperatures, which are necessary, because they are not miscible at room temperature.

Die approbierte gedruckte Originalversion dieser Dissertation ist an der TU Wien Bibliothek verfügbar.
The approved original version of this doctoral thesis is available in print at TU Wien Bibliothek.
TU Bibliothek Your knowledge hub WIEN

2.4.2.3. Swellability

Swellability tests of **pMISt2** samples without and with rubber **CB24** were performed to further investigate the reaction of the MI-St-systems with polybutadiene and also to prove the proposed cross-linking mechanism of **pMISt1** in chapter 2.3.7.

Therefore, samples were moulded at 100 °C, because **MISt2** formulations are not homogeneous at room temperature and **PhMI** precipitates again during cooling. Polymerised samples were submerged for 7 d in $CHCl_3$. Sample mass was recorded before and after swelling and after drying (see chapter 2.4.2.3 of the experimental part).
So swellability and gel fraction were calculated: Table 27.

Table 27: Swellability and gel fraction of **pMISt2**

Sample	Swellability [%]	Gel fraction [%]
pMISt2_0	- *	0*
pMISt2_10	1314	76.5
pMISt2_20	1270	77.8
pMISt2_30	1208	78.7
pMISt2_50	1033	83.7

* completely soluble

As can be seen in Table 27, pure **pMISt2** is completely soluble in $CHCl_3$. This behaviour proves the theory of H-abstraction next to the N atom of MI **PrMI** in **MISt1** (Figure 105, compare also chapter 2.3.7), since **PhMI** in **MISt2** exhibits no abstractable H atom in α-position and therefore gives an uncross-linked soluble polymer.

Die approbierte gedruckte Originalversion dieser Dissertation ist an der TU Wien Bibliothek verfügbar.
The approved original version of this doctoral thesis is available in print at TU Wien Bibliothek.
TU Bibliothek Your knowledge hub WIEN

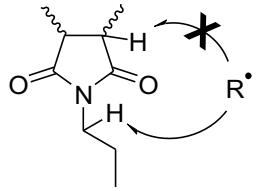

Figure 105: Cross-linking mechanism of **PrMI**

The swellability experiments further show similar findings as model system **pMISt1**: covalent cross-linking of the MI-St-system with BR **CB24** and a very high amount of swelling, which decreases with higher polybutadiene concentration.

Finally, **pMISt2_0** is completely soluble and thus conversions were calculated with ^{1}H-NMR spectroscopy and molecular weight was measured with GPC. So following results were obtained:

- DBC_{PhMI}: 98%
- DBC_{FESt}: 96%
- M_n = 182.5 kDa
- Đ = 6.3

These outcomes show again the high reactivity and also underline the high potential of MI-St-copolymers for application in photopolymerisation.

Hence, some interesting effects and influences on reactivity and (thermo)mechanical properties of aliphatic model MI-St-system **MISt1** and aromatic substituted MI containing **MISt2** could be elucidated. With this improved knowledge on MI-St-BR-terpolymerisation optimisation of material properties can be started.

Die approbierte gedruckte Originalversion dieser Dissertation ist an der TU Wien Bibliothek verfügbar.
The approved original version of this doctoral thesis is available in print at TU Wien Bibliothek.
TU Bibliothek Your knowledge hub WIEN

2.5. Variation of MI substituent

Model MI-St-system **MISt1** containing BR **CB24** exhibits very promising chemical as well as (thermo)mechanical properties (see chapter 2.3) and a better understanding of the MI-St-BR-based photopolymers is also already obtained (chapter 2.4). Nevertheless, there are still some challenges such as high volatility of the used monomers, which have to be solved.

Since **MISt1** resin consists of highly volatile monomers and in **MISt2** formulation the MI **PhMI** precipitates during cooling, new MI moieties are needed. In contrast, already introduced St monomer **FESt** will be used again in equimolar concentration as St component, due to its low volatility and easy synthesis. Additionally, PI TPO-L (0.2 w%) is applied in all formulations to preserve comparability of gained results. Finally, polybutadiene **CB24** is applied only in contents below 20 w% as toughening agent, because higher concentrations give a rubber swollen with monomer instead of a liquid formulation (compare **MISt1** in chapter 2.3.3). Furthermore, material properties suffer as well from the high BR amount (see **pMISt1** in chapter 2.3.8).

Thus, MI-St-systems 3-5 (**MISt3-5**) were studied regarding the optimisation of material properties and therefore also identifying potential applications of this new material class:

- Maleimide-styrene-system 3 (**MISt3**):

A meradimate substituted maleimide (**MMI**, Figure 106) was chosen as new MI compound, because in our working group already good results for reactive diluents with other menthyl esters could be obtained [51]. Furthermore, the additional cycloaliphatic structure of meradimate should dramatically increase solubility compared to MI **PhMI**, which is the main issue of **MISt2**.

Die approbierte gedruckte Originalversion dieser Dissertation ist an der TU Wien Bibliothek verfügbar.
The approved original version of this doctoral thesis is available in print at TU Wien Bibliothek.
TU Bibliothek Your knowledge hub WIEN

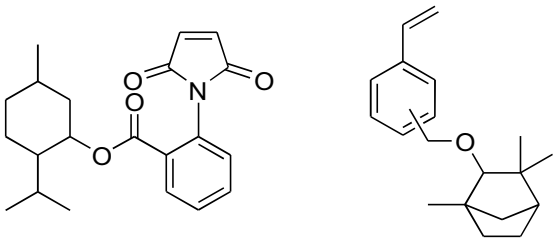

MMI **FESt**

Figure106: Used monomers for **MISt3**

- Maleimide-styrene-system 4 (**MISt4**):

Since aromatic substituted MIs exhibit reduced reactivity and thus maybe do not yield desired material properties, a MI with an aliphatic substituent on the N atom was used for MI-St-system **MISt4**. Hence, MI **CHMI** is applied (Figure 107) as a representative for cycloaliphatic substituted MIs. Furthermore, a high T_g of the polymers should be obtained due to the rigid cyclohexyl ring structure.

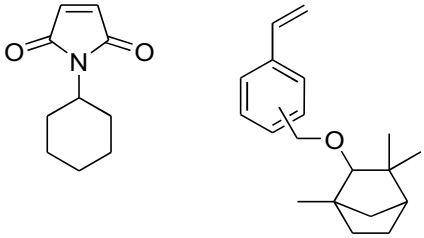

CHMI **FESt**

Figure 107: Used monomers for **MISt4**

A drawback of **CHMI** is, that it is solid at room temperature (T_m = 87 – 90 °C) and so **MISt4** (with and without BR **CB24**) gives completely homogeneous formulations only at temperatures > 75 °C. So all experiments with **MISt4**-based resins were performed at 80 °C to ensure a homogeneous resin. However, it takes quite some time (> 2 min) until it crystallises again, thus giving enough time for moulding specimen at room temperature for (thermo)mechanical tests. Nevertheless, this strongly limits comparability with other investigated MI-St-systems, which were tested always at 25 °C.

Die approbierte gedruckte Originalversion dieser Dissertation ist an der TU Wien Bibliothek verfügbar.
The approved original version of this doctoral thesis is available in print at TU Wien Bibliothek.
TU Bibliothek Your knowledge hub WIEN

- Maleimide-styrene-system 5 (**MISt5**):

A further aliphatic substituted MI was chosen, since it was shown already with model system **MISt1**, that linear aliphatic groups yield good material properties. So **EHMI** was used as MI component with St **FESt** for MI-St-system 5 (**MISt5**, Figure 108), because the higher molecular weight of **EHMI** compared to **PrMI** in **MISt1** should significantly decrease monomer volatility (compare chapter 2.3.1).

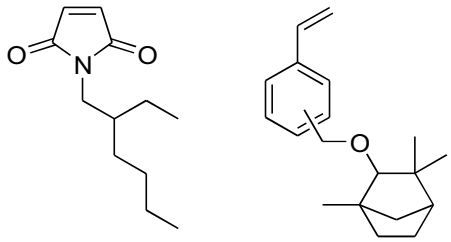

Figure 108: Used monomers for **MISt5**

2.5.1. Monomer syntheses

First of all, desired MI monomers **MMI** and **EHMI** had to be synthesised. In contrast, MI **CHMI** is commercially available.

*2.5.1.1. Synthesis of **MMI***

MI **MMI** had to be synthesised, since it is not commercially available. This was conducted with a standard procedure for the synthesis of MIs with sodium acetate and acetic anhydride (*e.g.* according to McLeod *et al.* [141], Figure 109). So **MMI** was obtained as a slightly yellow-orange highly viscous monomer in 80% yield in batch sizes of > 35 g (see chapter 2.5.1.1 of the experimental part).

Die approbierte gedruckte Originalversion dieser Dissertation ist an der TU Wien Bibliothek verfügbar.
The approved original version of this doctoral thesis is available in print at TU Wien Bibliothek.
TU Bibliothek Your knowledge hub WIEN

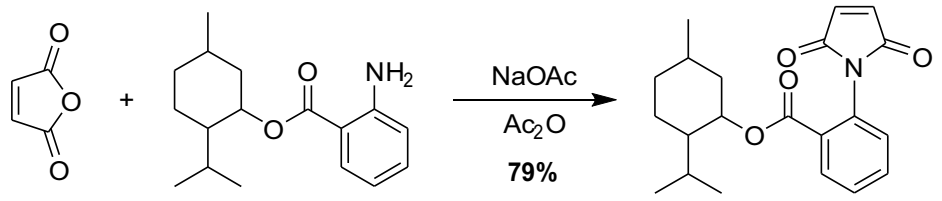

Figure 109: Synthesis of **MMI**

Additionally, it has to be mentioned, that no information on the stereochemistry of the menthyl structure is available. However, since the starting material meradimate is quite cheap (100 mL ~ 62 €[1]), it can be supposed, that it is enantiomerically pure, because only one enantiomer of meradimate is FDA approved as a UV filter in sunscreens.

It was also tried to synthesise **MMI** like the IIs and CIs before with toluene in a Dean-Stark-apparatus [118] (see chapter 2.2.1) or also in neat at high temperatures [142-143], but both approaches yielded only corresponding maleamic acid (Figure 110). Hence, usage of acetic anhydride and sodium acetate could not be avoided to obtain MI **MMI**.

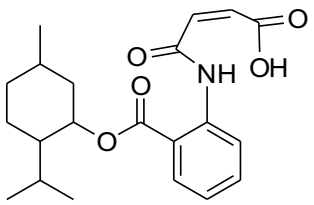

Figure 110: Intermediate product maleamic acid

Finally, it has to be mentioned, that harsh conditions are necessary to remove residual solvent from the product. Hence, phenothiazine has to be added to prevent polymerisation during work-up.

1 January 2019, Sigma-Aldrich

Die approbierte gedruckte Originalversion dieser Dissertation ist an der TU Wien Bibliothek verfügbar.
The approved original version of this doctoral thesis is available in print at TU Wien Bibliothek.

*2.5.1.2. Synthesis of **EHMI***

At the beginning the synthesis of **EHMI** was conducted according to patent WO 2005118537 [118] like itaconimides and citraconimides before using toluene and a Dean-Stark-apparatus (Figure 111). Unfortunately, obtained yield of MI **EHMI** was only 20%.

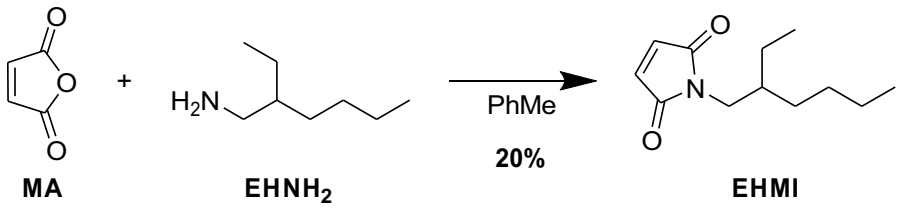

Figure 111: Low yield synthesis of **EHMI**

Therefore, another (more complex) procedure had to be applied to yield sufficient quantities of the desired monomer. Hence, the synthetic approach according to McLeod *et al.* [141] was used, which was already exploited for the synthesis of aromatic substituted MI **MMI** for **MISt3** (chapter 2.5.1.1). Thereby, the cyclisation reaction of the corresponding maleamic acid is promoted with Ac_2O (Figure 112; see chapter 2.5.1.2 of the experimental part). So the yield of MI **EHMI** could be raised successfully to 46% in batch sizes of more than 50 g.

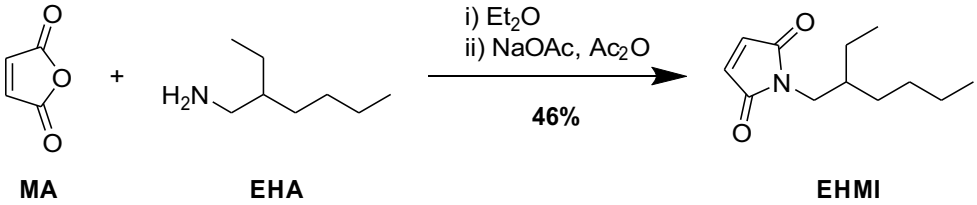

Figure 112: Synthesis of **EHMI**

Die approbierte gedruckte Originalversion dieser Dissertation ist an der TU Wien Bibliothek verfügbar.
The approved original version of this doctoral thesis is available in print at TU Wien Bibliothek.
TU Bibliothek Your knowledge hub WIEN

2.5.2. Volatility

First of all, again volatility of used MIs **MMI**, **CHMI** and **EHMI** had to be measured, since this is very important for further measurements and handling of **MISt3-5** formulations. Especially volatility of **CHMI** is crucial, because **MISt4**-based resins have to be polymerised at elevated temperatures, which are needed to obtain homogeneous mixtures.

Volatility measurements were performed on the STA in the same way than with all monomers before for 3 h under N_2 atmosphere (compare also chapter 2.3.1). Furthermore, the results were compared to MA **IBMA** as industrial relevant monofunctional monomer and additionally to the formerly used components in **MISt1**.

So the data summarised in Table 28 was obtained at 90 °C:

Table 28: Volatility at 90 °C after 3 h

Monomer	Mass loss [%]
IBMA	10
PrMI	53
tBuSt	16*
FESt	< 1
MMI	< 1
CHMI	8
EHMI	6

* polymerised

Table 28 shows, that MI **MMI** only looses < 1% mass over 3 h at 90 °C, which is comparable to St derivative **FESt**. Additionally, no homopolymerisation or degradation could be observed. Hence, **MISt3** formulations can be used with its non-volatile MI and St components also at high temperatures.

Furthermore, MIs **CHMI** and **EHMI** exhibit a slightly too big mass loss at 90 °C. So they were tested at lower temperatures as well: Table 29.

Die approbierte gedruckte Originalversion dieser Dissertation ist an der TU Wien Bibliothek verfügbar.
The approved original version of this doctoral thesis is available in print at TU Wien Bibliothek.
TU Bibliothek Your knowledge hub WIEN

Table 29: Volatility after 3 h

Temperature [°C]	Mass loss of **CHMI** [%]	Mass loss of **EHMI** [%]
90	8	6
80	1	5
60	< 1	3
50	n.d.*	2

* not determined

As can be seen in Table 29, MI **CHMI** is quite non-volatile and suitable to be utilised for some hours at higher temperatures up to 80 °C.
Volatility of MI **EHMI** is on an acceptable level at 50 °C. Thus, MI **EHMI** is an option also for applications, where only slightly increased temperatures or short heating times are used.

2.5.3. Storage stability

After promising volatility studies on used monomers, storage stability of resins was investigated, since it is a crucial property for applications in industrial scale. Hence, it was tested with **MISt3-5**-based formulations as well.

Therefore, **MISt3-5** resins without added polybutadiene **CB24** were chosen, because they would yield cross-linked polymers, which are not soluble any more and therefore no NMR spectroscopy is possible. The samples were stored under air and under light protection at room temperature. Furthermore, no additional inhibitors were added to the final resin. Evaluation of storage stability was done periodically by optical assessment and recording of ^{1}H-NMR spectra.

Die approbierte gedruckte Originalversion dieser Dissertation ist an der TU Wien Bibliothek verfügbar.
The approved original version of this doctoral thesis is available in print at TU Wien Bibliothek.
TU Bibliothek Your knowledge hub WIEN

Interestingly, **MISt3**-based resin does not gel/polymerise – even after 7 months, whereas **MISt1** formulations solidify already after few days. This good storage stability can be attributed to the reduced reactivity of the MI due to the aromatic substituent on the N atom [116].

In MI-St-system **MISt4_0** no polymerisation and no change in ^{1}H-NMR spectra could be observed after over 4 months.

Finally, also **MISt5_0** does not show polymerisation or a change in ^{1}H-NMR spectra after over 6 months.

2.5.4. UV-Vis absorbance

Since MI **MMI** has a slightly yellow to orange colour (see Figure 113) UV-Vis absorption spectra were measured to ensure, that no interference with the used PI TPO-L occurs.

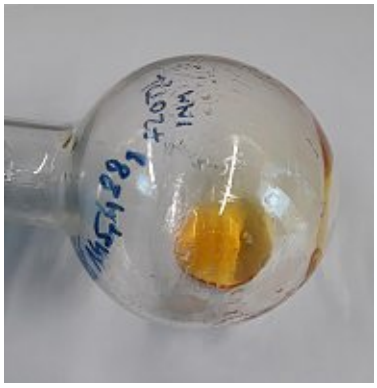

Figure 113: Flask containing **MMI**

Furthermore, MI **EHMI** strangely is a brownish liquid (which is in accordance with literature [144]; purity confirmed with TLC, ^{1}H and ^{13}C-NMR spectroscopy, HPLC and GC-MS). Hence, also a UV-Vis absorption spectrum of **EHMI** was recorded.

So UV-Vis absorption spectra were measured of both MIs and PI TPO-L in 1 mM DCM solutions: Figure 114.

Die approbierte gedruckte Originalversion dieser Dissertation ist an der TU Wien Bibliothek verfügbar.
The approved original version of this doctoral thesis is available in print at TU Wien Bibliothek.
TU Bibliothek Your knowledge hub WIEN

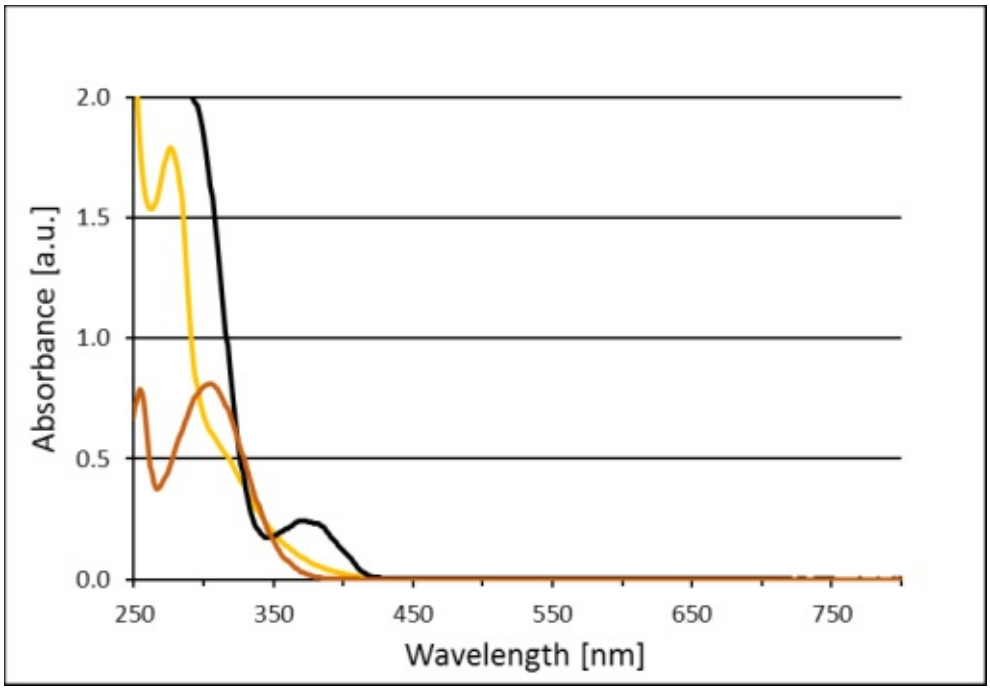

Figure 114: UV-Vis absorption spectra of TPO-L (—), **MMI** (—) and **EHMI** (—)

Spectra in Figure 114 show, that **MMI** absorbs until ~ 400 nm, whereas TPO-L runs out until ~ 415 nm. In addition, MI **EHMI** exhibits almost no overlapping with the n-π*-absorbance of TPO-L (~ 380 nm). Thus, molar extinction coefficients were calculated for different wavelengths according to Lambert-Beer law (equation 2) for a closer look: see Table 30.

$$A = \varepsilon * c * d \qquad (2)$$

A... Absorbance [-]
ε... Molar extinction coefficient [L mol^{-1} cm^{-1}]
c... Concentration [mol/L]
d... Optical path length [cm]

Table 30: Molar extinction coefficients of TPO-L, **MMI** and **EHMI**

Molecule	$\varepsilon_{365\ nm}$ [L mol^{-1} cm^{-1}]	$\varepsilon_{385\ nm}$ [L mol^{-1} cm^{-1}]	$\varepsilon_{400\ nm}$ [L mol^{-1} cm^{-1}]	$\varepsilon_{420\ nm}$ [L mol^{-1} cm^{-1}]
TPO-L	232	220	120	12
MMI	114	49	24	7
EHMI	52	6	2	1

Die approbierte gedruckte Originalversion dieser Dissertation ist an der TU Wien Bibliothek verfügbar.
The approved original version of this doctoral thesis is available in print at TU Wien Bibliothek.
TU Bibliothek Your knowledge hub WIEN

As can be seen in Table 30 above, slight absorption interference of the MIs and PI has to be expected during polymerisation, since in final photopolymerisable formulations monomer concentrations are considerably higher than PI content. However, for L-AMT – a potential application of MI-St-based photopolymers – the addition of a light absorber can possibly be avoided due to self absorbance of monomers.

2.5.5. Melt viscosity

As already mentioned several times before, viscosity of resins is an important property, because many application processes need a specific range of viscosity. Since formulations based on MI-St-system **MISt3-5** can be applied also at higher temperatures, melt viscosity was measured on a rheometer to further characterise the MI-St-systems and to evaluate potential fields of usage.

So the results depicted in Figure 115 and summarised in Table 31 were gained for formulations based on **MISt3**.

Die approbierte gedruckte Originalversion dieser Dissertation ist an der TU Wien Bibliothek verfügbar.
The approved original version of this doctoral thesis is available in print at TU Wien Bibliothek.
TU Bibliothek Your knowledge hub WIEN

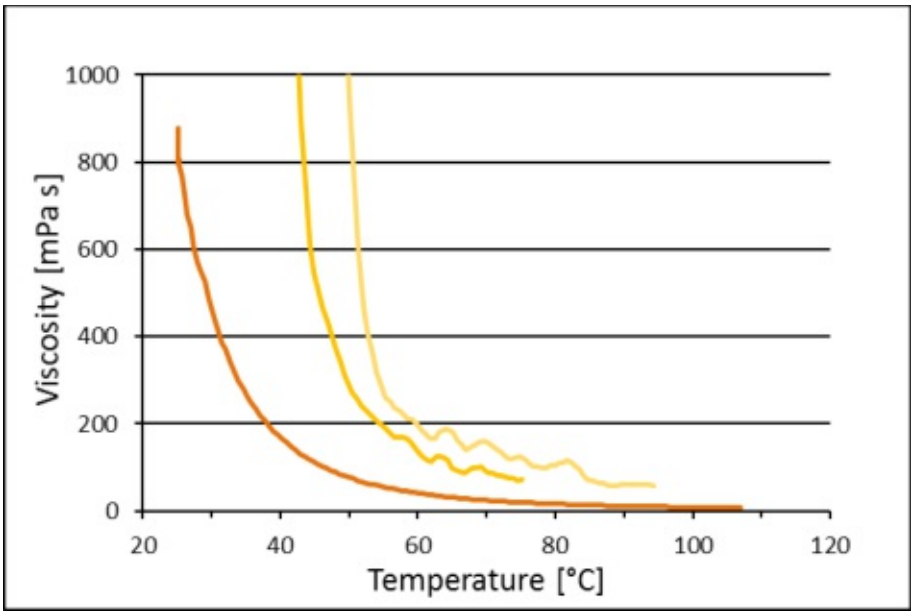

Figure 115: Melt viscosity of **MISt3** formulations without (—) and with 10 (—) or 20 w% (—) **CB24**

Table 31: Viscosity of tested **MISt3** formulations at 60 °C

Resin	Viscosity [mPa s]
MISt3_0	41
MISt3_10	115
MISt3_20	169

As expected and shown in Table 31 addition of high molecular weight rubber **CB24** induces an increase in viscosity. Interestingly, – and not fully understood yet – a very strong viscosity decline can be observed in all 3 formulations with increasing temperature.

Measurements of **MISt4**-based resins were started at 70 °C to ensure homogeneous resins. The obtained melt viscosity curves are presented in Figure 116 and viscosities at 80 °C are listed in Table 32 for comparison.

Die approbierte gedruckte Originalversion dieser Dissertation ist an der TU Wien Bibliothek verfügbar.
The approved original version of this doctoral thesis is available in print at TU Wien Bibliothek.
TU Bibliothek Your knowledge hub WIEN

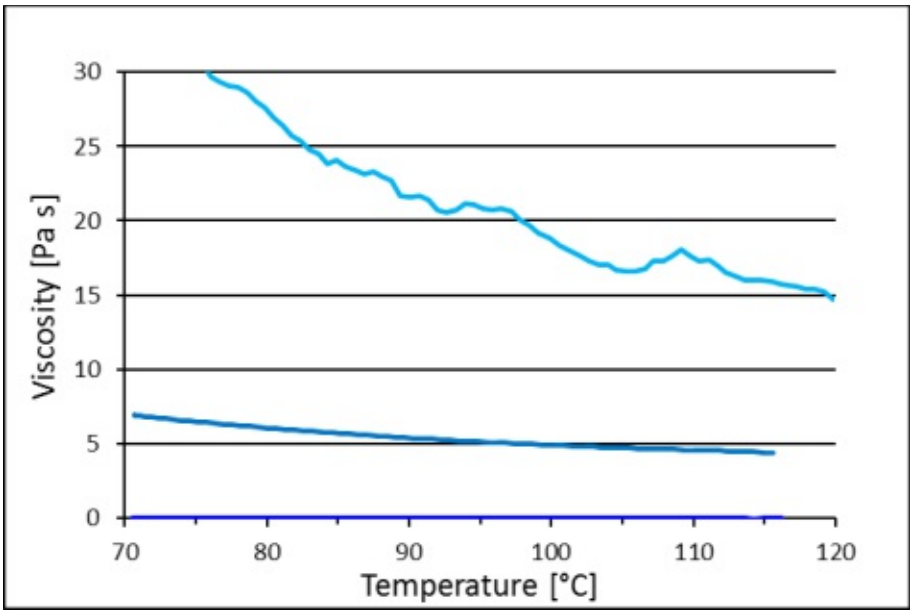

Figure 116: Melt viscosity of **MISt4** formulations without (—) and with 10 (—) or 20 w% (—) **CB24**

Table 32: Viscosity of tested **MISt4** formulations at 80 °C

Resin	Viscosity [mPa s]
MISt4_0	4
MISt4_10	6050
MISt4_20	26000

Results above again show a dramatic increase in viscosity when adding BR **CB24**, which was already observed in previous MI-St-systems, due to the high molecular weight of the rubber. Although **MISt4_20** is already very viscous, viscosity of **MISt4_10** is still on an acceptable level for many applications.

The results of **MISt5** are given in Figure 117 and summarised in Table 33 for 50 °C, which is the maximum working temperature for several hours of **MISt5**-based formulations.

Die approbierte gedruckte Originalversion dieser Dissertation ist an der TU Wien Bibliothek verfügbar.
The approved original version of this doctoral thesis is available in print at TU Wien Bibliothek.
TU Bibliothek Your knowledge hub WIEN

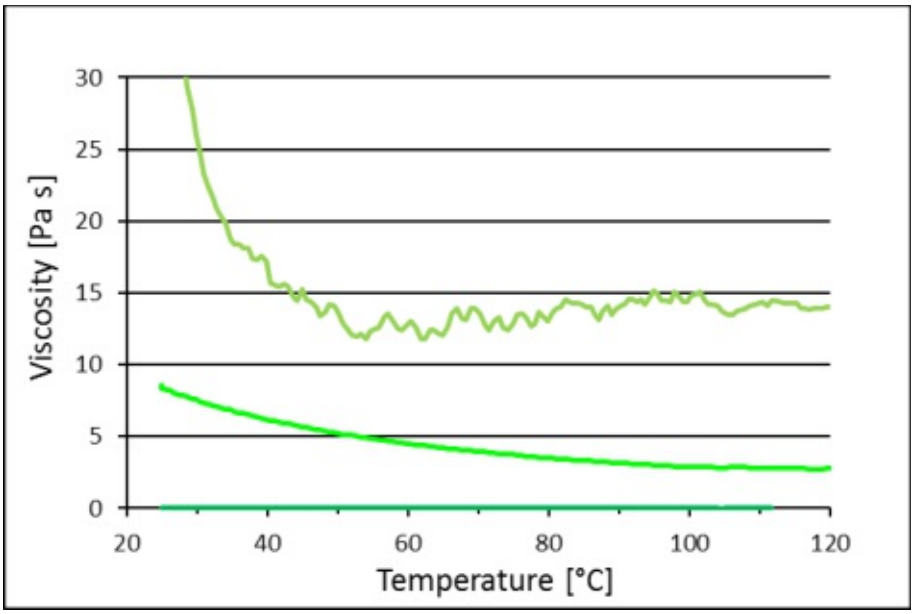

Figure 117: Melt viscosity of **MISt5** formulations without (—) and with 10 (—) or 20 w% (—) **CB24**

Table 33: Viscosity of tested **MISt5** formulations at 50 °C

Resin	Viscosity [mPa s]
MISt5_0	7
MISt5_10	5212
MISt5_20	13031

Determined viscosities of tested **MISt5** formulations are as well high, but on a level, which still allows processing.

As can be seen in Figures 115-117 and Tables 31-33 addition of high molecular weight rubber **CB24** to MI-St monomers induces a strong increase in viscosity. Nevertheless, viscosity of the resins is low especially at elevated temperatures and comparable to *e.g.* MA **IBMA** containing polybutadiene **CB24** at room temperature (see chapter 2.3.3).

Die approbierte gedruckte Originalversion dieser Dissertation ist an der TU Wien Bibliothek verfügbar.
The approved original version of this doctoral thesis is available in print at TU Wien Bibliothek.
TU Bibliothek Your knowledge hub WIEN

2.5.6. Photo-DSC

Since already performed preliminary experiments on the MI-St formulations give very promising results regarding resin properties, also photo-DSC studies were conducted to evaluate the photopolymerisation reaction of the different MI-St-systems.

Additionally, the influence of polybutadiene **CB24** content on polymerisation kinetics should be tested. Furthermore, a first comparison to model MI-St-system **MISt1** can be performed, to check the expected lower reactivity of MI **MMI** compared to **PrMI**, which was already indicated by the storage stability tests (chapter 2.5.3).

Photo-DSC experiments were conducted at 25 °C (**MISt3** and **MISt5**) or for **MISt4** formulations at 80 °C to ensure homogeneous resins. Samples were irradiated with a wavelength of 320 – 500 nm, since 0.2 w% TPO-L are applied as PI in all formulations. Additionally, ^{1}H-NMR spectroscopy and GPC of **MISt3_0** were performed. No NMR spectra and GPC of all the other tested samples were measured, because they are insoluble, which further underlines the proposed theory of cross-linking in MI-St-copolymers (see chapter 2.4.2).

Results of the photo-DSC study for MI-St-system **MISt3** are given in Figure 118 and summarised in Table 34.

Die approbierte gedruckte Originalversion dieser Dissertation ist an der TU Wien Bibliothek verfügbar.
The approved original version of this doctoral thesis is available in print at TU Wien Bibliothek.
TU Bibliothek Your knowledge hub WIEN

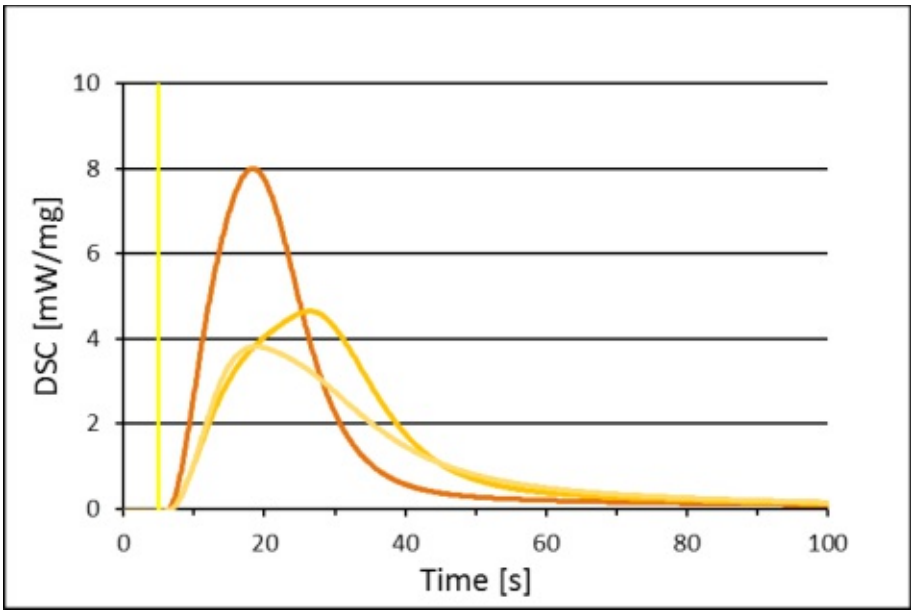

Figure 118: Photo-DSC curves of **MISt3** without (—) and with 10 (—) or 20 w% (—) **CB24**; start of irradiation (—)

Table 34: Results of photo-DSC, NMR spectroscopy and GPC measurements of **MISt3**-based formulations

Formulation	Photo-DSC			NMR spectroscopy		GPC	
	Peak max [s]	$t_{95\%}$ [s]	Area [J/g]	DBC MI [%]	DBC St [%]	M_n [kDa]	Đ [-]
MISt3_0	14.1	63.8	142.0	62	61	100.0	6.9
MISt3_10	21.5	92.8	133.9	not soluble		not soluble	
MISt3_20	14.0	98.3	122.5				

The data given in Table 34 shows that the addition of **CB24** to **MISt3** raises the necessary time to reach peak maximum and time to get 95% of conversion. But it has to be mentioned, that the variation of measured values is quite high. Additionally, the amount of generated heat is reduced with increasing rubber concentration, due to decreased volume of reactive double bonds in the formulation.

In contrast, photo-DSC curves of **MISt1** resins show faster polymerisation reactions with increasing BR content (see chapter 2.3.5). This occurs due to a much higher reaction heat and thus a much more distinct Trommsdorff effect

Die approbierte gedruckte Originalversion dieser Dissertation ist an der TU Wien Bibliothek verfügbar.
The approved original version of this doctoral thesis is available in print at TU Wien Bibliothek.
TU Bibliothek Your knowledge hub WIEN

compared to **MISt3** formulations. In addition, DSC curves in Figure 118 exhibit a few seconds inhibition time until photopolymerisation reaction is initiated. This can be attributed to dissolved O_2 or more probably to the higher inhibitor concentration in **MISt3** formulations (compare chapter 2.5.1.1). Furthermore, absorption of irradiation by the aromatic substituted MI **MMI** in **MISt3** may hinder efficient photopolymerisation as well (see chapter 2.5.4). So higher PI concentration or more reactive PIs would avoid this effect, but then comparison of different MI-St-systems and also the fabrication of thick specimens for mechanical testing would not be possible due to the high reaction heat (compare chapter 2.3).

As already known from MI-St-system **MISt2** (chapter 2.4.2), cross-linking of the MI-St-system with polybutadiene **CB24** occurs and therefore the samples are not soluble anymore. Since NMR spectroscopy and GPC are only possible in solution, only **pMISt3_0** can be analysed with these 2 techniques. So DBC was calculated with ^{1}H-NMR spectra and showed relatively low MI and St conversion of 62% and 61%, respectively. These results are in accordance with literature, that aromatic MIs are less reactive than aliphatic ones [116]. Additionally, measured molecular weights and DBCs are not as high as in previously tested **pMISt2_0**, where also an aromatic substituted MI (**PhMI**) is used, because it was photopolymerised at 100 °C (see chapter 2.4.2.3).

Furthermore, **MISt4** formulations were investigated as well. Results are depicted in Figure 119 and listed in Table 35.

Die approbierte gedruckte Originalversion dieser Dissertation ist an der TU Wien Bibliothek verfügbar.
The approved original version of this doctoral thesis is available in print at TU Wien Bibliothek.
TU Bibliothek Your knowledge hub WIEN

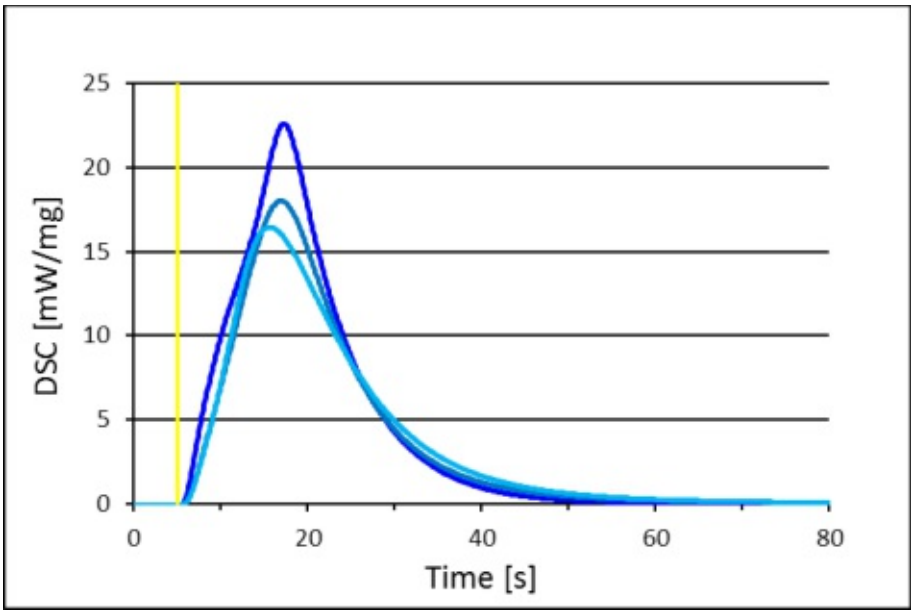

Figure 119: Photo-DSC curves of **MISt4** without (—) and with 10 (—) or 20 w% (—) **CB24**; start of irradiation (—)

Table 35: Results of photo-DSC studies of **MISt4**-based formulations

Formulation	Peak max [s]	$t_{95\%}$ [s]	Area [J/g]
MISt4_0	12.2	28.4	312.3
MISt4_10	11.8	32.4	290.9
MISt4_20	10.8	36.4	275.9

Obtained data of **MISt4** formulations above shows the same trends as the already investigated **MISt1** system, where also an aliphatic MI (**PrMI**) is used (chapter 2.3.5). Time to reach peak maximum is reduced and $t_{95\%}$ is increased with higher rubber concentrations, due to increased viscosity of the formulations. However, although MI-St-system **MISt4** reacts a lot faster than model system **MISt1**, it can hardly be compared, because they were tested at 25 °C and not at 80 °C and an increased temperature also enhances the reaction rate. Finally, a similar DBC can be assumed for all resins as heat of polymerisation (peak area) decreases approximately by the weight percent of polybutadiene content.

Die approbierte gedruckte Originalversion dieser Dissertation ist an der TU Wien Bibliothek verfügbar.
The approved original version of this doctoral thesis is available in print at TU Wien Bibliothek.
TU Bibliothek Your knowledge hub WIEN

Finally, results of photo-DSC experiments of **MISt5**-based resins are given in Figure 120 and Table 36.

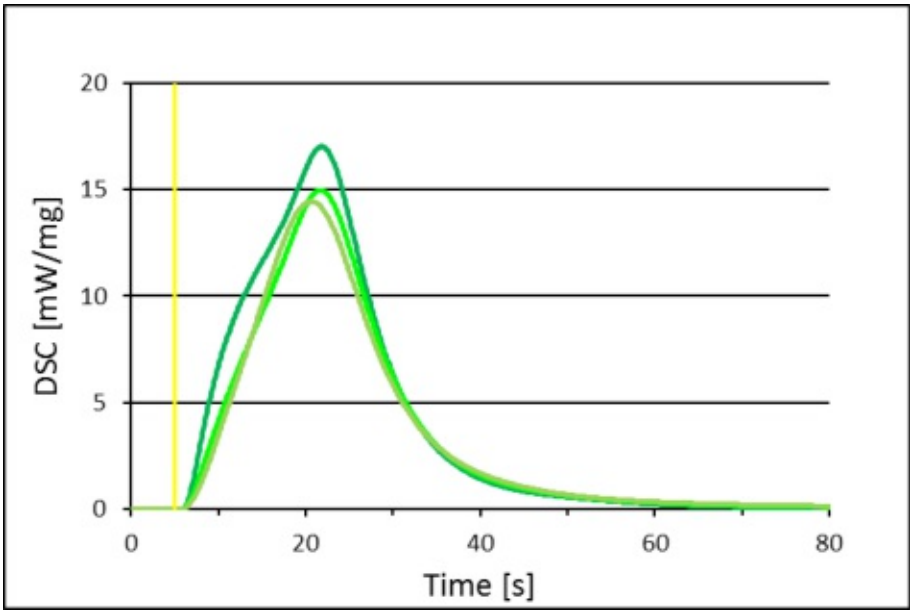

Figure 120: Photo-DSC curves of **MISt5** without (—) and with 10 (—) or 20 w% (—) **CB24**; start of irradiation (—)

Table 36: Results of photo-DSC studies of **MISt5**-based formulations

Formulation	Peak max [s]	$t_{95\%}$ [s]	Area [J/g]
MISt5_0	17.6	32.9	303.3
MISt5_10	17.3	38.0	273.8
MISt5_20	16.9	42.9	264.0

Photo-DSC data shows – as expected – again high reactivity for **MISt5**, which is similar to model MI-St-system **MISt1** (chapter 2.3.5) and **MISt4**, since they all contain aliphatic substituted MIs (**PrMI** or **CHMI**). Polymerisation is faster with increasing BR content and formulations without and with 10 w% **CB24** exhibit a Trommsdorff effect. Finally, similar DBCs can be assumed, due to comparable polymerisation heat, which decreases approximately according to their rubber concentration.

Die approbierte gedruckte Originalversion dieser Dissertation ist an der TU Wien Bibliothek verfügbar.
The approved original version of this doctoral thesis is available in print at TU Wien Bibliothek.
TU Bibliothek Your knowledge hub WIEN

The photo-DSC results for **MISt3**-based resins verified the expected lower reactivity caused by the aromatic substituent on the MI compound. In addition, determined molecular weights and DBCs of **pMISt3_0** are also not as high as in **pMISt2_0**, due to a lower reaction temperature.
Furthermore, although MI-St-system **MISt4** reacts a lot faster than model system **MISt1** and also **MISt5**, it can hardly be compared, because of the needed elevated measurement temperature and thus enhanced reaction rate. Nevertheless, both monomer generations **MISt4** and **MISt5** show promising results in the photo-DSC study.

So experiments on the photopolymerisation reaction of the monomer generations **MISt3-5** will be completed with RT-NIR-photorheology studies to determine also DBCs of the insoluble polymers.

2.5.7. RT-NIR-photorheology

RT-NIR-photorheology measurements were performed for further characterisation of the photopolymerisation reaction of MI-St-systems **MISt3-5**. Furthermore, rheological informations on the curing reaction can be gained on the rheometer device.

It should be mentioned once more, that NIR double bond signals from MI and St could not be distinguished due to strong overlapping of the peaks (compare Figure 84). Since effective alternating copolymerisation of MI and St was already elucidated in chapter 2.3.6, the following DBCs always refer to an overall conversion of both monomers.

Die approbierte gedruckte Originalversion dieser Dissertation ist an der TU Wien Bibliothek verfügbar.
The approved original version of this doctoral thesis is available in print at TU Wien Bibliothek.
TU Bibliothek Your knowledge hub WIEN

The experiments were conducted at 25 °C (**MISt3** and **MISt5**) and for **MISt4** formulations at 80 °C to ensure homogeneous resins. Since 0.2 w% TPO-L are applied as PI, samples were irradiated with a wavelength of 320 – 500 nm.

The results of the MI-St-system **MISt3** are presented in Figure 121 and summarised in Table 37. Furthermore, diagrams of the storage and loss modulus and the evolution of shrinkage force during polymerisation are given in the appendix (Figures 150 and 151).

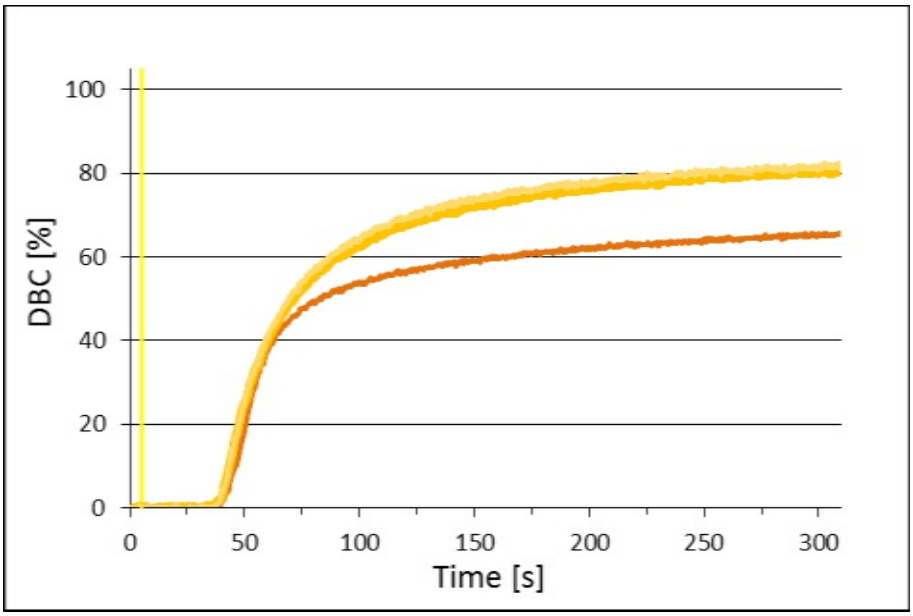

Figure 121: DBC of **MISt3** formulations without (—) and with 10 (—) or 20 w% (—) **CB24**; start of irradiation (—)

Table 37: Results of photorheology experiments of **MISt3**

Formulation	R_p [%/s]	t_{gp} [s]	DBC_{gp} [%]	$t_{95\%}$ [s]	DBC_{end} [%]	Shrinkage force [N]
MISt3_0	2.1	-	-	201.3	67	9.0
MISt3_10	2.2	45.1	27	203.0	81	11.8
MISt3_20	2.2	43.0	22	195.3	83	12.4

Die approbierte gedruckte Originalversion dieser Dissertation ist an der TU Wien Bibliothek verfügbar.
The approved original version of this doctoral thesis is available in print at TU Wien Bibliothek.
TU Bibliothek Your knowledge hub WIEN

As can be seen in results above, higher BR concentration in **MISt3** resins slightly increases polymerisation rate, reduces time needed to reach the gel point and also the DBC at this point. Nevertheless, in the end a higher DBC is obtained. The formed shrinkage force is a little bit increased with higher **CB24** content supposable due to higher conversion and/or degree of cross-linking.
When compared to model MI-St-system **MISt1**, where the aliphatic substituted MI **PrMI** is used, **MISt3** resins show the same trends with increasing rubber **CB24** concentration but photopolymerisation is much more retarded and less final conversion is reached. This effect can be explained again by the lower reactivity of aromatic substituted MI **MMI** in **MISt3** [116].
Finally, the absence of an intersection point of G' and G'' curves (gel point) for **MISt3_0** is probably produced due to a very high viscous part and no cross-linking in **pMISt3_0**.

Furthermore, data of the monomer generation **MISt4** are given in Figure 122 and listed in Table 38. Diagrams of the storage and loss modulus and the evolution of shrinkage force during polymerisation are again shown in the appendix in Figures 152 and 153.

Die approbierte gedruckte Originalversion dieser Dissertation ist an der TU Wien Bibliothek verfügbar.
The approved original version of this doctoral thesis is available in print at TU Wien Bibliothek.
TU Bibliothek Your knowledge hub WIEN

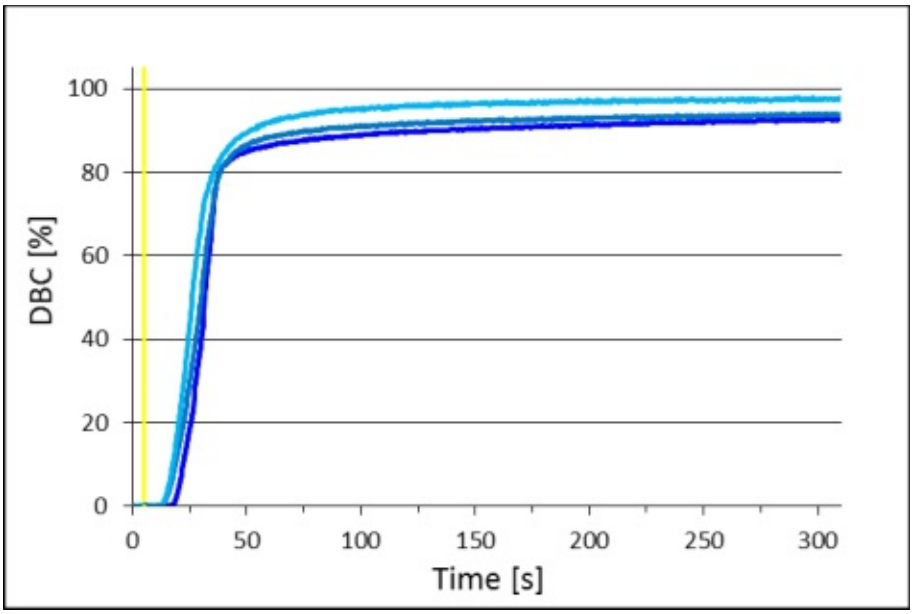

Figure 122: DBC of **MISt4** without (—) and with 10 (—) or 20 w% (—) **CB24**; start of irradiation (—)

Table 38: Results of photorheology experiments of **MISt4**

Formulation	R_p [%/s]	t_{gp} [s]	DBC_{gp} [%]	$t_{95\%}$ [s]	DBC_{end} [%]	Shrinkage force [N]
MISt4_0	3.8	33.7	79	79.0	93	11.4
MISt4_10	3.7	18.3	24	67.3	95	20.4
MISt4_20	4.5	16.1	24	63.7	97	20.2

MISt4-based formulations exhibit the same trends like previously tested MI-St-system **MISt3** before. Additionally, shrinkage force decreases somewhat already during the experiment due to the high temperature during the measurement, which makes stress relaxation in the material possible. Again the higher reactivity of **MISt4** can be attributed to the elevated measurement temperature, which is needed to guarantee a homogeneous formulation.

Finally, **MISt5**-based formulations were studied as well. So results illustrated in Figure 123 and summarised in Table 39 were gained. Diagrams of the storage and loss modulus and the evolution of shrinkage force during polymerisation are depicted in the appendix (Figures 154 and 155).

Die approbierte gedruckte Originalversion dieser Dissertation ist an der TU Wien Bibliothek verfügbar.
The approved original version of this doctoral thesis is available in print at TU Wien Bibliothek.
TU Bibliothek Your knowledge hub WIEN

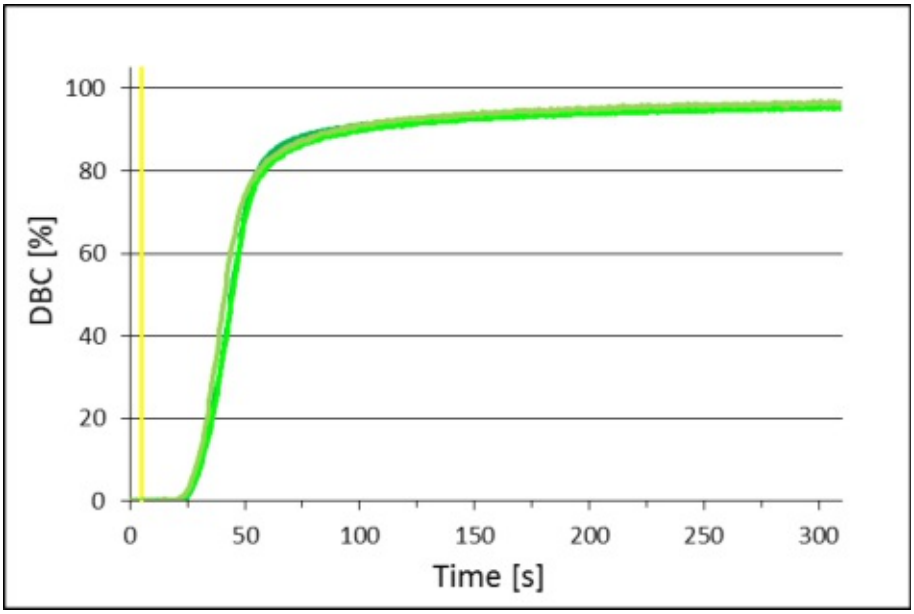

Figure 123: DBC of **MISt5** without (—) and with 10 (—) or 20 w% (—) **CB24**; start of irradiation (—)

Table 39: Results of photorheology experiments of **MISt5**

Formulation	R_p [%/s]	t_{gp} [s]	DBC_{gp} [%]	$t_{95\%}$ [s]	DBC_{end} [%]	Shrinkage force [N]
MISt5_0	3.1	45.3	73	90.5	95	18.5
MISt5_10	3.2	35.5	33	107.2	95	19.2
MISt5_20	3.4	30.1	27	103.1	97	19.9

Results for **MISt5** resins in Table 39 show, that t_{gp} and also DBC_{gp} again become lower with higher rubber **CB24** content, due to significant higher viscosities and therefore earlier gelation. In contrast, increasing BR concentration exhibits almost no influence on polymerisation rate, $t_{95\%}$, final DBC and shrinkage force.

Die approbierte gedruckte Originalversion dieser Dissertation ist an der TU Wien Bibliothek verfügbar.
The approved original version of this doctoral thesis is available in print at TU Wien Bibliothek.
TU Bibliothek Your knowledge hub WIEN

RT-NIR-photorheology experiments evidence the lower reactivity of **MISt3** formulations once more.

Results of **MISt4** and **MISt5** are comparable to monomer generation **MISt1**, which can be expected, because monomers with similar structures are utilised. While measurements with **MISt4** were always performed at 80 °C and thus are hardly comparable with other experiments due to higher reactivity at elevated temperatures, the main difference of the MI-St-systems **MISt1** and **MISt5** is, that **MISt5** formulations need longer time to gel and so higher DBC_{gp}s are gained. This effect is probably attributed due to less cross-linking reactions during the MI-St-copolymerisation of **MISt5** monomers caused by a more sterically hindered CH_2 group in α-position in MI **EHMI** than **PrMI**. Hence, a swellability study will clarify this idea.

2.5.8. Swellability

Swellability studies of **pMISt3-5** without and with BR **CB24** were performed to prove again (in)solubility and thus occurrence of the suggested cross-linking mechanism in the MI-St-BR-terpolymer (compare also swellability studies of **pMISt1** and **pMISt2** photopolymers in chapters 2.3.7 and 2.4.2.3). Furthermore, it should be tested, if retarded gelation of **MISt5** compared to **MISt1** in RT-NIR-photorheology experiments (chapter 2.5.7) originates from less cross-linking reactions.

Therefore, polymerised samples were submerged for 7 d in $CHCl_3$. Sample mass was recorded before and after swelling and after drying (see also chapter 2.5.8 of the experimental part).

So swellabilities and gel fractions of the different MI-St-system **pMISt3-5**, which are listed in Tables 40-42, were calculated.

Die approbierte gedruckte Originalversion dieser Dissertation ist an der TU Wien Bibliothek verfügbar.
The approved original version of this doctoral thesis is available in print at TU Wien Bibliothek.
TU Bibliothek Your knowledge hub WIEN

Table 40: Swellability and gel fraction of **pMISt3**

Sample	Swellability [%]	Gel fraction [%]
pMISt3_0	- *	0*
pMISt3_10	1840	10.6
pMISt3_20	1600	53.0

* completely soluble

Table 41: Swellability and gel fraction of **pMISt4**

Sample	Swellability [%]	Gel fraction [%]
pMISt4_0	28700	18.0
pMISt4_10	1240	78.1
pMISt4_20	900	85.1

Table 42: Swellability and gel fraction of **pMISt5**

Sample	Swellability [%]	Gel fraction [%]
pMISt5_0	16000	22.7
pMISt5_10	1770	81.9
pMISt5_20	1140	91.9

Results shown in Table 40 support again the proposed theory of cross-linking of the MI-St system by abstractable H atoms next to the N atom of the MI component, because **pMISt3_0** is soluble – like **pMISt2_0** before – as there is no possibility for H-abstraction next to a N atom. In contrast, **pMISt4_0** and **pMISt5_0** are insoluble due to cross-linking reactions of the MIs **CHMI** and **EHMI**. Additionally, also the low conversion (compare chapter 2.5.7) of the **pMISt3**-based polymers can be seen as the gel fraction is really low.

Furthermore, swellability values of **pMISt4_0** and **pMISt5_0** are a lot higher than **pMISt1_0**, which is caused by the sterical hindrance of the bulky side groups for H-abstraction in α-position next to the N atom. Swellabilities of **pMISt4** and **pMISt5** containing BR are lower compared to corresponding **pMISt2** and **pMISt3** polymers due to cross-linking reactions on the aliphatic substituted MIs **CHMI** and **EHMI**, which further underlines the theory of less cross-linking reactions

Die approbierte gedruckte Originalversion dieser Dissertation ist an der TU Wien Bibliothek verfügbar.
The approved original version of this doctoral thesis is available in print at TU Wien Bibliothek.
TU Bibliothek Your knowledge hub WIEN

because MI **EHMI** exhibits an increased steric hindrance for H-abstraction in α-position due to the ethyl group in β-position compared to cyclohexyl substituted MI **CHMI**.

In addition, – as known from previous experiments on MI-St-systems – higher rubber concentrations yield higher conversion, which can be seen at increased gel fractions. Furthermore, denser networks are obtained caused by more cross-linking reactions of the MI/St with the polybutadiene double bonds and thus less swelling occurs. As this reaction is more frequently with higher rubber concentrations, it leads to higher network densities. Therefore, the same trends as before for MI-St-systems **pMISt1** and **pMISt2** can be observed as well for **pMISt3-5**.

So **pMISt3**-based photopolymers were not studied further, because low reactivity, low conversion and low molecular weights will not yield suitable materials. Hence, only **pMISt4** and **pMISt5** without and with 10 or 20 w% rubber **CB24** are investigated regarding their (thermo)mechanical properties.

2.5.9. (Thermo)mechanical properties

In addition to physical and chemical properties of **MISt4** and **MISt5** resins the final photopolymers should also be tested regarding their (thermo)mechanical properties to complete studies on MI-St-BR-systems **pMISt4** and **pMISt5**.

The specimens for all (thermo)mechanical tests were prepared by moulding the resins according to the general procedure described in chapter 2.3.8 of the experimental part or for **MISt4** samples according to chapter 2.5.9 of the experimental part.

Die approbierte gedruckte Originalversion dieser Dissertation ist an der TU Wien Bibliothek verfügbar.
The approved original version of this doctoral thesis is available in print at TU Wien Bibliothek.
TU WIEN Bibliothek Your knowledge hub

2.5.9.1. DMTA

DMTA measurements were performed to estimate thermomechanical properties as well as thermal phase transitions like T_g.

All DMTA experiments were conducted in torsion mode with a heating rate of 2 °C/min and constant normal force.
The obtained results of the DMTA studies are depicted in Figure 124 (**pMISt4**) and Figure 125 (**pMISt5**).

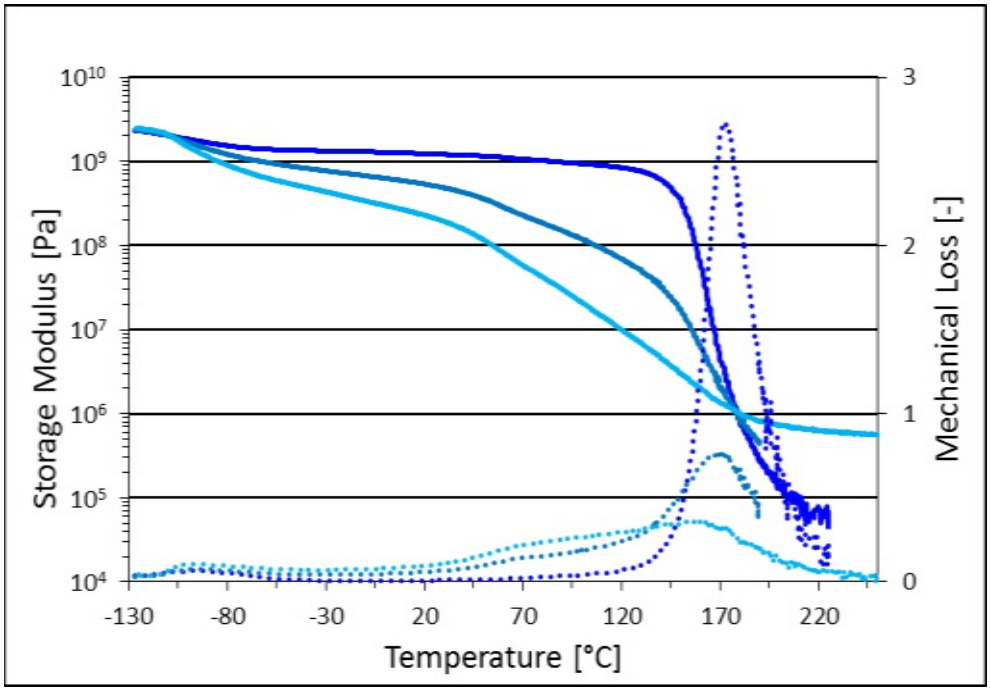

Figure 124: Storage modulus (—) and mechanical loss (▪▪▪) of **pMISt4** without (—) and with 10 (—) or 20 w% (—) **CB24**

Figure 124 shows interestingly quite high compatibility of rubber **CB24** and MI-St phase in **pMISt4**, which can be seen in the small glass transition peak in loss factor of the rubber (~ -95 °C) and the occurrence of a new peak at ~ 70 °C at higher BR concentrations. Additionally, – as expected – T_gs reach a very high level of > 170 °C, which are almost the same values like **pMISt1**.

Die approbierte gedruckte Originalversion dieser Dissertation ist an der TU Wien Bibliothek verfügbar.
The approved original version of this doctoral thesis is available in print at TU Wien Bibliothek.
TU Bibliothek Your knowledge hub WIEN

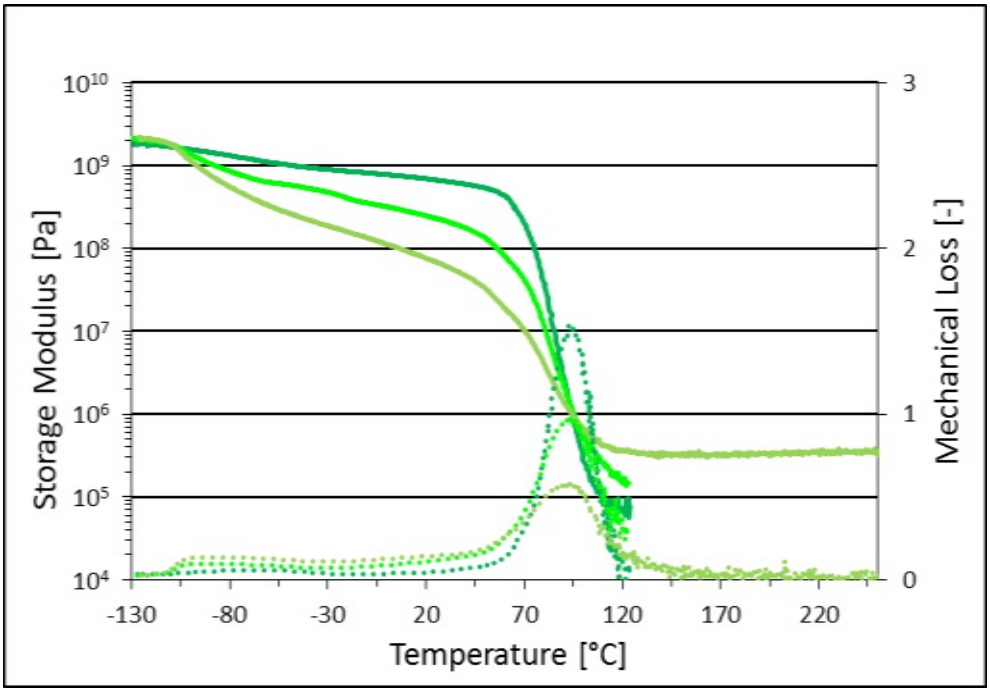

Figure 125: Storage modulus (—) and mechanical loss (▪▪▪) of **pMISt5** without (—) and with 10 (—) or 20 w% (—) **CB24**

Interestingly, also **pMISt5** matrix exhibits quite high compatibility with BR **CB24**. This behaviour can be attributed to the aliphatic 2-ethyl hexyl side chain of MI **EHMI**, which can be seen at the very small peak of the loss factor of the rubber glass transition at ~ -95 °C. Nevertheless, G' at room temperature decreases dramatically with increasing polybutadiene concentration. Furthermore, T_g of hard MI-St phase in **pMISt5**-based polymer is quite low (~ 90 °C) compared to the other tested MI-St-systems, because the long aliphatic substituent of the used MI **EHMI** acts as plasticiser.

In comparison of the 2 investigated MI-St-systems again the strong influence of the substituents on the utilised MI structure can be observed. The rigid cyclohexyl moiety in **pMISt4** increases glass transition temperature and yields

Die approbierte gedruckte Originalversion dieser Dissertation ist an der TU Wien Bibliothek verfügbar.
The approved original version of this doctoral thesis is available in print at TU Wien Bibliothek.
TU Bibliothek Your knowledge hub WIEN

also a high modulus at room temperature. In contrast, **pMISt5**, which contains **EHMI** with a 2-ethyl hexyl structure, exhibits a dramatic loss of T_g and G' due to the long aliphatic side chain.

2.5.9.2. Tensile tests

Additionally, tensile tests of **pMISt4** and **pMISt5** with various BR concentrations were conducted to gain further insights into mechanical properties of these MI-St-BR-terpolymers.

All tensile tests were performed according to ISO 527 with specimen shape 5B and a traverse velocity of 5 mm/min.
So stress-strain curves given exemplary in Figures 126-127 and summarised in Tables 43-44 were obtained for **pMISt4-5**.

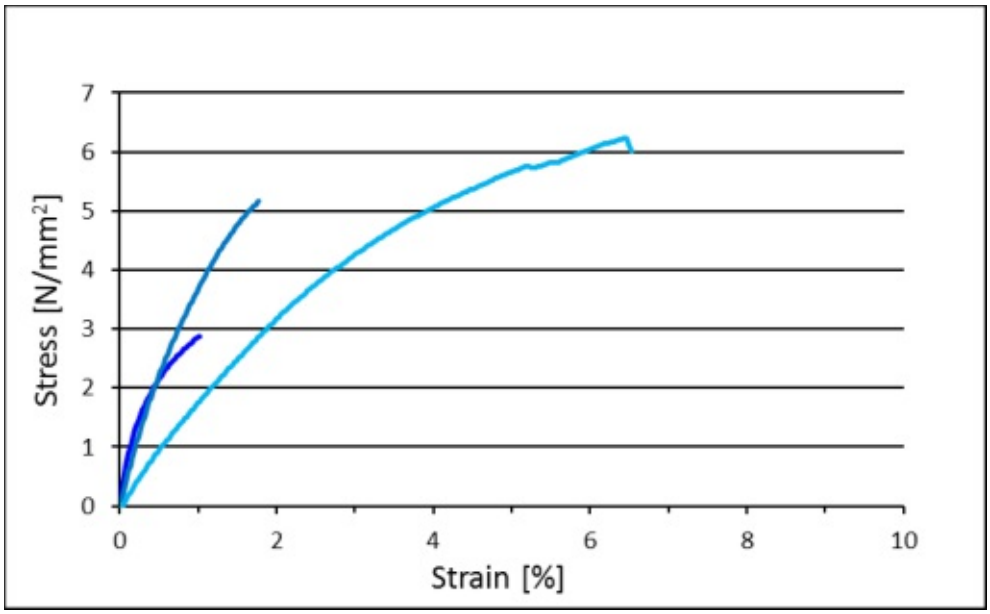

Figure 126: Stress-strain curves of **pMISt4** without (—) and with 10 (—) or 20 w% (—) **CB24**

Die approbierte gedruckte Originalversion dieser Dissertation ist an der TU Wien Bibliothek verfügbar.
The approved original version of this doctoral thesis is available in print at TU Wien Bibliothek.
TU Bibliothek Your knowledge hub WIEN

Table 43: Results of tensile tests of **pMISt4**

Sample	$Stress_{max}$ [MPa]		$Strain_{Break}$ [%]	
	Average	s	Average	s
pMISt4_0	3.0	0.2	1.3	0.3
pMISt4_10	5.0	0.2	1.9	0.2
pMISt4_20	6.4	0.4	6.2	1.6

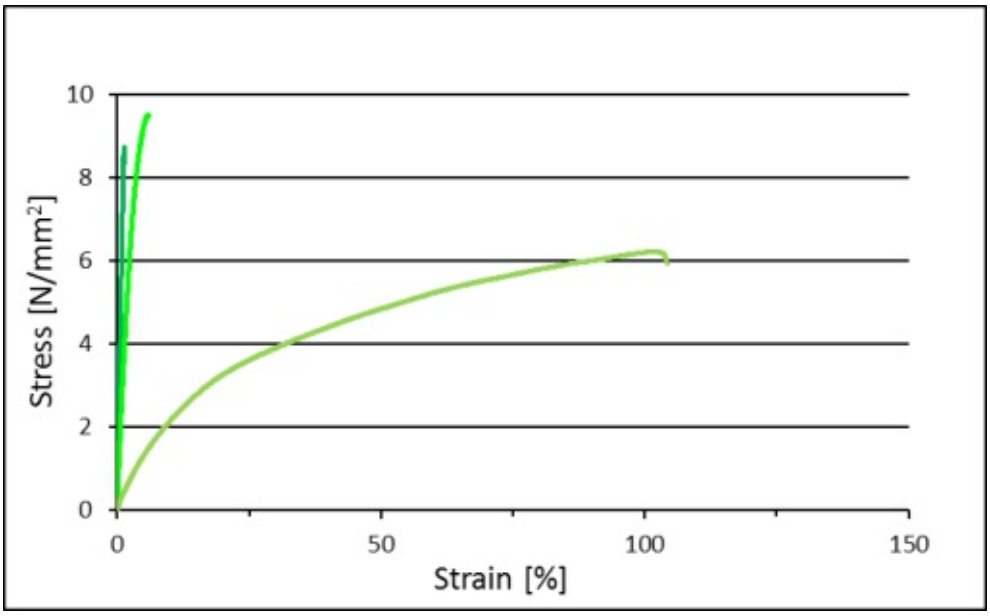

Figure 127: Stress-strain curves of **pMISt5** without (—) and with 10 (—) or 20 w% (—) **CB24**

Table 44: Results of tensile tests of **pMISt5**

Sample	$Stress_{max}$ [MPa]		$Strain_{Break}$ [%]	
	Average	s	Average	s
pMISt5_0	8.0	1.1	1.1	0.3
pMISt5_10	9.4	0.4	6.0	0.0
pMISt5_20	6.5	0.6	122.9	31.7

Tensile tests of **pMISt4** and **pMISt5** show the same trends as in model MI-St-system **pMISt1**: low concentrations of polybutadiene **CB24** increase σ_{max} and ε_{break}, before at higher rubber contents the rubbery behaviour dominates the

Die approbierte gedruckte Originalversion dieser Dissertation ist an der TU Wien Bibliothek verfügbar.
The approved original version of this doctoral thesis is available in print at TU Wien Bibliothek.
TU Bibliothek Your knowledge hub WIEN

material properties. Furthermore, the influence of the rigid cycloaliphatic structure of MI **CHMI** in **pMISt4** can be observed again, since it causes the low stress and strain at break compared to **pMISt5**.

Nevertheless, **pMISt1** exhibits still higher values than **pMISt4** and **pMISt5** (~ 3 – 4 times higher maximum stress) due to more cross-linking reactions, whereby higher network densities are achieved. Additionally, these low values may be attributed to higher brittleness compared to **pMISt1**-based polymers. Thus, impact resistance was tested as well.

2.5.9.3. Impact resistance

Finally, impact resistance of the **pMISt4**/**pMISt5**-**CB24**-terpolymers were measured to finalise characterisation of mechanical properties.

Impact resistance was determined with the Dynstat approach according to DIN 51230.

So results presented in Figures 128-129 and Tables 45-46 were calculated.

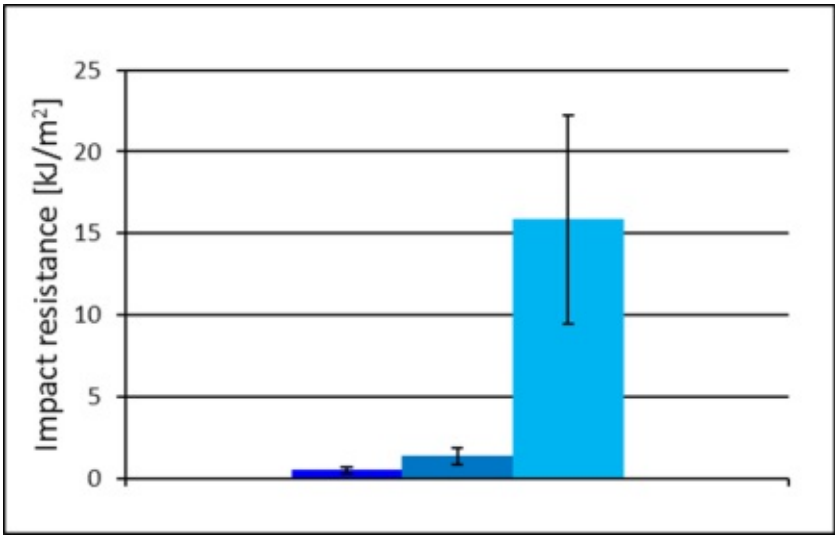

Figure 128: Dynstat impact resistance of **pMISt4** without (—) and with 10 (—) or 20 w% (—) **CB24**

Die approbierte gedruckte Originalversion dieser Dissertation ist an der TU Wien Bibliothek verfügbar.
The approved original version of this doctoral thesis is available in print at TU Wien Bibliothek.
TU Bibliothek Your knowledge hub WIEN

Table 45: Results of Dynstat impact tests of **pMISt4**

Sample	Impact resistance [kJ/m²]	
	Average	s
pMISt4_0	0.5	0.2
pMISt4_10	1.4	0.5
pMISt4_20	15.9*	6.4*

* hinge break

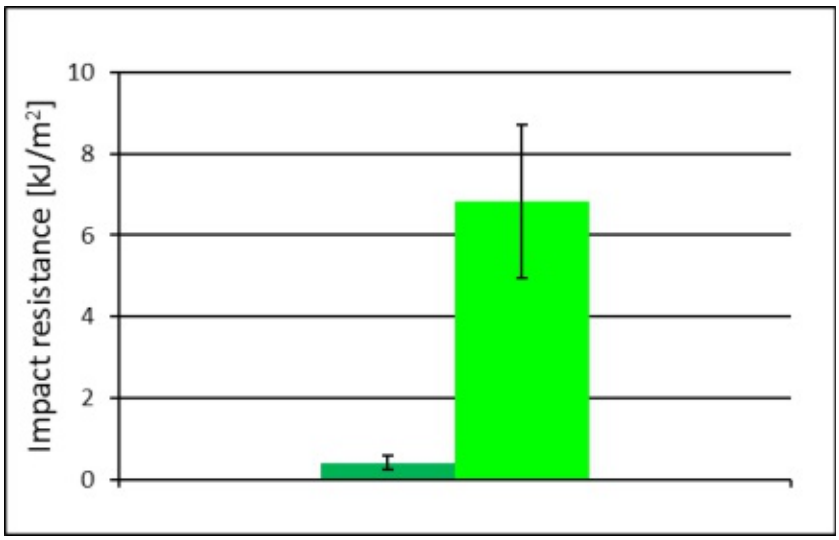

Figure 129: Dynstat impact resistance of **pMISt5** without (—) and with 10 w% (—) **CB24**

Table 46: Results of Dynstat impact tests of **pMISt5**

Sample	Impact resistance [kJ/m²]	
	Average	s
pMISt5_0	0.4	0.2
pMISt5_10	6.8*	1.9*
pMISt5_20	- **	- **

* hinge break

** does not break

As can be seen in Tables 45 and 46, **pMISt4** is more brittle than **pMISt5** and thus needs higher BR concentrations to obtain specimen that do not break anymore (compare also Figures 130 and 131). This behaviour can be attributed – as

Die approbierte gedruckte Originalversion dieser Dissertation ist an der TU Wien Bibliothek verfügbar.
The approved original version of this doctoral thesis is available in print at TU Wien Bibliothek.
TU Bibliothek Your knowledge hub WIEN

assumed before – to the substituents of the applied MIs: the cycloaliphatic ring structure (cyclohexyl moiety) in MI **CHMI**, which is applied in **pMISt4**, enhances rigidity but also brittleness.

Figure 130: pMISt4 specimen after impact test without (left) and with 10 (middle) or 20 w% (right) **CB24**

Figure 131: pMISt5 specimen after impact test without (left) and with 10 (middle) or 20 w% (right) **CB24**

However, even impact resistance of **pMISt5** is not as high as in **pMISt1** polymers (already **pMISt1_10** does not break), but still a BR **CB24** content of 20 w% is sufficient to obtain specimens, which do not fracture (compare also Figure 131). This drawback of **pMISt5** can be attributed to less effective phase separation of MI-St and BR phase, which was already observed in the DMTA measurements (compare chapter 2.5.9.1). Nevertheless, determined impact resistances are very high.

2.5.10. AFM

AFM experiments were performed again to visualise the phase separation and to measure the size of hard and soft domains in **pMISt4** and **pMISt5** containing rubber **CB24**.

Die approbierte gedruckte Originalversion dieser Dissertation ist an der TU Wien Bibliothek verfügbar.
The approved original version of this doctoral thesis is available in print at TU Wien Bibliothek.
TU Bibliothek WIEN Your knowledge hub

All AFM experiments were performed in an area of 5*5 µm^2 and with a resolution of 256*256 pixels.

So the images shown in Figures 132 and 133 were obtained from AFM measurements.

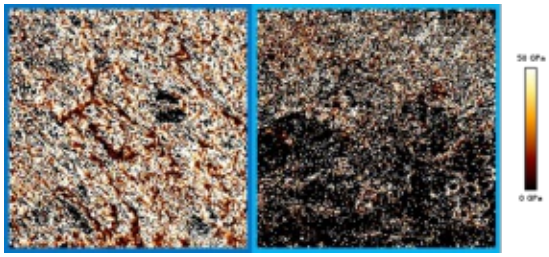

Figure 132: Young's moduli of **pMISt4** samples with 10 (—) or 20 w% (—) **CB24**

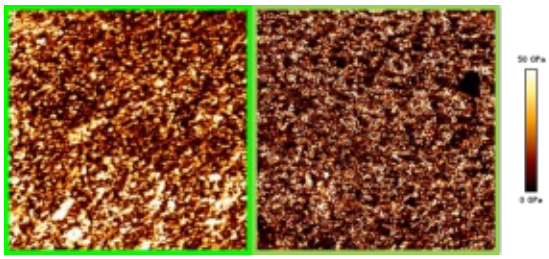

Figure 133: Young's moduli of **pMISt5** samples with 10 (—) or 20 w% (—) **CB24**

Although sample preparation was not perfect for these phase separated photopolymers, it still can be seen in Figures 132 and 133, that higher BR concentrations decrease the Young's moduli of the **pMISt4-5**-based terpolymers, which was already expected from the tensile tests (chapter 2.5.9.2) and previous investigated MI-St-BR-system **pMISt1** (see chapter 2.3). In addition, the lower moduli of **pMISt4**-based photopolymers are shown in the AFM pictures as well, since the rigid and brittle MI **CHMI** is used in **MISt4**. Furthermore, good compatibility of MI-St matrix and rubber phase is verified, which was observed in the DMTA curves of **pMISt4-5** terpolymers (see chapter 2.5.9.1). Finally, a more

Die approbierte gedruckte Originalversion dieser Dissertation ist an der TU Wien Bibliothek verfügbar.
The approved original version of this doctoral thesis is available in print at TU Wien Bibliothek.
TU Bibliothek Your knowledge hub WIEN

effective phase separation in **pMISt4** compared to **pMISt5**-based polymers is indicated as well due to smaller domains in the picture. Thus, AFM measurements further confirm previous experiments.

2.5.11. Thermal stability

Finally, **pMISt4-5** terpolymers were also investigated regarding their thermal stability in order to conclude studies on these monomer generations.

The measurements were conducted on the STA under N_2 atmosphere according to DIN EN ISO 11358.
So the results shown in Figures 134-135 and summarised in Tables 47-48 were gained for **pMISt4** and **pMISt5**.

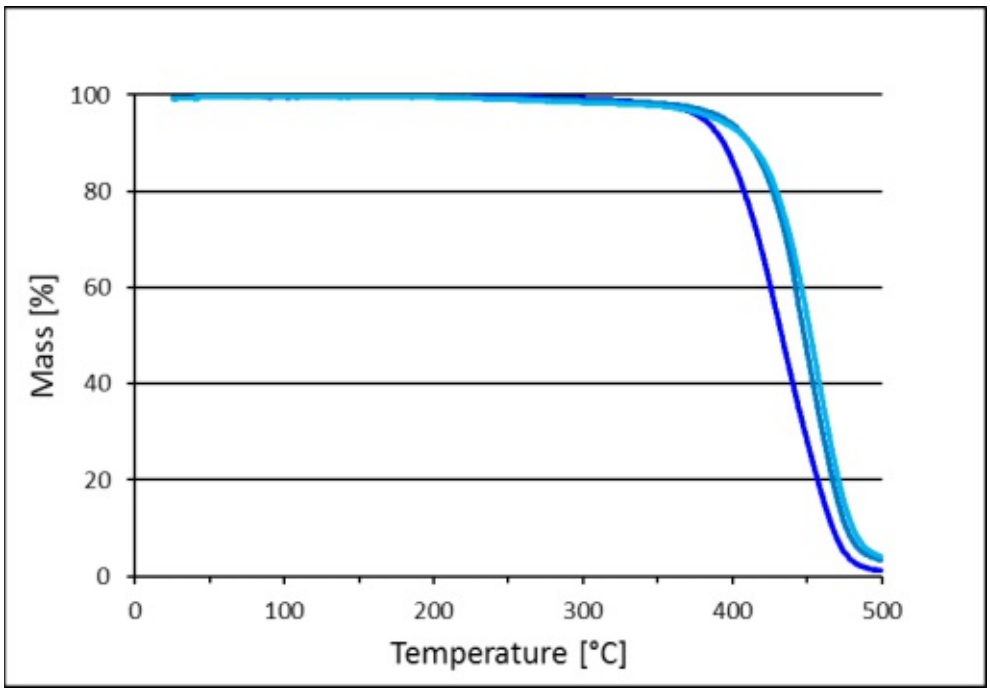

Figure 134: TGA of **pMISt4** without (—) and with 10 (—) or 20 w% (—) **CB24**

Die approbierte gedruckte Originalversion dieser Dissertation ist an der TU Wien Bibliothek verfügbar.
The approved original version of this doctoral thesis is available in print at TU Wien Bibliothek.
TU Bibliothek Your knowledge hub WIEN

Table 47: Thermal stability of **pMISt4**

Sample	T_A [°C]	T_C [°C]
pMISt4_0	395	432
pMISt4_10	419	444
pMISt4_20	424	454

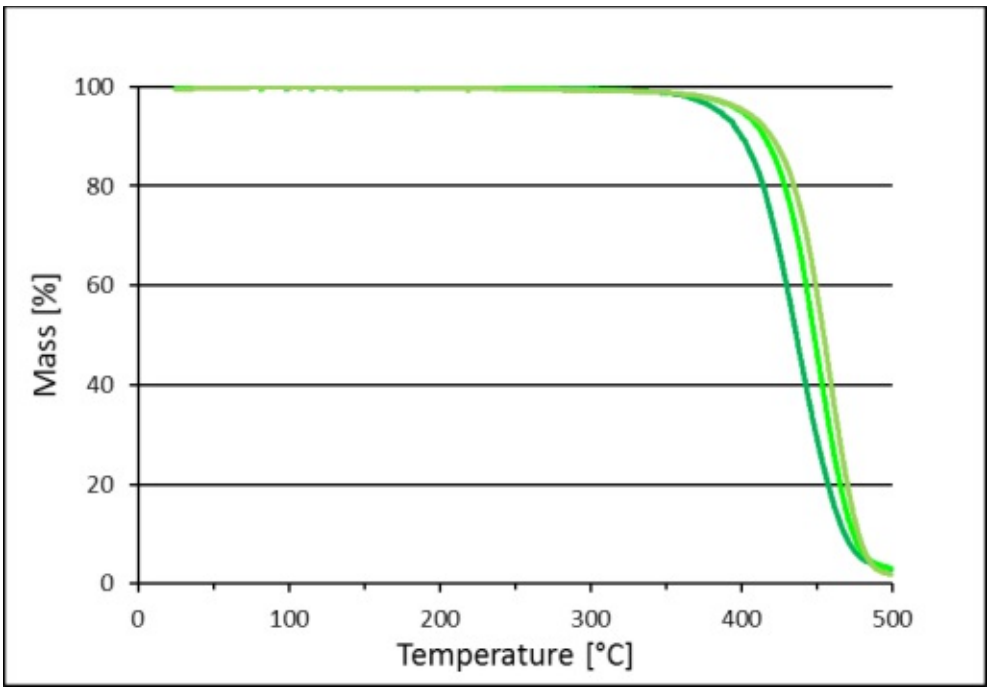

Figure 135: TGA of **pMISt5** without (—) and with 10 (—) or 20 w% (—) **CB24**

Table 48: Thermal stability of **pMISt5**

Sample	T_A [°C]	T_C [°C]
pMISt5_0	403	433
pMISt5_10	420	444
pMISt5_20	429	457

As expected – and also as already observed in former MI-St-BR-systems – higher polybutadiene **CB24** concentrations increase thermal stability. Nevertheless, stabilities of **pMISt4-5**-based photopolymers are again very high and only slightly reduced compared to **pMISt1**, which could be expected due to their similar monomer structures.

Die approbierte gedruckte Originalversion dieser Dissertation ist an der TU Wien Bibliothek verfügbar.
The approved original version of this doctoral thesis is available in print at TU Wien Bibliothek.
TU Bibliothek Your knowledge hub WIEN

2.5.12. Conclusion

Formulations based on **MISt3** monomers are not volatile and also storage stability is very high, but reactivity and thus DBC and obtained molecular weights are low compared to model MI-St-system **MISt1**. Hence, also (thermo)mechanical properties suffer from the lowered reactivity, which is caused by the aromatic substitution of the utilised MI **MMI**. On the other hand, higher reaction temperatures (compare **MISt2** in chapter 2.4.2.3) or an increased PI concentration would maybe enhance the reactivity, but then a comparison of the different MI-St-systems is not possible. Therefore, aliphatic MIs have to be applied to yield good material properties under used reaction conditions.

MI-St-system **pMISt4** exhibits good thermomechanical properties (*e.g.* high T_g) like **pMISt1** before, but in addition utilised monomers are offering also low volatility – even at higher temperatures. However, these elevated temperatures are needed to obtain homogeneous resins. On the other hand, the cyclohexyl moiety of the used MI **CHMI** is very rigid and hence tensile properties and toughness are reduced compared to MI **PrMI** in **MISt1**. So increased contents of toughening agent BR **CB24** are needed in **pMISt4**-based photopolymers to yield high toughness, which consequently lead also to a strong softening of the polymer.

MISt5 formulations again exhibit low volatility and viscosity as well as high reactivity, while a good storage stability is maintained. On the other hand, some (thermo)mechanical properties of **pMISt5** – especially a low T_g – limit the area of application for this MI-St-system.

Die approbierte gedruckte Originalversion dieser Dissertation ist an der TU Wien Bibliothek verfügbar.
The approved original version of this doctoral thesis is available in print at TU Wien Bibliothek.
TU Bibliothek Your knowledge hub WIEN

2.6. Potential applications

After successfully studying several different MI-St-systems with a variety of characteristics a set of resins/photopolymers with a wide range of properties is received. Hence, some typical applications for photopolymerisable monomers were tested with an introduced MI-St-BR-terpolymer, which fits with its qualities at the best for each different task.

2.6.1. Reactive diluent (RD)

Many conventional (meth)acrylates, which yield good material properties (*e.g.* toughness) due to their high molecular weight, cannot be processed because of their high viscosities. So the monomers are mixed with reactive diluents to tune the viscosity of the final resin to the desired level. Unfortunately, most RDs are small molecules and thus are volatile and/or reduce glass transition temperature dramatically.

The most common RD for photopolymer resins is isobornyl methacrylate (**IBMA**, compare chapter 2.3, where it was used for comparison as monofunctional MA). However, **IBMA** lacks applicability at elevated temperatures, since it is too volatile. Thus, a need for new non-volatile and high T_g RDs is given.

Since this specification profile perfectly fits to MI-St-system **MISt4** – and radical terpolymerisation of MI, St and MA was already successfully proven in chapter 2.2.5 – some studies were performed to test the potential application of a MI-St-system as RD for industrial high molecular weight methacrylic resins.

So the commercially available difunctional polyester urethane methacrylate Bomar XR-741MS (**Bomar**) was chosen as high molecular weight methacrylic monomer (M_w ~ 1000 g/mol), which cannot be processed at room temperature without the addition of RDs. Therefore, **Bomar** formulations containing 80 mol% **IBMA** (for comparison as reference RD) or an equimolar ratio of MI **CHMI** and St

Die approbierte gedruckte Originalversion dieser Dissertation ist an der TU Wien Bibliothek verfügbar.
The approved original version of this doctoral thesis is available in print at TU Wien Bibliothek.
TU WIEN Bibliothek Your knowledge hub

FESt (**MISt4**) were prepared and investigated. Ivocerin was used as PI (0.75 w%) [115, 145]. Both mixtures containing **Bomar** and one RD are given in Tables 49 and 50.

Table 49: Compositions of **Bomar** resin with **IBMA** as RD

Component	DB% [%]	mol% [%]	w% [%]
Bomar	33.3	20	52.53
IBMA	66.6	80	46.72
Ivocerin	-	-	0.75

Table 50: Compositions of **Bomar** resin with **MISt4** as RD

Component	DB% [%]	mol% [%]	w% [%]
Bomar	33.3	20	52.26
CHMI	33.3	40	18.73
FESt	33.3	40	28.26
Ivocerin	-	-	0.75

2.6.1.1. Melt viscosity

First of all, melt viscosity was measured, because viscosity reduction is the main aim of a RD.

So results depicted in Figure 136 and listed in Table 51 were obtained.

Die approbierte gedruckte Originalversion dieser Dissertation ist an der TU Wien Bibliothek verfügbar.
The approved original version of this doctoral thesis is available in print at TU Wien Bibliothek.
TU Bibliothek Your knowledge hub WIEN

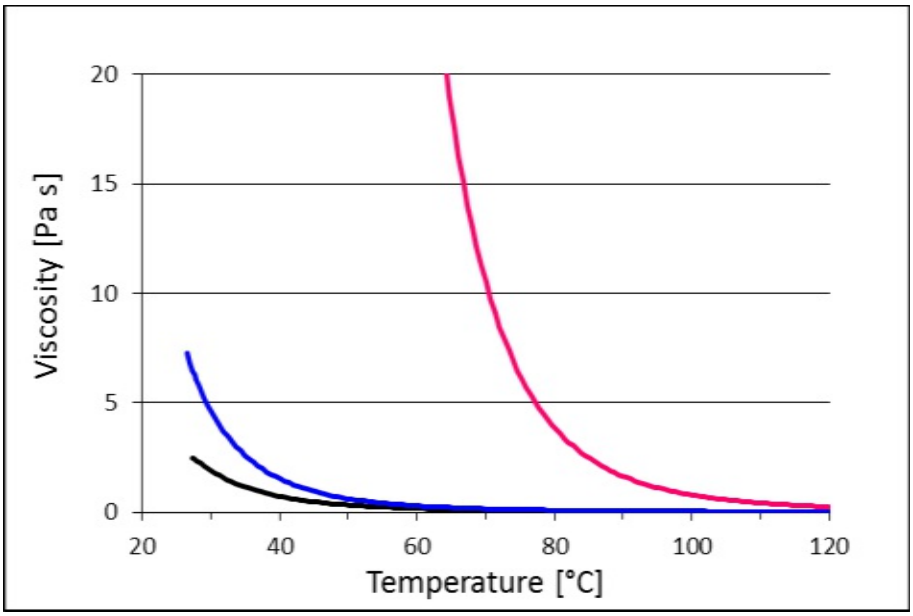

Figure 136: Melt viscosity of **Bomar** without (—) and with 80 mol% **IBMA** (—) or **MISt4** (—)

Table 51: Viscosity of tested **Bomar** formulations

Resin	Viscosity at 40 °C [Pa s]	Viscosity at 60 °C [Pa s]	Viscosity at 80 °C [Pa s]
Bomar	660	33	3.9
Bomar, 80 mol% **IBMA**	0.73	0.17	0.06
Bomar, 80 mol% **MISt4**	1.55	0.29	0.09

It can be seen above, that MA **IBMA** is slightly more powerful in viscosity reduction than MI-St-system **MISt4**. Nevertheless, both resins exhibit really low viscosity values.

2.6.1.2. DMTA

A further important property of RDs is their influence on (thermo)mechanical properties like T_g. Hence, DMTA was measured to determine the effect of the two different RDs on the **pBomar** matrix.

Die approbierte gedruckte Originalversion dieser Dissertation ist an der TU Wien Bibliothek verfügbar.
The approved original version of this doctoral thesis is available in print at TU Wien Bibliothek.
TU Bibliothek Your knowledge hub WIEN

All DMTA experiments were executed in torsion mode with a heating rate of 2 °C/min and constant normal force.

The results of the DMTA study are given in Figure 137.

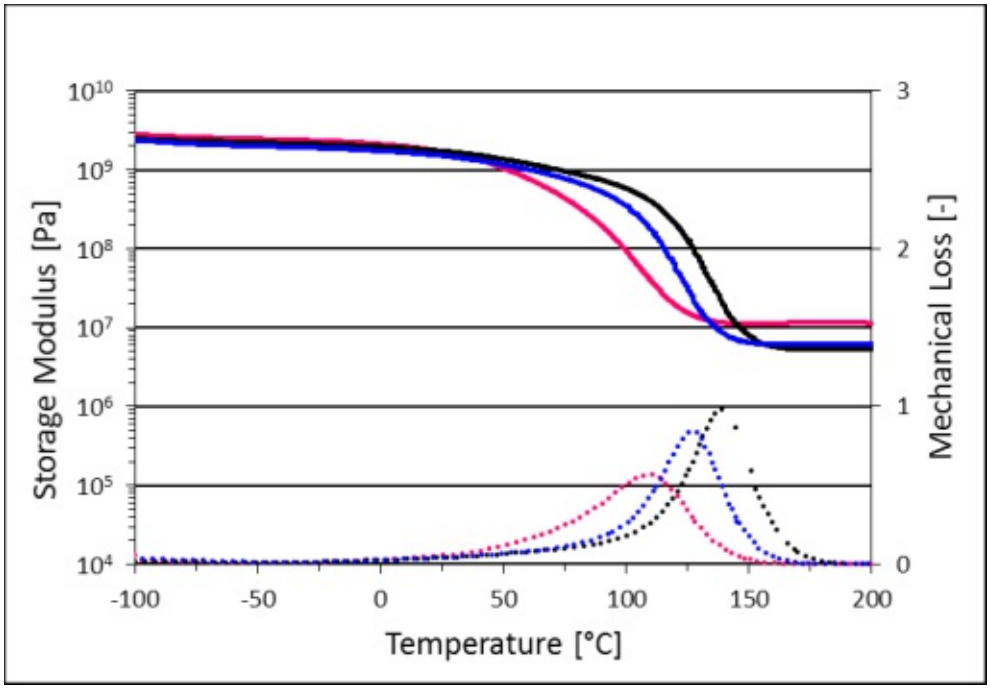

Figure 137: Storage modulus (—) and mechanical loss (▪▪▪) of **pBomar** without (—) and with 80 mol% **IBMA** (—) or **MISt4** (—)

Figure 137 shows, that both RDs raise the T_g of the polymer to higher values due to their rigid ring structures. Unfortunately, MA **IBMA** (T_g = 139 °C) is slightly more powerful than MI-St-system **MISt4** (T_g = 127 °C). Finally, also G' at the rubbery plateau indicates, that the network density is reduced to a similar level with both added RDs.

2.6.1.3. Tensile tests

In addition to DMTA studies tensile tests were performed to further characterise MI-St-system **MISt4** as RD and compare its properties in the **pBomar** matrix with MA **IBMA**.

Die approbierte gedruckte Originalversion dieser Dissertation ist an der TU Wien Bibliothek verfügbar.
The approved original version of this doctoral thesis is available in print at TU Wien Bibliothek.
TU Bibliothek Your knowledge hub WIEN

All tensile tests were executed according to ISO 527 with specimen shape 5B and a traverse velocity of 5 mm/min.

Hence, results depicted exemplary in Figure 138 and summarised in Table 52 were gained.

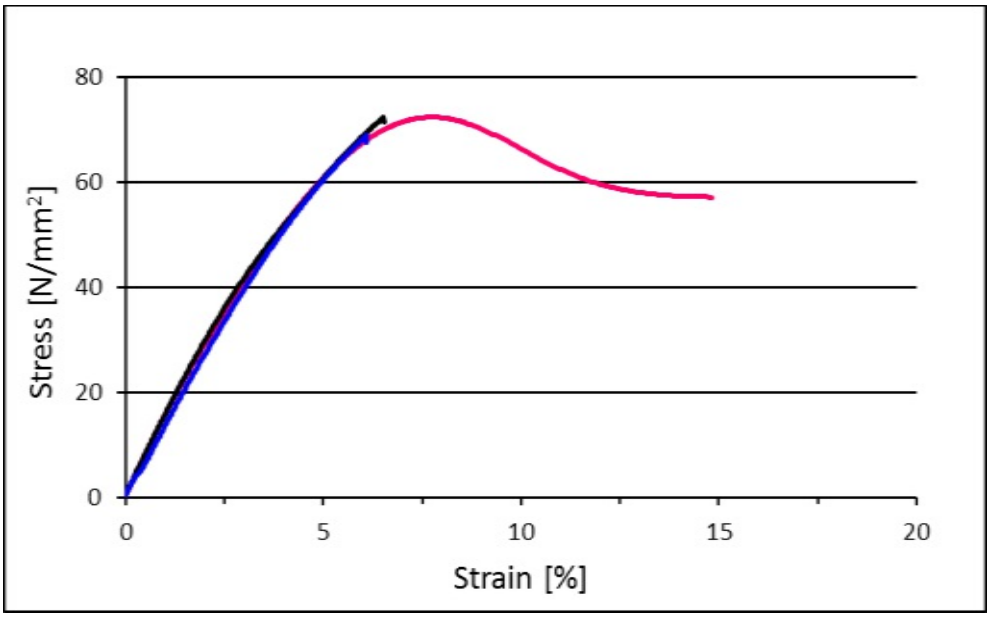

Figure 138: Stress-strain curves of **pBomar** without (—) and with 80 mol% **IBMA** (—) or **MISt4** (—)

Table 52: Results of tensile tests of **pBomar**

Sample	$Stress_{max}$ [MPa]		$Strain_{Break}$ [%]	
	Average	s	Average	s
pBomar	73.9*	3.2*	13.1	2.3
pBomar, 80 mol% **IBMA**	75.7	2.6	6.8	0.6
pBomar, 80 mol% **MISt4**	68.3	6.9	6.1	0.8

* yield point

As can be seen in the obtained data above, no significant difference of MA and MI-St RDs can be measured. Both RDs reduce strain at break with their rigid ring structures, which probably increase brittleness.

Die approbierte gedruckte Originalversion dieser Dissertation ist an der TU Wien Bibliothek verfügbar.
The approved original version of this doctoral thesis is available in print at TU Wien Bibliothek.
TU Bibliothek Your knowledge hub WIEN

2.6.1.4. Impact resistance

Finally, impact resistance was measured to conclude the evaluation of MI-St-system **MISt4** as RD.

Impact resistance was measured with the Dynstat approach according to DIN 51230.

So results shown in Figure 139 and listed in Table 53 were calculated.

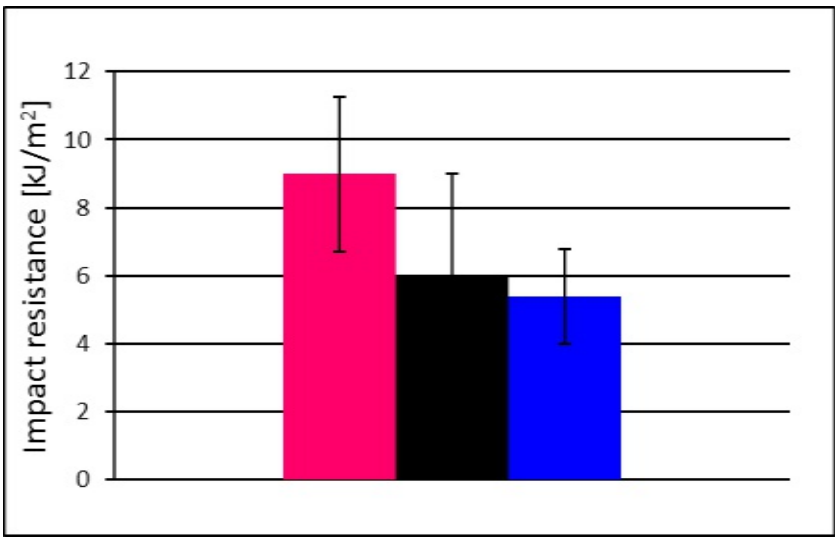

Figure 139: Dynstat impact resistance of **pBomar** without (—) and with 80 mol% **IBMA** (—) or **MISt4** (—)

Table 53: Results of Dynstat impact tests of **pBomar**

Sample	Impact resistance [kJ/m²]	
	Average	s
pBomar	9.0	2.3
pBomar, 80 mol% **IBMA**	6.0	3.0
pBomar, 80 mol% **MISt4**	5.4	1.4

Die approbierte gedruckte Originalversion dieser Dissertation ist an der TU Wien Bibliothek verfügbar.
The approved original version of this doctoral thesis is available in print at TU Wien Bibliothek.
TU Bibliothek Your knowledge hub WIEN

Again no significant difference in the influence of MA **IBMA** and MI-St-system **MISt4** can be observed. Furthermore, both RDs decrease impact resistance of **pBomar** due to their rigid (side) groups. This effect was already indicated in the tensile tests by the lower values for strain at break for photopolymers containing a RD (chapter 2.6.1.3).

So MI-St-system **MISt4** is definitely a promising alternative for MA **IBMA** as standard RD. Resin viscosities as well as (thermo)mechanical properties of a **pBomar** photopolymer containing 80 mol% of the MI-St-system are similar or only slightly worse compared to the MA as RD. In contrast, volatilities of MI **CHMI** and St **FESt** are dramatically lower than **IBMA** (see chapters 2.2.2, 2.4.2.2 and 2.5.2), which open a completely new area of applications, which deal with elevated temperatures.

2.6.2. Frontal polymerisation (FP)

Photopolymerisation is always limited by the penetration depth of light, which is needed to initiate the polymerisation reaction by generating reactive species from a PI. Thus, a strong limitation is given, when thick samples – or filled systems – should be cured. One approach to circumvent this drawback is to use FP [10-11, 146-148].

In UV-initiated thermal FP the reaction is started locally by light (or heat) and the so produced reaction heat induces cleavage of a thermal initiator, which again starts polymerisation in the surrounding monomer formulation. Thus, monomers are converted into a polymer in a localised self propagating thermal reaction zone, which moves through the whole resin (see Figure 140).

Die approbierte gedruckte Originalversion dieser Dissertation ist an der TU Wien Bibliothek verfügbar.
The approved original version of this doctoral thesis is available in print at TU Wien Bibliothek.
TU Bibliothek Your knowledge hub WIEN

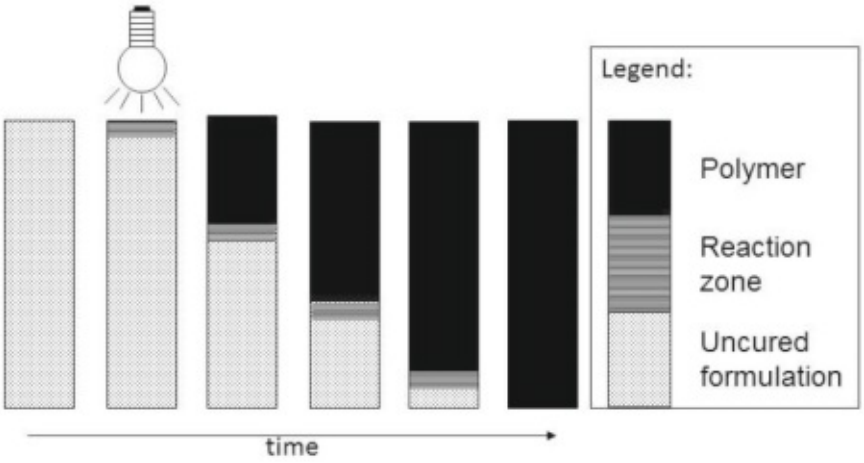

Figure 140: Scheme of light initiated FP [149]

For a proof-of-concept if production of composites is also possible with MI-St-systems, a MI-St-copolymer filled with carbon fibres (CF) should be fabricated by FP. CFs were used, because the black fibres usually allow photopolymerisation only on the surface due to their very efficient light absorption over a wide wavelength range.

So a resin based on the liquid and low volatile MI-St-system **MISt5** was filled with 20 w% CF. Irgacure 819 (1 w%, Figure 50) was applied as PI for starting the polymerisation and benzoyl peroxide (**BPO**, 5 w%, Figure 141) was utilised as thermal initiator, which is responsible for front propagation.

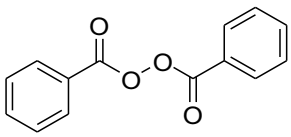

Figure 141: Structure of **BPO**

FP experiments were conducted with a set-up, which was developed previously in our group: Figure 142 [149].

Die approbierte gedruckte Originalversion dieser Dissertation ist an der TU Wien Bibliothek verfügbar.
The approved original version of this doctoral thesis is available in print at TU Wien Bibliothek.
TU Bibliothek Your knowledge hub WIEN

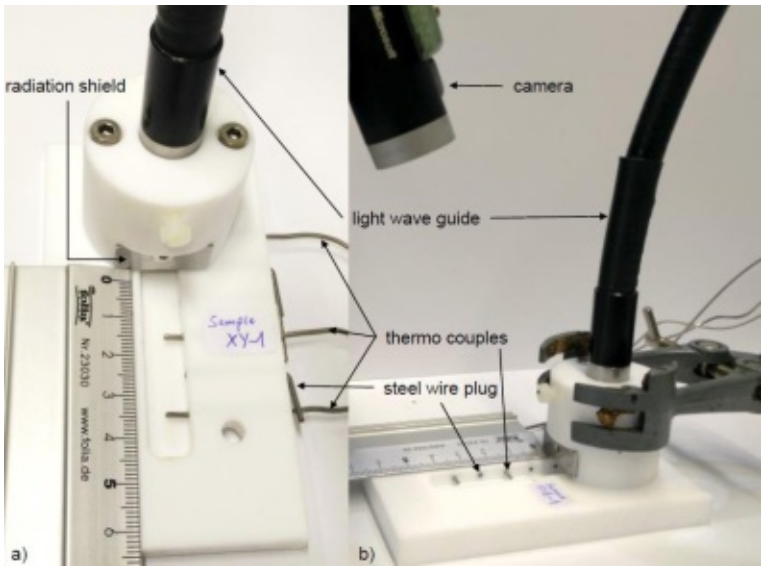

Figure 142: Experimental set-up for FP [149]

Further experimental parameters of the FP experiments are given in chapter 2.6.2 of the experimental part. Additionally, it has to be mentioned, that the length of the mould was reduced with a plasticine plug to minimise the amount of required resin for an experiment.

So following FP could be achieved with the CF-filled **MISt5** resin (Figure 143). In addition, the obtained sample is shown in Figure 144.

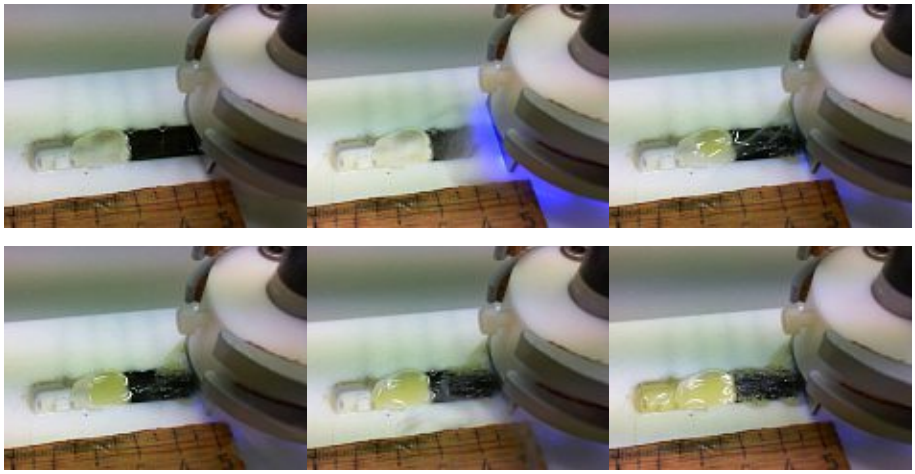

Figure 143: FP of **MISt5** containing 20 w% CF

Die approbierte gedruckte Originalversion dieser Dissertation ist an der TU Wien Bibliothek verfügbar.
The approved original version of this doctoral thesis is available in print at TU Wien Bibliothek.
TU Bibliothek Your knowledge hub WIEN

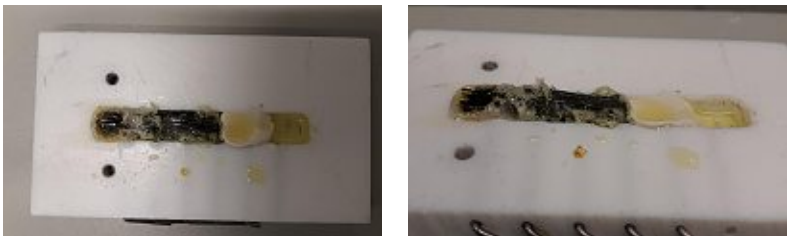

Figure 144: CF-filled **pMISt5** sample

Although there is still some room for optimisation of the FP (*e.g.* bubble formation probably caused by the high concentration of thermal initiator **BPO**), it can be claimed, that fabrication of CFR MI-St composites by FP could be established successfully.

2.6.3. 3D printing

Since the FP technology requires special (combinations of) initiators and monomers, the applicability is limited in some areas. Therefore, 3D printing as a second approach to fabricate bigger and/or filled parts with photopolymers was investigated as well to further underline the potential of the introduced MI-St-BR-terpolymers. So a photopolymerisable MI-St-system was tested for usage in lithography based additive manufacturing technologies (L-AMT).

Amongst other AMTs for polymers like fused deposition modelling (FDM) or selective laser sintering (SLS), L-AMTs experienced a tremendous growth over the last years and are nowadays very popular in industry as well as in the private sector [14, 150-151]. The key feature of these technologies is the layer-by-layer production of a part based on a computer model thereof (Figure 145).

Die approbierte gedruckte Originalversion dieser Dissertation ist an der TU Wien Bibliothek verfügbar.
The approved original version of this doctoral thesis is available in print at TU Wien Bibliothek.
TU Bibliothek Your knowledge hub WIEN

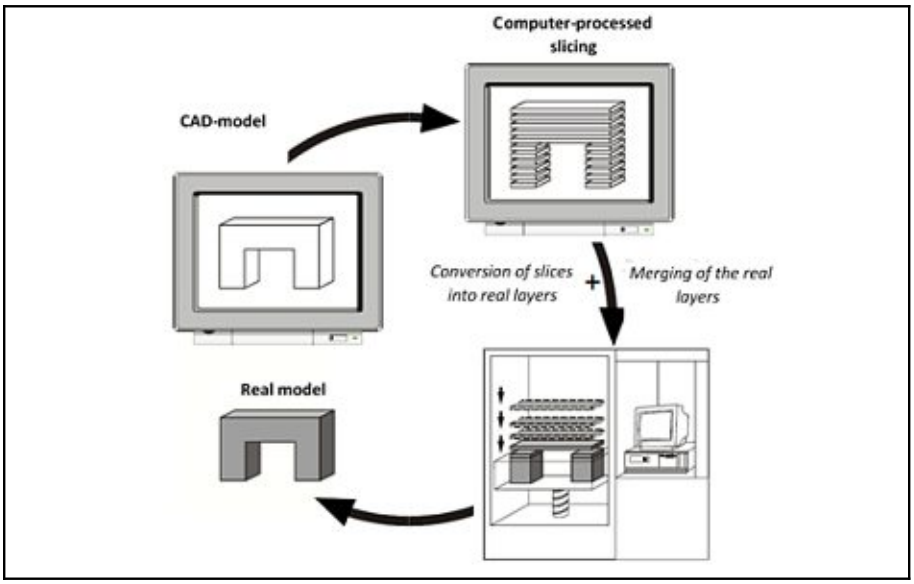

Figure 145: Principle of L-AMT [152]

L-AMTs utilise photopolymerisable resins and a spatially controlled light source to trigger solidification of monomers only in the desired areas. Thus, gelation occurs only where light meets the photopolymerisable resin in the vat. So a 3 dimensional structure is obtained by irradiating layer by layer. Furthermore, L-AMT was extended previously via “Hot-Lithography” by a heated vat, thus enabling processability of a huge variety of new monomers [124-125].

There are two different possibilities to initiate the photopolymerisation reaction only in the desired spots, either with a laser (SLA) or an LED light source with a digital micro mirror device chip (DLP) (see Figure 146).

Die approbierte gedruckte Originalversion dieser Dissertation ist an der TU Wien Bibliothek verfügbar.
The approved original version of this doctoral thesis is available in print at TU Wien Bibliothek.
TU Bibliothek Your knowledge hub WIEN

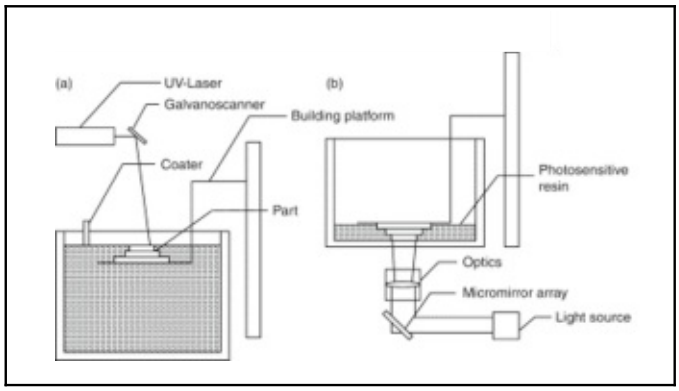

Figure 146: Scheme of SLA (a) and DLP (b) [12]

Whereas in SLA a laser is scanning very rapidly over the layer, in DLP higher exposure times are common. Thus, a DLP printer was used for a proof-of-concept towards transparent ABS-like photopolymers for L-AMT, since it is known from the reactivity studies of MI-St-based formulations, that they exhibit high reaction times (compare chapters 2.3-2.5).

Again the MI-St-BR-terpolymer with the most suitable properties was applied for the proof-of-concept of 3D printability. Thus, MI-St-system **MISt5_10** was chosen, due to a good balance between chemical reactivity and final thermomechanical properties.
First of all, some preliminary studies had to be performed to adjust the **MISt5_10** resin composition, since the set-up of the used DLP printer is fixed and therefore irradiation wavelength and intensity cannot be changed. After some exposure studies suitable experimental parameters like PI (concentration), light absorber (concentration), irradiation time and layer thickness could be determined. So following **MISt5_10*** formulation was optimised regarding given DLP printer and process parameters:

- PI: 1 w% Ivocerin
- Light absorber: 0.1 w% Sudan Yellow 177
- Layer thickness: 50 µm
- Irradiation time of each layer: 40 s

Die approbierte gedruckte Originalversion dieser Dissertation ist an der TU Wien Bibliothek verfügbar.
The approved original version of this doctoral thesis is available in print at TU Wien Bibliothek.
TU Bibliothek Your knowledge hub WIEN

It has to be mentioned, that interestingly addition of cross-linkers (difunctional styrene moieties) is not necessary and even more does not yield in enhanced mechanical integrity of test specimens, due to increased brittleness.

For 3D printing a structure was chosen, which is tough to manufacture with traditional methods like milling or casting. Hence, the cube shown in Figure 147 was printed with the experimental parameters given in chapter 2.6.3 of the experimental part.

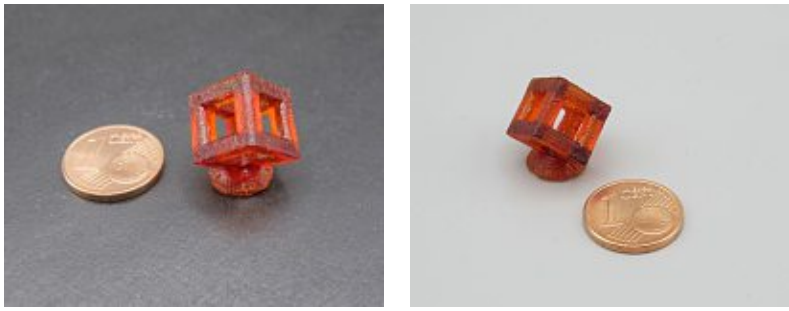

Figure 147: Pictures of 3D printed **pMISt5_10***

So another proof-of-concept of a possible application for MI-St-BR-terpolymers was successfully demonstrated. Thus, in the end three different potential uses could be presented for this new class of photopolymers, where the MI-St-system is equal or even superior to traditionally applied monomers.

Die approbierte gedruckte Originalversion dieser Dissertation ist an der TU Wien Bibliothek verfügbar.
The approved original version of this doctoral thesis is available in print at TU Wien Bibliothek.
TU Bibliothek Your knowledge hub WIEN

Experimental Part

1. UV-Curable (Meth)Acrylates containing Blocked Isocyanates

1.2. Model compounds

1.2.1. Model isocyanurates

1.2.1.2. Determination of deblocking temperature

In addition to a blank sample a BIC was dissolved as well in an excess (10 eq.) of 1-laurylamine to check, if a deblocking reaction occurs in the presence of an amine.

STA measurements were performed with the following experimental parameters to determine the deblocking temperature of used BICs and BIC-amine-mixtures:

- Temperature: 25 – 300 °C
- Heating rate: 10 K/min
- Atmosphere: N_2 (flow rate of 40 mL/min)

ATR-IR spectra were recorded before and after thermal treatment of a sample in an Al-block for 1 h at 160 °C under Ar atmosphere. Due to comparison of taken spectra information on deblocking reactions can be obtained.

Die approbierte gedruckte Originalversion dieser Dissertation ist an der TU Wien Bibliothek verfügbar.
The approved original version of this doctoral thesis is available in print at TU Wien Bibliothek.
TU Bibliothek Your knowledge hub WIEN

1.3. Syntheses of methacrylates containing BICs

1.3.1. Synthesis of C3D1

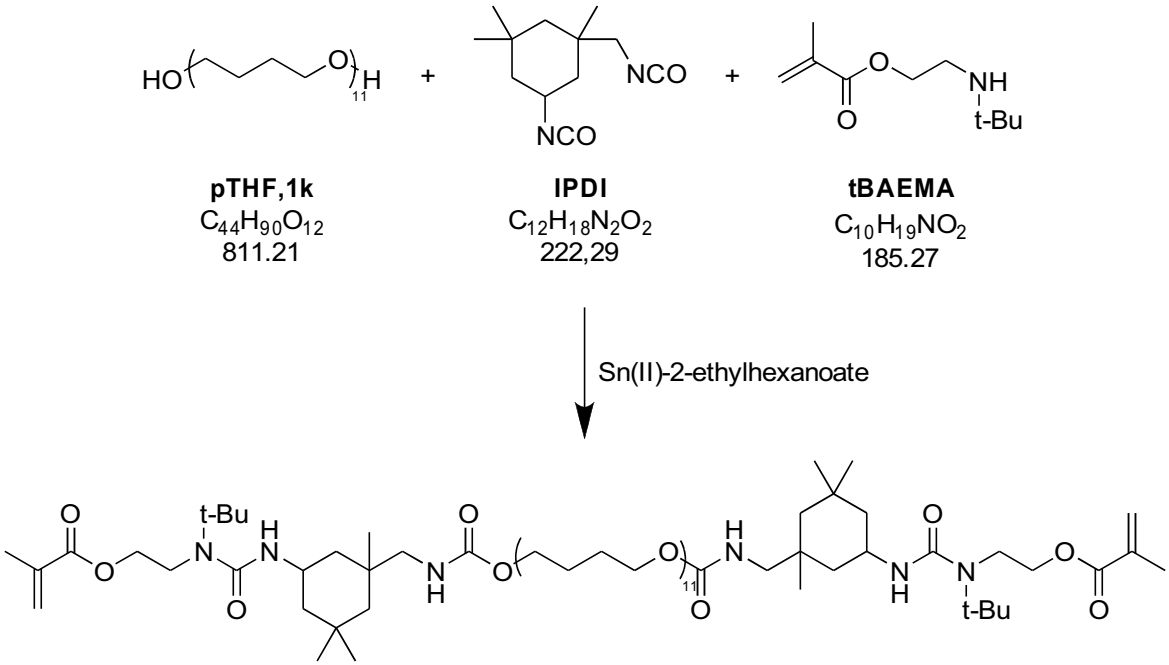

C3D1

Synthesis of **C3D1** was performed according to literature [98].

pTHF,1k (11.36 g, 14 mmol, 1 eq.), **IPDI** (6.24 g, 28 mmol, 2 eq.) and Sn(II)-2-ethylhexanoate (8 µL) were mixed under Ar atmosphere and stirred at 70 °C for 3 h. After cooling the reaction mixture to 40 °C, phenothiazine (1.8 mg, 100 ppm) and **tBAEMA** (5.19 g, 28 mmol, 2 eq.) were added slowly. Finally, the reaction was stirred 21 h at 50 °C to complete the reaction. The obtained high viscous clear liquid was used without any further purification.

R_f = 0.71 (PE : EE = 1 : 1)

Die approbierte gedruckte Originalversion dieser Dissertation ist an der TU Wien Bibliothek verfügbar.
The approved original version of this doctoral thesis is available in print at TU Wien Bibliothek.

^{1}H-NMR (400 MHz, $CDCl_3$, FID JST019/2): δ = 6.11-6.08 (m, 2 H, CH_2-DB), 5.61-5.53 (m, 2 H, CH_2-DB), 4.24-4.13 (m, 4 H, CH_2-O), 4.05-4.02 (m, 4 H), 3.43-3.34 (m, 44 H, CH_2-pTHF), 3.04-2.83 (m, 6 H), 1.94-1.89 (m, 6 H, CH_3-MA), 1.62-1.58 (m, 46 H, CH_2-pTHF), 1.40-1.37 (m, 14 H), 1.10 (s, 6 H, CH_3-IPDI), 1.06-1.04 (m, 18 H, CH_3-*t*-Bu), 0.90-0.84 (m, 12 H, CH_3-IPDI) ppm.

^{13}C-NMR (100 MHz, $CDCl_3$, FID JST019/3): δ = 167.8-167.4 (s, CO-MA), 159.5-159.2 (s, CO-urethane/urea), 158.7 (s, CO-urethane/urea), 157.2 (s, CO-urethane/urea), 156.1 (s, CO-urethane/urea), 136.4 (s, C-DB), 136.0 (s, C-DB), 135.9 (s, C-DB), 126.7-126.2 (t, CH_2-DB), 125.7 (t, CH_2-DB), 70.8-70.7 (t, CH_2-pTHF), 70.4 (t), 65.3 (t), 64.8-64.4 (t, CH_2-O), 56.2-55.1 (t), 54.8 (t), 54.4 (t), 50.6 (s, C-*t*-Bu), 47.7-46.3 (t), 44.8-43.9 (d), 43.5-43.2 (t), 42.6 (t), 42.2 (t), 41.4 (t, CH_2-N), 36.8-36.5 (t), 35.4-35.2 (d), 32.2-32.0 (t), 29.8-29.5 (q), 29.0 (q, CH_3-*t*-Bu), 27.9-27.8 (q), 26.7 (t, CH_2-pTHF), 26.4 (t), 26.0 (t), 23.8-23.5 (q, CH_3-IPDI), 18.5-18.4 (q, CH_3-MA) ppm.

1.3.2. Synthesis of BICMA1

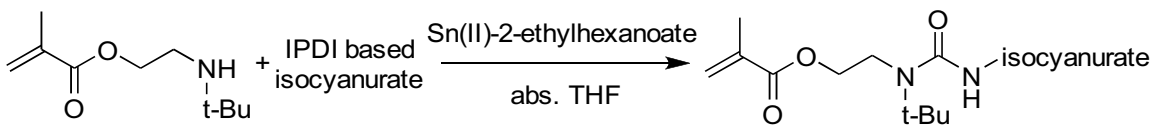

tBAEMA
$C_{10}H_{19}NO_2$
185.27

BICMA1

Synthesis of **BICMA1** was performed according to Cooper *et al.* [96].

Vestanat T1890/100 (**IPDI**-based isocyanurate) (9.786 g, 0.916 free IC/IPDI, 1.09 eq.) was dissolved in 20 mL dry THF. Then Sn(II)-2-ethylhexanoate (8 µL) and **tBAEMA** (7.416 g, 40 mmol, 1 eq.) were added. After 48 h stirring at room temperature phenothiazine (17 mg, 1000 ppm) was added. Finally, the solvent was removed under reduced pressure and the obtained white powder was used without any further purification.

Die approbierte gedruckte Originalversion dieser Dissertation ist an der TU Wien Bibliothek verfügbar.
The approved original version of this doctoral thesis is available in print at TU Wien Bibliothek.
TU Bibliothek Your knowledge hub WIEN

T_m = 91-100 °C

^{1}H-NMR (400 MHz, $CDCl_3$, FID JST018/13): δ = 6.13-6.08 (m, 1 H, CH_2-DB), 5.63-5.60 (m, 1 H, CH_2-DB), 5.22-4.99 (m, 1 H, CH-IPDI), 4.26-4.12 (m, 2 H, CH_2-O), 3.92-3.88 (m, 1 H), 3.73-3.63 (m, 1 H), 3.46-3.39 (m, 2 H), 3.09-2.87 (m, 1 H), 2.19-2.11 (m, 1 H), 1.96-1.92 (m, 3 H, CH_3-MA), 1.70 (bs, 1 H), 1.40 (s, 9 H, CH_3-*t*-Bu), 1.24-0.82 (m, 15 H, CH_3-*t*-Bu) ppm.

^{13}C-NMR (100 MHz, $CDCl_3$, FID JST018/14): δ = 167.8 (s, CO-MA), 159.5 (s, CO-urea), 158.7 (s, CO-urea), 150.7 (s, CO-isocyanurate), 149.8 (s, CO-isocyanurate), 136.1 (s, C-DB), 126.7 (t, CH_2-DB), 65.1-64.3 (t, CH_2-O), 56.2 (s, C-*t*-Bu), 48.5-27.7 (m), 23.5 (q, CH_3-IPDI), 18.5 (q, CH_3-MA) ppm.

1.5. Deblocking reactions in solution

A BIC was dissolved in an excess (10 eq.) of alcohol 1-lauryl alcohol or amine 1-laurylamine to check if a deblocking reaction occurs in solution. Furthermore, 5 mg phenothiazine were added.

Sampling was performed before and after thermal treatment for 5 h at 125 °C (**BICMA1**) or 15 min at 150 °C (**VIC2**) under Ar atmosphere. ATR-IR (**BICMA1**) or ^{1}H and ^{13}C-NMR spectra (**VIC2**) of the samples were recorded. Due to comparison of taken spectra information on deblocking reactions can be obtained.

1.6. (Thermo)mechanical properties

All resins were formulated according to DB% in literature (Table 54 [98] and Table 55). However, amine **DA** was used in an “equimolar” ratio for formulations based on **BICMA1** and **VIC2**, which means that one amino functionality is taken into account for each BIC moiety.

Die approbierte gedruckte Originalversion dieser Dissertation ist an der TU Wien Bibliothek verfügbar.
The approved original version of this doctoral thesis is available in print at TU Wien Bibliothek.
TU Bibliothek Your knowledge hub WIEN

Table 54: Composition of **REF** [98]

Component	w‰ [‰]	mol% [%]	eq. [-]	DB% [%]
C3D1	700	22.5	1.00	43.4
E3MA	206	57.2	2.54	55.2
PEGDMA (M_w = 750 Da)	10	0.7	0.03	1.4
HMDA	74	18.4	0.82	-
Irgacure 819	10	1.2	0.06	-

Table 55: Compositions of **RES1** and **RES2**

Component	DB% [%]	**RES1** [w%]	**RES2** [w%]
BICMA1	43.4	25.0	-
DA	-	58.4	-
VIC2	43.4	-	45.5
HMDA	-	-	15.0
E3MA	55.2	14.9	36.7
PEGDMA (M_w = 750 Da)	1.4	0.7	1.8
Irgacure 819	-	1.0	1.0

General procedure for moulding specimens: All samples were cured in transparent silicon moulds (*Wacker Elastosil RT 601*) 2 times 10 min in the Lumamat oven. Afterwards, half of the samples was stored over night (14 h) at 125 °C, where all specimens became darker, less sticky and seemed to be harder and tougher. Finally, the obtained polymer sticks were sanded to ensure a parallel shape.

Die approbierte gedruckte Originalversion dieser Dissertation ist an der TU Wien Bibliothek verfügbar.
The approved original version of this doctoral thesis is available in print at TU Wien Bibliothek.
TU Bibliothek Your knowledge hub WIEN

1.7. Influence of the matrix on deblocking reactions

1.7.2. Soft matrix

The components used in resin **RES3** are shown in Table 56. Furthermore, difunctional amine **HMDA** is again applied in equimolar ratio to BIC **VIC2**.

Table 56: Composition of **RES3**

Component	DB% [%]	w% [%]
VIC2	10	14.1
HMDA	-	4.6
E3MA	90	80.3
Irgacure 819	-	1.0

General procedure for specimen preparation: Photopolymerisation and thermal curing were performed at the same conditions as stated in chapter 1.6 to obtain comparable results. The samples were polymerised 2 times 10 min in a Lumamat oven. Afterwards, thermal treatment of the specimens was done for 14 h at 125 °C.

Die approbierte gedruckte Originalversion dieser Dissertation ist an der TU Wien Bibliothek verfügbar.
The approved original version of this doctoral thesis is available in print at TU Wien Bibliothek.
TU Bibliothek Your knowledge hub WIEN

2. ABS-like Photopolymers

2.2. Preliminary experiments

2.2.1. Syntheses of itaconimides and citraconimides

2.2.1.1. Synthesis of PrII and PrCI

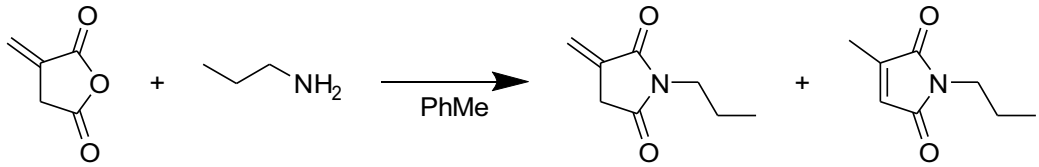

IA	**PrNH$_2$**	**PrII**	**PrCI**
$C_5H_4O_3$	C_3H_9N	$C_8H_{11}NO_2$	$C_8H_{11}NO_2$
112.08	59.11	153.18	153.18

Synthesis of *N*-propyl itaconimide (**PrII**) and *N*-propyl citraconimide (**PrCI**) was performed according to patent WO 2005118537 [118].

Itaconic anhydride **IA** (10.08 g, 90 mmol, 1 eq.) was dissolved under Ar atmosphere in 450 mL dry toluene. Subsequently, propylamine (5.33 g, 90 mmol, 1 eq.) and phenothiazine (55 mg, 3000 ppm) were added. The solution was stirred over night at 35 °C and then heated under reflux for 5 d in a Dean-Stark apparatus. Afterwards, the mixture was washed 3 times with 450 mL 2 M NaOH and once with 450 mL brine. After drying over Na_2SO_4 the solvent was removed under reduced pressure. Finally, 0.21 g (1.5% theoretical yield) of **PrII** and 0.73 g (5.3% theoretical yield) of **PrCI** were obtained as yellowish liquids after column chromatography (213 g silica, 17% EE in PE, 60 mL/min).

Die approbierte gedruckte Originalversion dieser Dissertation ist an der TU Wien Bibliothek verfügbar.
The approved original version of this doctoral thesis is available in print at TU Wien Bibliothek.
TU Bibliothek Your knowledge hub WIEN

PrII:

R_f = 0.25 (PE : EE = 5 : 1)

^{1}H-NMR (400 MHz, $CDCl_3$, FID JST031/10): δ = 6.34 (t, J = 2.4 Hz, 1 H, CH_2-DB), 5.61 (t, J = 2.1 Hz, 1 H, CH_2-DB), 3.54 (t, J = 7.4 Hz, 2 H, CH_2-N), 3.31 (t, J = 2.3 Hz, 2 H, CH_2-CO), 1.63 (sext, J = 7.4 Hz, 2 H, CH_2-CH_3), 0.91 (t, J = 7.5 Hz, 3 H, CH_3) ppm.

^{13}C-NMR (100 MHz, $CDCl_3$, FID JST031/11): δ = 174.1 (s, CO), 169.7 (s, CO), 133.5 (s, C-DB), 120.5 (t, CH_2-DB), 40.6 (t, CH_2-N), 33.9 (t, CH_2-CO), 21.3 (t, CH_2-CH_3), 11.5 (q, CH_3) ppm.

PrCI:

R_f = 0.58 (PE : EE = 5 : 1)

^{1}H-NMR (400 MHz, $CDCl_3$, FID JST031/8): δ = 6.30 (d, J = 1.8 Hz, 1 H, CH-DB), 3.45 (t, J = 7.3 Hz, 2 H, CH_2-N), 2.07 (d, J = 1.8 Hz, 3 H, CH_3-DB), 1.60 (sext, J = 7.3 Hz, 2 H, CH_2-CH_3), 0.89 (t, J = 7.5 Hz, 3 H, CH_3) ppm.

^{13}C-NMR (100 MHz, $CDCl_3$, FID JST031/9): δ = 172.2 (s, CO), 171.2 (s, CO), 145.6 (s, C-DB), 127.4 (d, CH-DB), 39.7 (t, CH_2-N), 22.1 (t, CH_2-CH_3), 11.4 (q, CH_3), 11.1 (q, CH_3-DB) ppm.

2.2.1.2. Synthesis of BnII and BnCI

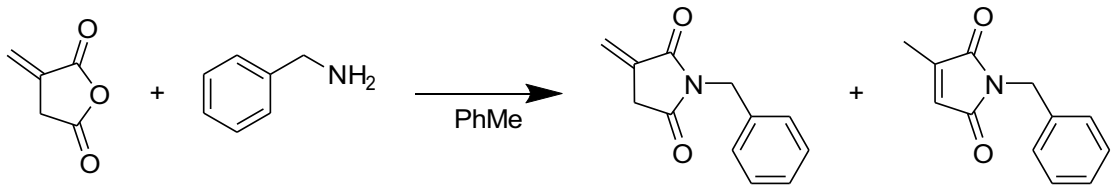

IA	**BnNH$_2$**	**BnII**	**BnCI**
$C_5H_4O_3$	C_7H_9N	$C_{12}H_{11}NO_2$	$C_{12}H_{11}NO_2$
112.08	107.16	201.23	201.23

Synthesis of *N*-benzyl itaconimide (**BnII**) and *N*-benzyl citraconimide (**BnCI**) was performed according to patent WO 2005118537 [118].

Die approbierte gedruckte Originalversion dieser Dissertation ist an der TU Wien Bibliothek verfügbar.
The approved original version of this doctoral thesis is available in print at TU Wien Bibliothek.
TU Bibliothek Your knowledge hub WIEN

Itaconic anhydride **IA** (7.33 g, 65 mmol, 1 eq.) was dissolved under Ar atmosphere in 325 mL dry toluene. Afterwards, benzylamine (7.01 g, 65 mmol, 1 eq.) and phenothiazine (40 mg, 3000 ppm) were added. Then the solution was heated under reflux for 24 h in a Dean-Stark apparatus. The next day the mixture was washed 3 times with 325 mL 2 M NaOH and once with 325 mL brine. After drying over Na_2SO_4 the solvent was removed under reduced pressure. Finally, 2.86 g (21.7% theoretical yield) of **BnII** and 2.73 g (20.7% theoretical yield) of **BnCI** were obtained as yellowish liquids after column chromatography (213 g silica, 10% EE in PE, 60 mL/min).

BnII:

R_f = 0.42 (PE : EE = 2 : 1)

^{1}H-NMR (400 MHz, $CDCl_3$, FID JST029/8): δ = 7.42-7.25 (m, 5 H, CH-Ar), 6.35 (t, J = 2.6 Hz, 1 H, CH_2-DB), 5.62 (t, J = 2.1 Hz, 1 H, CH_2-DB), 4.74 (s, 2 H, CH_2-N), 3.32 (t, J = 2.3 Hz, 2 H, CH_2-CO) ppm.

^{13}C-NMR (100 MHz, $CDCl_3$, FID JST029/7): δ = 173.6 (s, CO), 169.3 (s, CO), 135.8 (s, C-Ar), 133.4 (s, C-DB), 129.1 (d, CH-Ar), 128.8 (d, CH-Ar), 128.1 (d, CH-Ar), 121.0 (t, CH_2-DB), 42.6 (t, CH_2-N), 34.0 (t, CH_2-CO) ppm.

BnCI:

R_f = 0.68 (PE : EE = 2 : 1)

^{1}H-NMR (400 MHz, $CDCl_3$, FID JST029/4): δ = 7.34-7.22 (m, 5 H, CH-Ar), 6.31 (q, J = 1.8 Hz, 1 H, CH-DB), 4.64 (s, 2 H, CH_2-N), 2.06 (d, J = 1.8 Hz, 3 H, CH_3) ppm.

^{13}C-NMR (100 MHz, $CDCl_3$, FID JST029/5): δ = 171.7 (s, CO), 170.6 (s, CO), 145.9 (s, C-DB), 136.6 (s, C-Ar), 128.8 (d, CH-Ar), 128.5 (d, CH-Ar), 127.9 (d, CH-Ar), 127.5 (d, CH-DB), 41.6 (t, CH_2-N), 11.1 (q, CH_3) ppm.

Die approbierte gedruckte Originalversion dieser Dissertation ist an der TU Wien Bibliothek verfügbar.
The approved original version of this doctoral thesis is available in print at TU Wien Bibliothek.
TU Bibliothek Your knowledge hub WIEN

2.3. Model maleimide-styrene-system (MISt1)

2.3.7. Swellability

Three samples of each formulation were polymerised in the UV-chamber (5 min on each side with 100% intensity) as small discs (diameter 4 mm, thickness 2 mm, ~ 35 mg) for swellability studies. Then they were submerged for 7 d in $CHCl_3$ or EtOH (solvents were changed after 3 d). Sample mass was recorded before and after swelling and after drying in a vacuum oven at 60 °C until constant mass.

Swellability (S) and gel fraction (G) were calculated according to equations 3 and 4.

$$S = \frac{m_{swollen}}{m_{dry}} * 100 \quad (3)$$

S... Swellability [%]
$m_{swollen}$... Mass in swollen state [mg]
m_{dry}... Mass after drying [mg]

$$G = \frac{m_{dry}}{m_{start}} * 100 \quad (4)$$

G... Gel fraction [%]
m_{dry}... Mass after drying [mg]
m_{start}... Original mass [mg]

2.3.8. (Thermo)mechanical properties

General procedure for moulding specimens: All samples were cured in transparent silicon moulds (*Wacker Elastosil RT 601*) 2 times 5 min (100% intensity) in the UV-chamber. Finally, the obtained polymer sticks were sanded to ensure parallel shape.

Die approbierte gedruckte Originalversion dieser Dissertation ist an der TU Wien Bibliothek verfügbar.
The approved original version of this doctoral thesis is available in print at TU Wien Bibliothek.
TU Bibliothek Your knowledge hub WIEN

2.4. Further mechanistic studies on MI-St-copolymerisation

2.4.2. Cross-linking behaviour in MI-St-copolymers

2.4.2.1. Synthesis of FESt

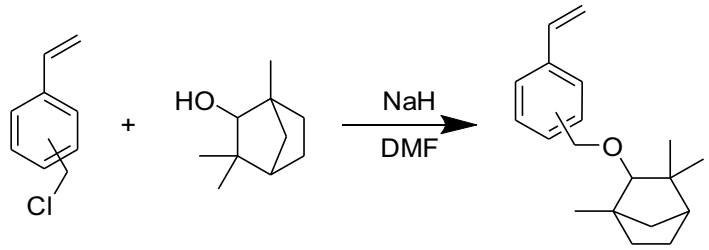

VBnCl C_9H_9Cl 152.62 | **Fenchol** $C_{10}H_{18}O$ 154.25 | **FESt** $C_{19}H_{26}O$ 270.42

Synthesis of **FESt**, a mixture of 1,3,3-trimethyl-2-((3-vinylbenzyl)oxy)bicyclo[2.2.1]heptane and 1,3,3-trimethyl-2-((4-vinylbenzyl)oxy)bicyclo[2.2.1]heptane, was performed according to Kobayashi *et al.* [140].

NaH (60 w% in paraffin; 7.81 g, 195 mmol, 1.5 eq.) was dispersed in 250 mL dry DMF and cooled to 0 °C. Afterwards, fenchol (24.09 g, 156 mmol, 1.2 eq.) was added and the solution was stirred for 15 min at 0 °C. Then **VBnCl** (19.86 g, 130 mmol, 1 eq.) was added slowly without heating the solution above 5 °C. After stirring over night at room temperature the reaction was diluted with 300 mL EE and quenched with 150 mL saturated aqueous NH_4Cl solution. The aqueous phase was diluted with deionized water until all precipitate was dissolved and then extracted 3 times with 200 mL EE. The combined organic phases were dried over anhydrous Na_2SO_4 and the solvent was evaporated under reduced pressure. Finally, the crude product was dissolved in 200 mL PE, washed with 200 mL deionized water and filtrated over 350 g silica. After removal of the solvent under reduced pressure, 27.55 g (78.3% theoretical yield) of **FESt** were obtained as a colourless liquid.

Die approbierte gedruckte Originalversion dieser Dissertation ist an der TU Wien Bibliothek verfügbar.
The approved original version of this doctoral thesis is available in print at TU Wien Bibliothek.
TU Bibliothek Your knowledge hub WIEN

R_f = 0.33 (PE : DCM = 9 : 1)

^{1}H-NMR (400 MHz, $CDCl_3$, FID JST043/4): δ = 7.40-7.24 (m, 8 H, CH-Ar), 6.76-6.68 (m, 2 H, CH-DB), 5.75 (dd, J_1 = 6.9 Hz, J_2 = 17.6 Hz, 2 H, CH_2-DB), 5.23 (dd, J_1 = 8.4 Hz, J_2 = 10.7 Hz, 2 H, CH_2-DB), 4.62-4.41 (m, 4 H, CH_2-Bn), 3.02 (d, J = 4.6 Hz, 2 H, CH-O), 1.86-1.78 (m, 2 H), 1.75-1.68 (m, 2 H), 1.64 (bs, 2 H), 1.46-1.36 (m, 4 H), 1.10-0.98 (m, 22 H) ppm.

^{13}C-NMR (100 MHz, $CDCl_3$, FID JST043/5): δ = 140.0 (s, C-Ar), 139.3 (s, C-Ar), 137.6 (s, C-Ar), 137.1 (d, CH-DB), 136.8 (d, CH-DB), 136.7 (s, C-Ar), 128.5 (d, CH-Ar), 127.7 (d, CH-Ar), 127.0 (d, CH-Ar), 126.2 (d, CH-Ar), 125.3 (d, CH-Ar), 113.9 (t, CH_2-DB), 113.6 (t, CH_2-DB), 92.7 (d, CH-O), 92.6 (d, CH-O), 73.5 (t, CH_2-Bn), 73.3 (t, CH_2-Bn), 49.4 (s, C-CH_3), 49.4 (s, C-CH_3), 49.0 (d, CH), 41.6 (t, CH_2), 39.7 (s, C-$(CH_3)_2$), 39.7 (s, C-$(CH_3)_2$), 31.8 (q, CH_3), 26.4 (t, CH_2), 26.2 (t, CH_2), 21.0 (q, CH_3), 21.0 (q, CH_3), 20.3 (q, CH_3), 20.3 (q, CH_3) ppm.

2.4.2.3. Swellability

Swellability studies of **pMISt2** samples without and with BR **CB24** were conducted in $CHCl_3$ with the procedure given in chapter 2.3.7 of the experimental part to obtain comparable data.

Die approbierte gedruckte Originalversion dieser Dissertation ist an der TU Wien Bibliothek verfügbar.
The approved original version of this doctoral thesis is available in print at TU Wien Bibliothek.
TU Bibliothek Your knowledge hub WIEN

2.5. Variation of MI substituent

2.5.1. Monomer syntheses

2.5.1.1. Synthesis of MMI

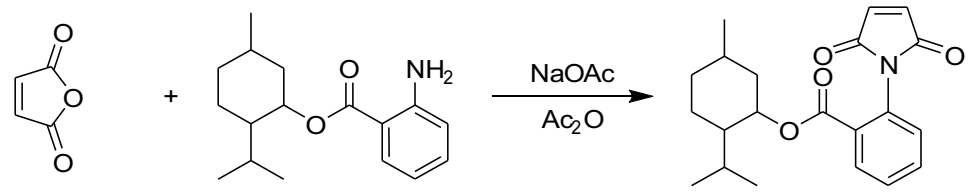

MA
$C_4H_2O_3$
98.06

meradimate
$C_{17}H_{25}NO_2$
275.39

MMI
$C_{21}H_{25}NO_4$
355.43

Synthesis of 2-isopropyl-5-methylcyclohexyl 2-(2,5-dioxo-2,5-dihydro-*1H*-pyrrol-1-yl)benzoate (**MMI**) was performed according to McLeod *et al.* [141].

MA (9.83 g, 100 mmol, 1 eq.) and menthyl anthranilate (meradimate) (27.55 g, 100 mmol, 1 eq.) were dissolved in 400 mL dry Et_2O under Ar atmosphere. After stirring 5 h at room temperature the solvent was decanted off and the white precipitate was dried under reduced pressure. Then anhydrous NaOAc (3.29 g, 40 mmol, 0.4 eq.), phenothiazine (60 mg, 3000 ppm) and 400 mL freshly distilled Ac_2O were added. Afterwards, the solution was stirred 5 h at 90 °C under Ar atmosphere. Then approximately 350 mL of the solvent were removed under reduced pressure. Subsequently, saturated aqueous $NaHCO_3$ solution was used to quench and neutralise the reaction mixture under ice cooling. The aqueous phase was extracted 3 times with 250 mL DCM. The combined organic phases were dried over anhydrous Na_2SO_4 and the solvent was removed under reduced pressure. Finally, the crude product was dissolved in DCM and filtrated over silica. After evaporation of the solvent under high vacuum at 60 °C 28.56 g (80.3% theoretical yield) of **MMI** were obtained as yellow-orange very high viscous liquid.

Die approbierte gedruckte Originalversion dieser Dissertation ist an der TU Wien Bibliothek verfügbar.
The approved original version of this doctoral thesis is available in print at TU Wien Bibliothek.
TU Bibliothek Your knowledge hub WIEN

R_f = 0.51 (PE : EE = 4 : 1)

^{1}H-NMR (400 MHz, $CDCl_3$, FID JST050/12): δ = 8.10 (d, J = 8.2 Hz, 1 H, CH-Ar), 7.64 (t, J = 7.6 Hz, 1 H, CH-Ar), 7.52 (t, J = 7.5 Hz, 1 H, CH-Ar), 7.30 (d, J = 7.9 Hz, 1 H, CH-Ar), 6.88 (s, 2 H, CH-DB), 4.83 (dt, J_1 = 10.8 Hz, J_2 = 4.3 Hz, 1 H, CH-O), 2.04-2.01 (m, 1 H, CH), 1.92-1.84 (m, 1 H, CH), 1.71-1.68 (m, 2 H, CH_2), 1.54-1.38 (m, 2 H, CH_2), 1.12-0.96 (m, 2 H, CH_2), 0.91-0.88 (m, 7 H, CH_3/CH-*i*-Pr), 0.74 (d, J = 7.0 Hz, 3 H, CH_3) ppm.

^{13}C-NMR (100 MHz, $CDCl_3$, FID JST050/11): δ = 169.9 (s, CO-MI), 164.5 (s, CO-ester), 134.7 (d, CH-DB), 133.2 (d, CH-Ar), 131.8 (d, CH-Ar), 131.3 (s, C-Ar), 130.6 (d, CH-Ar), 129.3 (d, CH-Ar), 129.0 (s, C-Ar), 75.4 (d, CH-O), 47.3 (d, CH-*i*-Pr), 40.9 (t, CH_2), 34.4 (t, CH_2), 31.6 (d, CH-CH_3), 26.3 (d, CH-*i*-Pr), 23.5 (t, CH_2), 22.1 (q, CH_3), 20.9 (q, CH_3-*i*-Pr), 16.3 (q, CH_3-*i*-Pr) ppm.

2.5.1.2. Synthesis of EHMI

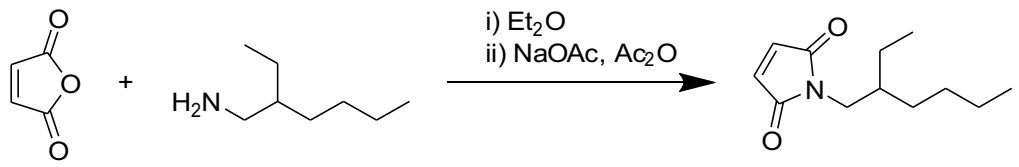

MA $C_4H_2O_3$ 98.06 | **EHA** $C_8H_{19}N$ 129.25 | **EHMI** $C_{12}H_{19}NO_2$ 209.29

Synthesis of 1-(2-ethylhexyl)-*1H*-pyrrole-2,5-dione (**EHMI**) was performed like the synthesis of MI **MMI** (chapter 2.5.1.1 of the experimental part) according to McLeod *et al.* [141].

MA (18.83 g, 192 mmol, 1 eq.) and freshly distilled **EHA** (84-85 °C at 60 mbar, 24.82 g, 192 mmol, 1 eq.) were dissolved in 500 mL dry Et_2O under Ar atmosphere. After stirring 5 h at room temperature, the solvent was removed under reduced pressure. Then anhydrous NaOAc (6.31 g, 76.8 mmol, 0.4 eq.), phenothiazine (115 mg, 3000 ppm) and 500 mL Ac_2O were added. Afterwards, the solution was stirred again 5 h at 90 °C under Ar atmosphere. Then,

Die approbierte gedruckte Originalversion dieser Dissertation ist an der TU Wien Bibliothek verfügbar.
The approved original version of this doctoral thesis is available in print at TU Wien Bibliothek.
TU Bibliothek Your knowledge hub WIEN

approximately 450 mL of the solvent were removed under reduced pressure at 70 °C. Subsequently, saturated aqueous $NaHCO_3$ solution was used to quench and neutralise the reaction mixture under ice cooling. The aqueous phase was extracted 3 times with PE. The combined organic phases were dried over anhydrous Na_2SO_4 and the solvent was removed under reduced pressure. Finally, the crude product was filtrated over silica (eluent PE : Et_2O = 9 : 1). After evaporation of the solvent 18.36 g (45.7% theoretical yield) of **EHMI** were obtained as slightly brownish liquid.

R_f = 0.43 (PE : EE = 10 : 1)
^{1}H-NMR (400 MHz, d_6-DMSO, FID JST077/3): δ = 7.02 (s, 2 H, CH-DB), 3.28 (d, J = 7.1 Hz, 2 H, CH_2-N), 1.60 (sept, J = 6.3 Hz, 1 H, CH), 1.24-1.15 (m, 8 H, CH_2), 0.86-0.81 (m, 6 H, CH_3) ppm.
^{13}C-NMR (100 MHz, d_6-DMSO, FID FID JST077/4): δ = 171.3 (s, CO-MI), 134.4 (d, CH-DB), 40.8 (t, CH_2-N), 37.7 (d, CH), 29.9 (t, CH_2), 27.9 (t, CH_2), 23.3 (t, CH_2), 22.4 (t, CH_2), 13.9 (q, CH_3), 10.3 (q, CH_3) ppm.

2.5.8. Swellability

Swellability studies of **pMISt3-5** without and with rubber **CB24** were performed in $CHCl_3$ with the procedure given in chapter 2.3.7 of the experimental part to obtain comparable data.

2.5.9. (Thermo)mechanical properties

General procedure for moulding specimens of **MISt4**-based resins: The formulations were homogenised at elevated temperatures and afterwards cooled down to room temperature. Then the samples were cured in transparent silicon moulds (*Wacker Elastosil RT 601*) 2 times 5 min (100% intensity) in the UV-chamber before precipitation of MI **CHMI** started. Finally, the obtained polymer sticks were sanded to ensure parallel shape.

Die approbierte gedruckte Originalversion dieser Dissertation ist an der TU Wien Bibliothek verfügbar.
The approved original version of this doctoral thesis is available in print at TU Wien Bibliothek.
TU Bibliothek Your knowledge hub WIEN

2.6. Potential applications

2.6.1. Reactive diluent (RD)

General procedure for moulding specimens: All samples were cured in transparent silicon moulds (*Wacker Elastosil RT 601*) 2 times 10 min in the Lumamat oven. Finally, the obtained polymer sticks were sanded to ensure parallel shape.

2.6.2. Frontal polymerisation (FP)

FP experiments were performed in a Teflon mould with a sample size of 3 g. The used CF exhibit a Köper texture and a weight of 245 g/m^2. An Omnicure lamp (320 – 500 nm) with 3 W/cm^2 at the light guide tip was applied for irradiation.

2.6.3. 3D printing

The 3D printing experiments were performed on a self made DLP printer equipped with a diamond-WXGA light engine (460 nm, 6 mW/cm^2 intensity at sample surface). Each layer of 50 µm thickness was irradiated for 40 s at room temperature and a contact pressure of 60 N.

Afterwards, the printed parts were post-cured in the UV-chamber for 5 min at 100% intensity.

Die approbierte gedruckte Originalversion dieser Dissertation ist an der TU Wien Bibliothek verfügbar.
The approved original version of this doctoral thesis is available in print at TU Wien Bibliothek.
TU WIEN Bibliothek Your knowledge hub

Materials, Devices and Analyses

Reagents and solvents

All commercial reagents and solvents were used without further purification, if not mentioned explicitly in a different way.

Dry solvents were taken from a *PURESOLV*-system from *it-innovative technology inc.* or were bought already in anhydrous form (*e.g.* EtOH, DMF).

Orange light laboratory

Handling of light sensitive substances/reactions/resins was carried out in an orange light laboratory, where windows were laminated with an *Asmetec metolight* SF-UV-filter foil (type ASR-SF-LY5) and *Osram* lumilux bulbs with chip-control (litght colour 62) were used instead of common fluorescent tubes.

Light sources

According to the used photoinitiator different (UV-)light sources were applied to irradiate the sample:

- UV-chamber: *Uvitron International INTELLI-RAY 600* with Hg broad band UV-bulb (600 W; UV-A: 125 mW/cm^2; Vis: 125 mW/cm^2)
- Light oven: *Lumamat 100* (400-500 nm) from *Ivoclar Vivadent AG* with 6 *Osram Dulux L Blue* 18 W bulbs
- Omnicure-system: *Omnicure Series 2000 EXFO* with a 200 W Hg-bulb and according to used filter 320 – 500 nm or 400 – 500 nm

Die approbierte gedruckte Originalversion dieser Dissertation ist an der TU Wien Bibliothek verfügbar.
The approved original version of this doctoral thesis is available in print at TU Wien Bibliothek.
TU Bibliothek Your knowledge hub WIEN

TLC

Silica gel 60 F_{254} TLC-aluminium foils from *Merck* were used for thin layer chromatography.

Column chromatography

For column chromatography a *Büchi Sepacore Flash System* with following parts was used:

- *Büchi* control unit C-620
- Pump system: 2 *Büchi* pump moduls C-605
- Detector: *Büchi* UV-photometer C-635 and *Büchi* RI-detector Refractom
- Collector: *Büchi* fraction collector C-660

The columns were filled with silica gel 60 (*Merck*, 40 – 63 µm). The exact process parameters (solvents, flow rates, etc.) were given in each case.

GPC

All GPC measurements were conducted at 40 °C on a *Malvern Viscotek GPCmax VE2001* system equipped with a *Malvern Viscotek TDA*, *Malvern Viscotek SEC-MALS 9* and RI detector VE3850. Three *Waters Styragel HR 0.5, 3 and 4 THF* columns were used with dry THF as mobile phase (1 mL/min). Calibration was performed with PS standards (0.370 – 177 kDa). The software OmniSEC 5.12 was used for data acquisition and analyses.

GC-MS

For GC-MS measurements a system from *Thermo Scientific* was used:

- Autosampler: *AS 3000*
- GC: *Trace GC Ultra* with a BGB-5 column (30 m length)
- MS: *ITQ 1100* with an ion trap detector and EI ionisation

Die approbierte gedruckte Originalversion dieser Dissertation ist an der TU Wien Bibliothek verfügbar.
The approved original version of this doctoral thesis is available in print at TU Wien Bibliothek.
TU WIEN Bibliothek Your knowledge hub

Melting points

Melting points were measured with an *OptiMelt* automated melting point system from *SRS Stanford Research Systems*.

NMR spectroscopy

NMR spectra were recorded at 20 °C on a *Bruker DPX-200* with 200 MHz for ^{1}H (50 MHz for ^{13}C), a *Bruker Avance DRX-400* with 400 MHz for ^{1}H (100 MHz for ^{13}C) or a *Bruker Avance IIIHD* with 600 MHz for ^{1}H (150 MHz for ^{13}C). If not mentioned otherwise, $CDCl_3$ was used as solvent. Data was recorded and evaluated with *Topspin* software.

The results of ^{1}H and ^{13}C spectra were given as follows:

- Chemical shifts are given in ppm and are referred to tetramethylsilane (TMS, δ = 0 ppm). The actual values are corrected according to the used solvent (^{1}H: $CDCl_3$ δ = 7.26 ppm, d_6-DMSO δ = 2.50 ppm; ^{13}C: $CDCl_3$ δ = 77.1 ppm, d_6-DMSO δ = 39.5 ppm).
- All multiplicities are stated as follows: ^{1}H: s = singlet, bs = broad singlet, d = doublet, t = triplet, q = quartet and m = multiplet; ^{13}C: s = quaternary C, d = CH, t = CH_2, q = CH_3; assignment of signals via APT, COSY or/and HSQC spectra.

ATR-IR spectroscopy

All ATR-IR spectra were recorded on a *PerkinElmer 65* FT-IR spectrometer with a golden-gate diamond ATR unit. No ATR correction was done.

Die approbierte gedruckte Originalversion dieser Dissertation ist an der TU Wien Bibliothek verfügbar.
The approved original version of this doctoral thesis is available in print at TU Wien Bibliothek.
TU Bibliothek Your knowledge hub WIEN

UV-Vis absorption

UV-Vis absorption spectra were recorded on a *Lambda 950* device from *PerkinElmer* equipped with a PMT detector.

For measuring an UV-Vis absorption spectrum the substances were dissolved in a defined concentration (1 mM) in dry DCM. After filtering the solutions through a syringe filter, spectra were recorded from 250 – 800 nm.

STA

All STA experiments were performed on a *Netzsch STA 449 F1 Jupiter*.

The volatility measurements were done for 3 h at various temperatures with following conditions:

- Sample size: 10 ± 1 mg
- Crucibles: Al with Al lid (with a hole)
- Atmosphere: N_2 (flow rate of 40 mL/min)

Sample mass loss was calculated after preheating phase, when the constant target temperature was reached.

Thermal stability of the photopolymers was measured on the STA according to DIN EN ISO 11358 with following experimental parameters:

- Sample size: 10 ± 1 mg
- Crucibles: Al, with Al lid (with a hole)
- Atmosphere: N_2 (flow rate of 40 mL/min)
- Temperature: 25 – 500 °C
- Heating rate: 10 K/min

The temperatures of beginning mass loss (T_A) and the temperatures of the inflexion points (T_C) were determined from the TGA curve.

Die approbierte gedruckte Originalversion dieser Dissertation ist an der TU Wien Bibliothek verfügbar.
The approved original version of this doctoral thesis is available in print at TU Wien Bibliothek.
TU Bibliothek Your knowledge hub WIEN

Thermal DSC

For thermal DSC measurements a *Shimadzu DSC-50* was used.

Photo-DSC

A *Netzsch DSC 204 F1* coupled with an Omnicure lamp for irradiation of the sample was used.

All photo-DSC studies were performed under following conditions:

- Sample size: 10 ± 0.5 mg
- Crucibles: Al (at elevated temperatures with glass lid)
- Atmosphere: N_2 (flow rate of 20 mL/min)
- Light source: Omnicure lamp, depending on used PI either 320 – 500 nm or 400 – 500 nm
- Irradiation intensity: 1 W/cm^2 at the light guide tip
- Irradiation time: 2*5 min exposure to UV-light after flushing the sample chamber 4 min with inert gas

Each formulation was tested 3 times. Additionally, a ^{1}H-NMR spectrum and a GPC of each polymer were recorded.

RT-NIR-photorheology [153]

RT-NIR-photorheology measurements were performed on an *Anton Paar MCR 302 WESP* equipped with a (quartz) glass plate and a PP25 measuring system. Furthermore, Peltier elements around the plate (*Anton Paar* P-PTD200/GL) and a heating hood (*Anton Paar* H-PTD200) were used as temperature control system. The rheometer device was combined with a *Bruker Vertex 80* FTIR spectrometer. An Omnicure lamp was used for irradiation of the sample (see Figure 148). The light intensity was adjusted with an *Ocean Optics USB 2000+* spectrometer on the surface of the optical window. The software *Anton Paar* Rheoplus V3.62 and OPUS 7.0 were used for data recording and analyses.

Die approbierte gedruckte Originalversion dieser Dissertation ist an der TU Wien Bibliothek verfügbar.
The approved original version of this doctoral thesis is available in print at TU Wien Bibliothek.
TU Bibliothek Your knowledge hub WIEN

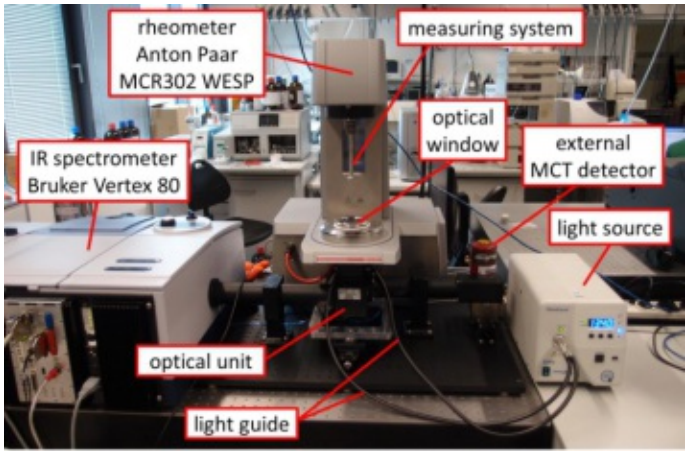

Figure 148: RT-MIR/NIR-photorheology set-up

The experiments on the RT-NIR-photorheology device were conducted under following experimental conditions:

- Sample size: 140 µL
- Measurement device: PP25
- Frequency: 1 Hz
- Amplitude: 1%
- Gap: 200 µm
- Optical window: Glass plate protected with a PE tape (*tesa extra power transparent*)
- Light source: Omnicure lamp with 320 – 500 nm
- Irradiation intensity: 10 mW/cm^2 at sample surface
- Irradiation time: 5 min

Each formulation was tested 3 times.

Double bond conversion (DBC) was calculated with IR spectroscopy via the drop of peak area during polymerisation of the first overtone vibration of the C=C double bond in the NIR at ~ 6100 cm^{-1}. Additionally, shrinkage force (F_N), storage (G') and loss modulus (G") were measured with the rheometer device.

Die approbierte gedruckte Originalversion dieser Dissertation ist an der TU Wien Bibliothek verfügbar.
The approved original version of this doctoral thesis is available in print at TU Wien Bibliothek.
TU Bibliothek Your knowledge hub WIEN

Viscosity

Viscosity was measured on an *Anton Paar MCR 300* rheometer with a Peltier PTD 150 system.

All viscosity measurements were conducted with following experimental parameters:

- Sample size: 80 µL
- Temperature: 25 °C
- Measuring system: CP25-1
- Gap: 48 µm
- Shear rate: 100 s^{-1}

Melt viscosity

Measurements were performed on an *Anton Paar MCR 301* rheometer with a CTD 450 oven.

All melt viscosity measurements were conducted with following parameters:

- Sample size: ~ 85 µL with additional 0.5 mg phenothiazine
- Measuring system: CP25-1 with 48 µm gap between tip and plate
- Shear rate: 100 s^{-1}
- Temperature: 25 – 120 °C
- Heating rate: 3 °C/min

Measurements were stopped manually, when a start of thermal polymerisation was observed.

Die approbierte gedruckte Originalversion dieser Dissertation ist an der TU Wien Bibliothek verfügbar.
The approved original version of this doctoral thesis is available in print at TU Wien Bibliothek.
TU Bibliothek Your knowledge hub WIEN

DMTA

DMTA measurements were performed on an *Anton Paar MCR 301* rheometer with a CTD 450 oven and a SRF 12 measuring system.

All DMTA experiments were conducted with rectangular shaped specimens (~ 5*2*40 mm^3) in torsion mode with constant normal force and following experimental parameters:

- Frequency: 1 Hz
- Amplitude: 0.1%
- Constant normal force: -1 N
- Temperature: -100 – 200 °C or -130 – 250 °C for MISt-based polymers
- Heating rate: 2 °C/min

Tensile tests

Tensile tests were performed on a *Zwick Z050* with a force sensor with a maximal force of 1 kN. *TestXpert II* was used for recording and evaluation of measured data.

All tensile tests were executed according to ISO 527 with specimen shape 5B (Figure 149) and a traverse speed of 5 mm/min. At least 5 specimen were tested for each photopolymer.

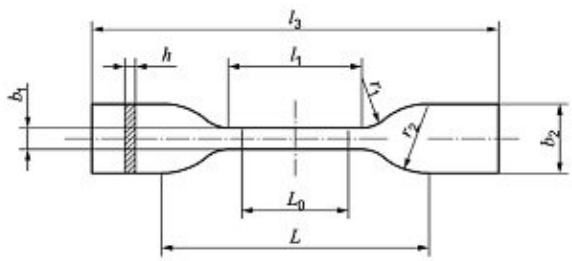

Figure 149: Scheme of specimen shape 5B [154]

Die approbierte gedruckte Originalversion dieser Dissertation ist an der TU Wien Bibliothek verfügbar.
The approved original version of this doctoral thesis is available in print at TU Wien Bibliothek.
TU Bibliothek Your knowledge hub WIEN

Specimen shape 5B, which is shown in Figure 149, exhibits following dimensions:

- Overall length l_3: ≥ 35 mm
- Width at the ends b_2: 6 ± 0.5 mm
- Length of the narrow parallel part l_1: 12 ± 0.5 mm
- Width of the narrow part b_1: 2 ± 0.1 mm
- Small radius r_1: 3 ± 0.1 mm
- Big radius r_2: 3 ± 0.1 mm
- Clamp starting distance L: 20 ± 2 mm
- Measuring length L_0: 10 ± 0.2 mm
- Thickness h: 1 ± 0.1 mm

Dynstat impact resistance

A *Karl Frank GmbH* Dynstat device (type 573) with 5, 10, 20 or 40 kpcm hammers was used.

Dynstat impact resistance was always measured according to DIN 51230. An appropriate hammer was applied for breaking the test pieces. Additionally, measured data was normalised to the real cross section of the corresponding sample. At least 4 specimens (~ 10*4*15 mm^3) were tested for each photopolymer.

SEM

SEM measurements were performed on a *FEI Philips XL 30*. Sample edges were coated with a conducting Ag-based paint. Additionally, samples were sputtered with a thin layer of Au.

Die approbierte gedruckte Originalversion dieser Dissertation ist an der TU Wien Bibliothek verfügbar.
The approved original version of this doctoral thesis is available in print at TU Wien Bibliothek.
TU Bibliothek Your knowledge hub WIEN

AFM

AFM experiments were performed on a *NanoWizard ULTRA SpeedA* AFM system from *JPK Instruments AG*, which was equipped with an *Axio Observer.D1* inverted optical microscope from *ZEISS*. Samples for AFM measurements were cut from the edge of tensile test specimens with a sharp scalpel, polished with sand paper and glued on a glass slide with commercial 2K epoxy glue.

The following parameters were applied in all nanoindentations experiments:

- 4XC-NN-17 rectangular cantilever with a tip with nominal radius of 10 nm
- The spring constant was calibrated with the thermal noise method
- The deflection sensitivity was determined by measuring 16 force measurements on the glass slide
- Quantitative imaging mode with a maximum applied force of 20 nN
- Measurement area: 5*5 μm^2
- Resolution: 256*256 pixels

The Young's moduli were calculated according to the Hertz analysis method.

Die approbierte gedruckte Originalversion dieser Dissertation ist an der TU Wien Bibliothek verfügbar.
The approved original version of this doctoral thesis is available in print at TU Wien Bibliothek.
TU Bibliothek Your knowledge hub WIEN

Summary

The aim of this thesis was to investigate approaches for toughening of photopolymers to enable possible new fields of application. Therefore, an extended literature search in scientific publications as well as patents was performed. Since a lot of research was conducted in the last decades and thus various concepts for enhancing toughness were developed, two different independent plans were pursued and studied in detail.

First, an approach based on changing the polymer architecture of photopolymers was investigated. Therefore, blocked isocyanates were incorporated into the spacer between the methacrylate moieties of a multifunctional methacrylate. Thus, thermally induced cleavage of cross-links in a polymer network is enabled. Additionally, a difunctional amine is added to the photopolymer resin and integrated into the polymer. After heating and regeneration of the isocyanate motive, the chain extender can react and a linear polyurea is formed. Hence, degradation of the highly cross-linked thermoset (methacrylic photopolymer) to a thermoplastic material (linear polymethacrylate and linear polyurea) can be accomplished.

Die approbierte gedruckte Originalversion dieser Dissertation ist an der TU Wien Bibliothek verfügbar.
The approved original version of this doctoral thesis is available in print at TU Wien Bibliothek.
TU Bibliothek Your knowledge hub WIEN

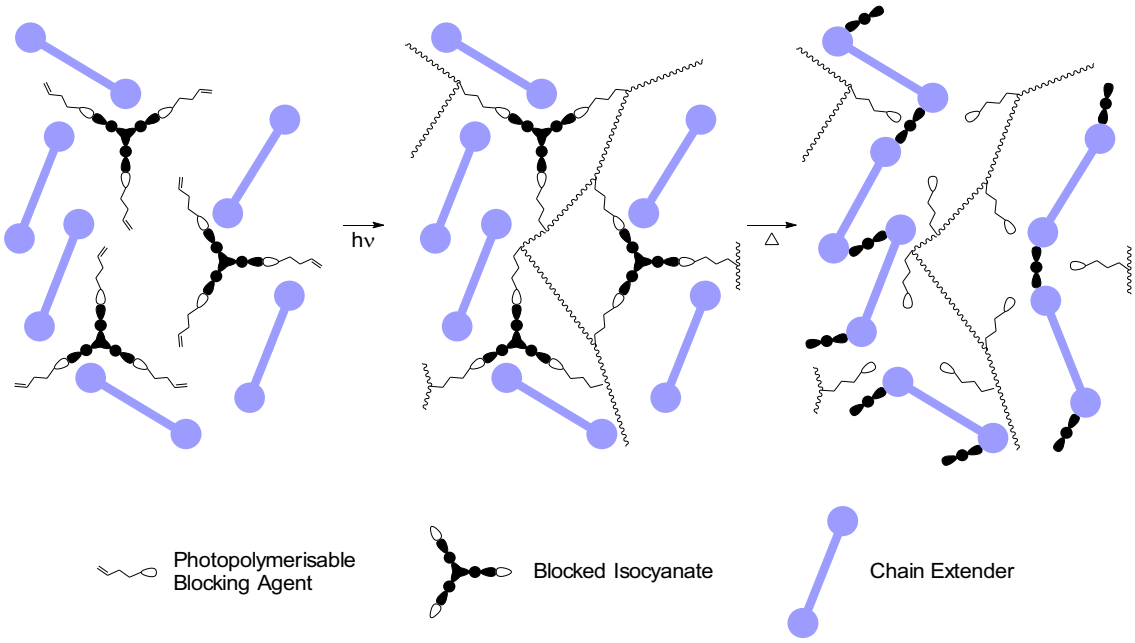

So two commercially available different isocyanurate model compounds based on difunctional isocyanates **HDI** and **IPDI** were chosen and tested regarding their capability of isocyanate liberation at suitable temperatures:

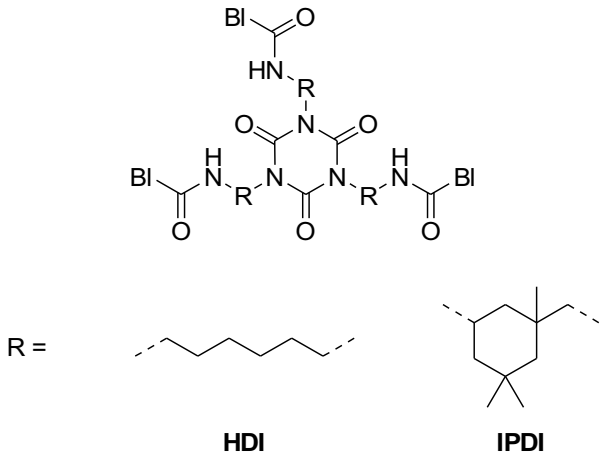

Deblocking reactions and regeneration of the isocyanate structures could be achieved successfully in preliminary experiments in the presence of an amine with an onset temperature of ~ 120 °C. Hence, a methacrylic monomer based on

Die approbierte gedruckte Originalversion dieser Dissertation ist an der TU Wien Bibliothek verfügbar.
The approved original version of this doctoral thesis is available in print at TU Wien Bibliothek.
TU Bibliothek Your knowledge hub WIEN

the **IPDI** isocyanurate model compound was synthesised (**BICMA1**). In addition, a literature known monomer (**C3D1**) and a monomer based on a C-H acidic blocking reagent (**VIC2**) were used for comparison.

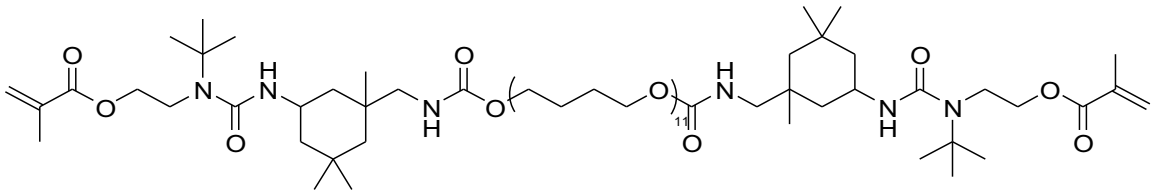

C3D1

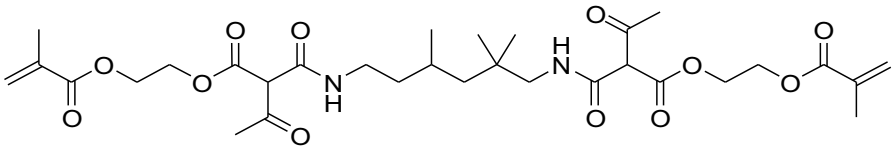

VIC2

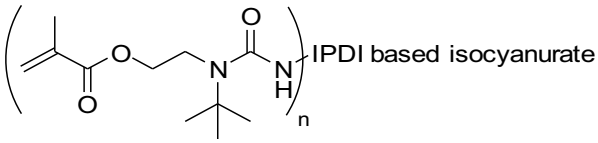

BICMA1

The synthesised methacrylates containing blocked isocyanates were formulated either with a high molecular weight and flexible difunctional diamine **DA** or with the rigid cycloaliphatic diamine **HMDA**.

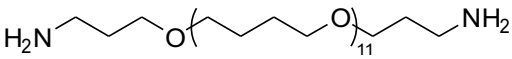

DA

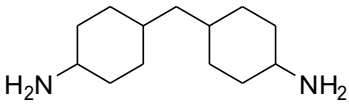

HMDA

Die approbierte gedruckte Originalversion dieser Dissertation ist an der TU Wien Bibliothek verfügbar.
The approved original version of this doctoral thesis is available in print at TU Wien Bibliothek.

Unfortunately, synthesised monomers showed a thermally induced deblocking reaction in the presence of an amine only in solution at 125 °C and not in bulk after polymerisation. Thus, the formulation, which was mixed in accordance with literature, was modified to a softer and more polar matrix. Since these resin alterations facilitate isocyanate regeneration, deblocking reactions and polyurea formation could be achieved and finally proved by tensile tests.

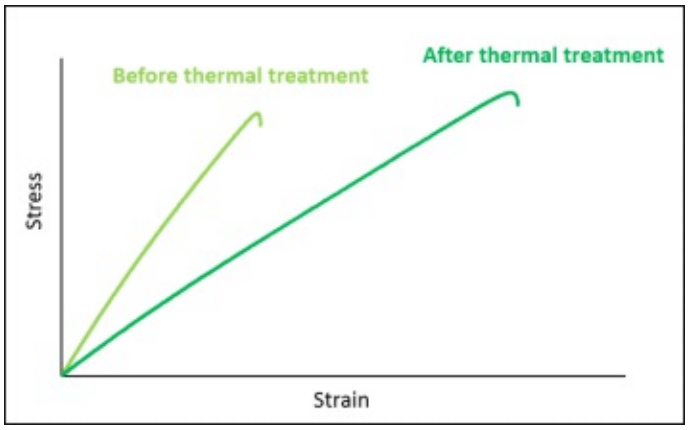

The second pursued concept is based on mimicking structure and morphology of ABS. Since ABS cannot be synthesised via photopolymerisation, the monomers (acrylonitrile, butadiene and styrene) were substituted to circumvent this issue. After some syntheses and preliminary photo-DSC studies suitable monomers were found, which exhibit an acceptable low degree of volatility and high reactivity: maleimides, styrene derivatives and polybutadiene.

Die approbierte gedruckte Originalversion dieser Dissertation ist an der TU Wien Bibliothek verfügbar.
The approved original version of this doctoral thesis is available in print at TU Wien Bibliothek.
TU Bibliothek Your knowledge hub WIEN

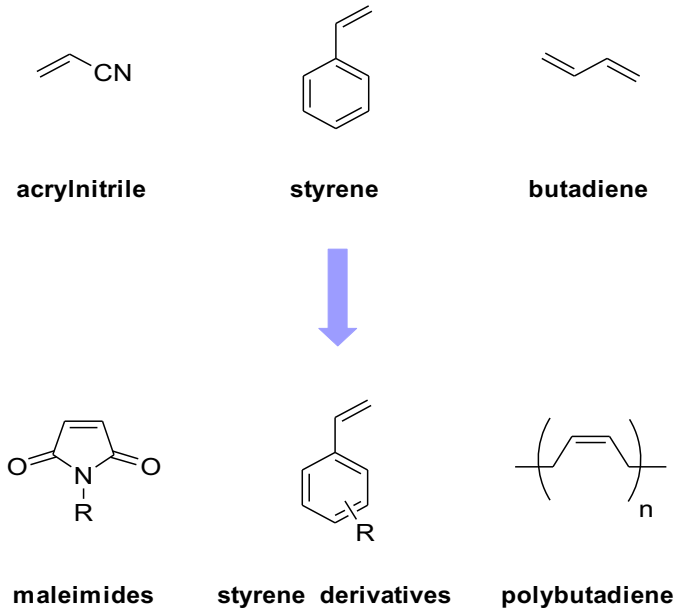

A first model system **MISt1** was selected and formulation characteristics, reactivity as well as material properties thereof were tested. While monomer volatility and storage stability are not ideal, fast photopolymerisation and high conversions (> 87%) could be achieved. In addition, **pMISt1** polymers exhibit a high T_g (> 160 °C), good tensile properties (*e.g.* a $stress_{max}$ of 28 MPa and a $strain_{break}$ of 46%) and superior toughness (calculated Dynstat impact resistance of > 100 kJ/m^2).

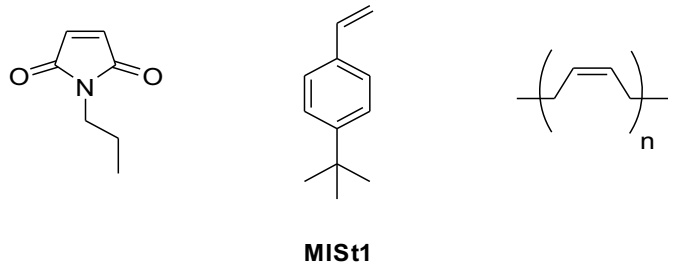

Die approbierte gedruckte Originalversion dieser Dissertation ist an der TU Wien Bibliothek verfügbar.
The approved original version of this doctoral thesis is available in print at TU Wien Bibliothek.
TU Bibliothek Your knowledge hub WIEN

With these very promising results of the first monomer generation further experiments were conducted and a better understanding and more insights into maleimide-styrene-polybutadiene terpolymers were obtained:

- Factors triggering phase separation
- Occurrence of cross-linking reactions of the maleimide substituent
- Cross-linking due to copolymerisation with polybutadiene double bonds
- Terpolymerisation behaviour of the maleimide-styrene-system with methacrylates

Moreover, different substituted monomer systems (**MISt2-5**) were tested to further optimise resin attributes such as volatility (< 1% after 3 h at 90 °C) and storage stability (> 4 m), while maintaining fast photopolymerisation with high double bond conversions (> 90%) and superior material properties (*e.g.* **pMISt4**-based terpolymers exceed T_gs of 170 °C).

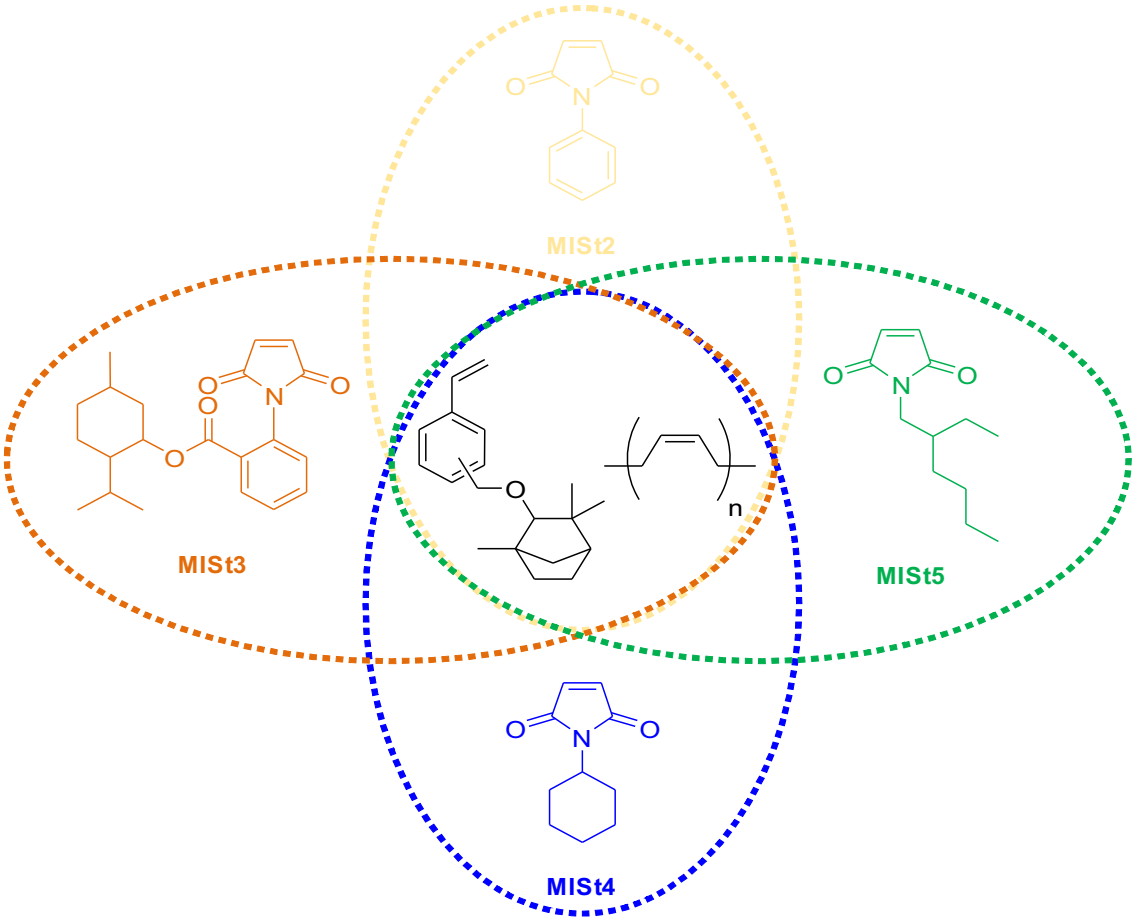

Die approbierte gedruckte Originalversion dieser Dissertation ist an der TU Wien Bibliothek verfügbar.
The approved original version of this doctoral thesis is available in print at TU Wien Bibliothek.

Thus, a broad variety of different formulation and material properties can be covered with this new photopolymer class.

Finally, 3 different potential applications for maleimide-styrene copolymers without and with butadiene rubber addition were shown:

- Reactive diluent for highly viscous methacrylic resins
- Frontal polymerisation
- 3D printing

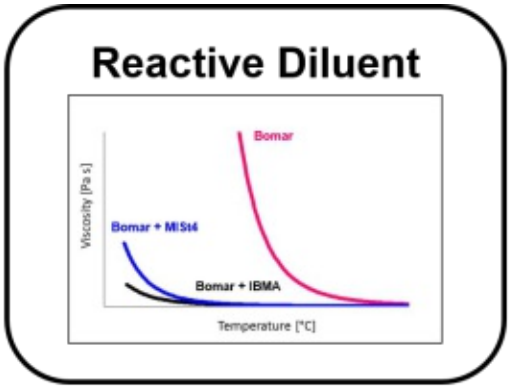

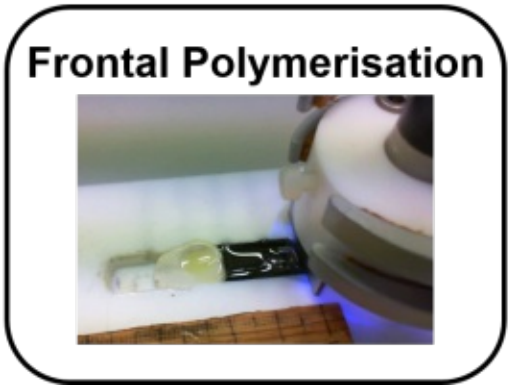

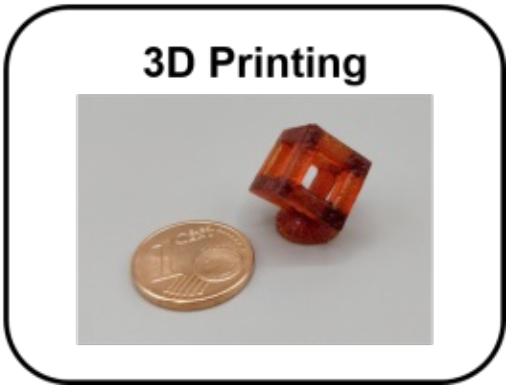

First, monomer system **MISt4** was successfully applied as non-volatile reactive diluent for a commercial highly viscous urethane methacrylate, which cannot be processed without heating or adding diluents. Additionally, formulation as well as

Die approbierte gedruckte Originalversion dieser Dissertation ist an der TU Wien Bibliothek verfügbar.
The approved original version of this doctoral thesis is available in print at TU Wien Bibliothek.
TU Bibliothek Your knowledge hub WIEN

final photopolymer properties were compared to the very popular reactive diluent isobornyl methacrylate (**IBMA**), which is known to be too volatile for application at elevated temperatures.

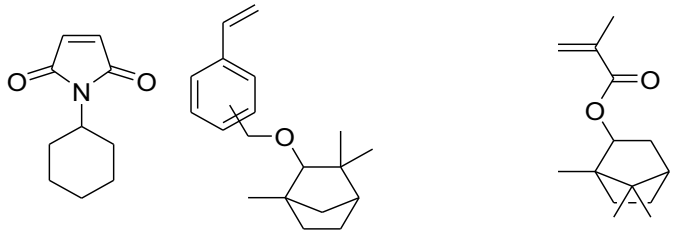

MISt4 **IBMA**

Both reactive diluent approaches result in low resin viscosities (< 1 Pa s at 45 °C). Furthermore, the obtained polymer characteristics are similar such as high glass transition temperatures (> 125 °C). However, the properties such as stress and strain at break suffer due to the rigid cycloaliphatic ring structures of the additive systems yielding materials with low impact resistance (~ 6 kJ/m^2).

In addition, fabrication of photopolymer parts with several millimetres thickness of a carbon fibre filled maleimide-styrene copolymer (20 w% fibres in **MISt5**) was achieved successfully via frontal polymerisation.

Lastly, feasibility of 3D printing (DLP) of a maleimide-styrene-polybutadiene terpolymer (**MISt5** with 10 w% rubber) was proven as well, which enables new fields of application for this new ABS-inspired photopolymer class in industry and research.

Die approbierte gedruckte Originalversion dieser Dissertation ist an der TU Wien Bibliothek verfügbar.
The approved original version of this doctoral thesis is available in print at TU Wien Bibliothek.
TU Bibliothek Your knowledge hub WIEN

Abbreviations

ABS	acrylonitrile butadiene styrene terpolymer
ACN	acetonitrile
AFM	atomic force microscopy
AMT	additive manufacturing technology
ATR	attenuated total reflectance
BIC	blocked isocyanate
BR	butadiene rubber
CI	citraconimide
DBC	double bond conversion
DMF	dimethylformamide
DMTA	dynamic mechanical thermal analysis
DSC	differential scanning calorimetry
EtOH	ethanol
G	shear modulus
G'	storage modulus
G''	loss modulus
GC	gas chromatography
GPC	gel permeation chromatography
HBR	hydrogenated butadiene rubber
HMDS	hexamethyldisilazane
IC	isocyanate
II	itaconimide
IR	infrared spectroscopy
MA	methacrylate
MI	maleimide
MIR	mid-infrared
MISt	maleimide styrene copolymer
MS	mass spectrometry
NIR	near-infrared
NMR	nuclear magnetic resonance
PE	petroleum ether
PI	photoinitiator
R_p	polymerisation rate
RT	real time
s	standard deviation
SEM	scanning electron microscopy
St	styrene
STA	simultaneous thermal analysis
tan δ	mechanical loss
T_{db}	deblocking temperature
T_g	glass transition temperature
THF	tetrahydrofuran
TLC	thin layer chromatography

Die approbierte gedruckte Originalversion dieser Dissertation ist an der TU Wien Bibliothek verfügbar.
The approved original version of this doctoral thesis is available in print at TU Wien Bibliothek.
TU WIEN Bibliothek Your knowledge hub

Bibliography

[1] Studer, K.; UV-curing: worth investing in a prosperous green technology. *Coating* **2007**, *40* (9), 33-37.

[2] Fouassier, J. P.; Allonas, X.; Burget, D.; Photopolymerization reactions under visible lights: principle, mechanisms and examples of applications. *Prog. Org. Coat.* **2003**, *47* (1), 16-36.

[3] Fleischer, J. E.; Coatings for plastics. UV-curable coatings for functional and decorative plastics applications is gaining popularity. *Mod. Paint Coat.* **2001**, *91* (4), 21-22.

[4] Abe, Y.; Current status and updates on the radiation curing technology for polymers for coatings. *DIC Tech. Rev.* **2005**, *11*, 1-20.

[5] Husar, B.; Heller, C.; Schwentenwein, M.; Mautner, A.; Varga, F.; Koch, T.; Stampfl, J.; Liska, R.; Biomaterials based on low cytotoxic vinyl esters for bone replacement application. *J. Polym. Sci., Part A: Polym. Chem.* **2011**, *49* (23), 4927-4934.

[6] Orman, S.; Hofstetter, C.; Aksu, A.; Reinauer, F.; Liska, R.; Baudis, S.; Toughness enhancers for bone scaffold materials based on biocompatible photopolymers. *J. Polym. Sci., Part A: Polym. Chem.* **2019**, *57* (2), 110-119.

[7] Moszner, N.; Salz, U.; New developments of polymeric dental composites. *Prog. Polym. Sci.* **2001**, *26* (4), 535-576.

[8] Cushing, M. C.; Anseth, K. S.; Hydrogel Cell Cultures. *Science* **2007**, *316* (5828), 1133-1134.

[9] Fedorovich, N. E.; Swennen, I.; Girones, J.; Moroni, L.; van Blitterswijk, C. A.; Schacht, E.; Alblas, J.; Dhert, W. J. A.; Evaluation of Photocrosslinked Lutrol Hydrogel for Tissue Printing Applications. *Biomacromolecules* **2009**, *10* (7), 1689-1696.

Die approbierte gedruckte Originalversion dieser Dissertation ist an der TU Wien Bibliothek verfügbar.
The approved original version of this doctoral thesis is available in print at TU Wien Bibliothek.
TU Bibliothek Your knowledge hub WIEN

[10] Khan, A. M.; Pojman, J. A.; The use of frontal polymerization in polymer synthesis. *Trends Polym. Sci.* **1996**, *4* (8), 253-257.

[11] Pojman, J. A.; Ilyashenko, V. M.; Khan, A. M.; Free-radical frontal polymerization: self-propagating thermal reaction waves. *J. Chem. Soc., Faraday Trans.* **1996**, *92* (16), 2825-2837.

[12] Husar, B.; Hatzenbichler, M.; Mironov, V.; Liska, R.; Stampfl, J.; Ovsianikov, A.; Photopolymerization-based additive manufacturing for the development of 3D porous scaffolds. *Biomaterials for Bone Regeneration* **2014**, *75*, 149-201.

[13] Tumbleston, J. R.; Shirvanyants, D.; Ermoshkin, N.; Janusziewicz, R.; Johnson, A. R.; Kelly, D.; Chen, K.; Pinschmidt, R.; Rolland, J. P.; Ermoshkin, A.; Samulski, E. T.; DeSimone, J. M.; Continuous liquid interface production of 3D objects. *Science* **2015**, *347* (6228), 1349-1352.

[14] Ligon, S. C.; Liska, R.; Stampfl, J.; Gurr, M.; Mulhaupt, R.; Polymers for 3D Printing and Customized Additive Manufacturing. *Chem. Rev.* **2017**, *117* (15), 10212-10290.

[15] https://trends.directindustry.de/edinburgh-instruments/project-25178-193661.html; 30.8.2020.

[16] Dietliker, K., *Photoinitiators for Free Radical and Cationic Polymerisation*. **1991**; Vol. 3.

[17] Fouassier, J. P., *Photoinitiation, Photopolymerization, and Photocuring. Fundamentals and Applications*. Hanser: **1995**.

[18] Green, W. A., *Industrial Photoinitiators. A Technical Guide*. **2010**.

[19] Husar, B.; Liska, R.; Vinyl carbonates, vinyl carbamates, and related monomers: synthesis, polymerization, and application. *Chem. Soc. Rev.* **2012**, *41* (6), 2395-2405.

[20] Husar, B.; Ligon, S. C.; Wutzel, H.; Hoffmann, H.; Liska, R.; The formulator's guide to anti-oxygen inhibition additives. *Prog. Org. Coat.* **2014**, *77* (11), 1789-1798.

Die approbierte gedruckte Originalversion dieser Dissertation ist an der TU Wien Bibliothek verfügbar.
The approved original version of this doctoral thesis is available in print at TU Wien Bibliothek.
TU Bibliothek Your knowledge hub WIEN

[21] Ligon, S. C.; Husar, B.; Wutzel, H.; Holman, R.; Liska, R.; Strategies to Reduce Oxygen Inhibition in Photoinduced Polymerization. *Chem. Rev.* **2014**, *114* (1), 557-589.

[22] Ligon-Auer, S. C.; Schwentenwein, M.; Gorsche, C.; Stampfl, J.; Liska, R.; Toughening of photo-curable polymer networks: a review. *Polym. Chem.* **2016**, *7* (2), 257-286.

[23] Sultan, J. N.; McGarry, F. J.; Effect of rubber particle size on deformation mechanisms in glassy epoxy. *Polym. Eng. Sci.* **1973**, *13* (1), 29-34.

[24] Hazot, P.; Pichot, C.; Maazouz, A.; Synthesis of hairy acrylic core-shell particles as toughening agents for epoxy networks. *Macromol. Chem. Phys.* **2000**, *201* (6), 632-641.

[25] Zhang, H.; Tang, L.-C.; Zhang, Z.; Friedrich, K.; Sprenger, S.; Fracture behaviours of in situ silica nanoparticle-filled epoxy at different temperatures. *Polymer* **2008**, *49* (17), 3816-3825.

[26] Bagheri, R.; Marouf, B. T.; Pearson, R. A.; Rubber-Toughened Epoxies: A Critical Review. *Polym. Rev.* **2009**, *49* (3), 201-225.

[27] Liu, J.; Thompson, Z. J.; Sue, H.-J.; Bates, F. S.; Hillmyer, M. A.; Dettloff, M.; Jacob, G.; Verghese, N.; Pham, H.; Toughening of Epoxies with Block Copolymer Micelles of Wormlike Morphology. *Macromolecules* **2010**, *43* (17), 7238-7243.

[28] Lee, T. Y.; Carioscia, J.; Smith, Z.; Bowman, C. N.; Thiol-Allyl Ether-Methacrylate Ternary Systems. Evolution Mechanism of Polymerization-Induced Shrinkage Stress and Mechanical Properties. *Macromolecules* **2007**, *40* (5), 1473-1479.

[29] Jiang, T.; He, Y.; Jian, Y.; Nie, J.; Exploration for decreasing the volume shrinkage for photopolymerization. *Prog. Org. Coat.* **2012**, *75* (4), 398-403.

[30] Braunecker, W. A.; Matyjaszewski, K.; Controlled/living radical polymerization: Features, developments, and perspectives. *Prog. Polym. Sci.* **2007**, *32* (1), 93-146.

Die approbierte gedruckte Originalversion dieser Dissertation ist an der TU Wien Bibliothek verfügbar.
The approved original version of this doctoral thesis is available in print at TU Wien Bibliothek.
TU Bibliothek Your knowledge hub WIEN

[31] Hoyle, C. E.; Lee, T. Y.; Roper, T.; Thiol-enes: Chemistry of the past with promise for the future. *J. Polym. Sci., Part A: Polym. Chem.* **2004**, *42* (21), 5301-5338.

[32] Hoyle, C. E.; Bowman, C. N.; Thiol-Ene Click Chemistry. *Angew. Chem., Int. Ed.* **2010**, *49* (9), 1540-1573.

[33] Kade, M. J.; Burke, D. J.; Hawker, C. J.; The power of thiol-ene chemistry. *J. Polym. Sci., Part A: Polym. Chem.* **2010**, *48* (4), 743-750.

[34] El-Roz, M.; Lalevee, J.; Allonas, X.; Fouassier, J.-P.; The silane-ene and silane-acrylate polymerization process: a new promising chemistry? *Macromol. Rapid Commun.* **2008**, *29* (10), 804-808.

[35] Steindl, J.; Svirkova, A.; Marchetti-Deschmann, M.; Moszner, N.; Gorsche, C.; Light-Triggered Radical Silane-Ene Chemistry Using a Monosubstituted Bis(trimethylsilyl)silane. *Macromol. Chem. Phys.* **2017**, *218* (9), n/a.

[36] Steindl, J.; Koch, T.; Moszner, N.; Gorsche, C.; Silane-Acrylate Chemistry for Regulating Network Formation in Radical Photopolymerization. *Macromolecules* **2017**, *50* (19), 7448-7457.

[37] Yagci, Y.; Reetz, I.; Addition-fragmentation reactions in polymer chemistry. *React. Funct. Polym.* **1999**, *42* (3), 255-264.

[38] Moad, G.; Rizzardo, E.; Thang, S. H.; Radical addition-fragmentation chemistry in polymer synthesis. *Polymer* **2008**, *49* (5), 1079-1131.

[39] Gorsche, C.; Griesser, M.; Gescheidt, G.; Moszner, N.; Liska, R.; β-Allyl Sulfones as Addition-Fragmentation Chain Transfer Reagents: A Tool for Adjusting Thermal and Mechanical Properties of Dimethacrylate Networks. *Macromolecules* **2014**, *47* (21), 7327-7336.

[40] Ligon, S. C.; Seidler, K.; Gorsche, C.; Griesser, M.; Moszner, N.; Liska, R.; Allyl sulfides and α-substituted acrylates as addition-fragmentation chain transfer agents for methacrylate polymer networks. *J. Polym. Sci., Part A: Polym. Chem.* **2016**, *54* (3), 394-406.

Die approbierte gedruckte Originalversion dieser Dissertation ist an der TU Wien Bibliothek verfügbar.
The approved original version of this doctoral thesis is available in print at TU Wien Bibliothek.
TU Bibliothek Your knowledge hub WIEN

[41] Seidler, K.; Griesser, M.; Kury, M.; Harikrishna, R.; Dorfinger, P.; Koch, T.; Svirkova, A.; Marchetti-Deschmann, M.; Stampfl, J.; Moszner, N.; Gorsche, C.; Liska, R.; Vinyl Sulfonate Esters: Efficient Chain Transfer Agents for the 3D Printing of Tough Photopolymers without Retardation. *Angew. Chem., Int. Ed.* **2018**, *57* (29), 9165-9169.

[42] Lu, H.; Stansbury, J. W.; Bowman, C. N.; Towards the elucidation of shrinkage stress development and relaxation in dental composites. *Dent. Mater.* **2004**, *20* (10), 979-986.

[43] Svajdlenkova, H.; Sausa, O.; Steindl, J.; Koch, T.; Gorsche, C.; Microstructural PALS study of regulated dimethacrylates: Thiol- versus β-allyl sulfone-based networks. *J. Polym. Sci., Part B: Polym. Phys.* **2016**, *54* (24), 2476-2484.

[44] Švajdlenková, H.; Šauša, O.; Maťko, I.; Koch, T.; Gorsche, C.; Investigating the Free-Volume Characteristics of Regulated Dimethacrylate Networks Below and Above Glass Transition Temperature. *Macromol. Chem. Phys.* **2018**, *219* (15), 1800119 (1-9).

[45] Gorsche, C.; Koch, T.; Moszner, N.; Liska, R.; Exploring the benefits of β-allyl sulfones for more homogeneous dimethacrylate photopolymer networks. *Polym. Chem.* **2015**, *6* (11), 2038-2047.

[46] Gorsche, C.; Synthesis and characterization of monomers and additives for photopolymer-based dental restoratives. PhD-Thesis, Technische Universität Wien, **2015**.

[47] Strong, A. B., *Plastics: materials and processing*. 3 ed.; **2006**.

[48] Meyers, M.; Chawla, K., *Mechanical Behavior of Materials*. 2 ed.; Cambridge University Press: **2008**.

[49] MacKnight, W. J.; Earnest Jr, T. R.; The structure and properties of ionomers. *Journal of Polymer Science: Macromolecular Reviews* **1981**, *16* (1), 41-122.

[50] Harakály, G. A.; Tough photopolymers for Hot Lithography application. PhD-Thesis, Technische Universität Wien, **2019**.

Die approbierte gedruckte Originalversion dieser Dissertation ist an der TU Wien Bibliothek verfügbar.
The approved original version of this doctoral thesis is available in print at TU Wien Bibliothek.
TU Bibliothek Your knowledge hub WIEN

[51] Kury, M.; Tough photopolymers for stereolithography. PhD-Thesis, Technische Universität Wien, **2020**.

[52] Bucknall, C. B.; New criterion for craze initiation. *Polymer* **2007**, *48* (4), 1030-1041.

[53] Bucknall, C. B.; Quantitative approaches to particle cavitation, shear yielding, and crazing in rubber-toughened polymers. *J. Polym. Sci., Part B: Polym. Phys.* **2007**, *45* (12), 1399-1409.

[54] Michler, G. H., *Kunststoff-Mikromechanik: Morphologie, Deformations- und Bruchmechanismen*. Hanser: **1992**.

[55] Wicks, D. A.; Wicks, Z. W.; Blocked isocyanates III: Part A. Mechanisms and chemistry. *Prog. Org. Coat.* **1999**, *36* (3), 148-172.

[56] Delebecq, E.; Pascault, J.-P.; Boutevin, B.; Ganachaud, F.; On the Versatility of Urethane/Urea Bonds: Reversibility, Blocked Isocyanate, and Non-isocyanate Polyurethane. *Chem. Rev.* **2013**, *113* (1), 80-118.

[57] Ying, H.; Zhang, Y.; Cheng, J.; Dynamic urea bond for the design of reversible and self-healing polymers. *Nature Communications* **2014**, *5*, 1-9.

[58] Rolph, M. S.; Markowska, A. L. J.; Warriner, C. N.; O'Reilly, R. K.; Blocked isocyanates: from analytical and experimental considerations to non-polyurethane applications. *Polym. Chem.* **2016**, *7* (48), 7351-7364.

[59] Hartmann, B.; Duffy, J. V.; Lee, G. F.; Balizer, E.; Thermal and dynamic mechanical properties of polyurethaneureas. *J. Appl. Polym. Sci.* **1988**, *35* (7), 1829-1852.

[60] Krol, P.; Synthesis methods, chemical structures and phase structures of linear polyurethanes. Properties and applications of linear polyurethanes in polyurethane elastomers, copolymers and ionomers. *Prog. Mater. Sci.* **2007**, *52* (6), 915-1015.

[61] Chattopadhyay, D. K.; Raju, K. V. S. N.; Structural engineering of polyurethane coatings for high performance applications. *Prog. Polym. Sci.* **2007**, *32* (3), 352-418.

[62] Szycher, M., *Szycher's Handbook of Polyurethanes*. 2 ed.; Taylor & Francis: **2012**.

Die approbierte gedruckte Originalversion dieser Dissertation ist an der TU Wien Bibliothek verfügbar.
The approved original version of this doctoral thesis is available in print at TU Wien Bibliothek.
TU Bibliothek Your knowledge hub WIEN

[63] Engels, H.-W.; Pirkl, H.-G.; Albers, R.; Albach, R. W.; Krause, J.; Hoffmann, A.; Casselmann, H.; Dormish, J.; Polyurethanes: Versatile Materials and Sustainable Problem Solvers for Today's Challenges. *Angew. Chem., Int. Ed.* **2013**, *52* (36), 9422-9441.

[64] Koshiba, M.; Hwang, K. K. S.; Foley, S. K.; Yarusso, D. J.; Cooper, S. L.; Properties of ultraviolet curable polyurethane acrylates. *J. Mater. Sci.* **1982**, *17* (5), 1447-1458.

[65] Viollaz, F.; Pascault, J. P.; Camberlin, Y.; Reactive blocked polyurethane systems. 2. Reaction kinetics in the presence of a chain extender. Structure and properties of the obtained poly(urethane-ureas). *Makromol. Chem.* **1984**, *185* (12), 2517-2532.

[66] Speckhard, T. A.; Hwang, K. K. S.; Lin, S. B.; Tsay, S. Y.; Koshiba, M.; Ding, Y. S.; Cooper, S. L.; Properties of UV-curable polyurethane acrylates: effect of reactive diluent. *J. Appl. Polym. Sci.* **1985**, *30* (2), 647-666.

[67] Lai, Y. C.; Baccei, L. J.; Synthesis and structure-property relationships of UV-curable urethane prepolymers with hard-soft-hard blocks. *J. Appl. Polym. Sci.* **1991**, *42* (7), 2039-2044.

[68] Yu, X.; Grady, B. P.; Reiner, R. S.; Cooper, S. L.; Mechanical and thermal properties of UV-curable polyurethane and polyurea acrylates. *J. Appl. Polym. Sci.* **1993**, *49* (11), 1943-1955.

[69] Krishnan, P. S. G.; Choudhary, V.; Varma, I. K.; Current status of urethane (meth)acrylate oligomers and polymers. *J. Macromol. Sci., Rev. Macromol. Chem. Phys.* **1993**, *C33* (2), 147-180.

[70] Kwon, J.-Y.; Yoo, H.-J.; Kim, H.-D.; Effect of chemical structure on the properties of UV-cured polyurethane acrylates films. *Fibers and Polymers* **2001**, *2* (3), 141-147.

[71] Sinh, L. H.; Harri, K.; Marjo, L.; Minna, M.; Luong, N. D.; Jurgen, W.; Torsten, W.; Matthias, S.; Jukka, S.; Novel photo-curable polyurethane resin for stereolithography. *RSC Adv.* **2016**, *6* (56), 50706-50709.

Die approbierte gedruckte Originalversion dieser Dissertation ist an der TU Wien Bibliothek verfügbar.
The approved original version of this doctoral thesis is available in print at TU Wien Bibliothek.
TU Bibliothek Your knowledge hub WIEN

[72] Yilgor, I.; Yilgor, E.; Wilkes, G. L.; Critical parameters in designing segmented polyurethanes and their effect on morphology and properties: A comprehensive review. *Polymer* **2015**, *58*, A1-A36.

[73] Ionescu, M., *Chemistry and Technology of Polyols for Polyurethanes*. Rapra Technology Limited: **2005**.

[74] Petrovic, Z. S.; Budinski-Simendic, J.; Study of the effect of soft-segment length and concentration on properties of polyetherurethanes. II. The effect on mechanical properties. *Rubber Chem. Technol.* **1985**, *58* (4), 701-712.

[75] Martin, D. J.; Meijs, G. F.; Renwick, G. M.; McCarthy, S. J.; Gunatillake, P. A.; The effect of average soft segment length on morphology and properties of a series of polyurethane elastomers. I. Characterization of the series. *J. Appl. Polym. Sci.* **1996**, *62* (9), 1377-1386.

[76] Yilgor, I.; Yilgor, E.; Guclu Guler, I.; Ward, T. C.; Wilkes, G. L.; FTIR investigation of the influence of diisocyanate symmetry on the morphology development in model segmented polyurethanes. *Polymer* **2006**, *47* (11), 4105-4114.

[77] Oprea, S.; Structure and properties of cross-linked polyurethane copolymers. *Adv. Polym. Technol.* **2009**, *28* (3), 165-172.

[78] Sami, S.; Yildirim, E.; Yurtsever, M.; Yurtsever, E.; Yilgor, E.; Yilgor, I.; Wilkes, G. L.; Understanding the influence of hydrogen bonding and diisocyanate symmetry on the morphology and properties of segmented polyurethanes and polyureas: Computational and experimental study. *Polymer* **2014**, *55* (18), 4563-4576.

[79] Barbeau, P. H.; Gerard, J. F.; Magny, B.; Pascault, J. P.; Vigier, G.; Morphological analysis of photocured polyurethane acrylate networks. Correlation with viscoelastic properties. *J. Polym. Sci., Part B: Polym. Phys.* **1999**, *37* (9), 919-937.

[80] Barbeau, P.; Gerard, J. F.; Magny, B.; Pascault, J. P.; Effect of the diisocyanate on the structure and properties of polyurethane acrylate prepolymers. *J. Polym. Sci., Part B: Polym. Phys.* **2000**, *38* (21), 2750-2768.

Die approbierte gedruckte Originalversion dieser Dissertation ist an der TU Wien Bibliothek verfügbar.
The approved original version of this doctoral thesis is available in print at TU Wien Bibliothek.
TU Bibliothek Your knowledge hub WIEN

[81] Klinedinst, D. B.; Yilgor, I.; Yilgor, E.; Zhang, M.; Wilkes, G. L.; The effect of varying soft and hard segment length on the structure-property relationships of segmented polyurethanes based on a linear symmetric diisocyanate, 1,4-butanediol and PTMO soft segments. *Polymer* **2012**, *53* (23), 5358-5366.

[82] Koch, B.; Tailored urethane methacrylates for tough, thermoplastic-like photopolymers via Hot Lithography. Master Thesis, Technische Universität Wien, **2019**.

[83] Dieterich, D.; Aqueous emulsions, dispersions and solutions of polyurethanes; synthesis and properties. *Prog. Org. Coat.* **1981**, *9* (3), 281-340.

[84] Wicks, Z. W., Jr.; New developments in the field of blocked isocyanates. *Prog. Org. Coat.* **1981**, *9* (1), 3-28.

[85] Wicks, D. A.; Wicks, Z. W.; Blocked isocyanates III Part B: Uses and applications of blocked isocyanates. *Prog. Org. Coat.* **2001**, *41* (1-3), 1-83.

[86] Wicks, Z. W., Jr.; Blocked isocyanates. *Prog. Org. Coat.* **1975**, *3* (1), 73-99.

[87] Le, T. P.; Viollaz, F.; Camberlin, Y.; Thanh, M. L.; Pascauli, J. P.; Blocked polyurethanes as reactive systems. 1. Thermal dissociation as a function of the type of isocyanate and of the type of blocking agent. Study by DSC and FTIR. *Makromol. Chem.* **1984**, *185* (2), 281-295.

[88] Muramatsu, I.; Tanimoto, Y.; Kase, M.; Okoshi, N.; Correlation between thermal dissociation and chemical structure of blocked isocyanates. *Prog. Org. Coat.* **1993**, *22* (1-4), 279-286.

[89] Wicks, D. A.; Wicks, Z. W.; Multistep chemistry in thin films; the challenges of blocked isocyanates. *Prog. Org. Coat.* **2001**, *43* (1-3), 131-140.

[90] Sankar, G.; Sultan Nasar, A.; Effect of isocyanate structure on deblocking and cure reaction of N-methylaniline-blocked diisocyanates and polyisocyanates. *Eur. Polym. J.* **2009**, *45* (3), 911-922.

[91] Zhang, L.; Rowan, S. J.; Effect of Sterics and Degree of Cross-Linking on the Mechanical Properties of Dynamic Poly(alkylurea-urethane) Networks. *Macromolecules* **2017**, *50* (13), 5051-5060.

Die approbierte gedruckte Originalversion dieser Dissertation ist an der TU Wien Bibliothek verfügbar.
The approved original version of this doctoral thesis is available in print at TU Wien Bibliothek.
TU Bibliothek Your knowledge hub WIEN

[92] Ma, S.; Webster, D. C.; Degradable thermosets based on labile bonds or linkages: A review. *Prog. Polym. Sci.* **2018**, *76*, 65-110.

[93] Kim, G. Y.; Sung, S.; Kim, M. P.; Kim, S. C.; Lee, S.-H.; Park, Y. I.; Noh, S. M.; Cheong, I. W.; Kim, J. C.; Reversible polymer networks based on the dynamic hindered urea bond for scratch healing in automotive clearcoats. *Appl. Surf. Sci.* **2020**, *505*, in press.

[94] Podgorski, M.; Fairbanks, B. D.; Kirkpatrick, B. E.; McBride, M.; Martinez, A.; Dobson, A.; Bongiardina, N. J.; Bowman, C. N.; Toward Stimuli-Responsive Dynamic Thermosets through Continuous Development and Improvements in Covalent Adaptable Networks (CANs). *Adv. Mater.* **2020**, e1906876.

[95] Velankar, S.; Cooper, S. L.; Pazos, J.; UV-curable urethane urea acrylates via deblocking urea linkages. *Polym. Mater. Sci. Eng.* **1995**, *73*, 506-507.

[96] Velankar, S.; Pazos, J.; Cooper, S. L.; High-performance UV-curable urethane acrylates via deblocking chemistry. *J. Appl. Polym. Sci.* **1996**, *62* (9), 1361-1376.

[97] Rolland, J. P.; Chen, K.; Poelma, J.; Goodrich, J.; Pinschmidt, R.; DeSimone, J. M.; Robeson, L.; Methods of producing three-dimensional objects from materials having multiple mechanisms of hardening. WO2015200201A1, **2015**.

[98] Rolland, J. P.; Chen, K.; Poelma, J.; Goodrich, J.; Pinschmidt, R.; DeSimone, J. M.; Robeson, L.; Three-dimensional objects produced from materials having multiple mechanisms of hardening. WO2015200189A1, **2015**.

[99] Rolland, J. P.; Chen, K.; Poeima, J.; Goodrich, J.; Pinschmidt, R.; DeSimone, J. M.; Robeson, L. M.; Polyurethane resins having multiple mechanisms of hardening for use in producing three-dimensional objects. US20160137839A1, **2016**.

[100] Chen, K.; Wright, A. G.; Zhang, M. S.; Production method for three-dimensional object, polymerizable liquid composition, and blocked prepolymer and monomer. WO2018226943A1, **2018**.

Die approbierte gedruckte Originalversion dieser Dissertation ist an der TU Wien Bibliothek verfügbar.
The approved original version of this doctoral thesis is available in print at TU Wien Bibliothek.
TU Bibliothek WIEN Your knowledge hub

[101] Gorsche, C.; Schnoell, C.; Koch, T.; Moszner, N.; Liska, R.; Debonding on Demand with Highly Cross-Linked Photopolymers: A Combination of Network Regulation and Thermally Induced Gas Formation. *Macromolecules* **2018**, *51* (3), 660-669.

[102] Schmitt, F.; Wenning, A.; Weiss, J.-V.; Dimeric isocyanates in polyurethane powder coatings. *Prog. Org. Coat.* **1998**, *34* (1-4), 227-235.

[103] Disteldorf, J.; Huebel, W.; Wolf, E.; Uretidinediones free of isocyanurate from isophorone diisocyanate. EP45995A1, **1982**.

[104] Wakeshima, I.; Kijima, I.; Synthesis of heterocyclic compounds by the reaction of tin(II) bis(acetylacetonate) with isocyanates. *Bull. Chem. Soc. Jpn.* **1975**, *48* (3), 953-955.

[105] Schnöll, C.; Investigation of various blocked isocyanates for Debonding on Demand. Master Thesis, Technische Universität Wien, **2016**.

[106] Wendisch, D.; Reiff, H.; Dieterich, D.; Kernresonanzspektroskopische beiträge zur struktur und stereochemie von (cyclo)aliphatischen isocyanaten und deren folgeprodukten. *Die Angewandte Makromolekulare Chemie* **1986**, *141* (1), 173-183.

[107] Jiang, X.; Zhu, X.; Arnold, A. A.; Kong, X. Z.; Claverie, J. P.; Polyurea Structure Characterization by HR-MAS NMR Spectroscopy. *Ind. Eng. Chem. Res.* **2017**, *56* (11), 2993-2998.

[108] Wei-Guang Qiu; Fei-Long Zhang; Xu-Bao Jiang; Kong, X.-Z.; NMR Analysis to Identify Biuret Groups in Common Polyureas. *Chin. J. Polym. Sci.* **2018**, *36*, 1150-1156.

[109] Achten, D.; Buesgen, T.; Golling, F.; Wagner, R.; Tomczyk, C.; Tillack, J.; Eggert, C.; Laas, H.-J.; Stempfle, F. J.; Method for producing an object from a precursor, and use of a radically cross-linkable resin in an additive production method. WO2018104223A1, **2018**.

[110] Achten, D.; Buesgen, T.; Faecke, T.; Mettmann, B.; Buechner, J.; Laas, H.-J.; Liu, T.; Method for producing products by means of additive manufacturing methods using reactive powders, and products thereof. WO2018206614A1, **2018**.

Die approbierte gedruckte Originalversion dieser Dissertation ist an der TU Wien Bibliothek verfügbar.
The approved original version of this doctoral thesis is available in print at TU Wien Bibliothek.
TU WIEN Bibliothek Your knowledge hub

[111] Okada, S.; Blocked isocyanate, photocuarble composition, resin, and method of manufacturing threedimensional object. US2019161573A1, **2019**.

[112] Brandrup, J.; Immergut, E. H.; Grulke, E. A., *Polymer Handbook*. 4 ed.; Wiley: **1999**.

[113] Batzer, H., *Polymere Werkstoffe*. Georg Thieme Verlag: **1984**; Vol. 2.

[114] Bucknall, C. B.; Paul, D. R.; Notched impact behavior of polymer blends: Part 1: New model for particle size dependence. *Polymer* **2009**, *50* (23), 5539-5548.

[115] Peer, G.; Dorfinger, P.; Koch, T.; Stampfl, J.; Gorsche, C.; Liska, R.; Photopolymerization of Cyclopolymerizable Monomers and Their Application in Hot Lithography. *Macromolecules* **2018**, *51* (22), 9344-9353.

[116] Dolci, E.; Froidevaux, V.; Joly-Duhamel, C.; Auvergne, R.; Boutevin, B.; Caillol, S.; Maleimides As a Building Block for the Synthesis of High Performance Polymers. *Polymer Reviews* **2016**, *56* (3), 512-556.

[117] Yamazaki, H.; Matsumoto, A.; Otsu, T.; Effect of N-substituents on polymerization reactivity of N-alkylitaconimides in radical polymerization. *Eur. Polym. J.* **1997**, *33* (2), 157-162.

[118] Salman, M.; Sharma, S.; Yadav, G. C.; Kapkoti, G. S.; Mishra, A.; Gupta, P.; Anand, N.; Chugh, A.; Nanda, K.; Preparation of piperazine derivatives, particularly piperazinyl-pyrrolidine-2,5-dione, piperazinyl-tetrahydroisoindole-1,3-dione, and piperazinyl-piperidine-2,6-dione derivatives, as adrenergic receptor antagonists for treating benign prostatic hyperplasia. WO2005118537A2, **2005**.

[119] Watanabe, H.; Matsumoto, A.; Otsu, T.; Polymerization of N-alkyl-substituted itaconimides and N-(alkyl-substituted phenyl)itaconimides and characterization of the resulting polymers. *J. Polym. Sci., Part A: Polym. Chem.* **1994**, *32* (11), 2073-2083.

[120] Solanki, A.; Anand, V.; Choudhary, V.; Varma, I. K.; Effect of structure on thermal behavior of homopolymers and copolymers of itaconimides. *J. Macromol. Sci., Polym. Rev.* **2001**, *C41* (4), 253-284.

Die approbierte gedruckte Originalversion dieser Dissertation ist an der TU Wien Bibliothek verfügbar.
The approved original version of this doctoral thesis is available in print at TU Wien Bibliothek.
TU Bibliothek Your knowledge hub WIEN

[121] Reddy, P. Y.; Kondo, S.; Toru, T.; Ueno, Y.; Lewis Acid and Hexamethyldisilazane-Promoted Efficient Synthesis of N-Alkyl- and N-Arylimide Derivatives. *J. Org. Chem.* **1997**, *62* (8), 2652-2654.

[122] Upadhyay, S. K.; Pingali, S. R. K.; Jursic, B. S.; Comparison of microwave-assisted and conventional preparations of cyclic imides. *Tetrahedron Lett.* **2010**, *51* (17), 2215-2217.

[123] Sippy, K. B.; Anderson, D. J.; Bunnelle, W. H.; Hutchins, C. W.; Schrimpf, M. R.; Preparation and characterization of N-(3-pyridinyl) spirocyclic diamines as ligands for nicotinic acetylcholine receptors. *Bioorg. Med. Chem. Lett.* **2009**, *19* (6), 1682-1685.

[124] Ebert, J.; Gmeiner, R.; Stereolithography device having heating device. WO2016078838A1, **2016**.

[125] Steyrer, B.; Busetti, B.; Harakaly, G.; Liska, R.; Stampfl, J.; Hot Lithography vs. room temperature DLP 3D-printing of a dimethacrylate. *Addit. Manuf.* **2018**, *21*, 209-214.

[126] Galanti, A. V.; A kinetic study of the polymerization of aliphatic imides. *J. Appl. Polym. Sci.* **1984**, *29* (5), 1611-1616.

[127] Cowie, J. M. G.; Reid, V. M. C.; McEwen, I. J.; Effect of side chain lengths on the glass transition of copolymers from styrene with N-alkyl citraconimides and with N-alkyl itaconimides. *Br. Polym. J.* **1990**, *23* (4), 353-357.

[128] Hoyle, C. E.; Clark, S. C.; Jonsson, S.; Shimose, M.; Photopolymerization using maleimides as photoinitiators. *Polymer* **1997**, *38* (22), 5695-5697.

[129] Clark, S. C.; Hoyle, C. E.; Jonsson, S.; Morel, F.; Decker, C.; Photopolymerization of acrylates using N-aliphatic maleimides as photoinitiators. *Polymer* **1999**, *40* (18), 5063-5072.

[130] Joensson, S.; Viswanathan, K.; Hoyle, C. E.; Clark, S. C.; Miller, C.; Nguyen, C.; Zhao, W.; Shao, L.; Morel, F.; Decker, C.; Recent Development in Free Radical Photopolymerization Direct and Sensitized Excitation of Maleimides. *J. Photopolym. Sci. Technol.* **2000**, *13* (1), 125-143.

Die approbierte gedruckte Originalversion dieser Dissertation ist an der TU Wien Bibliothek verfügbar.
The approved original version of this doctoral thesis is available in print at TU Wien Bibliothek.
TU Bibliothek Your knowledge hub WIEN

[131] Nguyen, C. K.; Cavitt, T. B.; Hoyle, C. E.; Kalyanaraman, V.; Jonsson, S.; A mechanistic description of the sensitized N-substituted maleimide initiated photopolymerization of an acrylate monomer. *ACS Symp. Ser.* **2003**, *847* (Photoinitiated Polymerization), 27-40.

[132] Vázquez, C. P.; Joly-Duhamel, C.; Boutevin, B.; Photoinitiator-Free, Open-Air Acceptor/Donor Copolymerization of Bismaleimides: Simple Polymerization Conditions for New Thermoplastic Elastomer Production. *Macromol. Chem. Phys.* **2013**, *214* (14), 1621-1628.

[133] Andersson, H.; Hult, A.; Initiator-free photopolymerization of an aliphatic vinyl ether-maleimide monomer. *J. Coat. Technol.* **1997**, *69* (865), 91-95.

[134] Lee, C.-W.; Kim, J.-M.; Han, D. K.; Ahn, K.-D.; Photopolymerization of bifunctional maleimides based on electron-donor/acceptor systems. *J. Macromol. Sci., Pure Appl. Chem.* **1999**, *A36* (10), 1387-1399.

[135] Bonneaud, C.; Burgess, J. M.; Bongiovanni, R.; Joly-Duhamel, C.; Friesen, C. M.; Photopolymerization of maleimide perfluoropolyalkylethers without a photoinitiator. *J. Polym. Sci., Part A: Polym. Chem.* **2019**, *57* (6), 699-707.

[136] Jonsson, S.; Sundell, P.-E.; Hultgren, J.; Sheng, D.; Hoyle, C. E.; Radiation chemistry aspects of polymerization and crosslinking. A review and future environmental trends in 'non-acrylate' chemistry. *Prog. Org. Coat.* **1996**, *27* (1), 107-122.

[137] Oswal, S.; Bhandari, V. K.; Bhamore, P.; Malek, N. I.; Free Radical Copolymerization of Methyl Methacrylate and Styrene with N-(4-Carboxyphenyl)maleimide. *International Journal of Polymeric Materials and Polymeric Biomaterials* **2007**, *56* (4), 421-435.

[138] Hisano, M.; Takashima, T.; Jin, Z.; Shiibashi, A.; Matsumoto, A.; Radical Copolymerization Reactivity of N-Substituted Maleimides with α-Substituted Styrenes with Various N- and α-Substituents and the Thermal and Optical Properties of the Resulting Copolymers. *Macromol. Chem. Phys.* **2013**, *214* (14), 1612-1620.

Die approbierte gedruckte Originalversion dieser Dissertation ist an der TU Wien Bibliothek verfügbar.
The approved original version of this doctoral thesis is available in print at TU Wien Bibliothek.
TU Bibliothek Your knowledge hub WIEN

[139] Polli, H.; Pontes, L. A. M.; Araujo, A. S.; Barros, J. M. F.; Fernandes, V. J., Jr.; Degradation behavior and kinetic study of ABS polymer. *J. Therm. Anal. Calorim.* **2009**, *95* (1), 131-134.

[140] Miyamura, H.; Min, H.; Soule, J.-F.; Kobayashi, S.; Size of Gold Nanoparticles Driving Selective Amide Synthesis through Aerobic Condensation of Aldehydes and Amines. *Angew. Chem., Int. Ed.* **2015**, *54* (26), 7564-7567.

[141] Ambrus, J. I.; Halliday, J. I.; Kanizaj, N.; Absalom, N.; Harpsoe, K.; Balle, T.; Chebib, M.; McLeod, M. D.; Covalent attachment of antagonists to the α7 nicotinic acetylcholine receptor: synthesis and reactivity of substituted maleimides. *Chem. Commun.* **2012**, *48* (53), 6699-6701.

[142] Curran, D. P.; Geib, S.; DeMello, N.; Rotational features of carbon-nitrogen bonds in N-aryl maleimides. Atroposelective reactions of o-tert-butylphenylmaleimides. *Tetrahedron* **1999**, *55* (18), 5681-5704.

[143] Emsermann, J.; Opatz, T.; Photochemical Approaches to the Bilobalide Core. *Eur. J. Org. Chem.* **2017**, *2017* (23), 3362-3372.

[144] Bryne, P.; Wen, L.; Waller, D. P.; Canteenwala, T.; Foyle, P.; Jackson, E.; Photoactive polymers for photovoltaic cells. WO2012149189A2, **2012**.

[145] Peer, G.; New monomers for radical photopolymerization. Master Thesis, Technische Universität Wien, **2017**.

[146] Crivello, J. V.; Falk, B.; Zonca, M. R., Jr.; Photoinduced cationic ring-opening frontal polymerizations of oxetanes and oxiranes. *J. Polym. Sci., Part A: Polym. Chem.* **2004**, *42* (7), 1630-1646.

[147] Mariani, A.; Bidali, S.; Fiori, S.; Sangermano, M.; Malucelli, G.; Bongiovanni, R.; Priola, A.; UV-ignited frontal polymerization of an epoxy resin. *J. Polym. Sci., Part A: Polym. Chem.* **2004**, *42* (9), 2066-2072.

[148] Bomze, D.; Knaack, P.; Koch, T.; Jin, H.; Liska, R.; Radical induced cationic frontal polymerization as a versatile tool for epoxy curing and composite production. *J. Polym. Sci., Part A: Polym. Chem.* **2016**, *54* (23), 3751-3759.

[149] Bomze, D.; Radical induced Cationic Frontal Polymerization as a new and versatile Curing Technique for Epoxy Resins. PhD-Thesis, Technische Universität Wien, **2016**.

Die approbierte gedruckte Originalversion dieser Dissertation ist an der TU Wien Bibliothek verfügbar.
The approved original version of this doctoral thesis is available in print at TU Wien Bibliothek.
TU Bibliothek Your knowledge hub WIEN

[150] Liska, R.; Stampfl, J.; Photopolymers for rapid prototyping. *Basics and Applications of Photopolymerization Reactions* **2010**, *3*, 147-173.

[151] Herzberger, J.; Sirrine, J. M.; Williams, C. B.; Long, T. E.; Polymer Design for 3D Printing Elastomers: Recent Advances in Structure, Properties, and Printing. *Prog. Polym. Sci.* **2019**, *97*, 1-44.

[152] Gebhardt, A., *Rapid Prototyping: Werkzeuge für die schnelle Produktentwicklung*. **2005**.

[153] Gorsche, C.; Harikrishna, R.; Baudis, S.; Knaack, P.; Husar, B.; Laeuger, J.; Hoffmann, H.; Liska, R.; Real Time-NIR/MIR-Photorheology: A Versatile Tool for the in Situ Characterization of Photopolymerization Reactions. *Anal. Chem.* **2017**, *89* (9), 4958-4968.

[154] DIN EN ISO 527. *2012*.

Die approbierte gedruckte Originalversion dieser Dissertation ist an der TU Wien Bibliothek verfügbar.
The approved original version of this doctoral thesis is available in print at TU Wien Bibliothek.
TU Bibliothek Your knowledge hub WIEN

Appendix

1. RT-NIR-photorheology

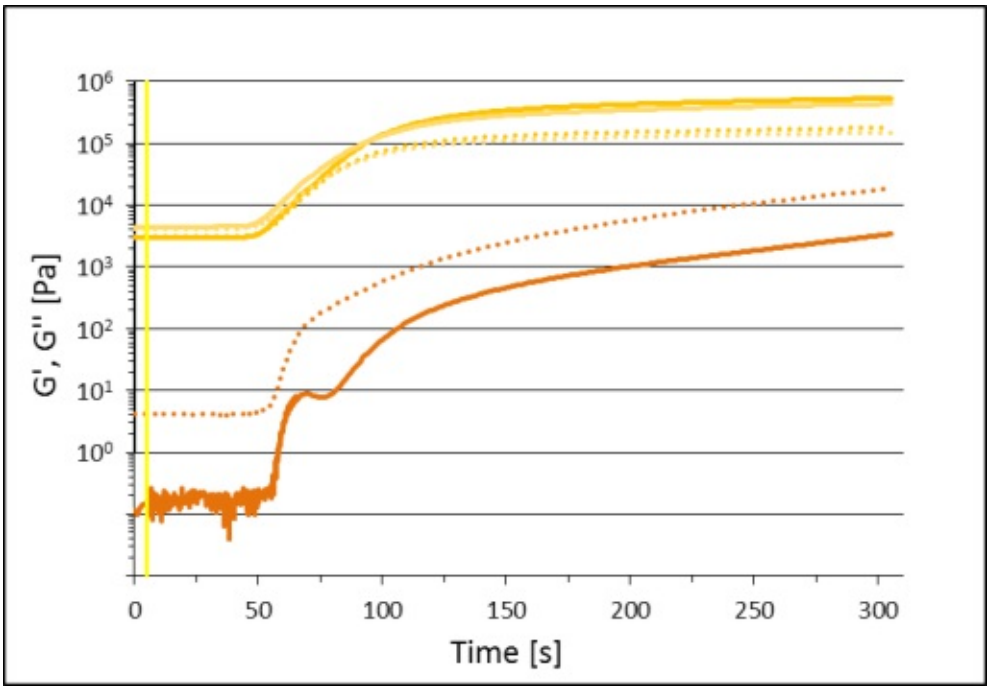

Figure 150: Storage modulus (—) and loss modulus (···) of **MISt3** without (—) and with 10 (—) or 20 w% (—) **CB24**; start of irradiation (—)

Die approbierte gedruckte Originalversion dieser Dissertation ist an der TU Wien Bibliothek verfügbar.
The approved original version of this doctoral thesis is available in print at TU Wien Bibliothek.

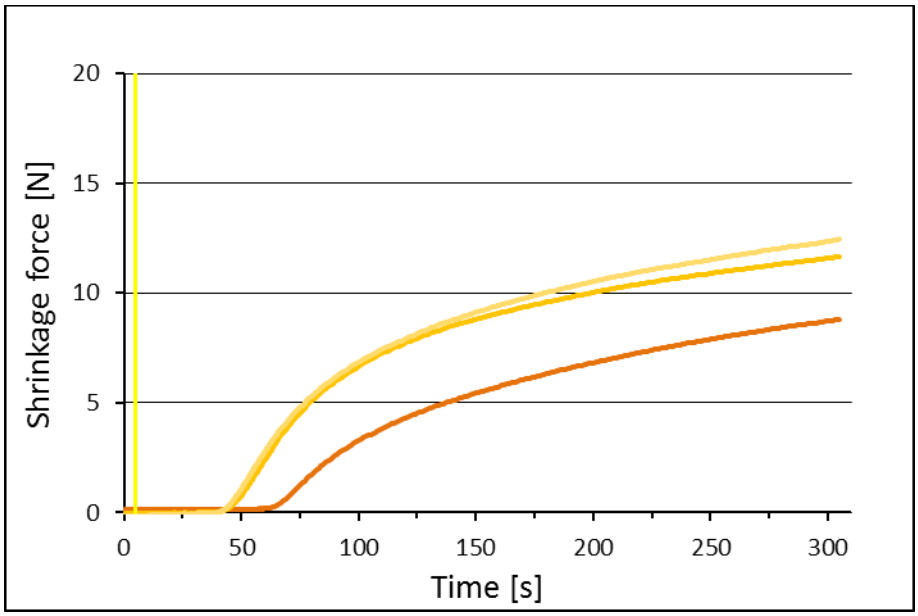

Figure 151: Evolution of shrinkage force of **MISt3** without (—) and with 10 (—) or 20 w% (—) **CB24**; start of irradiation (—)

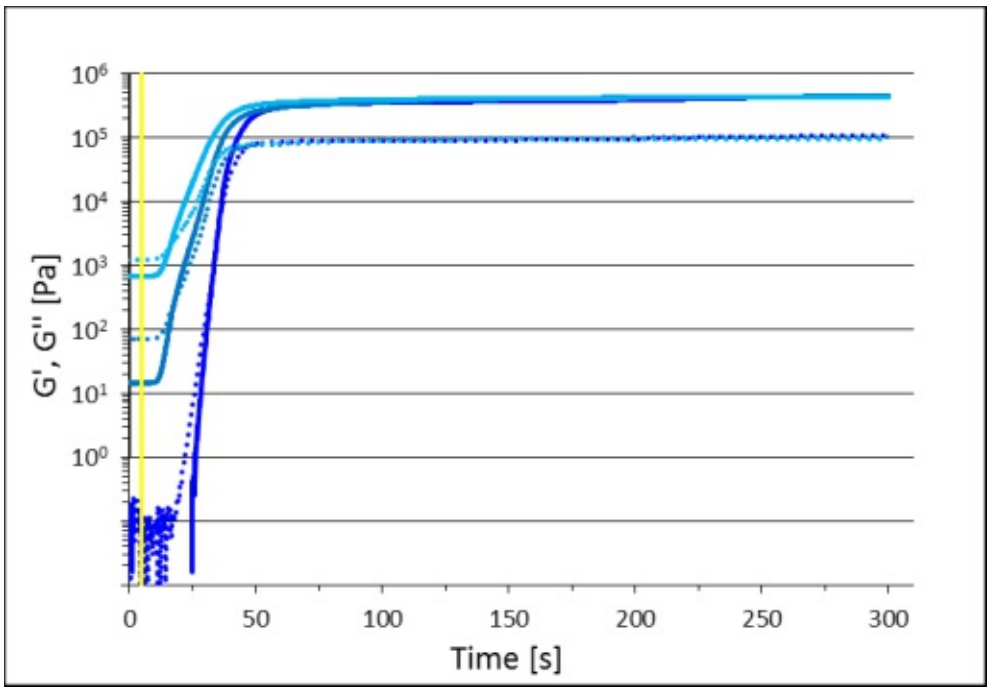

Figure 152: Storage modulus (—) and loss modulus (···) of **MISt4** without (—) and with 10 (—) or 20 w% (—) **CB24**; start of irradiation (—)

Die approbierte gedruckte Originalversion dieser Dissertation ist an der TU Wien Bibliothek verfügbar.
The approved original version of this doctoral thesis is available in print at TU Wien Bibliothek.
TU Bibliothek Your knowledge hub WIEN

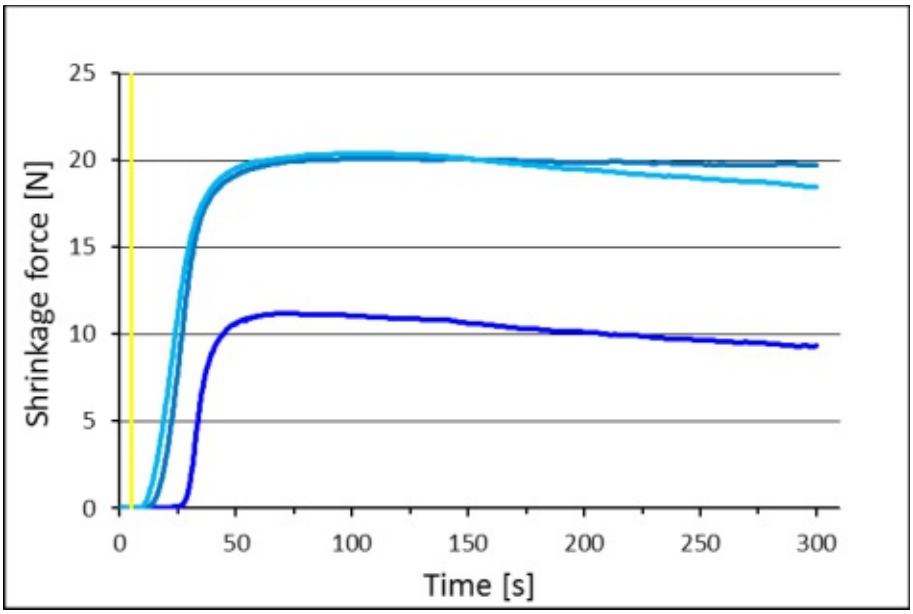

Figure 153: Evolution of shrinkage force of **MISt4** without (—) and with 10 (—) or 20 w% (—) **CB24**; start of irradiation (—)

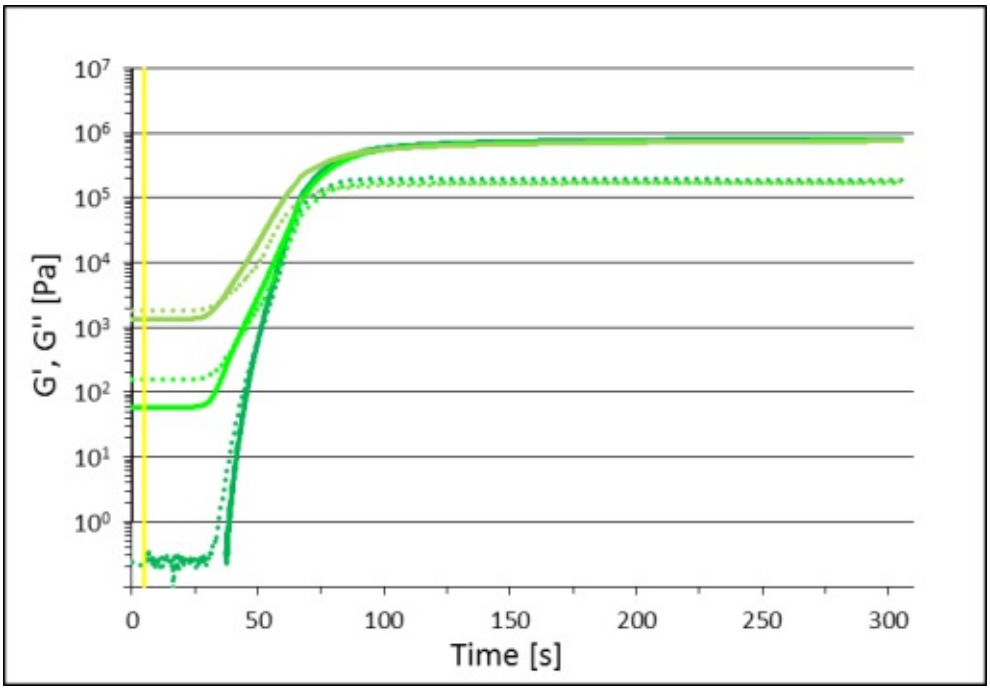

Figure 154: Storage modulus (—) and loss modulus (···) of **MISt5** without (—) and with 10 (—) or 20 w% (—) **CB24**; start of irradiation (—)

Die approbierte gedruckte Originalversion dieser Dissertation ist an der TU Wien Bibliothek verfügbar.
The approved original version of this doctoral thesis is available in print at TU Wien Bibliothek.
TU Bibliothek Your knowledge hub WIEN

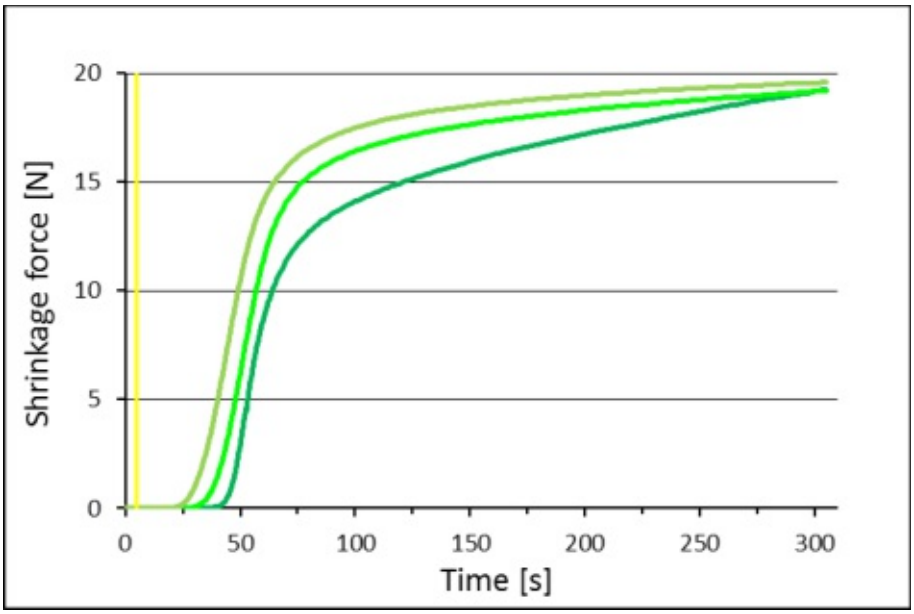

Figure 155: Evolution of shrinkage force of **MISt5** without (—) and with 10 (—) or 20 w% (—) **CB24**; start of irradiation (—)

Die approbierte gedruckte Originalversion dieser Dissertation ist an der TU Wien Bibliothek verfügbar.
The approved original version of this doctoral thesis is available in print at TU Wien Bibliothek.

Curriculum Vitae

DI Johannes Steindl

Date of birth:	6 August 1990 in Vienna
Nationality:	Austria
Address:	Withalmstraße 9/1B/16, 2120 Wolkersdorf
Phone:	+43 664 1500548
E-mail:	josteindl@gmx.at

Education

03/2016 – present	Doctoral programme in Engineering Science Technical Chemistry Technische Universität Wien, Institute of Applied Synthetic Chemistry, Division of Macromolecular Chemistry
11/2013 – 03/2016	Master programme Technical Chemistry (with distinction) Master thesis: “Chain Transfer Agents based on Silicon”, Technische Universität Wien, Institute of Applied Synthetic Chemistry, Christian Doppler Laboratory for Photopolymers in Digital and Restorative Dentistry
10/2009 – 11/2013	Bachelor programme Technical Chemistry Bachelor thesis: “Investigations on Thiophene Ring-Fragmentation (TRF) via Inline ATR-IR-Spectroscopy and Synthesis of NLO Materials”, Technische Universität Wien, Institute of Applied Synthetic Chemistry
09/2000 – 06/2008	BG/BRG Wolkersdorf

Die approbierte gedruckte Originalversion dieser Dissertation ist an der TU Wien Bibliothek verfügbar.
The approved original version of this doctoral thesis is available in print at TU Wien Bibliothek.
TU Bibliothek Your knowledge hub WIEN

Work experience

07/2019 – present	OMV Exploration & Production GmbH
04/2016 – 05/2019	Project assistant, FWF-Project Technische Universität Wien, Institute of Applied Synthetic Chemistry
10/2011 – 08/2015	Worker, Biomasse Obersdorf
09/2008 – 02/2009	Basic military service, NBC Defence School Korneuburg
07/2006	Worker, Stadtgemeinde Wolkersdorf

Personal skills

Languages:	German (mother tongue), English (fluent)
Computer skills:	MS Office, OpenOffice, ChemDraw, CorelDraw, Endnote, analysis software of various manufacturers (Bruker, Netzsch, Anton Paar, Thermo Fisher Scientific, Büchi, Waters, PerkinElmer,...)
Driving licenses:	A, B, C, E, F

Awards and Publications

- 5th European Symposium of Photopolymer Science 2018: 1st Prize Winner – Poster
- XXII. Bratislava International Conference on Macromolecules 2016: Best Student Poster Presentation Award
- J. Steindl, T. Koch, N. Moszner, C. Gorsche; "*Silane-Acrylate Chemistry for Regulating Network Formation in Radical Photopolymerization*"; Macromolecules, **50** (2017), 19; 7448 – 7457.

Die approbierte gedruckte Originalversion dieser Dissertation ist an der TU Wien Bibliothek verfügbar.
The approved original version of this doctoral thesis is available in print at TU Wien Bibliothek.
TU Bibliothek Your knowledge hub WIEN

- J. Steindl, A. Svirkova, M. Marchetti-Deschmann, N. Moszner, C. Gorsche; "*Light-Triggered Radical Silane-Ene Chemistry Using a Monosubstituted Bis(trimethylsilyl)silane*"; Macromolecular Chemistry and Physics, **218** (2017), 5; 1600563 – 1600569.
- D. Lumpi, J. Steindl, S. Steiner, V. Carl, P. Kautny, M. Schön, F. Glöcklhofer, B. Holzer, B. Stöger, E. Horkel, C. Hametner, G.A. Reider, M.D. Mihovilovic, J. Fröhlich; "*Thiophene ring-fragmentation reactions: Principles and scale-up towards NLO materials*"; Tetrahedron, **73** (2017), 5; 472 – 480.
- H. Svajdlenková, O. Sausa, J. Steindl, T. Koch, C. Gorsche; "*Microstructural PALS study of regulated dimethacrylates: Thiol- versus β-allyl sulfone-based networks*"; Journal of Polymer Science Part B: Polymer Physics, **54** (2016), 23; 2476 – 2484.

- (Co-)Author of 8 presentations on scientific conferences

Die approbierte gedruckte Originalversion dieser Dissertation ist an der TU Wien Bibliothek verfügbar.
The approved original version of this doctoral thesis is available in print at TU Wien Bibliothek.
TU Bibliothek Your knowledge hub WIEN